Ultrastructural Studies of Microalgae

Alanoud Jaber Rawdhan

A thesis submitted for the degree of Doctor of Philosophy (Integrated)

October, 2015

School of Agriculture, Food and Rural Development, Newcastle University

Newcastle upon Tyne, UK

Abstract

Ultrastructural Studies of Microalgae

The optimization of fixation protocols was undertaken for *Dunaliella salina*, Nannochloropsis oculata and Pseudostaurosira trainorii to investigate two different aspects of microalgal biology. The first was to evaluate the effects of the infochemical 2, 4decadienal as a potential lipid inducer in two promising lipid-producing species, Dunaliella salina and Nannochloropsis oculata, for biofuel production. D. salina fixed well using 1% glutaraldehyde in 0.5 M cacodylate buffer prepared in F/2 medium followed by secondary fixation with 1% osmium tetroxide. N. oculata fixed better with combined osmiumglutaraldehyde prepared in sea water and sucrose. A stereological measuring technique was used to compare lipid volume fractions in D. salina cells treated with 0, 2.5, and 50 µM and N. oculata treated with 0, 1, 10, and 50 µM with the lipid volume fraction of naturally senescent (stationary) cultures. There were significant increases in the volume fractions of lipid bodies in both D. salina (0.72%) and N. oculata (3.4%) decadienal-treated cells. However, the volume fractions of lipid bodies of the stationary phase cells were 7.1% for *D*. salina and 28% for N. oculata. Therefore, decadienal would not be a suitable lipid inducer for a cost-effective biofuel plant. Moreover, cells treated with the highest concentration of decadienal showed signs of programmed cell death. This would affect biomass accumulation in the biofuel plant, thus further reducing cost effectiveness.

The second investigation used the cell structure and gametogenesis of *Pseudostaurosira* trainorii to evaluate the cytoplasmic support for the molecular phylogeny of diatoms proposed by Medlin and Kaczmarska (2004) which divides diatoms into three clades that differ in their ultrastructure, where Clade 1 contains centric diatoms, Clade 2a centric bipolar and multipolar diatoms and Clade 2b pennate diatoms. *P. trainorii* is classified as araphid diatom which has a thread-like structure reported by Sato et al. (2011) that could resemble the flagella in centric diatoms. *P. trainorii* fixed better with combined osmiumglutaraldehyde prepared in sea water and sucrose, and it was found that its Golgi apparatus and auxospore were resemble those of Clade 2b, while the pyrenoid structure might represent a variation of the structures described for other members of Clade 2b. In addition, this study proved that the thread-like structures in *P. trainorii* were not flagella.

Dedication

I dedicate this work to my father "Jaber Rawdhan", whose belief in me inspired me to believe in myself.

Acknowledgements

This work is the product of support from many people - my advisors, colleagues, friends, and family.

Firstly, I would like to thank Dr. Gordon Beakes for his guidance, support, encouragement, and advice throughout my study.

I would like to thank too Dr. Gary Caldwell, Dr. Rebecaa Taylor, and Dr. Shina Sato, for supporting me and providing algal samples for my research.

My thanks also go to thank the electron microscopy research service staff at Newcastle University, especially Vivian Thompson, Tracey Davey, and Kathryn White, for their training and technical help.

I would like to thank Kuwait University for funding my Integrated PhD studies.

More personally, I would like to thank my friends: Gillian Libretto; Awar al-Hawge; Hanan Dashti; Zainab Afseri; Wafa Hussain; Zainab Ashkanani; Amerah Ibrahim and her family; and Howra Ben Hasan, for their support and encouragement.

Finally, I wish to thank my family for their living support – my father Jaber Rawdhan; my mother Warda al-Shamri; my sisters Hanouf, Ohoud, Narjes, Heba, Fatma, Anaam, and Hawraa; my brothers Ahmad and Hussain; and my lovely niece Laila Al-Shammari.

Table of contents

Abstract	ii
Dedication	
Acknowledgements	iv
Table of content	V
List of Tables	viii
List of Figures	. X
Chapter 1. Introduction	
1.1 Introduction	1
1.2 Thesis organization	
1.3 Project description	
1.3.1 Effects of an algal infochemical (decadienal) on the ultrastructure of	
Dunaliella salina and Nannochloropsis oculata	.3
1.3.2 Pseudostaurosira trainorii: ultrastructure and gametogenesis	
1.4 Aims and objectives	
Chapter 2. Methods	
2.1 Cultures	
2.1.1 Maintenance cultures of <i>Dunaliella salina</i> and <i>Nannochloropsis oculata</i>	
2.1.2 <i>Pseudostaurosira trainorii</i> : cultures and inducing gamete formation and	
mating	24
2.2 Light microscopy	
2.3 Transmission electron microscopy fixation protocols	
2.3.1 Optimizing the fixation of <i>Dunaliella salina</i>	
2.3.1.1 Protocol one: 2% glutaraldehyde 1% osmium in 0.1 M cacodylate	
buffer in seawater (2% GaOs, SW)	28
2.3.1.2 Protocol two: 2% glutaraldehyde 1% osmium in 0.1 M cacodylate	
buffer in buffered sterile F/2 medium (2% Ga/Os F/2)	29
2.3.1.3 Protocol three: 1% glutaraldehyde 1% osmium in 0.1 M cacodylate	
buffer in buffered sterile F/2 medium (1% Ga/Os F/2)	
2.3.2 Optimizing fixation protocols for <i>Nannochloropsis oculata</i>	
2.3.2.1 Protocol four: combined glutaraldehyde-osmium with sucrose (Ga-	
Os/Os suc)	
2.3.2.2 Protocol five: combined glutaraldehyde-osmium (Ga-Os/Os)	
2.3.3 Optimizing the fixation of <i>Pseudostaurosira trainorii</i>	
2.3.3.1 Protocol six: 1.25% glutaraldehyde 1% osmium in 0.1 M	_
cacodylate buffer in seawater (1.25% GaOs, 50% SW)	32
2.3.3.2 Protocol seven: 2.5% glutaraldehyde 1% osmium in 0.1 M	_
cacodylate buffer in seawater (2% GaOs, SW)	32
2.3.3.3 Protocol eight: combined 2% glutaraldehyde - 0.5% osmium - 1%	
osmium in 0.1 M cacodylate buffer in buffered sterile SW with	
sucrose (2% Ga-Os/Os 50% SW)	32
2.4 Preparation for scanning electron microscopy	
2.5 Evaluation of fixation protocols	
2.5.1 Optimizing fixation protocols for <i>Dunaliella salina</i>	
2.5.2 Optimizing fixation protocols for <i>Nannochloropsis oculata</i>	
2.5.3 Optimizing fixation protocols for <i>Pseudostaurosira trainorii</i>	
2.6 Conclusion	
Chapter 3. Effects of an algal infochemical (decadienal) on the ultrastructure of	-
Dunaliella salina and Nannochloropsis oculata	57
3.1 Introduction	

3.1.1 Importance of biofuels	57
3.1.2 Advantages of algal biofuel	59
3.1.3 Algal biofuel production schemes	60
3.1.4 Lipids in microalgae	61
2.1.5 Maximising the lipid content in algae	
3.1.6 Infochemicals	65
3.1.7 Study aims	66
3.2 Methods	68
3.2.1 Comparison of active versus stationary phase cell ultrastructure	68
3.2.1.1 Dunaliella salina CCAP19/30	68
3.2.1.2 Nannochloropsis oculata CCAP849/1	68
3.2.2 Assessing the effects of decadienal on <i>Dunaliella salina</i> and	
Nannochloropsis oculata cell structure	68
3.2.3 Stereological and statistical analysis	
3.2.3.1 <i>Dunaliella salina</i> : testing the differences between volume fraction	
of log and stationary phases	
3.2.3.2 <i>Dunaliella salina</i> : testing the differences between volume fraction	
of decadienal-treated cells	
3.2.3.3 Nannochloropsis oculata: testing the differences between volume	
fractions of log and stationary phases	74
3.2.3.4 <i>Nannochloropsis oculata</i> : testing the differences between volume	
fractions of decadienal-treated cells	. 75
3.3 Results	. 77
3.3.1 Dunaliella salina ultrastructure	77
3.3.1.1 Ultrastructure of actively growing 7-day-old cells	
3.3.1.2 Ultrastructure of 14-day-old stationary phase cells	
3.3.1.3 Ultrastructure of decadienal-treated cells	
3.3.2 Nannochloropsis oculata ultrastructure	97
3.3.2.1 Ultrastructure of actively growing 6-day-old cells	
3.3.2.2 Ultrastructure of 14-day-old stationary phase cells	
3.3.2.3 Ultrastructure of decadienal-treated cells	
3.4 Discussion	122
3.4.1 Ultrastructural differences between actively growing and stationary cells	s 122
3.4.1.1 Dunaliella salina	
3.4.1.1.1 General morphology	
3.4.1.1.2 Chloroplast structure and lipid reserves	
3.4.1.1.3 Other cell organelles	
3.4.1.2 Nannochloropsis oculata	
3.4.1.2.1 General morphology	
3.4.1.2.2 Chloroplast morphology and structure and lipid reserves	
3.4.2 Effects of decadienal and culture age on lipid accumulation in	
Dunaliella salina and Nannochloropsis oculata	129
3.4.3 Effect of decadienal on other cell organelles of <i>Dunaliella salina</i> and	
Nannochloropsis oculata	133
Chapter 4. Gametogenesis of <i>Pseudostaurosira trainorii</i>	
4.1 Introduction	
4.1.1 Diatom classification: historical perspectives based on morphological	
characteristics	. 144
4.1.2 Diatom classification: molecular phylogeny and ultrastructural	
characteristics	145
4.1.2.1 Golgi apparatus	. 146
4.1.2.2 Pyrenoid structure	
-	

4.1.2.3 Sexual reproduction	150
4.1.2.3.1 Sexual reproduction in centric diatoms	155
4.1.2.3.2 Sexual reproduction in pennate diatoms	157
4.1.2.4 Auxospore formation and structure in relation to molecular	
phylogeny	158
4.1.3 Aims of this diatom study	161
4.2 Methods	
4.3 Results	161
4.3.1 Vegetative cells	161
4.3.2 Gametogenesis	166
4.3.2.1 Male gametogenesis and gametes	166
4.3.2.2 Female gametogenesis and gametes	170
4.3.2.3 Fertilization and auxospore development	174
4.4 Discussion	177
4.4.1 Organelles with significance for molecular phylogeny	
4.4.2 Sexual reproduction, gametogenesis and auxosporulation	178
4.4.3 Auxospore development	181
Chapter 5. Conclusion	184
Appendices	189
Appendix 1	189
Appendix 2	190
References	203

List of Tables

Table	Title	Page
1.1	The conventional algal groups	9
1.2	The classification of eukaryotes at the highest ranks	11
1.3	The classification of the three organisms	12
1.4	Ultrastructural studies available of the genus <i>Dunaliella</i>	13
1.5	Studies available of the genus Nannochloropsis	16
1.6	Available studies of the genus <i>Pseudostaurosira trainorii</i>	17
2.1	The chemical composition of F/2 medium	23
2.2	Chemical components of the WC medium	26
2.3	Chemical components of Roshchin medium	27
2.4	Summary of preparative procedure used	31
2.5	Summary of preparative procedure used for <i>Pseudostaurosira trainorii</i>	33
2.6	Assessment of fixation techniques applied to <i>Dunaliella salina</i>	37
2.7	Assessment of fixation techniques applied to <i>Nannochloropsis oculata</i>	44
2.8	Assessment of fixation techniques applied to <i>Pseudostaurosira</i>	
	trainorii	52
3.1	Experimental set-up for <i>Dunaliella salina</i>	70
3.2	Experimental set-up for Nannochloropsis oculata	70
3.3	Results of t-tests for volume fractions of cytoplasm, mitochondria,	
	chloroplast, matrix, thylakoid membranes and starch in <i>Dunaliella</i>	
	salina active and stationary phase cells	81
3.4	Results of Mann-Whitney tests for volume fraction for nucleus, lipid,	
	vacuoles, plastoglobuli and pyrenoid in <i>Dunaliella salina</i> active and	
	stationary phase cells	81
3.5	Results of ANOVA tests on the effects of decadienal treatments on the	
	volume fractions of cytoplasm, thylakoid membrane, starch, and	
	matrix in Dunaliella salina	90
3.6	Results of Kruskal-Wallis tests for volume fractions of nucleus,	
	mitochondria, lipid, vacuoles, chloroplast, pyrenoid and plastoglobuli	
	in Dunaliella salina decadienal-treated cells	90
3.7	Results of Mann-Whitney tests for significant differences between	
	volume fractions of nucleus, mitochondria, lipid and vacuoles in	
	Dunaliella salina decadienal-treated cells	91
3.8	Results of t-tests of volume fractions of cytoplasm, cell wall,	
	chloroplast, matrix and thylakoid membranes and starch in	
	Nannochloropsis oculata active and stationary phase cells	100
3.9	Results of Mann-Whitney tests of volume fractions of nucleus, lipid,	
	vacuoles, plastoglobuli and mitochondria in Nannochloropsis oculata	
	active and stationary phase cells	100
3.10	Results of ANOVA tests on the effects of decadienal treatments on the	
	volume fractions of cytoplasm and matrix in Nannochloropsis oculata	110
3.11	Results of Kruskal-Wallis test of volume fractions of nucleus,	
	mitochondria, lipid, vacuoles, chloroplast, cell wall, plastoglobuli and	
	thylakoid membranes in <i>Nannochloropsis oculata</i> decadienal-treated	110
0.15	cells	110
3.12	Results of Mann-Whitney tests for significant differences between	
	volume fractions of lipid and cell wall in Nannochloropsis oculata	
	decadienal-treated cells	111

3.13	Programmed cell death mechanisms, their signs and mediator with the	
	key reference	136
3.14	Similarities and differences between results of this present study for	
	Dunaliella salina programmed cell death and the results of Jimenez et	
	al. (2009)	143
4.1	Comparison of morphological features across the three molecular	
	clades	148
4.2	Summary of pyrenoid characteristics as described by Schmid (2001)	
	together with diagrammatic interpretations of the present writer	152

List of Figures

Figure	Title	Page
1.1	A phylogeny of the major groups of eukaryotic organisms	18
1.2	Dunaliella salina cell structure	19
1.3	Nannochloropsis oculata cell structure	20
1.4	The diatom cell structure	21
2.1	Gametogenesis induction in Pseudostaurosira trainorii	25
2.2	Dunaliella salina fixation protocol one	38
2.3	Dunaliella salina fixation protocol two	39
2.4	Dunaliella salina fixation protocol three	40
2.5	Nannochloropsis oculata cells fixed with fixation protocol one	46
2.6	Nannochloropsis oculata cells fixed with fixation protocol two	47
2.7	Nannochloropsis oculata cells fixed with fixation protocol three	48
2.8	Nannochloropsis oculata cells fixed with fixation protocol four	19
2.9	Nannochloropsis oculata cells fixed with fixation protocol five	50
2.10	Pseudostaurosira trainorii life cycle stages fixed using protocol six	53
2.11	Pseudostaurosira trainorii life cycle stages fixed using protocol seven	54
2.12	Pseudostaurosira trainorii 24 hours induced male gamete fixed using	
	protocol eight	55
3.1	Basic structure of triacylglycerides	67
3.2	Decadienal structure	67
3.3	Experimental set-up	71
3.4	Stereological analysis	76
3.5	Dunaliella salina cell structure under light, scanning electron microscopy and	
	comparison between exponential and stationary growth phases of <i>Dunaliella</i>	
	salina under lower magnification transmission electron microscopy	82
3.6	Comparison of exponential and stationary growth phases of <i>Dunaliella salina</i>	
	at higher magnification of transmission electron microscope.	83
3.7	Mean and 95% confidence intervals of volume fractions of the cell organelles	
	in Dunaliella salina log and stationary phase cells	84
3.8	Median and 95% confidence intervals of volume fractions of the cell	
	organelles in <i>Dunaliella salina</i> log and stationary phase cells	85
3.9	Comparisons of cell structures of two <i>Dunaliella salina</i> control samples	92
3.10	Dunaliella salina decadienal-treated cells	93
3.11	Detailed structural distortion of <i>Dunaliella salina</i> cells treated with 50 µM	_
	decadienal	94
3.12	Means and 95% confidence intervals of volume fractions of the cytoplasm	
	and chloroplast constituents in <i>Dunaliella salina</i> treated with decadienal	95
3.13	Figure 3.13: Medians and 95% confidence intervals of volume fractions of	0.5
2.1.1	organelles in <i>Dunaliella salina</i> treated with decadienal	96
3.14	Nannochloropsis oculata cell structure under light and scanning electron	101
2.15	microscopy and exponential growing cells under electron microscopy	101
3.15	Higher magnification of the fine structure of exponentially growing cells of	100
2.16	Nannochloropsis oculata	102
3.16	Nannochloropsis oculata stationary phase growing cells	103
3.17	Higher magnification of fine structure of stationary phase growing cells of	104
1	Nannochloropsis oculata	1104

3.18	Mean and 95% confidence interval of volume fractions of the cell organelles	
	and chloroplast constituents in Nannochloropsis oculata log and stationary	
	phase samples	105
3.19	Median and 95% confidence interval fractions of cell organelles and	
	chloroplast constituents in <i>Nannochloropsis oculata</i> log and stationary phase	
	samples	106
3.20	Nannochloropsis oculata controls	112
3.21	Higher magnification of <i>Nannochloropsis oculata</i> cell organelles of both 0	
	μM decadienal and ethanol control cells	113
3.22	Nannochloropsis oculata cells treated with 1 µM decadienal	114
3.23	Higher magnification of <i>Nannochloropsis oculata</i> cells treated with 1 μM	
	decadienal	115
3.24	Nannochloropsis oculata cells treated with 10 μM decadienal	116
3.25	Higher magnification of <i>Nannochloropsis oculata</i> cells treated with 10 μM	
	decadienal	117
3.26	Nannochloropsis oculata cells treated with 50 µM decadienal	118
3.27	Higher magnification of <i>Nannochloropsis oculata</i> cells treated with 50 μM	
	decadienal	119
3.28	Mean and 95% confidence intervals of volume fraction of the cytoplasm and	
	matrix in Nannochloropsis oculata cells treated with deacadienal	120
3.29	Median and 95% confidence intervals of volume fraction of the cell	
	organelles in Nannochloropsis oculata cells treated with deacadienal	121
4.1	Golgi arrangements	149
4.2	Different types of sexual reproduction in different diatom groups as	
	summarised by Mann (1993)	154
4.3	Sperm formation in centric diatoms	156
4.4	The three types of auxospore	160
4.5	Light, scanning and transmission electron micrographs of <i>Pseudostaurosira</i>	
	trainorii	164
4.6	Cytological features of <i>Pseudostaurosira trainorii</i>	165
4.7	Male dividing cells and gametogenesis	168
4.8	Mature male gamete	169
4.9	Female dividing cells and gametogenesis	172
4.10	Egg differentiation and maturation	173
4.11	Fertilization and auxospore in the 20 minutes fertilized sample	175
4.12	Mature auxospore from 24 hours fertilized sample	176

Chapter 1. Introduction

1.1 Introduction

Eukaryotic organisms that are photosynthetic and have chlorophyll *a* with a thallus not differentiated into roots, stem and leaves are defined as algae (Lee 1999). Algae occur in almost all habitats and exhibit a huge morphological diversity, ranging from tiny unicells to large kelps over 50 m long (Lee 1999). However, algae also include cyanobacteria, which are only prokaryotic. Microalgae (or microscopic algae), which are algae that are generally invisible to the naked eye, which are both prokaryotic and eukaryotic (Tomaselli 2004). Microalgae include a variety of mostly unicellular organisms with different cellular organizations, and also include colony forming organisms that may have specialised structures that help them to adapt to their environment.

The conventional approach to classifying algae was generally based on their colour. New criteria were added later to classify algae, including the types of pigments, the chemistry of their storage products, cell wall composition, the presence and structure of flagella, patterns of nuclear division, and the relationship between the endoplasmic reticulum envelope and the nuclear envelope and chloroplast. Then Lee (1989) reviewed algal groups. He stressed the importance in algae classification of the additional membranes that surround the chloroplast envelope. Using this as a basis, he proposed that eukaryotic algae can be separated into three groups. They differ from one another based on chloroplast evolution in accordance with endosymbiosis theory (Table 1.1). The first eukaryotic algal group is of algae that have chloroplasts surrounded by no extra membranes and includes Rhodophyta, and Chlorophyta. The molecular phylogeny of Adl et al. (2012) placed these two groups together with Glaucophyta in Archaeplastida. The Glaucophyta have endosymbiotic cyanobacteria in the cytoplasm instead of chloroplasts (Lee 1999). The second group includes both the Dinophyta and Euglenophyta, which have one additional membrane of endoplasmic reticulum surrounding the plastid. In the final group, the algae have two additional membranes of endoplasmic reticulum surrounding the chloroplast and this group includes the Cryptophyta, Chrysophyta, Prymnesiophyta, Bacillarophyta, Xanthophyta,

Eustigmatophyta, Raphidophyta and Phaeophyta (Lee 1999). The scheme used for classifying algae is summarized in Table 1.1.

The development of molecular phylogeny and the Tree of Life project resulted in amendments to the classification of all eukaryotic organisms, which includes algae. The latest classification has been summarised by Adl et al. (2012). The present thesis is concerned with three algae Dunaliella salina, Nannochloropsis oculata, and Pseudostaurosira trainorii. They belong to two major super-groups described by Adl et al. (2012). D. salina belongs to the super-group Archaeplastida, and both N.oculata and P. trainorii belong to the super-group SAR (Table 1.2, Figure 1.1). The super-group Archaeplastida includes Glaucophyta, Rhodophyceae (red algae) and Chloroplastida (green lineages, including land plants). These three groups arose from the symbiosis of a heterotrophic eukaryotic ancestral organism with a photosynthetic cyanobacterium, and are considered to have the primary plastids (Reyes-Prieto et al. 2007). Following the evolution of red and green algae, the ancestors of the Chromalveolata were thought to have evolved through the engulfment of forms of red algae by a non-photosynthetic protist (Cavalier-Smith 1999). The Chromalveolata include the algal lineages of cryptophytes, haptophytes, stramenopiles, and dinoflagellates and the nonphotosynthetic ciliates and apicomplexans (Adl et al. 2005). However, more recent research suggests that this is a polyphyletic assemblage (Adl et al. 2012). Other algal groups evolved through the secondary symbiosis of either a green or a red alga (Falkowski et al. 2004). The euglenids evolved by the engulfment of the green alga cell by the ancestor of the euglenoid (Excavata), and chlorarachniophytes evolved by the engulfment of the green alga cell by the ancestor of the chlorarachniophyte amoebae (Rhizaria) (Falkowski et al. 2004; Reyes-Prieto et al. 2007). The red algal plastid groups such as cryptomonads, heterokonts, haptophytes, apicomplexans and dinoflagellates were acquired by a single secondary endosymbiosis by their common ancestor (Archibald 2005; Archibald 2008). However, Adl et al. (2012) reported that Stramenopiles (heterokonts, apicomplexans, diatoms, chrysophytes and brown seaweeds), Alveolata (dinoflagellates) and Radiolaria (Foraminifera) are now thought to share a common ancestor and have now been placed in the so-called SAR super-group. However, the cryptomonads and haptophytes still present challenges with regard to their phylogenetic placement in the tree of life (Adl et al. 2012).

1.2 Thesis organization

Algal ultrastructure is well documented and has been reviewed by Dodge (1973) and Berner (1993). This thesis examined two different and unrelated problems, using the common tool of transmission electron microscopy. The first problem investigated was the effect of the infochemical decadienal on the cell structure and lipid production of two algal species, *Dunaliella salina* and *Nannochloropsis oculata*, which are considered to be potential biofuel stock species (a full review of the issue is presented in the introduction to Chapter 3, section 3.1). The second problem was describing the cell structure and gametogenesis of the diatom *Pseudostaurosira trainorii*. This species is described for the first time in this thesis using transmission electron microscopy and this is considered important because it is the first species in which a thread-like structure in the male gametes has been reported (Sato et al. 2011).

The evolution of diatom diversity is an area that requires the study of different biological processes in order to be fully understood. For example, it requires the study of frustule (cell valve) morphology and ontogeny, of sexual reproduction, which includes gamete and auxospore ontogeny, and of cell structure organization. Different systems have been used historically to classify diatoms, but the use of molecular phylogeny changed the situation and erased the link between cell structure and classification again. A comprehensive, detailed description and review of the problem is presented in Chapter 4. The following section (1.3) gives a brief description of both problems, stating the aims of the two studies and the important cell ultrastructure features of the organisms studied.

1.3 Project description

1.3.1 Effects of an algal infochemical (decadienal) on the ultrastructure of Dunaliella salina and Nannochloropsis oculata

The aim of the experimentation described in Chapter 3 was first to use electron microscopy to permit the differentiation between two types of lipid-rich structures within the cell, namely, lipid bodies and membrane constituents, since chemical extraction methods only provide a measure of the total lipids in the cell. Electron microscopy was used as part of a quantitative technique using stereological measurements of randomly-taken thin sections of cells in their exponentional and stationary growth phases, and in a range of decadienal concentrations. This allowed an

estimation of the volume fraction of lipid production, which would enable assessment of whether decadienal triggers a shift to lipid body content or just increases the overall membrane constituents in the cell and, in particular, the extensive plastid thylakoid system. Furthermore, the effect of decadienal on the cell structure of *N. oculata* and *D. salina* could be evaluated in these two species of microalgae, which are already widely cultured and many of whose characteristics are well known. Finally, the effectiveness of decadienal as a lipid production inducer in both species could be assessed by comparing cell structure in the absence and presence of decadienal.

D. salina is green alga (Table 1.3) that has diverse features, some of them shared with land plants (van den Hoek et al. 1995; Graham et al. 2009). The chloroplasts are encircled by a double membrane with thylakoids grouped in lamellae, and contain chlorophyll *a* and *b* along with a set of accessory pigments such as carotenes and xanthophylls. Pyrenoids, when present, are embedded within the chloroplast and are surrounded by starch, which is the main reserve polysaccharide (Figure 1.2). While the majority of the green algae have firm cell walls, *D. salina* lacks a cell wall and, instead, has a thin glycocalyx coat (Ginzburg 1987). *D. salina* has two flagella which are similar in structure to each other (isokont).

The genus *Dunaliella* is considered a model organism, both for studying the evolution of higher plants and for studying the effect of stress factors, owing to its ubiquity and ability to survive in harsh environmental conditions such as high salinity, temperature fluctuation, nitrogen starvation, and irradiance (Ginzburg 1987; Cowan et al. 1992). It is industrially important because it can accumulate huge amounts of β -carotene in the cells which can be collected for commercial purposes (Borowitzka et al. 1984; Borowitzka and Borowitzka 1990). In addition, it has potential as a feedstock for biofuel production (Oren 2005; Gouveia and Oliveira 2009; Tafresh and Shariati 2009). Devi et al. (2012) demonstrated that the direct transesterification of microalgae biomass showed a good biodiesel yield, where *D. salina* yielded 66.6%. The total lipid content of *D. salina* was 21.2% (Devi et al. 2012).

Under some stress-inducing conditions, such as increased salt concentration (halostress), *D. salina* shows increased lipid production (Alhasan et al. 1987). In contrast, nitrogen limitation, which is a common way of inducing lipid production in other microalgae species, does not induce increased lipid production in *D. salina* (Griffiths and Harrison 2009). However, there has been relatively little research into

lipid accumulation in D. salina in response to halostress, as most of the earlier work in this area has focused principally on β -carotene production (Ben-Amotz and Avron 1983). D. salina is reported to produce 35% lipid content in non-stressed conditions (Griffiths and Harrison 2009). The effect of several physical stress factors on lipid production in D. salina has been studied previously (reviewed in Sharma et al. 2012). The majority of these studies used chemical extraction and dry weight as a method to quantify lipids (detailed in Chapter 3, section 3.1). However, only a limited number of studies, listed in Table 1.4, have been conducted using electron microscopy. To the best of the present writer's knowledge, this is the first ultrastructural study that has examined the effect of a chemical factor on D. salina cell structure.

The other organism considered was *Nannochloropsis oculata*. The genus Nannochloropsis belongs to the Eustigmatales, which is classified in the Stramenopiles that occur within the superclade SAR (Adl et al. 2012). It belongs to the class Eustigmatophyta, which has both ecological significance and economic uses (van den Hoek et al. 1995). It is a unicellular alga with spherical cell shape that ranges in size from two to four micrometres and has a simple cell structure (Figure 1.3). Growing in marine environments, it is characterized by its high content of eicosap entaenoic acid, an omega three fatty acid [205ω3] (Brown et al. 1993). Consequently, it has been used in many marine-culture hatcheries in Europe since the late 1980s to provide this important nutrient supplement (Cheng-Wu et al. 2001). Many studies have been conducted to optimise the mass production of Nannochloropsis cultivation in order to produce pharmaceuticals and fish feed (Rebolloso-Fuentes et al. 2001; Richmond and Cheng-Wu 2001; Rodolfi et al. 2003). Recently Nannochloropsis has been considered a candidate for the production of biofuel (Chisti 2007; Rodolfi et al. 2009; Brennan and Owende 2010). The genus Nannochloropsis is known to synthesise triacylglyceride (TAG) lipids (Vieler et al. 2012). As with other algal species, stress conditions trigger the accumulation of increased amounts of TAGs in Nannochloropsis spp. The stress factors that have been studied in this respect in *Nannochloropsis* spp. include changing nitrogen concentration, level of irradiation, temperature and salinity conditions.

Rodolfi et al. (2009) screened thirty microalgal species and assessed the best lipid producers as those strains showing the best combination of biomass productivity and lipid content. Three members of the marine genus *Nannochloropsis* had a lipid content of 30% or higher and a lipid productivity ranging from 55 to 61 mg l⁻¹ day⁻¹. The authors reported that *Nannochloropsis* species could produce 20 tons of lipid per

hectare in the Mediterranean climate and more than 30 tons of lipids per hectare in sunny tropical areas. *Nannochloropsis* could attain 60% lipid content by weight when subjected to nitrogen deficiency and high irradiances (Rodolfi et al. 2009; Pal et al. 2011). In addition, Devi et al. (2012) showed that *Nannochloropsis* sp. yielded 68.5% lipid content by direct transesterification. The total lipid content of *Nannochloropsis* sp. was 27.5% (Devi et al. 2012). Ultrastructural studies of *N. oculata*, however, are very limited and are summarized in Table 1.5.

1.3.2 Pseudostaurosira trainorii: ultrastructure and gametogenesis

Diatoms are unicellular or colonial algae with a unique cell wall. This wall (frustule) is composed of silica and has a complex architecture, as summarized in Figure 1.4. Variation in diatom frustule structure has been widely used to classify diatoms, in addition to features such as mode of sexual reproduction and plastid number and structure (Round et al. 1990). Diatoms have been traditionally split into two major taxonomic groups: the radially symmetrical centric diatoms and the bilaterally symmetrical pennate diatoms (Figure 1.4). In centric diatoms the valve is radially symmetric, organized around one central point, with pores and ribs radiating out from a central ring called the "annulus". Their overall cell shape varies from circular to short elliptical, triangular, or polygonal (Mann and Evans 2007). In contrast, in pennate diatoms, the valves are bilaterally symmetric and have their ribs and pores arranged on each side of a centre line (called the sternum) which divides the valve into two equal parts with an elongated cell shape (Lee 1999). Some pennate diatoms have a longitudinal slot in the valve called a raphe. The raphe divides the valve of the pennate diatom into two bilateral symmetrical halves. Valve ornamentation is caused by the presence of pores in the silica wall, which are called are loculi or areolae and are arranged in rows called a striae. The molecular phylogenetic study of diatoms (Medlin and Kaczmarska 2004) has revealed a slightly different classification as it results in two major clades at the level of subdivision. The first is Coscinodiscophytina (Clade 1) which includes those centric diatoms that have valves with radial symmetry (representing the class Coscinodiscophyceae), and the second is Bacillariophytina (Clade 2). This has two subgroups (class level) that are different from those recognised in conventional classification schemes. The first subgroup is the so-called Clade 2a and includes the bi- or multipolar centrics and the radial Thalassiosirales (resembleing traditional Mediophyceae); and the second is so-called Clade 2b that includes all the traditional pennate diatoms (equivalent to the traditional Bacillariophyceae) (Medlin

and Kaczmarska 2004). Medlin and Kaczmarska (2004) carried out a detailed analysis to see what ultrastructural and cytological features (e.g. the structure of the Golgi apparatus, chloroplast, pyrenoid organisation, auxospore structure and pattern of sexual reproduction) correlated with their molecularclades. A more detailed account of this is given in Chapter 4, section 4.1.2. This chapter documents the relationship between ultrastructural features and molecular phylogeny through the study of Pseudostaurosira trainorii, which belongs to the araphid pennate diatoms that have so far only been described by light and scanning electron microscopy (Table 1.6). Its shape is circular to elliptical with parallel striae (30 in 10 µm) and a distinct sternum along the long axis (Sato et al. 2011) (Figure 1.4). Only centric diatoms have anteriorly uniflagellate sperm whereas all pennate diatoms lack flagella (van den Hoek et al. 1995). Thus the presence of thread-like structures in *P. trainorii* make it an interesting organism to investigate as regards cell ultrastructure so as to determine the nature of this structure, which has been considered might be a vestigial flagellum (Sato et al. 2011). In addition, the cell ultrastructure determined by transmission electron microscopy of this hitherto undescribed species can be used to investigate the significance of cell structure in the context of the recent molecular phylogenetic concepts of the diatoms proposed by Medlin and Kaczmarska (2004).

1.4 Aims and objectives

The aim of this thesis was to use transmission electron microscopy to address two unrelated biological problems. The first was to assess the effects of the infochemical decadienal on the cell structure of two important biofuel producing species, *Dunaliella salina* and *Nannochloropsis oculata*, qualitatively and quantitatively through stereological technique. In order to assess whether this infochemical was simply speeding up the normal cell aging processes in the algal cells, the cytological effects of decadienal were compared using cells from two groups. One group consisted of exponentially growing decadienal-treated cells and the other of normal stationary phase cells. Further, estimating the volume fraction of lipid globules in decadienal-treated cells and normal aged cells would help to assess the usage of decdienal as a lipid induction substance in biofuel production plan.

The second problem addressed here was to describe the cell structure and gametogenesis of *Pseudostaurosira trainorii*, not hirherto described. This species had recently been shown to have a unique pattern of gametogenesis, with motile male

gametes that appeared to glide along fine cytoplasmic threads, which might or might not be related to flagella (Sato et al. 2011). Transmission electron microscopy should resolve this issue. Finally, these cytological ultrastructural features were to be placed in the context of the modern molecular phylogeny of diatoms, such as outlined by Medlin and Kaczmarska (2004).

Table 1.1: The conventional algal groups (Source: Berner 1993)

	No:	No membrane		membrane
	Rhodophyta	Chloroplyta	Euglenophyta	Dinophyta
Flagellum	-	Two anterior (whiplash) acronematic Or isokont flagella; sometimes pantone stephanokont		Transverse pantonematic flagellum, located in groove or a girdle and shorter
				posterior acronematic flagellum
Hairs	-	Fibrillar solid hairs (tripartite tubular hairs in some primitive Chlorophyta)	Nontubular fibrillary hairs	Nontubular fibrillary hairs
Chloroplast	Two-layered chloroplast envelope	Two-layered chloroplast envelope	CER membrane not continuous with nuclear membrane	CER membrane not continuous with nuclear membrane
Thylakoid membrane	1	-7; sometimes pseudograna	3	3
Girdle lamella	-	-	-	-
Storage product location	Outside chloroplast	Within the chloroplast stroma, often as a sheath around the pyrenoid	Outside chloroplast	Within the chloroplast stroma, often as a sheath around the pyrenoid
Chromosomes	Condensed at mitosis	Condensed at mitosis	Persistently condensed	Persistently condensed; attached to nuclear envelope
Kinetochore	+	-or +	+	-
Nucleolus	Not persistent at mitosis	Not persistent at mitosis	Persistent at mitosis (endosome)	Not persistent at mitosis
Nuclear envelope				
Intact	+	+	+	+
Polar gaps				
Breaks down		(+)		
Spindle type	Closed nuclear and cytoplasmic	Nuclear and cytoplasmic or intranuclear	Intranuclear and subspindles	Cytoplasmic tunnels
Polar structure	Polar rings; no true centrioles	Centrioles	?	?
Cytokinesis	Annular wall plus septal plug	Phycoplast and phragmoplast	Cleavage	Cleavage

Table 1.1: The conventional algal groups (continued)

	Two membranes							
	Cryptophyta	Chrysophta	Prymnesiophyta	Bacillariophyta	Xanthophyta	Eustigmatophyta	Raphidophyta	Phaeophyta
Flagellum	Two anterior	Two unisokont with	Two unisokont	One posterior	Two unisokont with	One anterior	Two unisokont with	Two unisokont with
	pantonematic	long anterior	acronematic flagella	pantonemtic flagellum	long anterior	pantonematic	long anterior	long anterior
	flagella	pantonematic and			pantonematic and	flagellum	pantonematic and short	pantonematic and short
		short posterior			short posterior		acronematic flagellum	posterior acronematic
		acronematic			acronematic flagellum			flagellum
		flagellum						
Hairs	Tripartite tubular	Tripartite tubular	Tripartite tubular	Tripartite tubular hairs	Tripartite tubular hairs	Tripartite tubular	Tripartite tubular hairs	Tripartite tubular hairs
	hairs	hairs	hairs			hairs		
Chloroplast	?	Outer CER	Outer CER	Outer CER membrane	Outer CER membrane	CER membrane not	Outer CER membrane	Outer CER membrane
		membrane	membrane	continuous with outer	continuous with outer	continuous with	continuous with outer	continuous with outer
		continuous with	continuous with	membrane of nuclear	membrane of nuclear	nuclear membrane	membrane of nuclear	membrane of nuclear
		outer membrane of	outer membrane of	envelope	envelope		envelope	envelope
		nuclear envelope	nuclear envelope					
Thylakoid	2	3	3	3	3	3	3	3
membrane								
Girdle lamella	-	+	+	+	+	-	-	+
Storage product	Between chloroplast	Outside the	Outside the	Outside the	Outside the	Outside the	Outside the chloroplast	Outside the chloroplast
location	envelope and CER	chloroplast	chloroplast	chloroplast	chloroplast	chloroplast		
Chromosomes	Persistently	Condensed at	Condensed at	Condensed at mitosis	Condensed at mitosis	Condensed at	Condensed at mitosis	Condensed at mitosis
	condensed	mitosis	mitosis			mitosis		
Kinetochore	+	-	-	-	-	-	+	+
Nucleolus	Persistent at mitosis	Not persistent at	Not persistent at	Not persistent at	Not persistent at	Not persistent at	Not persistent at mitosis	Not persistent at
		mitosis	mitosis	mitosis	mitosis	mitosis		mitosis
Nuclear envelope								
Intact	+					+	+	(+)
Polar gaps								+
Breaks down	+	+	+	+	+			
Spindle type	Nuclear and	Nuclear and	Nuclear and	Cytoplasmic (?)	Extended intranuclear	Nuclear and	Intranuclear	Intranuclear
	cytoplasmic	cytoplasmic	cytoplasmic			cytoplasmic		
Polar structure	Flagellarbasis; no true centriole	Rhizoplast	No centrioles	Spindle "precursor"	Centrioles	Flagellar bases act as centrioles	Centrioles	Extranuclear centrioles
Cytokinesis	Cystokinetic ring	Cleavage	Cleavege	Furrowing	Cleavage		Cleavage	Cell plate
Cytokinesis	Cystokinetic fing	Cicavage	Cleavage	FullOwing	Cicavage	Cleavage	Cicavage	Cen piate

Table 1.2: The classification of eukaryotes at the highest ranks (Source: Adl et al. 2012)

		Super-groups	Examples
Eukaryota		Amboebozoa	Tubulinea
			Mycetozoa
		Opisthokonta	Fungi
	Amorphea		Choanomonada
			Metazoa
			Apusomonnada
			Breviata
		Excavata	Metamonada
			Malawimonas
			Discoba
	Diaphoretickes		Cryptophyceae
			Centrohelida
			Telonemia
			Haptophyta
		Sar	Cercozoa
			Foraminifera
			"Radiolaria"
			Alveolata
			Stramenopiles
		Archaeplastida	Glaucophyta
			Rhodophyceae
			Chloroplatida
	Incertae sedis Eukaryota		Incertae sedis

Table 1.3: The classification of the three organisms

	D. salina	N. oculata	P. trainorii
Super-group	Archaeplatida	Sar	Sar
Higher Level	Chloroplastida	Stramenopiles	Stramenopiles
Phylum	Chlorophyta	Heterokontophyta	Bacillariophyta
Class	Chlorophyceae	Eustigmatophyta	Fragilariophyceae
Order	Volvocales	Eustigmatales	Fragilariales
Family	Dunaliellaceae	Monodopsidaceae	Fragilariceae

Table 1.4: Ultrastructural studies available of the genus *Dunaliella*

Factor	Ultrastructural effect	Microscope	Study
Comparison between logarithmic and	Stationary phase was marked by:	LM and TEM	Eyden (1975)
stationary phase growing cells of <i>D</i> .	- Changes in content and size of cytoplasmic vacuoles		
primolecta.	- Accumulation of cytoplasmic lipids		
	- Accumulation of starch in plastid		
	- Formation of autophagosome-like bodies		
3.5% and 25% NaCl	thylakoid membranes was numerous at low NaCl and	TEM	Pfeifhofer and Belton (1975)
	stacked or compressed at high NaCl		
Comparison between <i>D. tertiolecta</i> cell	- D. tertiolecta similar to D. salina and D.	TEM	Hoshaw and Maluf (1981)
structure and three other species.	bioculata in having two flagellar basal bodies		
	while <i>D. primolecta</i> has four basal bodies.		
	- The stigma in <i>D. tertiolecta</i> flat in shape, <i>D</i> .		
	salina elongated in shape, D. bioculata dense		
	plaque, and plate-like in D. primolecta		
Light intensity and temperature	At low light intensity the thylakoids had intensive	TEM	Vladimirova (1978)
	structure and condensed membranes, while the		
	thylakoid was reduced under high light intensity		
	Lipid globules appeared in all studied variants		
Ultrastructural comparison between D.	-	TEM	Melkonian and Preisig (1984)
salina and Spermatozopsis			
Hypoosmotic shock	Swollen cells	TEM and stereology	Maeda and Thompson (1986)
	Expanded organelles		
Low and high CO ₂ concentrations			Tsuzuki et al. (1986)
Review of English and non-English	-	-	Ginzburg (1987)
literature			

7

Table 1.4: Ultrastructural studies available of the genus *Dunaliella* (continued)

Factor	Ultrastructural effect	Microscope	Study
2.5%, 5% and 30% NaCl	 Accumulation of dark osmiophilic carotenoid globules at the cell periphery and the degeneration of the chloroplast with increasing salinity At 30% NaCl, thylakoids were still intact 	TEM	Alhasan et al. (1987)
Effect of different sources of organic nitrogen on <i>D. tertiolecta</i>	 Hypoxanthine affected endoplasmic reticulum, mitochondria and vacuoles structure Lipid granules were more frequent in allantoic acid-grown cells in comparison to nitrate and urea grown cells 	TEM and stereology	Oliveira and Huynh (1989)
Taxonomic identification	-	TEM	Parra et al. (1990)
Review of English and non-English literature	-	TEM an LM	Preisig (1992)
Effects of acute and chronic Copper and Cadmium on <i>D. salina</i> cells	 Increase in the relative lipid volume of <i>D. salina</i> exposed to acute sub-lethal concentration of cadmium Chronic exposure to either Copper or Cadimum also increased lipid volume. 	TEM and Stereology	Visviki and Rachlin (1994a)
Comparison of young and adult <i>D. salina</i> cell structure	 Adult cells had cell coat with variable pattern Young cells had three Golgi, while adult cells had six to eight Golgi Nucleus of young cell had anterior concavity, while adult cell had nucleus with anterior conical portion The chloroplast occupied 50% of cell volume with pyrenoid with small starch plates in young cells, while adult chloroplast occupied up to 75% of cell volume with pyrenoid and large starch plates 	TEM and SEM	Leonardi and Caceres (1994)

Table 1.4: Ultrastructural studies available of the genus *Dunaliella* (continued)

Factor	Ultrastructural effect	Microscope	Study
Salinity and irradiance	 High salinity induced salt-containing vacuoles Changes in salinity and irradiance changed the chloroplast structure by increasing invaginations and protuberances, lowring number of thylakoids and starch grains 	TEM	Stoynova-Bakalova and Toncheva-Panova (2003)
Darkness	- Cromatin condensation - Loss of nuclei - Intact mitochondria - Intact pyrenoids and starch were lost.	TEM	Segovia et al. (2003)
Chronic selenium intoxication	Different selenium concentrations cause: - Increase in excretory vacuoles - Chloroplast devoid of thylakoid - Autolysed mitochondria - Lysed cytoplasm - Fusing vacuoles	TEM and stereology	Reunova et al. (2007)
-UV irradiation - Acute heat-shock - Hyperosmotic shock - Nutrient starvation and nitrogen limitation - Stationary phase	 Aponecrosis-like Necrotic like Paraptotic Autophagic/vascular cell death Chromatin aggregation, nuclear fragmentation, membrane blebs, cytoplasmic disassembling 	TEM	Jimenez et al. (2009)
UV-B radiation Light-stress	 Swelled thylakoids Lipid globule accumulation Increased starch grains Disintegrated mitochondrial cristae Cisternae of Golgi dictyosomes became loose and swollen 	TEM SEM	Tian and Yu (2009) Lamers et al. (2010)
	 Lipid globule accumulation and disappearance of most thylakoid membranes 		
Dodecane	Distorted membranes, decomposed completely	LM	Kleinegris et al. (2011)

Table 1.5: Studies available of the genus Nannochloropsis

Study	Microscope	Main findings	
Antia et al. (1975)	TEM	Detailed description of <i>N. oculata</i> cell structure suggesting	
		its similarity to Eustigmatophyceae rather than Chlorophyta.	
Maruyama et al.	LM and TEM	Identification of two marine <i>Chlorella</i> species as members	
(1986)		of Eustigmatophyceae, and evidence of ultrastructure and	
		biochemistry of <i>N. oculata</i> .	
Solomon et al.	TEM	In comparison with healthy cells, nutrient stressed cells of	
(1986)		N. oculata contained more cytoplasmic lipid droplets. In	
		nitrogen-deficient cells small lipid droplets (plastoglouli)	
		were numerous within the chloroplast and disrupted the	
		orderly arrangement of thylakoid membranes.	
Karlson et al.	TEM	Comparison of cell structures of the genus <i>N. granulate</i> with	
(1996)		N. oculata and N. salina	
		N. granulate did not have pyrenoid and lamella vesicles,	
		which are present in the other two species.	
Rodolfi et al.	TEM	Medium recycling changed the cell structure of	
(2003)		Nannochloropsis sp. by producing two types of storage	
		bodies, accumulation bodies and pigmented bodies, which	
		differed in their osmiophility.	
Murakami and	TEM	Description of unusual nuclear division of <i>N. oculata</i> .	
Hashimoto (2009)			
Khairy (2009)	TEM	Exposure of <i>N. oculata</i> to high concentration of copper	
		resulted in increased numbers of vacuoles, cell swelling,	
		clumping.	
Simionato et al.	TEM	Cell volume of the nitrogen-deficient cells were occupied by	
(2013)		oil bodies, intact chloroplast in N. gaditana in comparison	
		with control cells.	

Table 1.6: Available studies of the genus *Pseudostaurosira trainorii*

Study	Microscope	Main findings
Williams and Round (1987)	SEM	Systematic study based on valve morphology separated the following genera from the Genus Fragilaria
Morales (2001)	SEM	Morphological study based on SEM, that aiming to identify isolated strains from Lake Connecticut waters in the USA. All these isolates were suspected to belong to the genus Fragilaria. The author identified the Species <i>Pseudostaurosira trainorii</i> Morales, sp. Nov. with the following description: "Frustules rectangular in girdle view, usually forming chains with the aid of spines, valve elliptical to round, valves 1.88-8.57 µm long/ 1.72- 4.41 µm wide, striae typically 20-25 per 10 µm, spines interrupting the striae, spines with lateral projections". He mentioned that this species were previously reported under the names: <i>Fragilaria elliptica</i> by Archibald 1983; Poulin et al. 1984 and <i>Staurosira elliptica</i> by Snoeijs and Balashova 1998.
Morales (2005)	LM and SEM	Morphological study based on SEM, that aiming to identify isolated strains from rivers in USA. Identified and described the species <i>Pseudostaurosira subsalina</i>
Morales et al. (2010)	LM and SEM	Description of several diatom species, including <i>Pseudostaurosira trainorii</i> Morales as the following: "Valve elliptical to flattened spheroids, valves 4-5 μm long/ 3.5- 4.0 μm wide, striae typically 16.5-19.5 per 10 μm, spines are not always visible at the valve margin but can be clearly seen on the girdle view "
Medlin et al. (2008)	Molecular Phylogeny and SEM	The new araphid genera separated from <i>Fragilaria</i> fell into several clades and they deserved taxonomic ranking but not as individual genera. The Genus <i>Pseudostaurosira</i> was one of these genera that occured in both sub-clades (2a and 2b) of the send clade within the araphid diatoms. The four isolates of the genus <i>Pseudostaurosira</i> studied had variable valve structure.
Sato et al. (2011)	SEM and LM	First detailed study of the gametofensis of <i>Pseudostaurosira trainorii</i> proved the induction of gametogenesis by cell-free exudates. Proved the presence of sticky threads structure in male gametes that resembled flagella in containing microtubules. However, they lacked mastigonemes and could catch and draw female gametes.

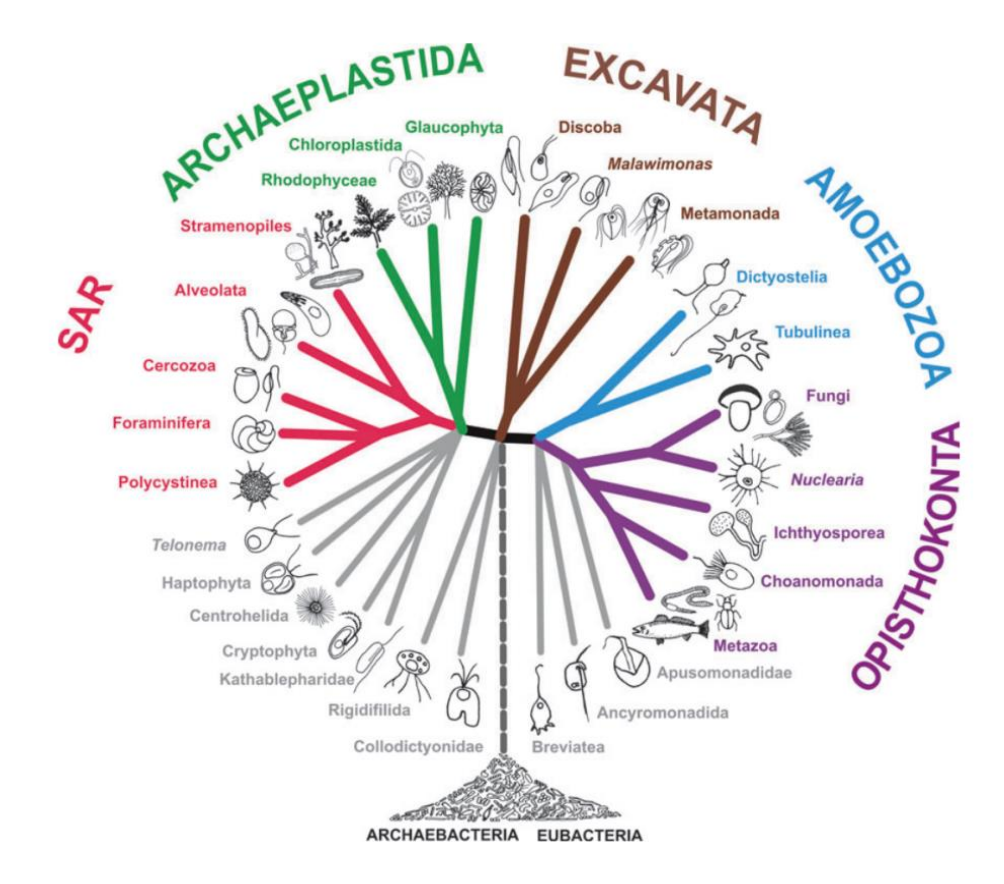


Figure 1.1: A phylogeny of the major groups of eukaryotic organisms (Source: Adl el al. 2012)

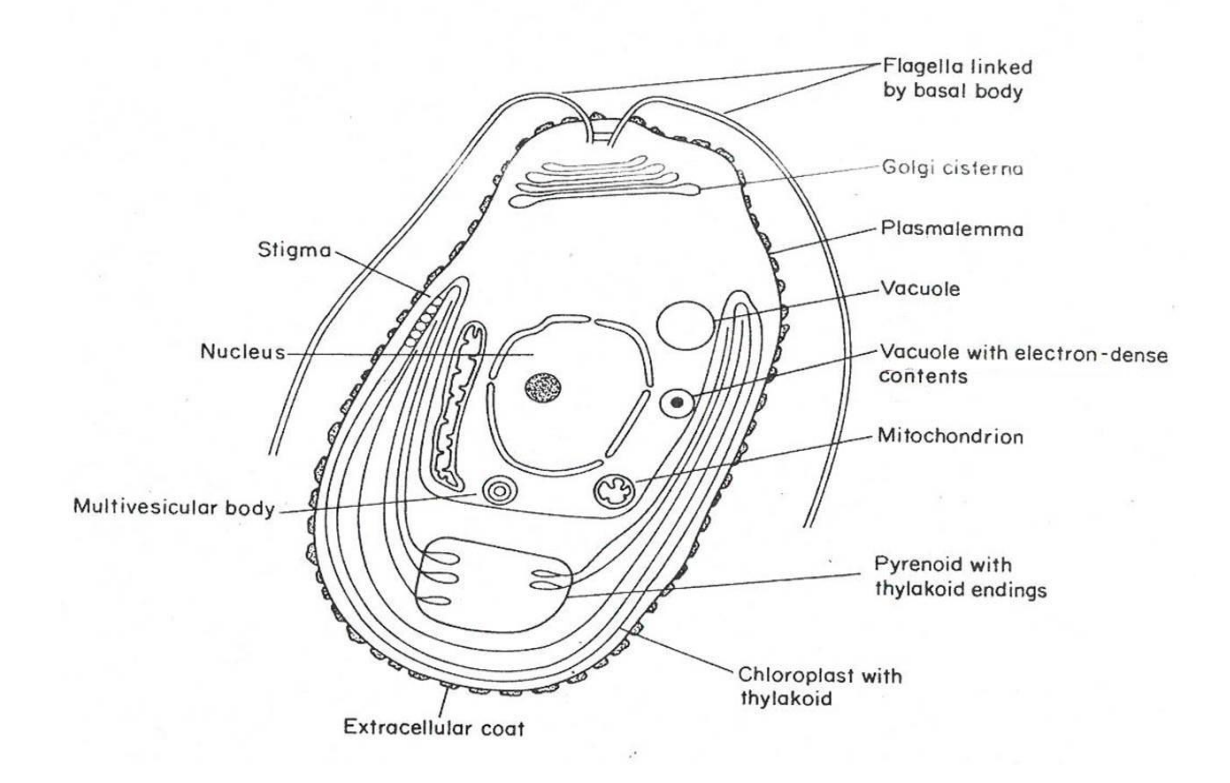


Figure 1.2: *Dunaliella salina* cell structure (Source: Ginzburg 1987)

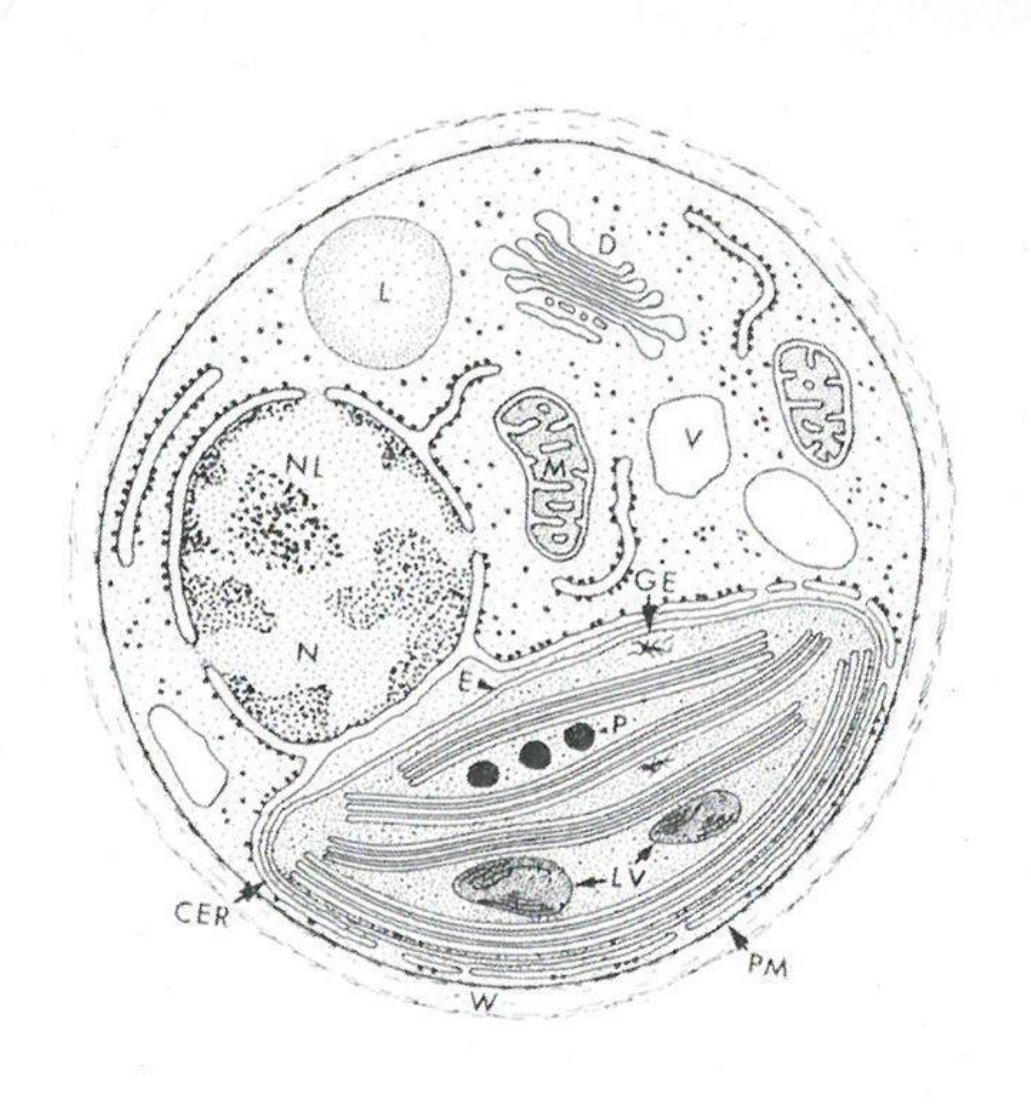


Figure 1.3: Nannochloropsis oculata cell structure

(Source: Antia et al. 1975)

CER: chloroplast endoplasmic reticulum; D: dictyosome; E: chloroplast envelope; GE: chloroplast genophore; L: lipid droplet; LV: lamellate vesicle; M: mitochondrion; N: nucleus; NL: nucleolus; P: plastoglobuli; PM: plasma membrane; V: vacuole; W: cell wall.

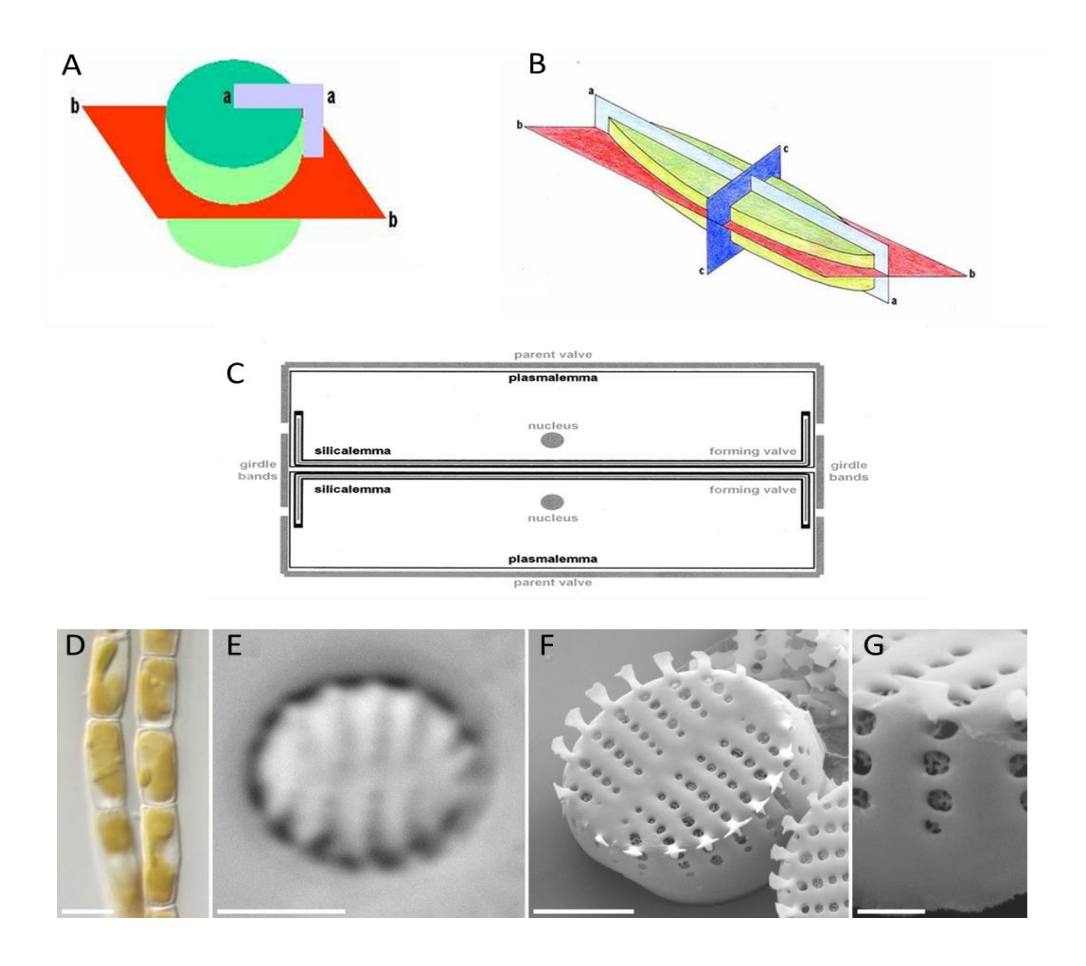


Figure 1.4: The diatom cell structure

A) Centric diatom. B) Pennate diatom. C) Diatom cell section from the side showing two newly formed cells within the mother cell. It consists of two parts called valves, which have different perforation patterns and ornamentations in different genera (Cox 2011). Of the two valves, one is slightly smaller and fits into the other in a way resembling the two parts of a Petri dish. The larger outer (upper) part is called the epitheca, whilst the smaller inner (lower) valve is called the hypotheca. At the periphery of each valve there are connecting bands (strips of silica) called the girdle bands. Therefore, the diatom cells have two different surface views. The valve view sees the diatom cell from the upper or lower surface (like looking at a Petri dish from the top or bottom surface), while the girdle view sees the diatom cell from the side (like viewing a Petri dish side-on). D) *P. trainorii* under the light microscope; scale bar 5 μ m. E) Inner valve showing the bilateral symmetry of the pennate diatom of the *P. trainorii* scale bar 2 μ m. F) Cell shell of *P. trainorii* with its circular appearance scale bar 2 μ m. G) Close view of the loculi. Scale bar 5 μ m.

Sources:

A-C: Kelly et al. (2005) D-G: Sato et al. (2011)

Chapter 2. Methods

2.1 Cultures

2.1.1 Maintenance cultures of Dunaliella salina and Nannochloropsis oculata

Dunaliella salina (CCAP19/30) and Nannochloropsis oculata (CCAP849/1) were purchased from the Culture Collection of Algae and Protozoa. These two strains were maintained as suspended cultures in 10 litre Nalgene polycarbonate carboys containing 9 litres of culture. The carboys were kept in an algal growth room within the School of Marine Science and Technology of Newcastle University. The growth room was illuminated by a combination of warm and cold fluorescent tubes giving a range luminance of 2200-2800 Lux with photoperiods of 16 hours light: 8 hours dark at 19 ± 2 °C. The carboys were aerated by connecting them to a pump, and the air coming from the pump was filtered through the use of a 0.45 μ m HePA-vent disposable in-line filter device, which is a glass microfibre filter with polypropylene housing (Whatman plc, Maidstone, Kent).

The medium used to culture both species was an F/2 medium (Guillard and Ryther 1962), which was prepared using natural seawater filtered to 1 μm, UV sterilised and autoclaved at 121°C for 25 min. The medium stock solutions consisted of NaNO₃ (0.075 g l⁻¹), NaH₂PO₄.2H₂O (0.00565 g l⁻¹), trace elements stock solution (1.0 ml l⁻¹), and vitamin mix stock solution (1.0 ml l⁻¹). The contents of the trace element solution are explained in Table 2.1. The medium was adjusted to pH 8.0 with 1 M NaOH or HCl. The medium was sterilized by autoclaving for 15 minutes at 121°C and used when cooled to room temperature.

These cultures were used to obtain samples for the evaluation of the fixation protocols and in the experiments described in Chapter 3 (sections 3.2.1 and 3.2.2).

Table 2.1: The chemical composition of F/2 medium

Component		Concentration
NaNO ₃		0.075 g l ⁻¹
NaH ₂ PO ₄ .2H ₂ O		0.00565 g l ⁻¹
Trace element stock solution (1.0 ml l ⁻¹)	Na ₂ EDTA	4.16 g l ⁻¹
	FeCl ₃ .6H ₂ O	3.15 g l ⁻¹
	CuSO ₄ .5H ₂ O	0.01 g l ⁻¹
	ZnSO ₄ .7HO	0.022 g l ⁻¹
	CoCl ₂ .6H ₂ O	0.01 g l ⁻¹
	MnCl ₂ .4H ₂ O	0.18 g l ⁻¹
	Na ₂ MoO ₄ .2H ₂ O	0.006 g l ⁻¹
Vitamin mix stock solution (1.0 ml l ⁻¹)	Cyanocobalamin (Vitamin B12)	0.0005 g l ⁻¹
	Thiamine HCl (Vitamin B1)	0.1 g l ⁻¹
	Biotin	0.0005 g l ⁻¹

2.1.2 Pseudostaurosira trainorii: cultures and inducing gamete formation and mating

Cultures of *Pseudostaurosira trainorii* were provided by Shinya Sato from the Royal Botanic Garden, Edinburgh. They were derived from *P. trainorii* cells that were collected from the bottom sands at Obuchi-numa Lake, Aomori Pref., Japan, on 25 July 2010. The methods for inducing gametogenesis were as described by Sato et al. (2011) and are as follows. Single cells were isolated from the original field sample to obtain clonal cultures. Eighteen clones were successfully established, of which six were male and twelve female. Clone numbers 3 (male) and 7 (female) were used for all ultrastructural fixations. Cultures were maintained in a 1:1 mixture of WC medium (Table 2.2) and Roshchin medium (Table 2.3) at 15 °C under cool-white fluorescent light on a 14 hours light: 10 hours dark photoperiod at a photon flux density of 5-20 mmol photons m⁻² s⁻¹.

Gamete induction was achieved by the release of the pheromone, as described by Sato et al. (2011). A Petri dish with 3% solid agar was used and two holes were prepared one centimetre apart from each other. Male and female compatible clones were placed into the separate holes. This allowed the pheromone to diffuse into the agar and induce the counterpart to produce gametes without mixing the compatible clones. This facilitated the ultrastructural study of male and female clones gametogenesis because it enabled populations of solely male or female gametes (together with their parent clone cells) to be collected for fixation. Samples were fixed after 24 hours induction of gametogenesis in Petri dishes (Figure 2.1). The observations of fertilization and zygote (auxospore) development were made from two compatible clones that were mixed in a liquid medium prepared as above and fixed 20 minutes, 3 hours and 48 hours after mixing the female and male compatible clones.

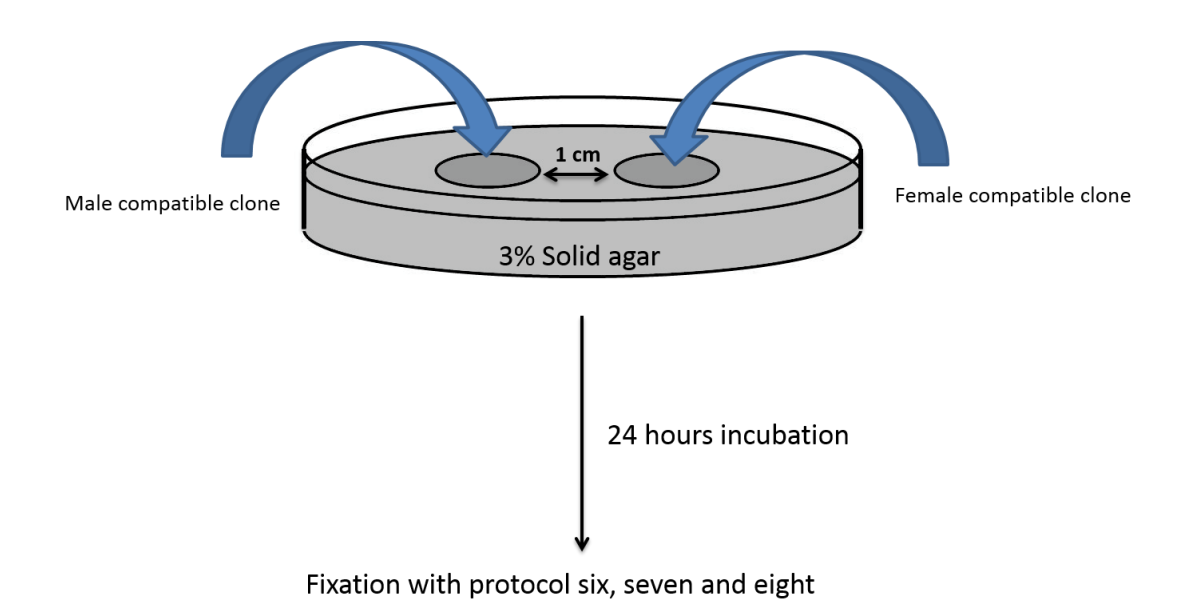


Figure 2.1: Gametogenesis induction in *Pseudostaurosira trainorii*

Table 2.2: Chemical components of the WC medium

Comp	ponent	Amount	Stock solution	Final concentration
Nal	NO ₃	1 ml 1 ⁻¹	85.1 g l ⁻¹	1 mM
CaCl ₂	•2H ₂ O	1 ml 1 ⁻¹	36.76 g l ⁻¹	0.25 mM
MgSO	4•7H ₂ O	1 ml l ⁻¹	36.97 g l ⁻¹	0.15 mM
NaH	ICO ₃	1 ml l ⁻¹	12.6 g l ⁻¹	0.15 mM
Na ₂ SiO	9H ₂ O	1 ml l ⁻¹	28.42 g l ⁻¹	0.1 mM
K ₂ H	IPO ₄	1 ml l ⁻¹	8.71 g l ⁻¹	0.05 mM
H ₃ I	$3O_3$	1 ml l ⁻¹	24 g l ⁻¹	0.39 mM
	Na ₂ EDTA·2H ₂ O	4.36 g l ⁻¹		11.7 μM
	FeCl ₃ •6H ₂ O	3.15 g l ⁻¹		11.7 μM
	CuSO ₄ •5H ₂ O	1 ml l ⁻¹	2.5 g l ⁻¹	10 nM
WC trace elements	ZnSO ₄ •7H ₂ O	1 ml l ⁻¹	22 g l ⁻¹	76.5 nM
solution (1 ml ⁻¹)	CoCl ₂ •6H ₂ O	1 ml l ⁻¹	10 g l ⁻¹	42 nM
	MnCl ₂ •4H ₂ O	1 ml 1 ⁻¹	180 g l ⁻¹	910 nM
	Na ₂ MoO ₄ •2H ₂ O	1 ml l ⁻¹	6.3 g l ⁻¹	26 nM
	Na ₃ VO ₄	1 ml l ⁻¹	18 g l ⁻¹	98 nM
	HEPES buffer pH 7.8 (Sigma H-3375)	2.4 g/200 ml dH ₂ O		
Vitamin B ₁₂ (1 ml ⁻¹)	Vitamin B ₁₂ (cyanocobalamin, Sigma V-6629)	0.027 g/200 ml dH ₂ O		
Thiamine vitamin	HEPES buffer pH 7.8 (Sigma H-3375)	2.4 g/200 ml dH ₂ O		
solution (1 ml ⁻¹)	Thiamine (Sigma T-1270)	0.067 g/200 ml dH ₂ O		
Biotin vitamin	HEPES buffer pH 7.8 (Sigma H-3375)	2.4 g/200 ml dH ₂ O		
solution (1 ml ⁻¹)	Biotin (Sigma B-4639)	0.005 g/200 ml dH ₂ O		

Table 2.3: Chemical components of Roshchin medium

Component	Concentration
Seawater	16%o
KNO ₃	202 mg l ⁻¹
Na ₂ HPO ₄ .12H ₂ O	17.9 mg l ⁻¹
FeSO ₄ .7H ₂ O	0.29 mg l ⁻¹
MnCl ₂ .4H ₂ O	0.19 mg l ⁻¹
CoCl ₂ .6H ₂ O	0.24 mg l ⁻¹
Na ₂ EDTA	3 mg l ⁻¹
Na ₂ S ₂ O ₃ .5H ₂ O	1.2 mg l ⁻¹
Na ₂ SiO ₃ .9H ₂ O	10 mg l ⁻¹
Vitamin B ₁₂	2 μg l ⁻¹

2.2 Light microscopy

The three species *D. salina*, *N. oculata*, and *P. trainorii* were examined by light microscopy under a Leica DMRB microscope (Leica Microsystems, Wetzlar, Germany), fitted with differential interference contrast (DIC) optics. A drop of the culture was placed on a glass slide and covered by a coverslip. Images of cells were recorded using an Olympus 5050 (Olympus Corp, Tokyo, Japan) 5 Mp digital camera.

2.3 Transmission electron microscopy fixation protocols

Fixation was optimized by undertaking initial trials using a range of different fixation protocols that were evaluated based on the overall quality of organelle preservation, reduced shrinkage and best overall visual appearance. The most appropriate protocol for each of the three algal species was then adopted for the main experimental investigations.

2.3.1 Optimizing the fixation of Dunaliella salina

Samples of cultures of *D. salina*, strain (CCAP19/30) were subjected to three different chemical fixation protocols to choose the best fixation protocol. The protocols were as follows:

2.3.1.1 Protocol one: 2% glutaraldehyde 1% osmium in 0.1 M cacodylate buffer in seawater (2% GaOs, SW)

D. salina cells were concentrated by centrifugation. Cells were transferred into 1.5 ml micro-centrifuge tubes (6 tubes) and centrifuged for 15 minutes at room temperature at 8000 rpm in a Hettich Microliter bench top centrifuge. The excess media were discarded and cells were embedded in agarose. These were fixed with 2% glutaraldehyde in a 0.1M cacodylate buffer (pH 7) prepared in sterile filtered seawater for 3 hours at room temperature (ca 20 °C) in 5 ml snap-capped glass vials under a fume hood. The fixed cells were rinsed three times (15 minutes each) with a fresh cacodylate buffer and then post-fixed in 1% osmium tetroxide for 1 hour at room temperature, again under a fume hood. The rinsing procedure with cacodylate buffer was repeated and then the specimens were dehydrated in a graded series of acetone solutions (25%, 50%, 75% and 100%), allowing 30 minutes in each dilution. Then the samples were infiltrated in a TAAB Premix epoxy resin kit (TAAB Laboratories Equipment Ltd, Aldermaston, Berks), in a series of graded mixes (25%, 50%, 75%, 100% resin: acetone) and left in

100% resin overnight in a refrigerator. The infiltrated agarose embedded blocks were then transferred to embedding capsules and polymerized overnight in a 60 °C oven.

Blocks were selected and trimmed into pyramids by hand with a razor blade. The trimmed blocks were sectioned to a thickness of 80 nm using a Reichert Ultracut E ultramicrotome (Leica Microsystems, Wetzlar, Germany) with a DiATOME (Diatome AG, Biel, Switzerland) diamond knife. Ultrathin sections were picked up on 100-mesh copper grids, stained with 2% aqueous uranyl acetate for 15 minutes, washed in three separate distilled water rinses, dried with filter paper and post-stained in lead citrate for 10 minutes at 20 °C in a Leica AC20 staining machine (Leica Microsystems, Wetzlar, Germany) prior to examination in a Philips CM100 TEM (Philips-FEI, Eindhoven, Netherlands). Images were recorded using an AMT CCD camera (Advanced Microscopy Techniques, Woburn, MA, USA). The optronics 1824 x 1824 pixel with AMT40 version 5.42 image capture engine was supplied by Deben, UK.

2.3.1.2 Protocol two: 2% glutaraldehyde 1% osmium in 0.1 M cacodylate buffer in buffered sterile F/2 medium (2% Ga/Os F/2)

This fixation protocol was the same as that described in Section 2.3.1.1 above, except that the cells were buffered in an F/2 medium (Table 2.1) rather than seawater (2% Ga/Os f/2).

2.3.1.3 Protocol three: 1% glutaraldehyde 1% osmium in 0.1 M cacodylate buffer in buffered sterile F/2 medium (1% Ga/Os F/2)

This fixation was the same as that described in Section 2.3.1.1 above, except that the primary fixation was 1% glutaraldehyde (1% GaOs F/2).

2.3.2 Optimizing fixation protocols for Nannochloropsis oculata

Samples of cultures of *N. oculata* (CCAP849/1) were fixed using the three different protocols described above, together with the following additional two protocols, as described by Karlson et al. (1996).

2.3.2.1 Protocol four: combined glutaraldehyde-osmium with sucrose (Ga-Os/Os suc)

Cells of *N. oculata* were fixed using a combined osmium-glutaraldehyde fixation protocol as developed by Karlson et al. (1996) for fixing *Nannochloropsis*. Cells were

concentrated by filtration using $0.22~\mu m$ Millipore membrane filters, embedded with agarose and mixed with a mixture of 5 ml osmium tetroxide (1% in 0.1 M cacodylate buffer, pH 7), 2 ml sucrose (2 mol 1^{-1} in filtered seawater), and 0.8 ml 25% glutaraldehyde. They were post-fixed with 1% osmium tetroxide in a cacodylate buffer for 1 hour. The samples were dehydrated as described above (section 2.3.1.1) and embedded in a TAAB low viscosity resin kit (TLV, TAAB Laboratories Equipment Ltd, Aldermaston, Berks).

2.3.2.2 Protocol five: combined glutaraldehyde-osmium (Ga-Os/Os)

Cells of *N. oculata* were fixed using a combined osmium-glutaraldehyde modified fixation protocol from Karlson et al. (1996) as described above but without the addition of sucrose to the fixative medium.

31

Table 2.4: Summary of preparative procedure used

Procedure Number	Primary fixation	Duration	Secondary fixation	Duration	Temperature	Dehydration	Embedding	Organism
Protocol one (2% GaOs, SW)	2% glutaraldehyde in 0.1 M cacodylate buffer (pH 7) prepared in sterile filtered seawater	3 hours	1% osmium tetroxide	1 hour	Room temperature	25%, 50%, 75% and 100% Acetone	TAAB epoxy resin, impregnated with 25%, 50%, 75%, 100% resin in acetone	D. salina, N. oculata
Protocol two (2% Ga/Os F/2)	2% glutaraldehyde in 0.1 M cacodylate buffer (pH 7) prepared in F/2 medium	3 hours	1% osmium tetroxide	1 hour	Room temperature	25%, 50%, 75% and 100% Acetone	TAAB epoxy resin, impregnated with 25%, 50%, 75%, 100% resin in acetone	D. salina, N. oculata
Protocol three (1% Ga/Os F/2)	1% glutaraldehyde in 0.5 M cacodylate buffer (pH 7) prepared in F/2 medium	3 hours	1% osmium tetroxide	1 hour	Room temperature	25%, 50%, 75% and 100% Acetone	TAAB epoxy resin, impregnated with 25%, 50%, 75%, 100% resin in acetone	D. salina, N. oculata
Protocol four (2%Ga-Os/Os suc)	osmium-glutaraldehyde: Mixture of 5 ml osmium tetroxide (1% in 0.1 M cacodylate buffer, pH 7), 2 ml sucrose (2 mol 1-1 in filtered sea water), and 0.8 ml glutaraldehyde	3 hours	1% osmium tetroxide	1 hour	Room temperature	25%, 50%, 75% and 100% Acetone	TAAB epoxy resin, impregnated with 25%, 50%, 75%, 100% resin in acetone	N. oculata
Protocol Five (2%Ga-Os/Os)	osmium-glutaraldehyde: Mixture of 5 ml osmium tetroxide (1% in 0.1 M cacodylate buffer, pH 7), and 0.8 ml glutaraldehyde	3 hours	1% osmium tetroxide	1 hour	Room temperature	25%, 50%, 75% and 100% Acetone	TAAB epoxy resin, impregnated with 25%, 50%, 75%, 100% resin in acetone	N. oculata

2.3.3 Optimizing the fixation of *Pseudostaurosira trainorii*

Four samples were fixed representing different stages of the life cycle (Table 2.5). These were: 24 hours induced male gamete; 24 hours induced female gamete; 3 hours mated male and female gametes; and 48 hours mated male and female gametes. Three fixation protocols were used to determine the optimum fixation conditions for *P. trainorii* cells (Table 2.5).

2.3.3.1 Protocol six: 1.25% glutaraldehyde 1% osmium in 0.1 M cacodylate buffer in seawater (1.25% GaOs, 50% SW)

P. trainorii cells were fixed with 1.25% glutaraldehyde in a 0.05 M cacodylate buffer in 50% sterile seawater (pH 7) at room temperature for 3 hours and post fixed with 1% osmium tetroxide for 1 hour at room temperature. The samples were dehydrated and stained as described in Protocol One of *D. salina* (section 2.3.1.1) and embedded with TAAB low viscosity resin.

2.3.3.2 Protocol seven: 2.5% glutaraldehyde 1% osmium in 0.1 M cacodylate buffer in seawater (2% GaOs, SW)

P. trainorii cells were fixed with 2.5% glutaraldehyde in a 0.1 M cacodylate buffer in 50% sterile filtered seawater (pH 7) at room temperature for 3 hours and post fixed with 1% osmium tetroxide in a 0.1 M cacodylate buffer for 1 hour at room temperature. Subsequently, they were centrifuged, dehydrated and stained as described for *D. salina* in section 2.3.1.1 and embedded with TAAB low viscosity resin.

2.3.3.3 Protocol eight: combined 2% glutaraldehyde-0.5% osmium-1% osmium in 0.1 M cacodylate buffer in buffered sterile SW with sucrose (2% Ga-Os/Os 50% SW)

Cells of *P. trainorii* were fixed using a combined osmium-glutaraldehyde fixation protocol as described by Karlson et al. (1996). Seven ml of each sample were mixed with a mixture of 5 ml osmium tetroxide (2%), 6 ml 0.2 M cacodylate buffer, 2 ml sucrose (2 mol 1⁻¹ in filtered seawater), and 1 ml 25% glutaraldehyde for 30 minutes, centrifuged at 1500 rpm and washed 3 times in a 0.1 M sodium cacodylate buffer in 50% sea water. They were post-fixed with 1% osmium tetroxide in a 50% cacodylate buffer for 1 hour and washed 3 times in 0.1 M sodium cacodylate buffer in 50%

seawater. The samples were dehydrated and stained as described for *D. salina* in section 2.3.1.1 and embedded with TAAB low viscosity resin.

Table 2.5: Summary of preparative procedure used for *Pseudostaurosira trainorii*

Fixation protocol	Sample	Figure
	24 hours induced male gamete	Figure 2.11A, B
	24 hours induced female gamete	Figure 2.11C, D
Protocol six (1.25 % GaOs, 50% SW)	3 hours mated male and female gametes (zygote)	Figure 2.11E, F
	48 hours mated male and female gametes (zygote)	Figure 2.11G
	24 hours induced male gamete	Figure 2.10A-C
	24 hours induced female gamete	Figure 2.10D, E
Protocol seven (2% GaOs, SW)	3 hours mated male and female gametes (zygote)	Figure 2.10F
	48 hours mated male and female gametes (zygote)	Figure 2.10G, H
Protocol eight (2% Ga-Os/Os 50% SW)	24 hours induced male gamete	Figure 2.9

2.4 Preparation for scanning electron microscopy

The samples of *Dunaliella* and *Nanochloropsis* were prepared using 2% glutaraldehyde in a 0.1 M Sorenson's phosphate buffer overnight. Circular coverslips (13 mm diameter) were washed with liquid detergent to remove grease and rinsed lightly. The cleaned coverslips were then coated in the adhesive agent poly-1-lysine (0.025%) and left to dry for 30 minutes. One 40 mm Petri dish was used for each sample, filled with Sorenson's phosphate buffer. The poly-1-lysine-coated coverslips were placed under the buffer and fixed suspensions pipetted onto the poly-1-lysine-covered coverslips and allowed to settle for 10 minutes, to enable the cells to attach firmly to the slide surface. Samples were dehydrated in stages of ethanol, starting with 25%, 50%, 70% for 10 minutes each, and then 100% twice for 15 minutes each. They were then placed in a coverslip holder and placed in a Baltec critical point dryer using carbon dioxide. Samples were viewed with a Cambridge S240 scanning electron microscope (Cambridge Instrument Company, Cambridge, UK) which has an analogue-digital converter. Images were captured using Orion version 6 software.

2.5 Evaluation of fixation protocols

The aim of fixation is to stabilize cellular organization so that the ultrastructure of a cell is not changed by the following treatments of the sample preparation such as dehydration, embedding and exposure to an electron beam (Glauert and Lewis 1998). There is no one perfect fixation for all types of cells. Therefore, a given fixation protocol was selected based upon the overall appearance of cell structure and the absence of obvious artefacts such as shrinkage, excessive membrane or breakage. There are some objective criteria for assessing fixation quality (Brand and Arnold 1986; Hayat 1989; McDonald and Morphew 1993; Glauert and Lewis 1998; Cribb et al. 2004). The absence of any obvious preservation artefacts was the main criterion by which the preservation protocols of the present writer were evaluated. Examples of such artefacts include membrane breakage or proliferation, the distortion (obvious swelling or shrinkage) and disorganization of organelles, and the presence of empty spaces in the cytoplasm or shrinkage of plasma membrane away from the cell wall in the case of plants (Glauert and Lewis 1998). Other criteria for assessing well-preserved cells involve the evaluation of the preservation of individual cell organelles. For example, organelle membranes should be intact and continuous. The nucleus of a well-preserved cell should have an intact structure with well-preserved contents and nuclear envelope.

The nucleoplasm should be of uniform density and contain visible heterochromatin and nucleolus. The cytoplasmic matrix must be finely granulated and contain no empty spaces. The mitochondria profiles must show clear and intact outer double membrane and cristae with a denser matrix than the cytoplasm. Finally, vacuoles must be bounded by an unbroken single membrane.

2.5.1 Optimizing fixation protocols for *Dunaliella salina*

Selecting the fixation protocol for *Dunaliella salina* was based on the comparison of protocols listed in the literature with the standard fixation protocol recommended by the Electron Microscopy Unit at Newcastle University (Appendix 1). Maeda and Thompson (1986), Einspahr et al. (1988) and Berube et al. (1999) fixed Dunaliella with 2% glutraldehyde, which matches the standard procedure of the Electron Microscopy Unit at Newcastle University. Oliveira and Huynh (1989) and Tian and Yu (2009) fixed Dunaliella with 2.5% glutaraldehyde. Since Dunaliella salina lacks a cell wall this would facilitate the diffusion of the fixative and the present writer decided to compare two different glutaral dehyde concentrations (1% and 2%) to determine the effect of different osmolarities on the fixation in sea water and F/2 medium used to prepare the stock solution of the glutaraldehyde. This was compared with protocols described in the literature in which only buffered solutions were used. Because fixative penetration into fixed cells depends primarily on simple diffusion in aqueous solution, this would be affected by the cell's internal osmolality (Glauert and Lewis 1998). The second factor that affects diffusion is the different constituents of the fixative, which have different diffusion coefficients and thus diffuse at different rates (Glauert and Lewis 1998). It was difficult to predict the result of fixation as the F/2 medium used had not been previously reported in the literature. The third factor which affects the diffusion of fixative into specimens is that the fixed parts of the cell may change the diffusion coefficients of the different fixative constituents, and this may result in poor penetration of the fixative to the deeper parts of the cell (Glauert and Lewis 1998).

The different fixation protocols here used all resulted in slightly different appearances of the cells (Table 2.6). The general appearance of fixed cells and an overall evaluation of the main organelle appearance and preservation are presented in Figures 2.2-2.4 and Table 2.6. The results of fixation with protocol one (2% GaOs, SW) were the most satisfactory, since no obvious fixation artefacts were detected. The whole cell and its different subcellular components were intact and easily differentiated from one another

and met the criteria of well-fixed cell components as defined by Hayat (1989). The description of each organelle and the assessment of its fixation quality are presented in Table 2.6 and Figure 2.2. In contrast, protocol two (2% Ga/Os, F/2) resulted in many fixation defects and artefacts, and therefore it was not considered to be satisfactory. The fixation quality for each organelle using protocol two is presented in Table 2.6 and Figures 2.3. The organelles that appeared adversely affected were mitochondria and chloroplast membranes and their constituents. The mitochondrial membranes were not clearly visible, the chloroplast thylakoid membranes were merged, and starch and pyrenoid contents showed signs of extraction, which indicated poor penetration of the fixatives. These observations indicated that the constituents of the F/2 medium reacted differently with the fixative than with seawater. Nor did fixation with protocol three (1% Ga/Os F/2) meet the criteria for well-preserved cells. The cytoplasmic matrix was densely granulated and the protoplast showed signs of shrinkage, which, again, is an indicator of poor penetration of the fixative into the cell, or an osmotic imbalance between the cytoplasm and fixative solution. As a result cells lost their water and shrank. Since protocol three had only 1% glutaraldehyde in comparison to protocol two (2%), it is likely that the cells were in hypertonic solution, resulting in the observed shrinkage.

It is clear that the higher glutaraldehyde fixative concentration (2% in protocols one and two) resulted in better overall cytoplasmic preservation and less membrane breakage than did the lower concentration (protocol three). Although most organelles appeared quite similar in appearance, the chloroplast thylakoid membranes appeared less regular and well-organised in the cells fixed in an F/2 medium, compared with seawater (cf Figures 2.2 and 2.3). In general, protocol one (2% Ga/Os, SW) appeared to give the best overall quality of fixation, with the half-strength fixative solution (1% Ga/Os) the poorest. Consequently, the former was the protocol selected for all forthcoming experiments on this organism.

Table 2.6: Assessment of fixation techniques applied to *Dunaliella salina*

Organelles Protocol one (2% GaOs, SW)			Protocol two (2% Ga/Os, F/2)		Protocol three (1% Ga/Os, F/2)	
	Features	Figure	Features	Figure	Features	Figure
Cytoplasm	Finely granulated showing no empty space	2.2A, B, D	Densely granulated, showing empty spaces	2.3A, D	Densely granulated showing no empty spaces	2.4A-D
Mitochondria	Outer double membrane and cristae and intact dense matrix in comparison with cytoplasm, not shrunk or swollen	2.2C	Not the same in all cells: outer double membrane was intact; cristae were lost in some cells. However, some cells had no intact mitochondrial shape. Matrix was the same density as cytoplasm	2.3B- D	Shrinkage in some cell outer double membranes and cristae were lost in dense matrix in comparison with cytoplasm	2.4A, D
Chloroplast	Outer double membrane intact Thylakoid membranes, starch, and pyrenoids were intact and showed no sign of extraction	2.2A, C, D	Outer double membrane lost its continuity, thylakoid membrane clear, condensed and merged in different parts. Starch and pyrenoid showed sign of extraction	2.3C	Outer double membrane lost its continuity, thylakoid membrane clear, condensed and merged in different parts. Starch and pyrenoid showed sign of extraction	2.4A, B, D
Nuclear content	Uniformly dense, visible chromatin and nucleolus	2.21A, B	Density varied, visible chromatin and nucleolus	2.3A	Uniformly dense	2.4A, B
Nuclear envelope	Double membrane intact and essentially parallel to each other and showed pores	2.2B	Difficult to identify membrane	2.3A, D	Double membrane intact and essentially parallel to each other but loss of continuity	2.4A
Cell membrane	Intact	2.2B, D	Loss of continuity	2.3A, D	Loss of continuity	2.4A, B
Vacuoles	Bound by unbroken single membrane	2.2A, D	Bound by unbroken single membrane	2.3A	Loss of membrane continuity	2.4D

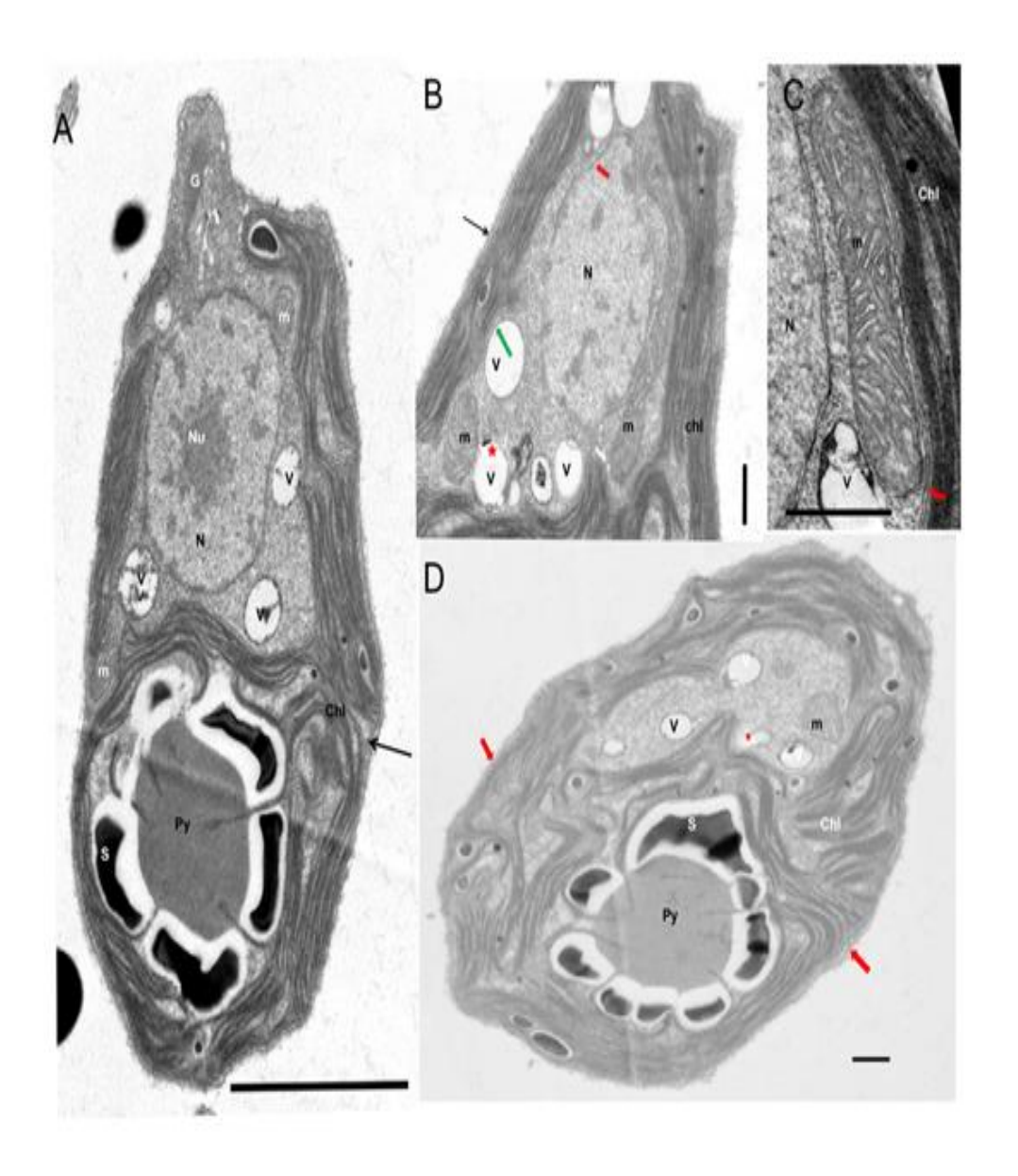


Figure 2.2: Dunaliella salina fixation protocol one

A) Longitudinal section. The cytoplasm matrix is finely granulated showing no empty spaces and intact membranes. The chloroplast's outer double membrane is unbroken (black arrow). Thylakoid membranes, starch, and pyrenoids are intact and show no sign of matrix extraction. Scale bar 2 μm. B) High power magnification of nucleus showing intact nucleus structure with uniform density and visible heterochromatin and nucleolus. The intact nuclear envelope has well-preserved double membranes which are parallel to each other and show the nuclear pores (red arrow). Scale bar 0.5 μm. C) Higher magnification of mitochondria. The mitochondria are undamaged (not shrunken or swollen, with a well-preserved matrix). The outer double membrane of the mitochondrion and cristae are all intact and clearly seen. The dense matrix of well-preserved mitochondria appears denser than that of the background cytoplasm. The chloroplast has intact double outer membrane (red arrow). Scale bar 0.5 μm. D) transverse section. Cell membrane is intact and visible (red arrows) Scale bar 0.5 μm. Chl: chloroplast; M: mitochondria; N: nucleus; Nu: nucleolus; Py: pyrenoid; S: starch; V: vacuoles.

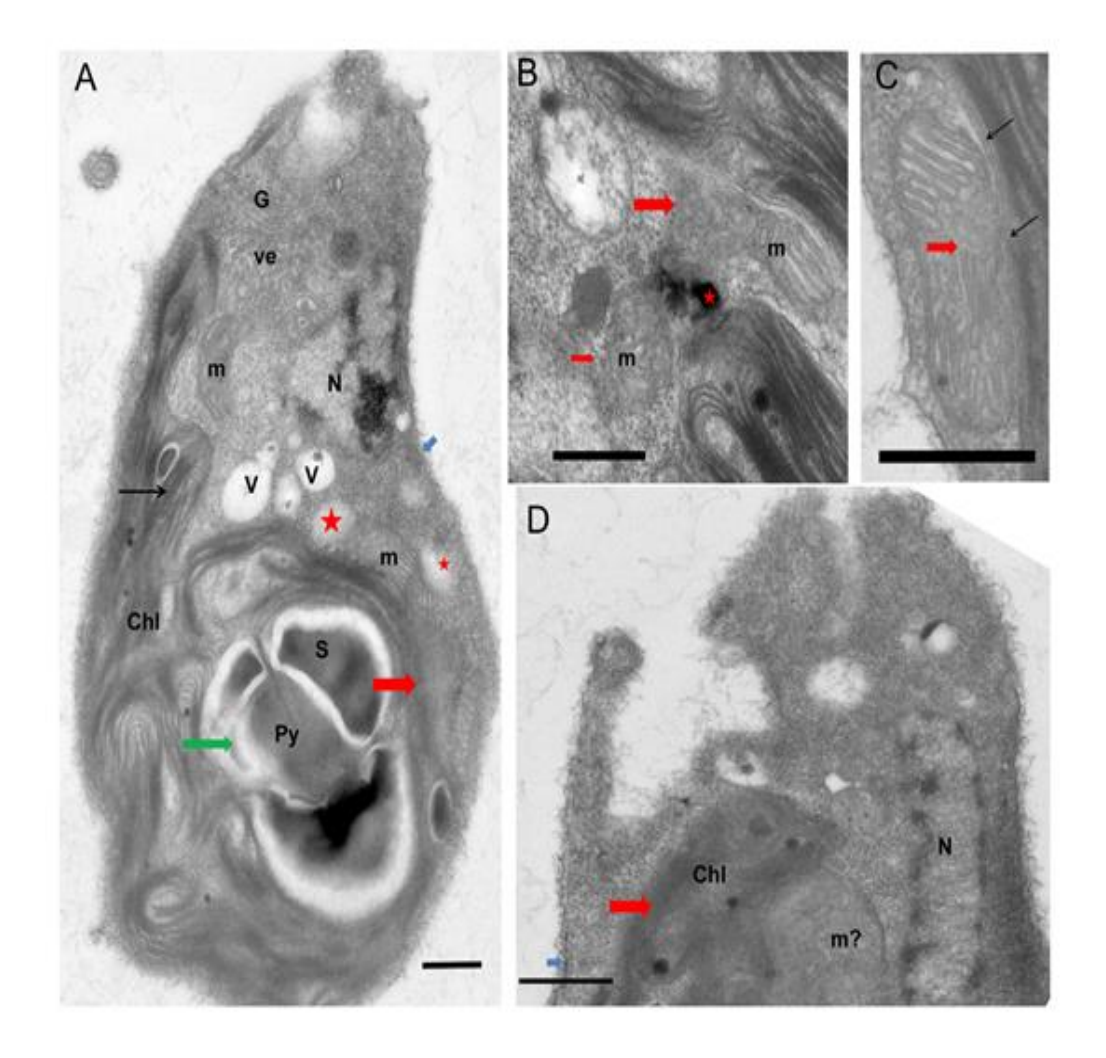


Figure 2.3: *Dunaliella salina* fixation protocol two

A) Longitudinal section shows the densely granulated cytoplasm matrix with empty spaces (red stars). The thylakoid membranes can be either clearly resolved or intact (black arrow) or condensed and merged in different parts (red arrow), and starch and pyrenoid show sign of extraction (green arrow). The nuclear content has a variable density and visible chromatin and nucleolus. Vacuoles are bound by unbroken single membrane. Scale bar 0.5 µm. B) High power magnification of cytoplasm with mitochondrial and vacuoles shows the lost cristae (red arrows). Mitochondrial matrix has the same density as background cytoplasm. Scale bar 0.5 μm. C) Higher magnification of mitochondrion showing intact double outer membrane and many cristae (red arrow). Chloroplast's double outer membrane is swollen in places (black arrows). Scale bar 0.5 μm. D) High power magnification of nucleus and surrounded cytoplasm. Mitochondria are difficult to discern from background matrix. The nuclear envelope is also hard to identify. Cell membrane has lost its continuity (blue arrow). Scale bar 0.5 µm. Chl: chloroplast; G: Golgi; L: lipid bodies; M: mitochondria; m?: mitochondria difficult to discern; N: nucleus; Nu: nucleolus; Py: pyrenoid; S: starch; V: vacuoles.

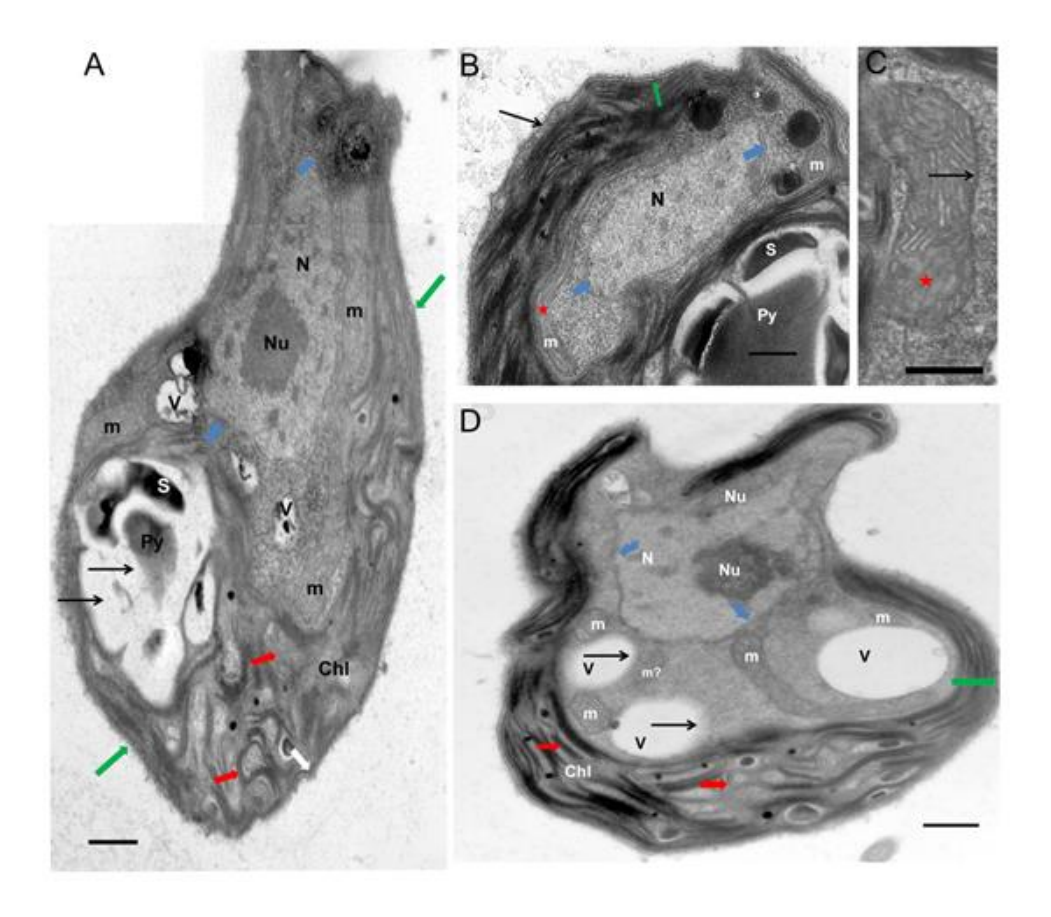


Figure 2.4: Dunaliella salina fixation protocol three

A) Longitudinal section where cytoplasm matrix is densely granulated showing no empty spaces. Chloroplast outer double membrane lost its continuity (white arrow). Starch and pyrenoid show signs of extraction (black arrows). Nuclear content is uniformly dense with clear nucleolus and chromatin. Cell membrane shows some breakage (green arrows). Scale bar 0.5 µm. B) High power magnification of vacuoles and cytoplasm. Chloroplast's outer double membrane has lost its continuity (green arrows), cell membrane has loss its continuity (black arrow). Scale bar 0.5 μm. C) Higher magnification of intact mitochondria with loss of some cristae membranes and outer double membranes (red star). The mitochondrial matrix is dense in comparison with cytoplasm. Scale bar 0.5 µm. D) High power magnification of nucleus and surrounding cytoplasm. Chloroplast outer double membrane has lost its continuity (green arrows). Mitochondria is either shrunken (red star) or intact with loss of some cristae membranes and outer double membranes. The double membranes of the nuclear envelope are intact and parallel to each other but show some breakage (blue arrows). Vacuoles show loss of membrane continuity (black arrows). Scale bar 0.5 µm. Chl: chloroplast; L: lipid bodies; M: mitochondria; m?: mitochondria difficult to discern; N: nucleus; Nu: nucleolus; Py: pyrenoid; S: starch; V: vacuoles.

2.5.2 Optimizing fixation protocols for Nannochloropsis oculata

The fixation of *Nannochloropsis oculata* cells was more difficult and challenging than that for *Dunaliella*. Previous studies used a number of different protocols as follows. Two studies (Maruyama et al. 1986 and Mohammady et al. 2005) used the standard fixation protocol used her (Appendix 1), which is 2% glutaraldehyde as the primary fixative and 1% osmium tetroxide as secondary fixative, and the quality of their fixation appeared good. Using these studies as a basis, the present writer decided to use 2% glutaraldehyde (protocols one and two) compared with 1% glutaraldehyde (protocol three) as well as both in seawater (protocol one) and Guillard's F/2 medium (protocols two and three). The differences in cell constituent structures with the three different fixation protocols are summarised in Table 2.7. The appearance of *N. oculata* cells using the three different fixation protocols that were tested are summarised in Figures 2.4 (protocol one: 2% Ga/Os, SW), 2.5 (protocol two: 2% Ga/Os F/2) and 2.6 (protocol three: 1% Ga/Os F/2).

Unfortunately, with the particular strain of *N. oculata* and growth conditions, none of the three protocols gave very satisfactory preservation of the cells. *N. oculata* cells after all sequential glutaraldehyde, osmium fixations (Protocols one-three) generally appeared very dense and often irregular in shape, suggesting shrinkage and deformation during subsequent infiltration with resin. The thylakoid membranes were often difficult to discriminate from the matrix (Figures 2.4A, D; 2.5A, B; 2.6A) and the mitochondria in some cells were swollen with an electron transparent matrix and disrupted cristae indicative of poor fixation (Figures 2.4B; 2.5D).

The fixation by using protocol one resulted in an unsatisfactory fixation, with the cytoplasm appearing densely granulated and showing signs of the loss of cell components and empty spaces (Figure 2.5A-D). Mitochondrial profiles could hardly be seen in micrographs, and it was suspected that some of the cytoplasmic spaces represented the location of poorly preserved mitochondria (Figure 2.5 A-D). However, it was hard to confirm this due to the massive distortion in organelle structure, with no clear mitochondrial shape, membranes and cristae. Nor were the results of fixation in protocol three satisfactory. The cytoplasm was densely granulated, showing signs of extraction and empty spaces (Figure 2.6A-D). Cell organelles appeared distorted and often could not be easily differentiated from the dense cytoplasmic matrix.

Therefore, as a result of the poor fixation results obtained using the first fixation protocols a new fixation protocol was tested based on that described by Karlson et al. (1996), who used a combined glutaraldehyde-osmium tetroxide primary fixative protocol. In addition to using a combined primary fixative, the inclusion of sucrose (2) mol l⁻¹) was also examined, as used by Karlson et al. (1996), in the fixative mix (protocol four), compared with seawater alone (protocol five). The cell structures of N. oculata cells under protocols four and five are presented in Figures 2.8 (protocol four: 2% Ga-Os/Os suc SW) and 2.9 (protocol five: 2% Ga-Os/Os SW). This simultaneous fixation resulted in a significant improvement in the fixation of the N. oculata (Figure 2.8 protocol four: 2% Ga-Os/Os suc SW, and Figure 2.8 protocol five: 2% Ga-Os/Os SW) and, therefore, was the protocol that was adopted in all subsequent studies. The differences in the major cell constituent structures with all the different fixation protocols that were used for N. oculata are summarized in Table 2.7. In the combined Ga-Os/Os fixations (protocols four and five; Figures 2.8, 2.9) the overall cell shape was smooth and rounded and the mitochondrial matrix uniform with generally dispersed tubular cristae (Figures 2.8A-C; 2.9B, D). The addition of sucrose to the fixative mix seemed to reduce cell shrinkage and gave better overall preservation of mitochondria. In general, cytoplasmic shrinkage was well controlled, although there was some slight shrinkage in protocol five (2% Ga-Os/Os in SW; Figure 2.9D). In protocol four, in which sucrose was also added to the filtered seawater (Table 2.7), the overall plastid matrix appeared less dense and the bands of closely depressed thylakoids were well preserved (Figure 2.8-D). In protocol five, the thylakoids often appeared less electron dense overall (Figure 2.9A, D), although there was some variability in this. Protocols four and five gave much better overall cell appearance (Figure 2.8, 2.9) and fixation quality in comparison with the other protocols (protocols one-three, Figures 2.5-2.7, Table 2.7). Although both protocols of the combined Os-Ga/Os fixation were satisfactory it was her preferred to use protocol four to fix *N. oculata* in subsequent fixations, since it was superior to protocol five in membrane preservation.

The reason for the combined fixative proving to be more effective for preserving *N. oculata* could be due to the fact that glutaraldehyde reacts rapidly with proteins and stabilizes the structures by cross-linking before there is any opportunity for extraction by the buffer (Glauert and Lewis 1998). At the same time, osmium tetraoxide penetrates the cell slowly and it reacts particularly with lipids that are not fixed by the aldehyde (Glauert and Lewis 1998). It reacts with the olfinic double bond of unsaturated lipid

(Glauert and Lewis 1998). However, if osmium tetraoxide is used solely as a primary fixative it usually leads to protein extraction due to the fact that it causes breakages in the polypeptide chains (Glauert and Lewis 1998). Therefore, in the simultaneous glutaraldehyde-osmium fixation, the former would fix the proteins, followed by the rapid fixation of lipids by osmium tetraoxide.

Table 2.7: Assessment of fixation techniques applied to Nannochloropsis oculata

Organelles	Protocol one (2% Ga	Os, SW)	Protocol two (2% Ga/Os, F/2)		Protocol three (1% Ga/Os F/2)		Protocol four (Ga-Os/Os suc)		Protocol five (Ga-Os/Os)	
	Feature	Figure	Feature	Figure	Feature	Figure	Feature	Figure	Feature	Figure
Cytoplasm	Densely granulated, showed sign of extraction and empty spaces	2.5A-D	Densely granulated, showed sign of extraction and empty spaces	2.6A-D	Densely granulated, showed sign of extraction and empty spaces	2.7A-D	Finely granulated, showed no sign of extraction or empty spaces	2.8A-D	Finely granulated, showed no sign of extraction or empty spaces	2.9A-D
Mitochondria	No clear membrane, swollen	2.5B, D	No clear mitochondrial shape, membranes and cristae	2.6A-D	Broken cristae	2.7A-D	Outer double membrane and cristae and intact dense matrix in comparison with cytoplasm, not shrunk nor swollen	2.8A-D	Outer double membrane and cristae were broken with signs of extraction	2.9A-D
Chloroplast	Loss of continuity of outer double membrane, thylakoid membrane condensed and merged	2.5A, C	Loss of continuity of outer double membrane, thylakoid membrane could be clear, condensed and merged in different parts, signs of extraction	2.6A-D	Outer double membrane lost its continuity. Thylakoid membrane could be clear, condensed and merged in different parts, signs of extraction	2.7A-D	Outer double membrane intact. Thylakoid membranes were intact and showed no sign of extraction	2.8A-D	Loss of continuity of outer double membrane. Thylakoid membranes were intact and showed no sign of extraction	2.9A-D

5

Table 2.7: Assessment of fixation techniques applied to *Nannochloropsis oculata* (continued)

Organelles	Protocol one (2	Protocol one (2% GaOs, SW)		Protocol two (2% Ga/Os, F/2)		Protocol three (1% Ga/Os F/2)		Protocol four (Ga-Os/Os suc)		Protocol five (Ga-Os/Os)	
	Feature	Figure	Feature	Figure	Feature	Figure	Feature	Figure	Feature	Figure	
Nuclear content	No clear nucleus	2.5B	Very dense, no visible chromatin or nucleolus	2.6A-D	Very dense, no visible chromatin but visible nucleolus	2.7A-D	Uniformly dense, visible chromatin and nucleolus	2.8A-D	Uniformly dense, visible chromatin and nucleolus	2.9A-D	
Nuclear envelope	Not clear	2.5B	Not clear	2.6A-D	Not clear	2.7A-D	Double membrane intact and essentially parallel to each other and showing pores		Double membrane visible but continuity lost	2.9A-D	
Cell membrane	Not clear and detached from cell wall in some cases	2.5C	Not clear and detached from cell wall in some cases	2.6A-D	Not clear and detached from cell wall	2.7A-D	Intact	2.8A-D	Not clear and detached from cell wall in some cases	2.9A-D	
Vacuoles	Loss of membrane continuity	2.5A-D	Loss of membrane continuity	2.6B	Loss of membrane continuity	2.7A-D	Bound by unbroken single membrane	2.8A-D	Bound by unbroken single membrane	2.9A-D	

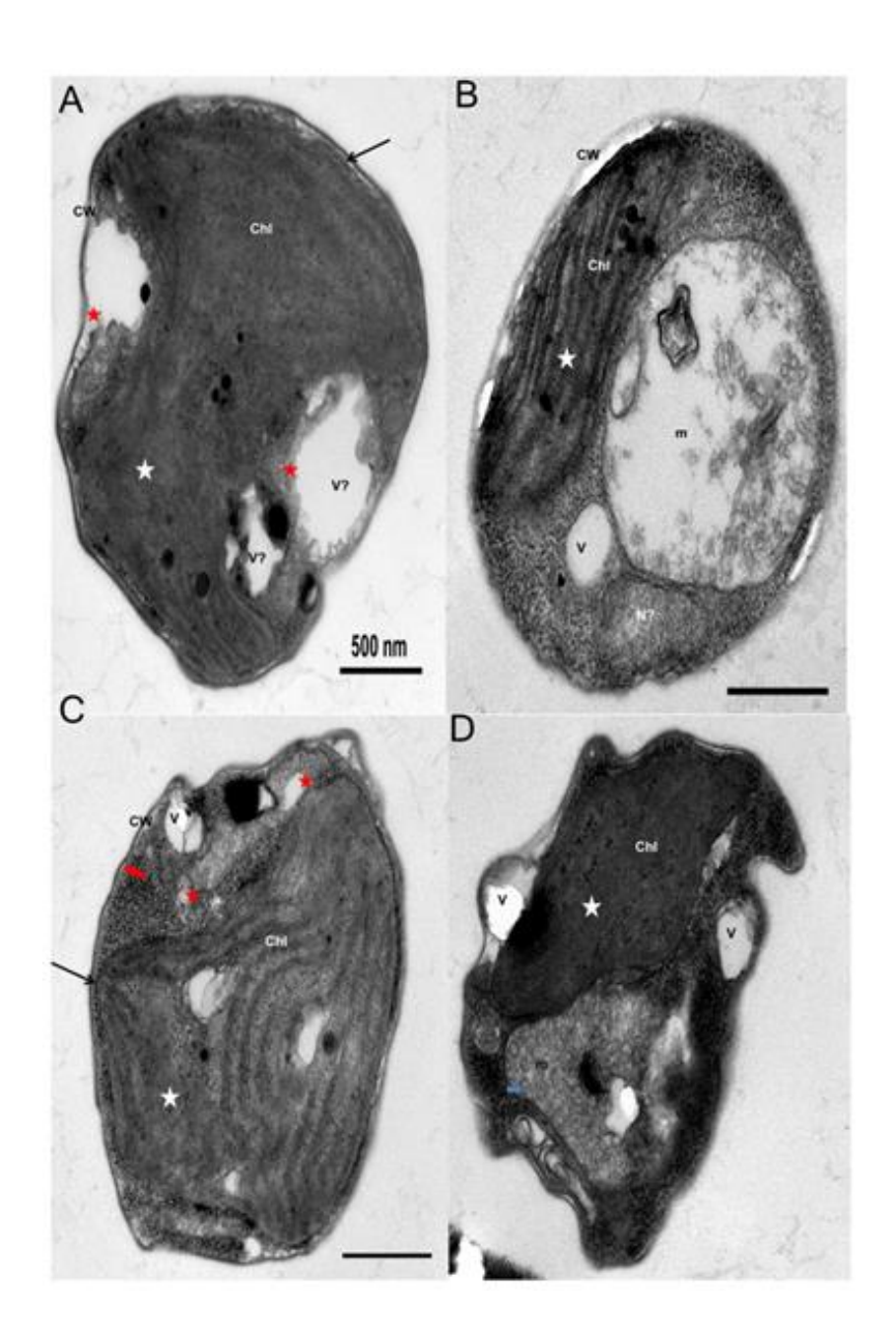


Figure 2.5: *Nannochloropsis oculata* cells fixed with fixation protocol one A) Densely granulated cytoplasm, shows sign of extraction and empty spaces (red stars). Chloroplast outer double membrane shows breakages (black arrow). Thylakoid membranes are condensed and merged (white star). Vacuole membranes are not clear. B) Mitochondrial profiles are swollen. Thylakoid membranes are condensed and merged (white star). Poor nucleus fixation as no clear nucleus is observed and no clear nuclear envelope. C) Densely granulated cytoplasm, shows sign of extraction and empty spaces (red stars). Chloroplast outer double membrane shows breakages (black arrow). Thylakoid membrane appears condensed and merged (white star). The cell membrane is not clear and appears only when detached from cell wall (red arrow). Vacuoles membranes show breakages. D) Mitochondrial profiles show no clear membranes (blue arrow). Thylakoid membrane condensed and merged (white star). Scale bar 0.5 μm. Chl: chloroplast; M: mitochondria; V: vacuoles.

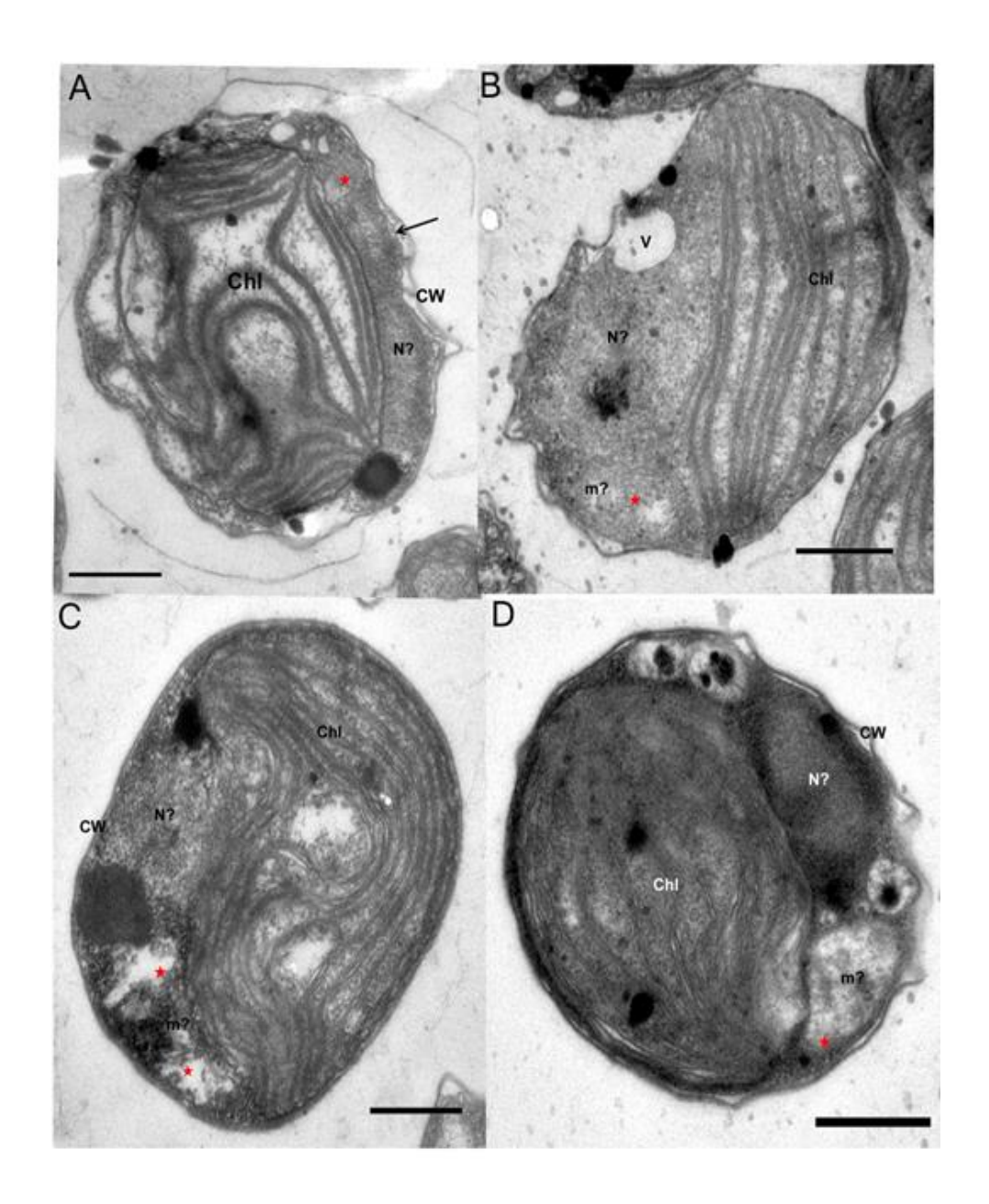


Figure 2.6: *Nannochloropsis oculata* cells fixed with fixation protocol two A) Distorted chloroplast structure: outer double membrane hard to discriminate from thylakoids; thylakoid membranes are clear or condensed and merged in different parts; very dense nuclear contents. Signs of matrix loss on unclear mitochondrial profile (red star). B) Chloroplast outer double membrane lost its continuity and is condensed and merged in different parts. Nucleus profiles with no clear nuclear envelope. Vacuoles have lost their membranes. Mitchondrial profile with distorted cristae and matrix loss (red star). C) Clear thylakoid membranes, with some evidence of matrix loss (red stars). Cell membrane not well-resolved and no clear nuclear profile in cells. D) Thylakoid membranes are clear or condensed in places. Cell membrane detached from cell wall. Scale bar 0.5 μm. Chl: chloroplast; CW: cell wall; m?: mitochondria difficult to discern; N?: nucleus difficult to discern; V: vacuoles.

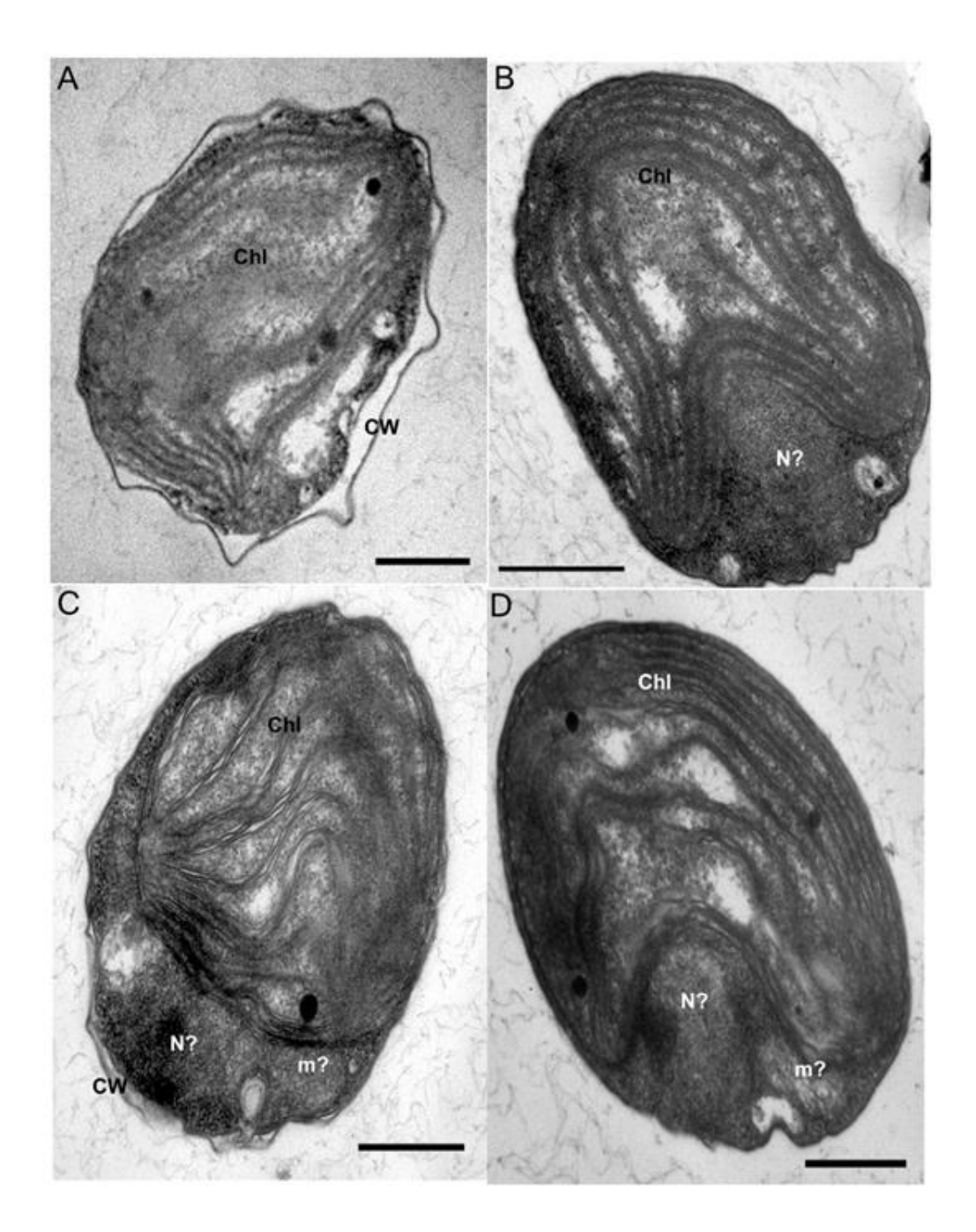


Figure 2.7: *Nannochloropsis oculata* cells fixed with fixation protocol three A) Clearly separated cell wall with closely depressed thylakoid membranes. B-D) No clear mitochondria. The nuclear envelope is not easily resolved and there is no visible heterochromatin, but a visible nucleolus. Chloroplast and thylakoid membranes are mostly condensed and merged, although some are clear and intact. Scale bar 0.5 μm. Chl: chloroplast; CW: cell wall; m?: mitochondria difficult to discern; N?: nucleus difficult to discern; V: vacuoles.

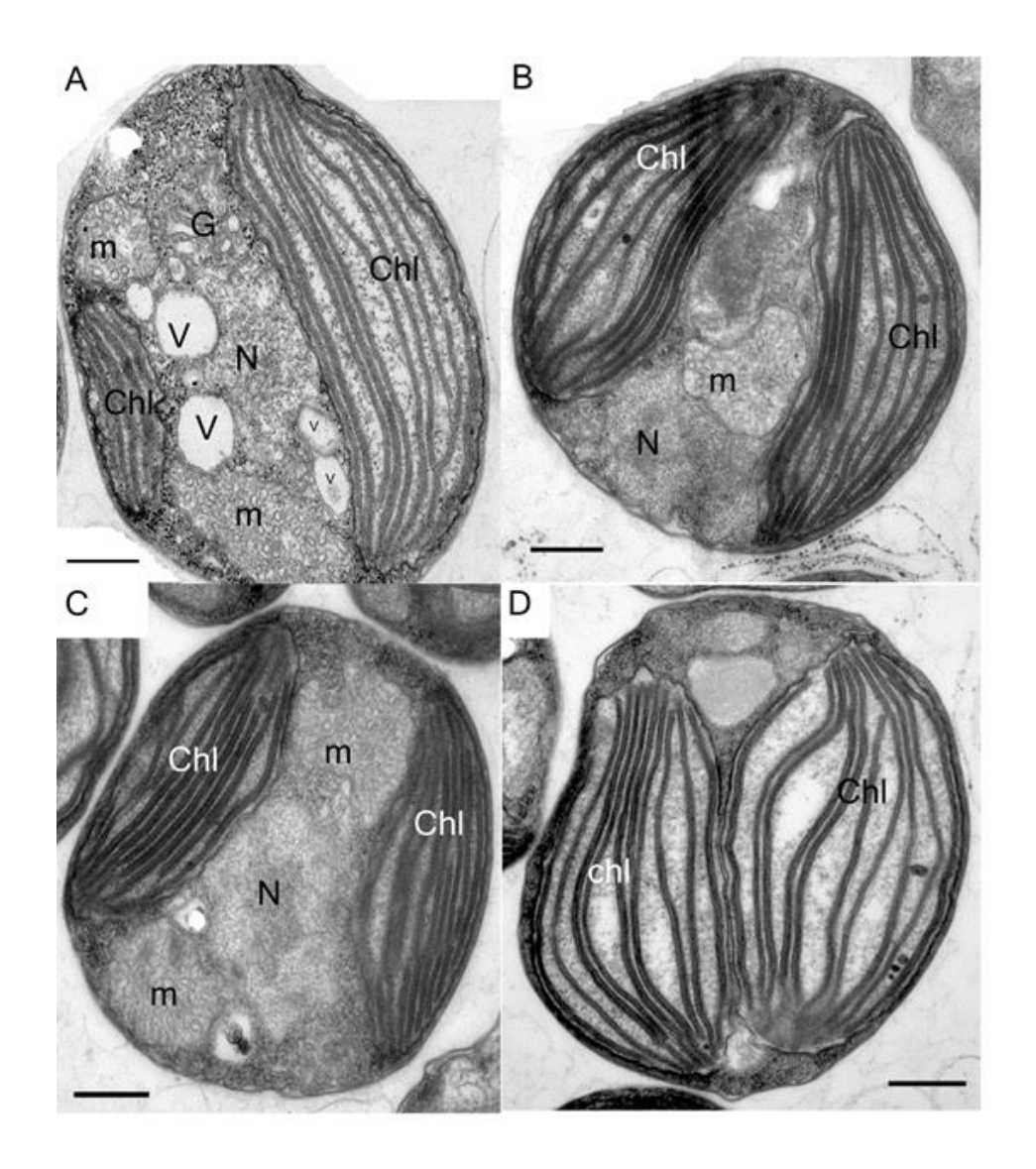


Figure 2.8: Nannochloropsis oculata cells fixed with fixation protocol four A-D) Finely granulated cytoplasm with no signs of matrix loss or empty spaces. Well-preserved mitochondrial profiles; neither shrunk nor swollen. Intact outer double membrane of chloroplast. Thylakoid membranes are intact and show no sign of swelling. Nucleus is well preserved with uniformly dense nuclear content and clearly visible heterochromatin and nucleolus. Double membrane of nuclear envelope is intact and not swollen. Cell membrane is intact and vacuoles are bound by unbroken single membranes. Scale bar $0.5~\mu m$. Chl: chloroplast; G: Golgi; M: mitochondria; N: nucleus; V: vacuoles.

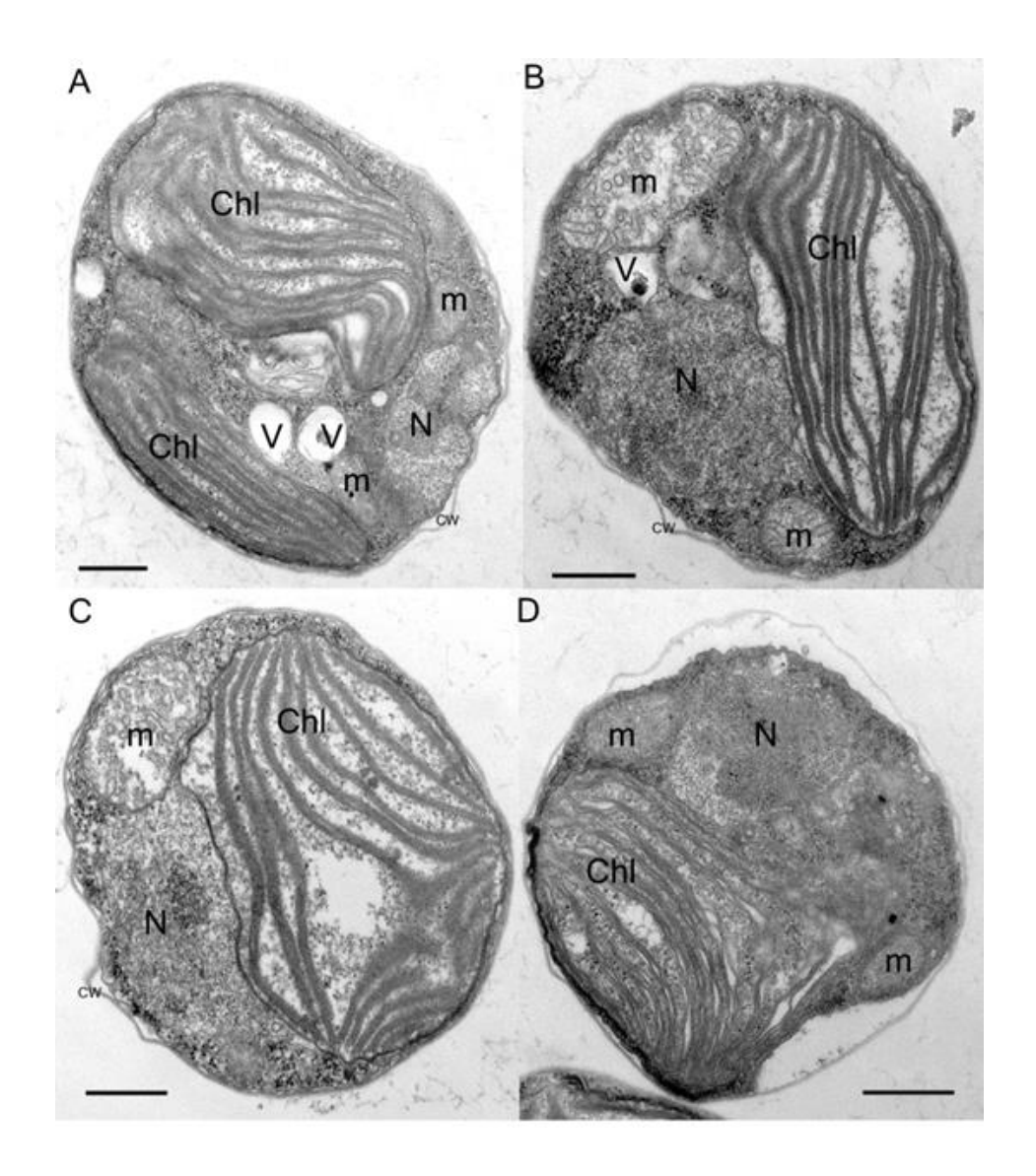


Figure 2.9: *Nannochloropsis oculata* cells fixed with fixation protocol five A-D) Cytoplasm is finely granulated with no signs of matrix loss or empty spaces. Mitochondrial profiles have broken outer double membrane and there is poorly defined cristae and matrix loss. Chloroplast has an outer double membrane which is broken in places. Thylakoid membranes are intact and show signs of swelling. Nuclear content is uniformly dense with visible heterochromatin and nucleolus and the nuclear envelope membranes are hard to discern. Cell membrane is not clear and in some cases detached from the cell wall. Vacuoles are bounded by unbroken single membranes. Scale bar 0.5 µm. Chl: chloroplast; CW: cell wall; M: mitochondria; N: nucleus; V: vacuoles.

2.5.3 Optimizing fixation protocols for *Pseudostaurosira trainorii*

The fixation of *Pseudostaurosira trainorii* for transmission electron microscopy was undertaken for the first time. It is recommended by Hayat (1989) to fix diatoms through the use of a range from 1%-3% which suits different diatom species and to post-fix with either 1% or 2% osmium tetraoxide. A concentration of 1.25% glutaraldehyce was chosen here followed by 1% osmium in 50% sea water for protocol six and a concentration of 2% glutaraldehyde followed by 1% osmium tetraoxide in seawater for protocol seven. The combined glutaraldehyde-osmium fixation (protocol eight) that was used successfully with *N. oculata* (section 2.5.2) was also employed as a better fixation protocol for *P. trainorii*, as the combined glutaraldehyde-osmium primary fixation has the advantage of fixing protein and lipids efficiently. Table 2.8 summarizes the ultrastructural features of different organelles fixed with protocols six, seven, and eight. The results of fixation with protocols seven and eight were not satisfactory as the cells showed considerable shrinkage and malformation in structures (Table 2.8, Figures 2.10-2.12).

The fixation by protocols six and seven resulted in poor quality. Protocol six was the worst protocol, with complete loss and shrinkage of the cytoplasm (Figure 2.10). This indicates that the cells were in hyposmotic solution because of the low concentration of glutaraldehyde 1.25% and 50% of seawater. Cell components were not-distinguishable from one another, with no clear differentiation between mitochondria, nucleus and chloroplast. Protocol seven was better than protocol six, yet it was not perfect. Cytoplasm shrinkage occurred and organelle details were unclear. For example, the mitochondrial cristae were not visible (Figure 2.11). Cell organelles could not be easily discriminated from one another and the dense cytoplasmic matrix.

The combined primary fixative (protocol eight) was the best fixative protocol for the diatom cells (Figure 2.12). As in the case of *Nannochloropsis*, the nucleus was clear and the mitochondrial matrix uniform, with generally dispersed tubular cristae (Figure 2.12A, C). Cell shrinkage was absent. The plastids were less condensed and the thylakoids were visible (Figure 2.12A-C). Therefore, protocol eight was used to fix *P. trainorii*. Detailed descriptions of the fixation protocols are presented in Table 2.8 and Figures 2.10-2.12.

Table 2.8: Assessment of fixation techniques applied to *Pseudostaurosira trainorii*

Organelles	Protocol six (1.25% Ga/Os, 50%	Protocol seven (2% Ga/O	s, SW)	Protocol eight (2%Ga-Os/Os 50% SW)		
Organetics	Feature	Figure	Feature	Figure	Feature	Figure
Cytoplasm	Densely granulated, showing signs of extraction and shrinking	2.10	Densely granulated, showing shrinkage	2.11	Densely granulated, showing no empty space in vegetative cells	2.12
Mitochondria	Unclear	2.10	Unclear	2.11	Outer double membrane and cristae and intact dense matrix in comparison with cytoplasm, not shrunken or swollen	2.12
Chloroplast	Distorted	2.10	Intact but condensed	2.11	Intact. Thylakoid membranes and pyrenoids were intact and showed no sign of extraction	2.12
Nuclear content	Unclear	2.10	Unclear	2.11	Intact	2.12
Nuclear envelope	Unclear	2.10	Unclear	2.11	Intact	2.12
Cell membrane	Loss of continuity	2.10	Loss of continuity	2.11	Intact	2.12
Vacuoles	Loss of membrane continuity	2.10	Bound by unbroken single membrane	2.11	Bound by unbroken single membrane	2.12
Cell wall	Extracted	2.10	Extracted	2.11	Intact	2.12

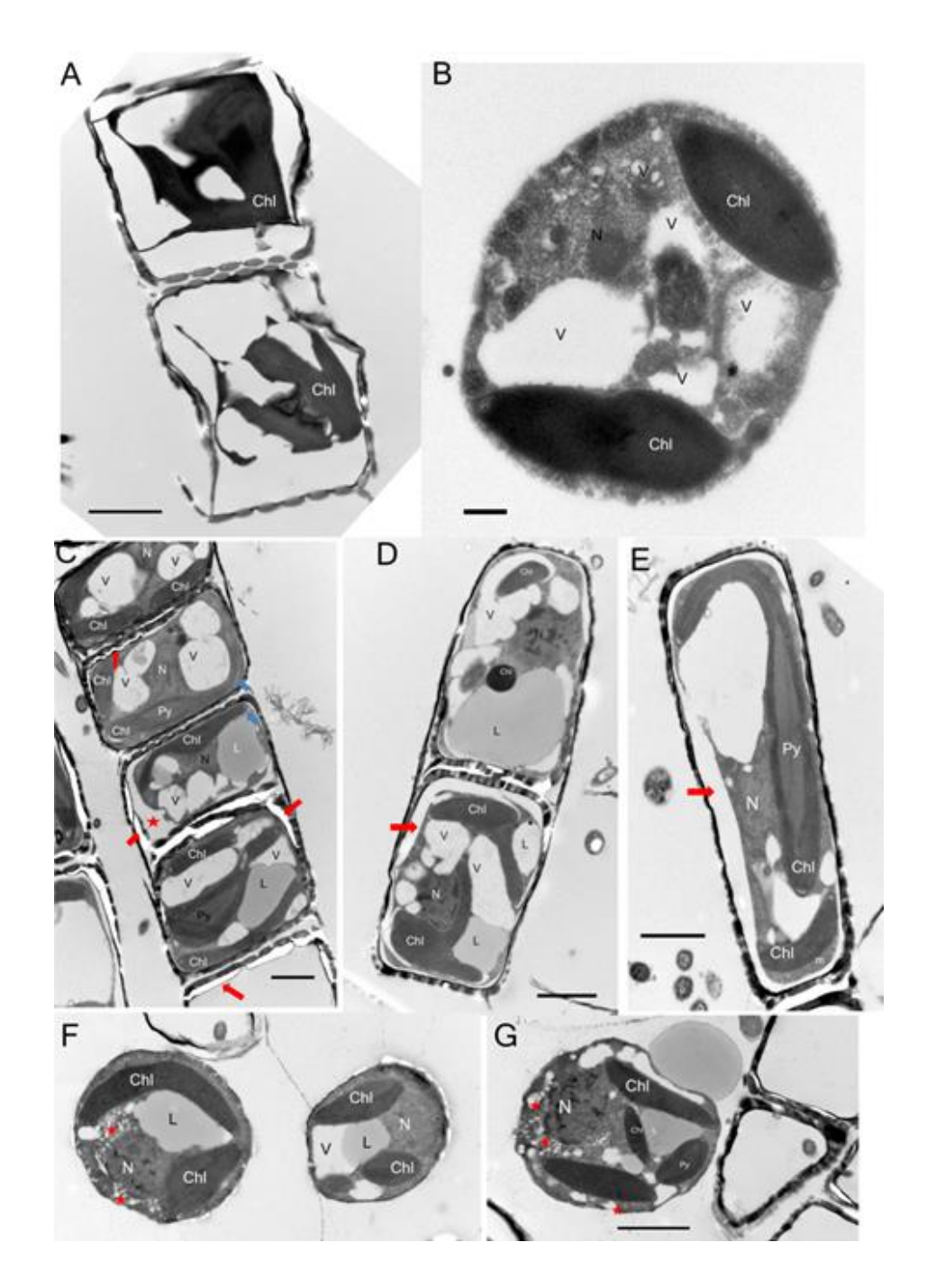


Figure 2.10: *Pseudostaurosira trainorii* life cycle stages fixed using protocol six A-B) 24 hours induced male gamete. C) 24 hours induced female gamete. D-F) 3 hours mated male and female gametes. G) 48 hours mated male and female gametes. The common features of poor preservation are: densely granulated cytoplasm with signs of matrix loss and shrinkage (red arrows); no visible mitochondrial profiles; chloroplast either distorted or dense; nuclear content and the nuclear envelope membranes not clearly visible; cell membrane not clear and if present has lost its integrity; vacuoles have lost their membranes; cell wall extracted. Chl: chloroplast; L: lipid bodies; N: nucleus; Py: pyrenoid; V: vacuoles.

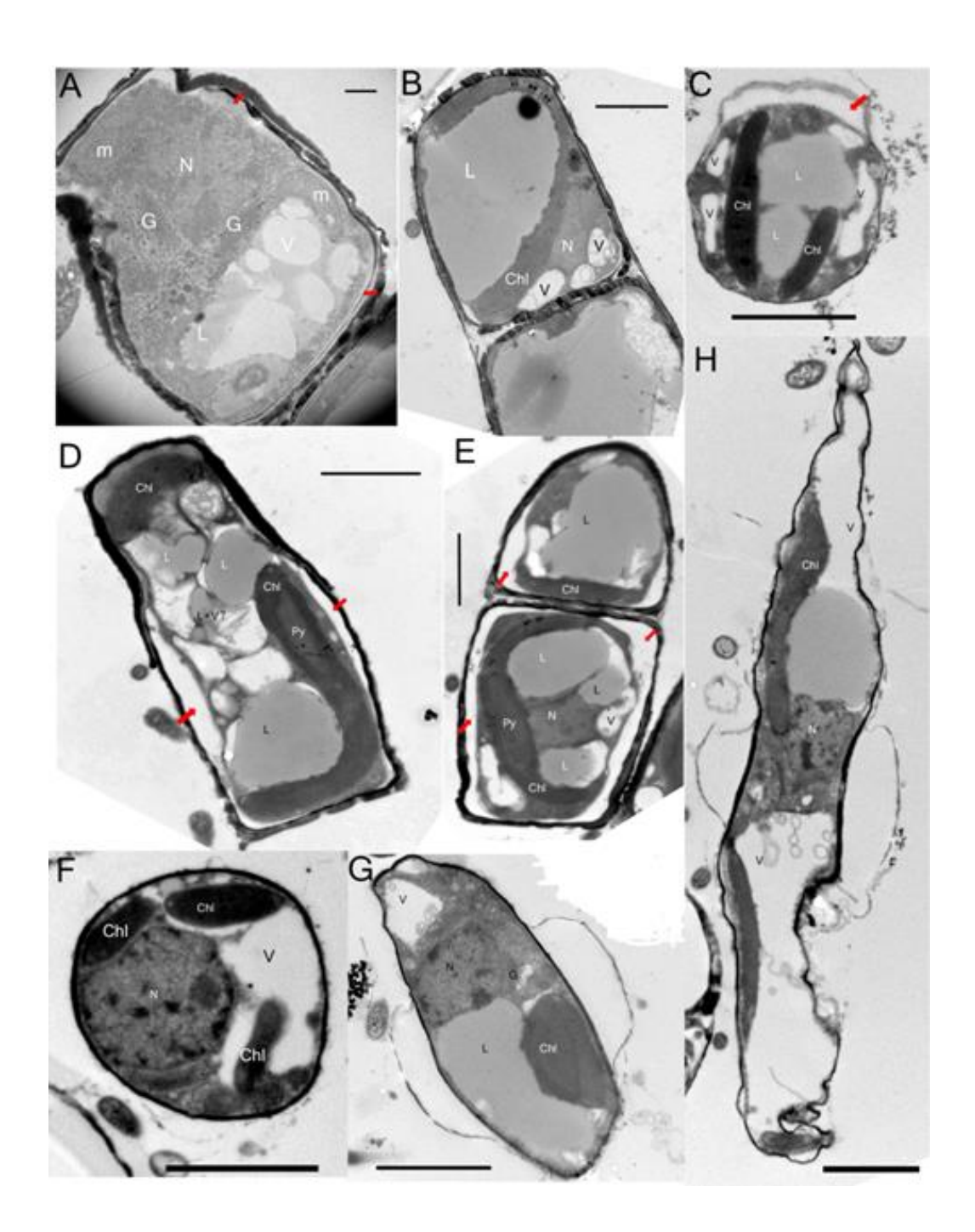


Figure 2.11: *Pseudostaurosira trainorii* life cycle stages fixed using protocol seven A-C) 24 hours induced male gamete. Scale bar 2 μ m. D-E) 24 hours induced female gamete. Scale bar 2 μ m. F) 3 hours mated male and female gametes Scale bar 2 μ m. G-H) 48 hours mated male and female gametes. Scale bar 2 μ m. The common features of the fixation are: the cytoplasm is densely granulated with signs of extraction and shrinkage (red arrows); mtochondrial profiles are dense with no clear cristae (m), and if clear there are sign of extraction (m?). Chloroplasts are intact but highly compact and condensed. Thylakoid membranes are not clearly differentiated. Nuclear content and the nuclear envelope membranes are not clearly visible. Cell membrane unclear and if present it has lost its continuity. Vacuoles are bounded by unbroken single membrane. Cell wall was extracted. Chl: chloroplast; G: Golgi; L: lipid bodies; M: mitochondria; N: nucleus; Py: pyrenoid; V: vacuoles.

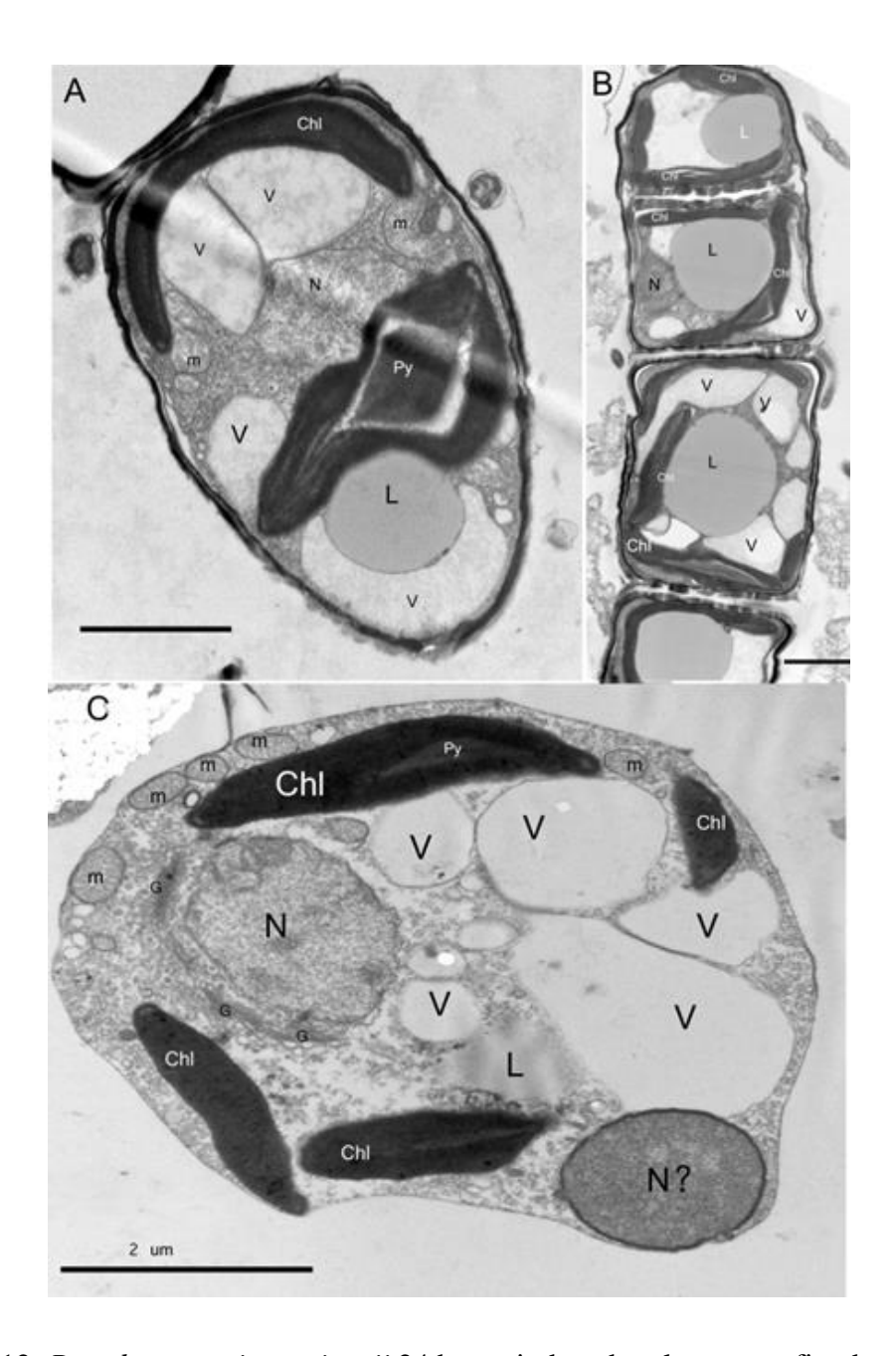


Figure 2.12: *Pseudostaurosira trainorii* 24 hours induced male gamete fixed using protocol eight

A) Male vegetative cell gird view. Scale bar 2 μ m. B) Male vegetative cell valve view. Scale bar 2 μ m. C) Male gametes. Scale bar 2 μ m. The common features of cell organelle fixation are that the cytoplasm is densely granulated with no signs of extraction or empty spaces. Mitochondrial profiles show good fixation since the outer double membrane and cristae are intact; matrix dense in comparison with cytoplasm; mitochondrial profiles not shrunken or swollen. The chloroplast is intact and thylakoid membranes and pyrenoids are intact and show no signs of extraction. Nuclear content, nuclear envelope and plasma membrane are intact. Vacuoles are bounded by unbroken single membrane. Cell wall is intact. Chl: chloroplast; G: Golgi; L: lipid bodies; M: mitochondria; N: nucleus; N?: second nucleus; Py: pyrenoid; V: vacuoles.

2.6 Conclusion

In conclusion, although there were no standard fixation protocols that suited all algal species and cell types, an optimal fixation protocol was selected that gave the best overall appearance of cell organelles. In addition, the selected protocol minimized fixation artefacts, particularly, in sensitive marker organelles such as mitochondria. These should not be swollen but have intact membranes and a well preserved matrix. Glutaraldehyde has been a widely used primary fixative, followed by post fixation with osmium tetroxide as a secondary fixative, and this combination generally worked well here with *D. salina*. However, combined fixation using both glutaraldehyde and osmium as a primary fixative followed by further secondary fixation with osmium tetraoxide gave better preservation of cells in both *N. oculata* and *P. trainorii*. This is because the fixatives react differently with each cell constituent and other factors such as the diffusion coefficients of the fixatives, osmolality, and time.

Chapter 3. Effects of an algal infochemical (Decadienal) on the ultrastructure of *Dunaliella salina* and *Nannochloropsis oculata*

3.1 Introduction

3.1.1 Importance of biofuels

Energy consumption in the form of fossil fuels is increasing globally (Singh and Gu 2010). Petroleum is currently the main energy source for the transport and logistics industries and will become depleted in the future, leading to unstable prices (Sorrell et al. 2009). Furthermore, the increasing consumption of fossil fuels causes an increase in greenhouse gas emissions, which results in global warming and climate change (Chisti 2007). Therefore, finding alternative sources of low-carbon, renewable and sustainable energy is of great importance. One such solution is biofuels (fuels produced from a source of organic biomass).

Biofuel production on a large scale will reduce greenhouse gas emissions because it relies directly on photosynthesis, a process that converts CO₂ into organic compounds, and thus is attracting great interest (Gavrilescu and Chisti 2005). There are different types of biofuels produced from different crops (such as edible as well as non-edible oil seeds) as well as from several aquatic algae, all of which have been recognized as biooil sources (Singh and Gu 2010). In addition, firewood, biogas, bio-hydrogen, bioethanol and biodiesel are examples of biofuels. There are commercial or pilot experimental procedures to use some of these (Gavrilescu and Chisti 2005). However, bioethanol produced from corn starch, sugar cane or sugar beet and biodiesel produced from oil crops such as palm and oil seed rape are the most widely produced biofuels (Chisti 2008; Scott et al. 2010). However, their production is unsustainable (Hill et al. 2006; Stephenson et al. 2008).

There are two important problems with the use of bioethanol and biodiesel from oil crops. One problem is that cultivating such crops to meet energy demand will compete with food security, as it will occupy huge areas of arable land. For example, to produce the amount of fuel needed in the UK for transport in 2008 would require more than half the land area of the UK to grow biodiesel crops (Scott et al. 2010). Another problem is that the production of biodiesel requires high amounts of energy. Both factors have

negative effects on ecosystem stability and food security (Chisti 2008; Christenson and Sims 2011).

The successful use of microalgae in other industries marks them as potentially better candidates for biofuel production. They can be sources of high-value products such as polyunsaturated fatty acids, natural colourants, biopolymers, and therapeutics (Belarbi et al. 2000; Lorenz and Cysewski 2000; Metzger and Largeau 2005; Singh et al. 2005; Walter et al. 2005; Spolaore et al. 2006). Microalgae are used to solve various environmental problems as they can be used in wastewater treatment plants and as bioremediating microorganisms (Mallick 2002; Kalin et al. 2005; Munoz and Guieysse 2006) and as biofertilizers because of their nitrogen fixing capabilities (Vaishampayan et al. 2001). In addition, microalgae can be used as feedstock for other forms of biofuel such as methane produced by anaerobic digestion of the algal biomass (Spolaore et al. 2006). Another way to utilize algae is to photobiologically produce biohydrogen (Ghirardi et al. 2000; Fedorov et al. 2005). Finally, microalgal lipids could be used to produce energy, either by simple direct combustion in boilers or in diesel engines (Converti et al. 2009). However, Chisti (2007) has recently shown that, theoretically, the best option to produce energy from algae is by transforming their lipids to produce more highly refined biofuels (Sawayama et al. 1995; Dunahay et al. 1996; Gavrilescu and Chisti 2005).

There are two main routes for the production of biofuels. In the first method, the algal biomass is fermented by other microbes. In the second, the algal lipid is transformed into biofuel through different chemical or thermochemical reactions, such as transesterification, direct hydrogenation of oils, pyrolysis of whole biomass, or gasification (Hill et al. 2006; Stephenson et al. 2008). In the transesterification reaction the reactants are triacylglycerides (TAGs), which are lipids produced by microalgae to store their energy, and methanol (Fukuda et al. 2001). Triacylglycerides are also called neutral lipids and are composed of three long-chain fatty acids (FAs) attached to a glycerol molecule (Figure 3.1). The methanol in the transesterification reaction substitutes glycerol. The results are methyl esters (biodiesel). This method is well-known and has been used to produce methyl esters for pharmaceutical use (Belarbi et al. 2000; Barnwal and Sharma 2005; Gerpen 2005).

3.1.2 Advantages of algal biofuel

The possibility of using microalgal biodiesel as an alternative to petroleum-derived transport fuels has increased in recent years as research shows it has many advantages that make it a preferable option. Some of the reported advantages include the ability to grow microalgae in shallow lagoons, raceway ponds, closed ponds or photobioreactors, which makes them available all year round. Microalgae have rapid growth since they are able to double their biomass (during the exponential growth phase) in a short time. The species of microalgae that are suitable for use as biofuel feedstock are abundant with variable lipid content in the range of 20–50% dry weight of biomass (Chisti 2007; Singh and Gu 2010). In addition, some microalgae can, under certain circumstances, have an oil content of 80% by weight of dry biomass (Metting 1996; Spolaore et al. 2006). This increases the potential to produce the required quantities of biodiesel demanded world-wide. In contrast, seed crops are limited by their cultivation season. In addition, seed crops need huge land areas and produce low biodiesel quantities when compared with microalgae. According to Chisti (2007), replacing 50% percent of United States transport consumption by biodiesel produced from oil palm cultivation will require 24% of United States agricultural land. In contrast, using microalgae as feedstock would need only 1-3% of total agricultural land (Chisti 2007). Together with the ability to cultivate microalgae on marginal lands, this makes algae the best option to replace fossil fuels without competing with food or other crops (Chisti 2007; Singh and Gu 2010). Furthermore, due to the high lipid content of microalgae cells (ranging from 20% to 50% of dry weight depending on species) their oil yields are much higher than those of oil crops. Singh and Gu (2010) showed that if microalgae oil content is 70% oil by weight this can yield 136,900 l ha⁻¹ biodiesel, and if it drops to 30% the biodiesel yield will be 58,000 l ha⁻¹. However, the yield from rapeseed is only 1190 l ha⁻¹ (Schenk et al. 2008) and for jatropha it is 1892 l ha⁻¹ (Chisti 2007). Therefore, microalgae could be an oil source which might meet the global demand for transport fuels.

Microalgae can help the environment in different ways if used as biofuel. Firstly, algae need CO₂ to grow, and Chisti (2008) estimated that producing 100 tons of algal biomass fixes roughly 183 tons of CO₂. This CO₂ can be provided from electricity power plants that burn fossil fuels (Sawayama et al. 1995; Yun et al. 1997), thus reducing emissions of a major greenhouse gas. Secondly, microalgae not only grow in the sea but also in brackish or saline waters and contaminated water. Therefore, they will help in the remediation of contaminated water since they utilize nutrients therefrom (Hu et al.

2008). For example, they can use nitrogen and phosphorus from agricultural run-off, concentrated animal feed operations, and industrial and municipal wastewaters (Hu et al. 2008). Thirdly, in contrast to oil crops, algae do not require herbicide or pesticide application (Rodolfi et al. 2009). Fourthly, livestock waste resulting from agriculture can be used to grow algae (Cantrell et al. 2008). Finally, the residual biomass resulting from lipid extraction can be used as feed or fertilizer (Spolaore et al. 2006).

The sustainable production of biodiesel from microalgae can be carbon-neutral and save energy. The algal biomass that remains after lipid extraction can be used in several ways, either as a further source of energy in the biodiesel production process or to produce products that can be sold for profit. For instance, the biomass can be fermented to bioethanol or biomethane (Chisti 2008), thereby providing another source of energy, or the residual biomass can be sold as high-protein animal feed or high-value microbial products (Molina et al. 1999; Gavrilescu and Chisti 2005; Chisti 2006).

3.1.3 Algal biofuel production schemes

A practical algal biofuel production scheme consists of several steps. Many factors affect the sustainability of the production scheme. In all cases, there is a necessity for biomass feedstock which is cheap to produce, sustainable, available in large amounts and preferably non-food based (Tang et al. 2011). It is started by growing the algae, which requires a supply of nutrients, under controlled growth conditions. Many factors have to be taken into consideration when choosing a viable production scheme. These are: i) the choice of the best bioreactor; ii) the prevention of contamination with invading organisms; and iii) controlling growth conditions to ensure that the algae will produce the highest amount of lipids (Scott et al. 2010). The second stage is harvesting and processing the algal biomass. It is important that the energy required for the production of biodiesel must be less than that obtained in the final product (Scott et al. 2010). The energy production and energy required for the production of biofuels is analysed by life-cycle analysis (LCA). One factor which adds considerable expense to the process is the need to separate algae from the water before lipid extraction. There are currently no efficient technologies available for this other than those which are very costly indeed (Brennan and Owende 2010). Lipids can be released from the cell by chemical extraction, but this must be done using both cost-effective and environmentally friendly techniques. Two solutions have been suggested to solve the issue of the prohibitive costs of biofuel production from microalgae (Scott et al. 2010).

One solution is to increase both the rate of growth and the concentration of cells in the culture. This will assist in the offset of the embodied energy within materials utilised in the ponds or photobioreactors. Additionally, this will bring down the expense involved in downstream processing. The second solution involves subjecting algae to nutrient starvation, which will induce them to maximise their lipid production. In this way the amount of nutrients needed to feed the algae will be decreased. Furthermore, the amount of residual biomass will be reduced. In turn, this will reduce the total energy needed for production (Scott et al. 2010).

The selection of suitable algal strains is also of crucial importance. Typically, the algal strain must be fastgrowing and at the same time produce large quantities of lipid in the cells (Scott et al. 2010). Algal genera that have been used for biofuel production include *Chlorella*, *Dunaliella*, *Haematococcus* and *Botryococcus* (Wolf et al. 1985). The latter have a high hydrocarbon content (Knights et al. 1970). *Dunaliella* spp. have been widely studied, cultivated and commercialized as a source of natural β -carotene (Ben-Amotz and Avron 1983).

3.1.4 Lipids in microalgae

Two categories of lipids are produced by microalgae according to their functions inside the cell: structural lipids (polar lipids) and storage lipids (non-polar lipids). Polyunsaturated fatty acids (PUFAs) are normally discovered in high amounts within structural lipids. They are also vital nutrients for aquatic animals and humans. Polar lipids (phospholipids) and sterols are important components of cell membrane structure. They can perform the role of a selective yet permeable barrier for both cells and organelles. Other roles polar lipids play in the cell are to enable the membrane to be functional, act as a medium for the provision of metabolic processes, take part in the membrane fusion process, and have a role in cell signalling pathways, so they can play a role in the adaptation of algae to environmental stresses (Hu et al. 2008; Sharma et al. 2012).

Lipids found in microalgae as storage reserves include neutral lipids, polar lipids, wax esters, sterols, hydrocarbons and prenyl derivatives (Hu et al. 2008; Sharma et al. 2012). Storage lipids are mainly in the form of triacylglycerides (TAGs) made of predominately saturated fatty acids and some unsaturated fatty acids which can be transesterified to produce biodiesel. Lipid production is increased under a range of stress conditions (Chisti 2006, 2007; Greenwell et al. 2010). TAGs are stored in

cytosolic lipid droplets. Research efforts over the last couple of decades have changed the perception of lipid droplets from static, energy-dense particles to dynamic organelles found across all Kingdoms (Beller et al. 2010). All lipid droplets share common features: a hydrophobic core typically comprising of TAGs or sterols surrounded by a monolayer of polar glycerolipids into which lipid droplet-associated proteins are embedded (Vieler et al. 2012). Despite these similarities, lipid droplets are versatile organelles that vary in size, shape, and function, depending on cell type (Sheehan et al. 1998; Vieler et al. 2012).

3.1.5 Maximising the lipid content in algae

Algal productivity is defined as the overall increase in algal biomass, whereas oil productivity is defined by Chisti (2007) as "the mass of oil produced per unit volume of the microalgal broth per day", and is the key factor that affects the success of an alga in biofuel production. It is controlled by the algal genome (Sharma et al. 2012) and depends on the algal growth rate and the oil content of the cells (Scott et al. 2010). Different factors that affect oil productivity in an algae can be grouped as physical, chemical and environmental. Examples include nutrients (particularly nitrogen and phosphorous), light irradiation, pH, temperature and heavy metals. All of these factors affect algal cells either on their own or synergistically and in each case have different effects (Hu et al. 2008). The effect of environmental factors on Nannochloropsis lipid production has been tested in various studies (Boussiba et al. 1987; Sukenik et al. 1989, 1993a, b; Zittelli et al. 1999). Culture age, light intensity, salinity levels and temperature limit Nannochloropsis growth, while at the same time they cause increases in saturated and monosaturated fatty acids (Renaud et al. 1991; Sukenik et al. 1993b; Renaud and Parry 1994). On the other hand irradiance levels affect the balance between structural membranes and storage lipids (Pal et al. 2011). Microalgae have the ability to adapt to different environmental conditions because they can change their metabolic pathways to synthesise different types of lipids (Thompson 1996; Guschina and Harwood 2006). When microalgal cells are stressed they will typically start to synthesise neutral lipids (storage lipids) which can constitute anything from 25-50% of their dry weight (Wang et al. 2009) or, in some extreme cases, as high as 80% of their lipid content (Klyachko-Gurvich 1974; Suen et al. 1987; Tonon et al. 2002). The green alga Chlorella vulgaris changed its metabolism during nitrogen starvation to synthesise lipids containing TAGs, while it is used to synthesis fatty acid rich lipids under normal conditions in a study by Widjaja et al. (2009).

The most common factor affecting lipid production in microalgae is nutrient starvation, which is defined as depletion of nutrients such as nitrogen or phosphorus (Hu et al. 2008; Sharma et al. 2012). Algal growth rate is reduced when subjected to nutrient reduction. However, algal cells can continue synthesising fatty acids if enough light and CO₂ are available for photosynthesis (Thompson 1996). Since growth and nutrients are directly related, the reduction in nutrients will generally cause a reduction in growth; therefore, requiring no new membrane synthesis. This leads to a shift in fatty acid metabolism to accumulate and store them as TAGs (Hu et al. 2008; Sharma et al. 2012). It is thought that this conversion in lipid metabolism during stress conditions is a protective mechanism, because photosynthesis does not cease in the presence of CO₂ and light irradiation, which results in the formation of ATP and NADPH (Hu et al. 2008; Sharma et al. 2012). In the presence of nutrients, the cellular energy stored as ATP and NADPH resulting from photosynthesis is used to construct new cells (biomass), but under nutrient starvation growth is limited and no new cells are formed. Therefore, ATP and NADPH start to accumulate and the cells will be depleted in ADP and NADP⁺, which are needed for photosynthesis to continue (Hu et al. 2008; Sharma et al. 2012). This may cause injuries to the cell (Hu et al. 2008; Sharma et al. 2012). As a result, consuming the energy stored in ATP and NADPH by synthesising TAGs will make ADP and NADP⁺ available for photosynthesis.

The effect of limitations in different nutrients has been extensively investigated (Hu et al. 2008; Sharma et al. 2012). The most studied nutrient is nitrogen. The increase in amount of lipid in algal cells during nitrogen starvation has been shown by several studies (Guschina and Harwood 2006; Griffiths and Harrison 2009; Hsieh and Wu 2009; Rodolfi et al. 2009; Wang et al. 2009; Praveenkumar et al. 2012). Algal genera have different lipid productivity responses following nutrient depletion. For instance, the diatom *Phaeodactylum tricornutum* showed a 6% increase in lipid content (Alonso et al. 2000), whereas *C. vulgaris* increased its lipid content by 40% (Illman et al. 2000). The actual composition of algal lipids may also vary in different species in response to nutrient starvation.

Converti et al. (2009) studied the effects of nitrogen reduction on the growth of *Nannochloropsis oculata* and *C. vulgaris*. When the nitrogen concentration was reduced by 50% compared with the standard medium concentration, the growth rate of *N. oculata* decreased but its lipid content doubled. In contrast, the growth rate of *C. vulgaris* was not affected and its lipid content increased threefold. Rodolfi et al. (2009)

carried out a large-scale study on the induction of lipid production in *Nannochloropsis* and other algal species using nitrogen and phosphorous depletion. Their results confirmed that nitrogen starvation increased lipid content and overall lipid productivity in an outdoor algal culture (Rodolfi et al. 2009). They showed that *Nannochloropsis* species could produce 20 tons of lipid per hectare in the Mediterranean climate and more than 30 tons of lipids per hectare in sunny tropical areas. The main limitation in using nitrogen depletion as a means to increase lipid production is the time required. This varied from two to five days, during which biomass increase was low and lipid productivity limited (Widjaja et al. 2009).

Other studies have investigated the effects of phosphorus, silicon and potassium deficiencies on lipid production in different algae. The effects of phosphorus deficiency showed contradictory results in different species. Whilst it increased lipid content (< 53%) in *Scenedesmus* sp. (Xin et al. 2010) and in *P. tricornutum*, *Chaetoceros* sp., *Isochrysis galbana* and *Pavlova lutheri* (Reitan et al. 1994), it resulted in a reduction of lipid content in *Nannochloris atomus* and *Tetraselmis* (Reitan et al. 1994). In addition, phosphorous deficiency affects fatty acid composition in a number of different ways. It has been shown to increase the production of unsaturated and monosaturated fatty acids and decrease the production of polyunsaturated fatty acids (Reitan et al. 1994).

Meanwhile it increased unsaturated fatty acids in *Chlorella kessleri* (El-Sheek and Rady 1995). Silicon deficiency induced lipid (mainly TAGs) production in the diatom *Cyclotella cryptica*, as illustrated by Miao and Wu (2006) and in *Chlorella* (Griffiths and Harrison 2009). Finally, both potassium and iron deficiency induced lipid production in *C. vulgaris* (Liu et al. 2008).

The major effect of temperature changes on microalgae is in altering fatty acid composition (Sharma et al. 2012). This is thought to be a protective mechanism, as the trend is to increase the proportion of unsaturated fatty acids as temperature decreases in order to maintain membrane fluidity (Sharma et al. 2012). Conversely, increasing temperature will increase the proportion of saturated fatty acids (Sharma et al. 2012). In *Dunaliella salina*, whose lipid-globules contain elevated levels of triacylglycerols (Rabbani et al. 1998), unsaturated lipids increased by 20% when growth temperature was decreased from 30 °C to 12 °C (Thompson 1996). Temperature elevation increased the growth rate of *Ochromonas danica* and the total lipid content was increased (Aaronson 1973). Elevated temperatures increased both the growth rate and total lipid production in *Nannochloropsis salina* (Boussiba et al. 1987). In contrast, the growth

rate of *Nannochloropsis oculata* was decreased in both elevated and reduced temperatures compared with the optimum (Converti et al. 2009). Therefore, the effects of temperature changes are not only genus-specific but also strain-specific. Increasing temperature cannot be considered as a practical way to improve lipid content in biofuel production, as it would be energetically expensive to maintain high temperatures in large-scale cultivation bioreactors (Sharma et al. 2012).

3.1.6 Infochemicals

Infochemicals are defined as secondary metabolites that serve as means of communication between different organisms (including microalgae) in aquatic environments (Dicke and Sabelis 1988). They convey information from the producer to the receiver organism to induce certain behavioural or physiological responses. This chemical communication is important for organisms that live in aquatic environments, to enable them to adapt to continual fluctuations in environmental factors such as levels of nutrients, light and temperature. Such communication is supported by the physical properties of water (Falciatore et al. 2000; Pohnert et al. 2007). These infochemical compounds belong to several different chemical groups, including dissolved gases (Steinke et al. 2002), hydrocarbons (Yasumoto et al. 2005), peptides (Rittschof and Cohen 2004) and proteins (Hallmann et al. 1998). Infochemicals are important factors that play major roles in managing the ecology of aquatic environments.

One group of infochemicals is the polyunsaturated aldehydes (PUAs). These are reported to have variable effects on invertebrates, algae, bacteria and yeast (Adolph et al. 2004; Caldwell et al. 2005; Casotti et al. 2005; Fontana et al. 2007; Taylor et al. 2007). Their effect on calanoid copepods is to reduce egg viability, produce abnormal morphological development in nauplii, and reduction in naupliar survival (Ban et al. 1997; Paffenhöfer 2002; Ianora et al. 2003; Taylor et al. 2007). PUAs are also toxic to many taxa other than copepods, such as polychaetes, echinoderms, and ascidians (Buttino et al. 1999; Caldwell et al. 2002; Simon et al. 2010).

Decadienal is one of the PUAs and has been reported to play an important role in the algal growth cycle and the formation of blooms. For example, Vardi et al. (2006) showed that when cells of the diatom *Phaeodactylum tricornutum* are exposed to 19.8 μ M (3 μ g ml⁻¹) of decadienal, cell death results, probably as a result of it triggering intracellular calcium transients which, in turn, leads to the generation of nitric oxide

(NO) by a calcium-dependent NO synthase-like activity (Vardi et al. 2006). However, subjecting cells to sublethal doses of decadienal can induce resistance to lethal doses, which is reflected in altered calcium signatures and the kinetics of NO production (Vardi et al. 2006). Decadienal belongs to the α,β-unsaturated aldehydes, which are reactive compounds that can receive electrons because of the double bond found in their aldehyde group (Hansen et al. 2004). These compounds affect the cell in various ways. They can react with proteins and enzymes (Witz 1989), DNA (Uchida 1999) and DNA polymerase (Wawra et al. 1986). They are reported to cause apoptosis in copepods (Miralto et al. 1999; Poulet et al. 2003; Romano et al. 2003) and diatoms (Casotti et al. 2005). In addition, they cause necroptosis in human cancer cells (Sansone et al. 2014). Apoptosis and necroptosis are types of programmed cell death (PCD).

Since microalgal cultivation for biofuel production resembles an open water environment, it is important to explore the effect of infochemicals such as decadienal on microlagal cultures, with the aim of enhancing biofuel production. Previous work by Taylor et al. (2012) indicated that, by treating algae cultures with decadienal, the lipid yield increased, but at the expense of reducing growth rate. Also, treatment with algae extracts promoted autoflocculation responses in the cultures. Given that decadienal is known to be broadly toxic to a range of cellular processes, it is important to gain an understanding of what the chemical is doing to the algae at the cellular and sub-cellular levels. High lipid yield per unit area is the result of both overall biomass productivity and individual cell lipid content. Both parameters need to be optimized in a successful biofuel production plant (Rodolfi et al. 2009). In this present study, sub-lethal concentrations of decadienal were investigated to determine the effects on overall yield and speed of lipid production (i.e. increased lipid yields more quickly) in Nannochloropsis oculata and Dunaliella salina, both of which have been intensively investigated as practical organisms for biofuel production (Hu et al. 2008; Rodolfi et al. 2009; Kilian et al. 2011).

3.1.7 Study aims

The main focus of this chapter is investigation of the effect of decadienal on the production of lipid droplets within the algal cellular structure. Electron microscopy was used, as it permits differentiation between the two types of lipid-rich structure, whereas chemical extraction methods only provide a measure of the total lipids in the cell. Stereological measurement techniques were used on randomly selected thin sections of

cells in their exponential growth phase and in a range of decadienal concentrations (0, 2.5, $50 \,\mu\text{M}$ for *D. salina*) and (0, 1, 10, $50 \,\mu\text{M}$ for *N. oculata*), to assess whether decadienal triggers a shift in lipid body content or increases the overall membrane constituents in the cell, particularly the extensive plastid thylakoid system.

Figure 3.1: Basic structure of triacylglycerides Triacylglycerides are composed of a glycerol backbone to which 3 fatty acids are esterified. (Source: King (2014))

$$H_3C$$

Figure 3.2: Decadienal structure (Source: Sigma-Aldrich (2015))

3.2 Methods

3.2.1 Comparison of active versus stationary phase cell ultrastructure

The two algal species used throughout this investigation were obtained from the Culture Collection of Algae and Protozoa, Oban. The *Dunaliella salina* strain (CCAP 19/30) and the *Nannochloropsis* strain (CCAP 849/1) were grown under the same conditions as the maintenance cultures described in Chapter 2 (section 2.1.1). To compare cell structure between active and stationary growth phases, standard growth curves were determined using optical density measurements (at 690 nm wavelength) using a Varian UV-VIS spectrophotometer. For each of the two species, two samples (one actively growing in the linear phase and one in the stationary phase) were fixed as described in Chapter 2 (section 2.3.1.1).

3.2.2.1 Dunaliella salina CCAP19/30

Two *D. salina* samples were fixed concurrently. Sample one was taken from a 10-day-old culture which was in the linear growth phase and had a culture cell density of 2.5×10^7 cells ml⁻¹. Sample two was taken from a 14-day-old culture in stationary phase with a culture density of 10.5×10^7 cells ml⁻¹. Samples were fixed using protocol one as described in Chapter 2 (section 2.3.1).

3.2.1.2 Nannochloropsis oculata CCAP849/1

For *N. oculata*, the first sample was fixed from a 6-day-old culture in the linear growth phase with a culture density of 1.95×10^7 cells ml⁻¹. The second sample was fixed from a 20-day-old culture that had entered stationary phase with a cell density of 8.77×10^7 cells ml⁻¹. Samples were fixed using protocol four as described in Chapter 2 (Section 2.3.2.1).

3.2.2 Assessing the effects of decadienal on *Dunaliella salina* and *Nannochloropsis* oculata cell structure

The effects of a range of *trans*, *trans*-2, 4-decadienal (Sigma Aldrich UK Ltd) (decadienal) concentrations on cell structure and lipid content was investigated using a randomized factorial experimental design. Four replicate cultures of *D. salina* and *N. oculata* per decadienal concentration were set up and distributed randomly in a LabHeat free standing incubator fitted with florescent light tubes, as shown in Figure 3.3. The factorial design minimized the effects of any minor temperature and light variations

during the experimental period. A 100 mM decadienal stock solution was prepared by dissolving 28.7 ml of 0.174 M decadienal (Mwt= 152.23 g mol⁻¹, density= 0.872 g ml⁻¹) in 21.3 ml methanol in the case of *D. salina* or 21.3 ml ethanol in the case of *N. oculata*. Specific volumes of the stock solution were added to sterile 50-ml conical flasks containing 40 ml of F/2 medium to give the test range of decadienal concentrations (Figure 3.3). The proportions of ethanol and methanol solvent controls were equal to the equivalent dose of the highest concentration of the treated samples (8.5 μl in the case of the 50 μM decadienal treatment).

D. salina treatments were inoculated with 1.8×10^6 cells ml⁻¹ in replicate flasks containing 0 μM, 2.5 μM, and 50 μM decadienal (Table 3.1). *N. oculata* treatments were inoculated with 2.0×10^6 cells ml⁻¹ in flasks containing 0 μM, 1 μM, 10 μM, and 50 μM decadienal (Table 3.2). A solvent control was run with 8.5 μl methanol. All flasks were maintained at 19 °C with a 16 hours light: 8 hours dark photoperiod for 24 hours.

Due to restrictions on the number of samples that can be effectively processed for electron microscopy at any one time, only one replicate flask was processed for each of the two growth phases and decadienal treatments using the optimal fixation protocols described in Chapter 2, section 2.3.1.1.

Table 3.1 Experimental set-up for *Dunaliella salina*.

Sample	Flask constituents
0 μΜ	40 ml of <i>D. salina</i> culture
Methanol control	39.9915 ml <i>D. salina</i> culture, 0.00852 ml 99% methanol
2.5 μΜ	39.999 ml D. salina culture, 0.001 ml of 100 mM decadienal
50 μΜ	39.98 ml <i>D. salina</i> culture. 0.02 ml of 100 mM decadienal

Table 3.2: Experimental set-up for *Nannochloropsis oculata*.

Sample	Flask constituents
0 μΜ	40 ml of <i>N. oculata</i> culture
Ethanol control	39.9915 ml <i>N. oculata</i> culture, 0.00852 ml 99% ethanol
1 μΜ	39.9996 ml N. oculata culture, 0.0004 ml of 100 mM decadienal
10 μΜ	39.996 ml <i>N. oculata</i> culture, 0.004 ml of 100 mM decadienal
50 μΜ	39.98 ml <i>N. oculata</i> culture. 0.02 ml of 100 mM decadienal

A

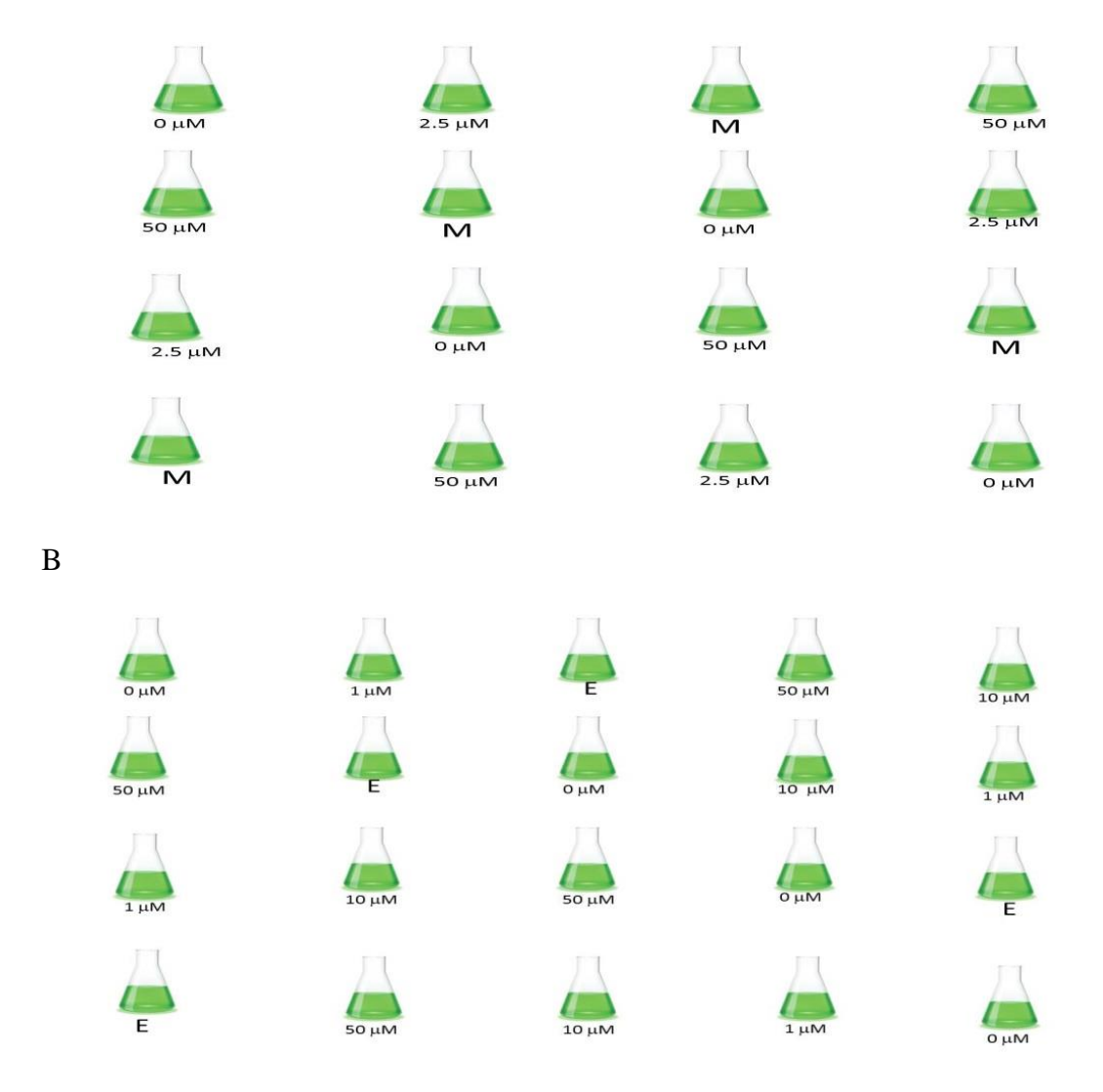


Figure 3.3: Experimental set-up

A) Dunaliella salina experimental design. Each flask contained:

0 μM: 40 ml of *D. salina* culture.

M (methanol control): 39.9915 ml D. salina culture, 0.00852 ml 99% methanol

2.5 μM: 39.999 D. salina culture, 0.001 ml of 100 mM decadienal

50 μM: 39.98 D. salina culture. 0.02 ml of 100 mM decadienal

B) Nannochloropsis oculata experimental design. Each flask contained:

0 μM: 40 ml of N. oculata culture.

E (methanol control): 39.9915 ml *N. oculata* culture, 0.00852 ml 99% ethanol.

1 μM: 39.9996 ml N. oculata culture, 0.0004 ml of 100 mM decadienal

10 μM: 39.996 ml N. oculata culture, 0.004 ml of 100 mM decadienal

50 μM: 39.98 ml N. oculata culture, 0.02 ml of 100 mM decadienal

3.2.3 Stereological and statistical analysis

Thirty micrographs representing a random sample from cells for each treatment were acquired by sectioning two to three blocks for each treatment in various planes (Visviki and Rachlin 1994a). These micrographs were analysed using a 1cm x 1 cm point lattice grid as described by Steer (1981) and shown in Figure 3.4 A and B. Using a grid point counting procedure, the volume fraction (Vv) of the following selected organelles was calculated (for definition and illustration see Figure 3.4): nucleus, mitochondria, lipid, cell wall, cytoplasm, vacuoles and chloroplast. In addition, chloroplasts were further analysed to determine the volumes of thylakoid membranes, starch, plastoglobuli, background matrix and pyrenoid (see Figure 3.4A, B). The mean organelle volume fraction and standard error was calculated for each organelle in each treatment. Data acquired from the calculation of Vv for the desired organelles were subjected to statistical analysis using Minitab 16.

3.2.3.1 *Dunaliella salina*: testing the differences between volume fractions of log and stationary phases

Anderson-Darling tests were conducted, one for each organelle, for active and stationary growth phases. For the active growth phase, the data for the nucleus, mitochondria, chloroplast, cytoplasm, thylakoid membrane, starch grains and matrix conformed to normal distributions (Anderson-Darling test, Table A1, Appendix 2, p>0.05); however, data for lipid, vacuoles, plastoglobuli, and pyrenoid were not normal (Anderson-Darling test, Table A1, Appendix 2, p>0.05). Data remained non-normal despite arcsine transformation (Anderson-Darling test, Table A3, Appendix 2 p<0.05). For the stationary phase growing cells, the data for lipid, cytoplasm, chloroplast, thylakoid membrane, and starch grains conformed to normal distributions (Anderson-Darling test, Table A2, Appendix 2, p>0.05); however, data for the nucleus, mitochondria, vacuoles, plastoglobuli, pyrenoid, and matrix were not normal (Anderson-Darling test, Table A2, Appendix 2, p<0.05) but data for the matrix and mitochondria were normalised by arcsine transformation (Anderson-Darling test, Table A4, Appendix 2, p>0.05).

Differences in volume fraction for non-normally distributed data (nucleus, lipid, vacuoles, plastoglobuli and pyrenoid) between the log and stationary phases were tested using Mann-Whitney *U*-tests (results, section 3.3.1.2). The volume fractions of normally distributed data (mitochondria, cytoplasm, chloroplast, matrix, thylakoid

membranes and starch) in the active and stationary phases were tested using t-tests (results, section 3.3.1.2). Equal variance tests (F-test) were conducted before t-tests. The variances of the log and stationary phase volume fractions for cytoplasm, chloroplast, thylakoid membrane and starch could be considered as equal (F-test, F values are shown in Table A5 in Appendix 2, p>0.05); therefore a t-test for equal variances was conducted to test significant differences in volume fractions of the organelles mentioned in actively growing and stationary phase growing cells. The variances of the active and stationary phase volume fractions for mitochondria and matrix could not be considered as equal (F-test, p<0.0, F values Table A5, Appendix 2). Therefore, a t-test for non-equal variances was used to test the significant differences in volume fraction of the cell's organelles in exponential and stationary phase growing cells (results section 3.3.1.2).

3.2.3.2 *Dunaliella salina*: testing the differences between volume fractions of decadienal-treated cells

The same procedure (section 3.2.3.1) was carried out to test the normality of volume fraction data for zero control, methanol control, 2.5 μ M and 50 μ M. Data for the chloroplast, cytoplasm, thylakoid membrane, starch grains and matrix conformed to normal distributions in all the four treatments (Anderson-Darling test, Tables A6-A10, Appendix 2, p>0.05). Data for nucleus, lipid, mitochondria, vacuoles, plastoglobuli, and pyrenoid did not conform to normal distribution (Anderson-Darling test, Tables A6-A10, Appendix 2, p>0.05). Arcsine transformation of the zero control non-normally distributed organelles did not achieve normality (Anderson-Darling test, Table A7, Appendix 2, p<0.05). Detailed results of the statistical analysis are shown in Appendix 2.

The differences in volume fractions for organelles that are non-normally distributed in zero control, methanol control, 2.5 μ M and 50 μ M samples (which are nucleus, mitochondria, lipid, vacuoles, cytoplasm, chloroplast, plastoglobuli and pyrenoid) were tested using the Kruskal-Wallis test (results, section 3.3.1.3). The data of organelles that were normally distributed (which are chloroplast, cytoplasm, thylakoid membrane, starch and matrix) were subjected to Levene's test of homogeneity of variances and showed no significant differences in the variances of cytoplasm, thylakoid membrane, starch and matrix for the four treatments (zero control, methanol control, 2.5 μ M and 50 μ M). Therefore, it can be assumed that cytoplasm, thylakoid membrane, starch and

matrix were drawn from populations with equal or similar variances (Levene's tests, L-values are shown in Table A11, Appendix 2, p>0.05) and ANOVA was used to test whether there were any significant differences in volume fractions of the organelles mentioned in the four treatments (results, section 3.3.2). Levene's test of homogeneity of variances showed significant differences in the variance of chloroplast for the four treatments (zero control, methanol control, 2.5 μ M and 50 μ M). Therefore, it cannot be assumed that the chloroplast were drawn from populations of equal variance (Levene's tests, L-value are shown in Table A11, Appendix 2, p<0.05) and the Kruskal-Wallis test were used to test whether there were any significant differences in volume fractions of the chloroplast for the four treatments (zero control, methanol control, 2.5 μ M and 50 μ M) (results, section 3.3.1.3).

3.2.3.3 Nannochloropsis oculata: testing the differences between volume fractions of log and stationary phases

Anderson-Darling tests were conducted for each organelle for active and stationary growth phases. For actively growing (log phase) cells the data for the mitochondria, chloroplast, cytoplasm, thylakoid membrane, cell wall and matrix conformed to normal distributions (Anderson-Darling test, Table A12, Appendix 2, p>0.05), whereas the data for nucleus, lipid, vacuoles, and plastoglobuli did not (Anderson-Darling test, Table A12, Appendix 2, p<0.05). The absence of storage body in log phase cells prevented a statistical analysis. The use of arcsine did not transform the data to normality (Anderson-Darling test, Table A14, Appendix 2, p<0.05). For stationary phase cells, the data for the lipid and cell wall conformed to normal distributions (Anderson-Darling test, Table A13, Appendix 2, p>0.05), whereas the data for nucleus, mitochondria, vacuoles, chloroplast, thylakoid membrane, plastoglobuli, matrix and storage bodies were not normal (Anderson-Darling test, Table A13, Appendix 2, p<0.05). The use of arcsine transformed the data of cytoplasm, chloroplast, matrix, and thylakoid membranes to normality (Anderson-Darling test, Table A15, Appendix 2, p>0.05).

Based on the normality results, the volume fractions for nucleus, lipid, vacuoles, mitochondria, and plastoglobuli in the active and stationary phases were tested using Mann-Whitney *U*-tests (results, section 3.3.2.2), whereas the volume fractions of cytoplasm, chloroplast, matrix, thylakoid membranes and cell wall were tested using t-tests. Equal variance tests (F-test) were conducted before the t-tests. The active and stationary phase volume fractions for cytoplasm, chloroplast, matrix, thylakoid

membrane and cell wall had equal variances (F-test, F values are shown in Table A16, Appendix 2, p<0.05). Therefore, a t-test for equal variances was used to test that there were no significant differences in volume fractions of the organelles mentioned in active and stationary phase growing cells (results section 3.3.2.2).

3.2.3.4 *Nannochloropsis oculata*: testing the differences between volume fractions of decadienal-treated cells

The testing for normality of volume fraction data for zero control, ethanol control, 1 μ M, 10 μ M and 50 μ M was conducted using the Anderson-Darling test. Data for the matrix conformed to normal distributions in all five treatments (Anderson-Darling test, Tables A17-A21, Appendix 2, p>0.05). Data of the cytoplasm volume fraction was successfully arcsine-transformed (Anderson-Darling test, Table A22, Appendix 2, p>0.05), whereas data for cell wall, nucleus, mitochondria, lipid, vacuoles, chloroplast, plastoglobuli, and thylakoid membrane were not normal (Anderson-Darling test, Tables A17-A21, Appendix 2, p<0.05).

The volume fractions for nucleus, mitochondria, lipid, vacuoles, cell wall, chloroplast, thylakoid membranes and plastoglobuli were tested using the Kruskal-Wallis test and showed there was no significant difference in volume fractions of different organelles between the four different treatments (results, section 3.3.2.3). The volume fractions of cytoplasm and matrix had no significant difference in variance between the four treatments (Levene's test, L-vales are shown in Table A23, Appendix 2, p>0.05) and were therefore analysed using ANOVA to test that there were no significant differences in volume fractions of the cytoplasm and matrix in the four treatment samples (zero control, ethanol control, $1\mu M$, $10\mu M$ and $50\mu M$) (results section 3.3.2.3).

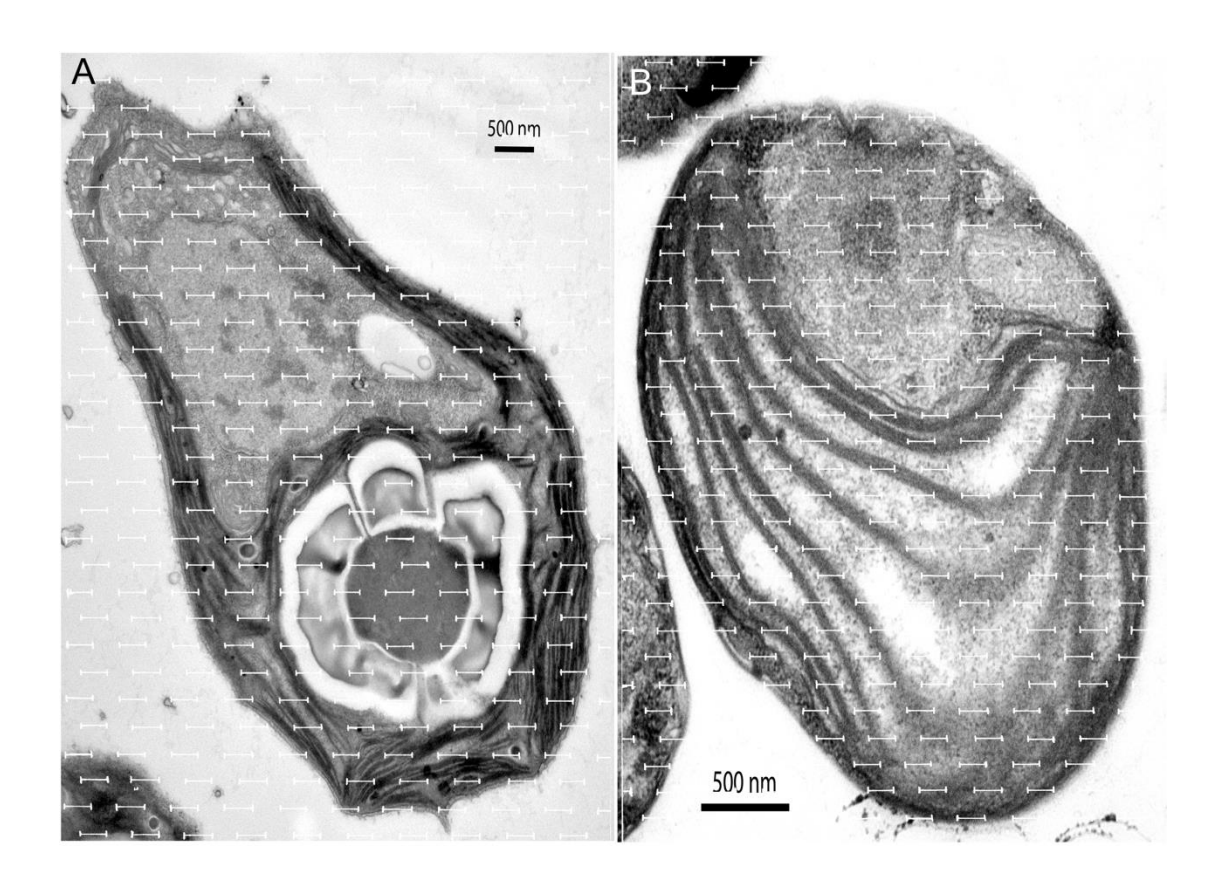


Figure 3.4: Stereological analysis

A) Longitudinal section of cell of *Dunaliella salina*, showing superimposed 1cm x 1cm lattice used to calculate volume fractions of the main organelle components. B) Longitudinal section of cell of *N. oculata*, showing superimposed 1cm x 1cm lattice used to calculate volume fractions of the main organelle components. Stereology is a discipline of science based on a complex set of mathematical principles that provide methods of calculating the three-dimensional structure of cells and cell organelles based on their two-dimensional appearance in the thin section (Weibel 1969; Steer 1981; Russ 1986). The volume fraction (Vv: the volume occupied by an organelle within the whole cell volume) occupied by an organelle is found by grid point counting. In grid point counting, a lattice grid containing 1 cm lines separated from each other by 1 cm is inserted over the micrograph. The number of points (at the end of each 1 cm line) that lies over each organelle is counted then divided by the total number of points that cover the cell. Steer (1981) showed that this method reduces the loss of accuracy.

3.3 Results

3.3.1 Dunaliella salina ultrastructure

3.3.1.1 Ultrastructure of actively growing 7-day-old cells

Dunaliella salina (CCAP19/30) cells were ovoid (Figure 3.5A-D, G) to pyriform (Figure 3.5E, F and H) and somewhat variable in size, with the average cell length 9 μm (ranging from 6 μm to 14 μm), and an average cell width of 5.5 μm (ranging from 4 μm to 8 μm). The lower part of the cell contained the bright green cup-shaped plastid, whereas the apical region, where the nucleus is located, was more translucent (Figure 3.5A-G). In some cells, the red plastid eyespot was seen (Figure 3.5B), as was the more round pyrenoid (Figure 3.5A, B, G). Each cell had a pair of isokont (equal length) flagella (Figure 3.5A-I, K), which were inserted in a small apical boss (projection, Figure 3.5H, K). Under the SEM, the two smooth flagella (average length of around 15 μm) had gently tapering tips (Figure 3.5I). Although appearing perfectly smooth at low magnification (Figure 3.5I), at higher power there appeared to be two rows of bubble-like projections either side of the axoneme (Figure 3.5K). In the SEM, the cell surface could be seen to be coated with larger bubble-like structures or granules (Figure 3.5H and J) which were not apparent under the light microscope (Figure 3.5A-G).

The internal cytoplasmic organisation of 10-day-old active growth phase *D. salina* cells under the TEM revealed a cell structure similar to that previously described for this species (Preisig 1992). *D. salina* cells lack rigid cell walls and have a thin flexible cell coat, which presumably accounts for the variable cell shape (Figure 3.5H-M). The cell coat layer that overlies the electron-dense plasma membrane was composed of an outer layer of fine granular/fibrillar material (Figure 3.5L, M and J) from which there were occasional stalked projections (Figure 3.5M arrowed).

The single cup-shaped chloroplast occupied just over half the cell volume (55%, Figure 3.7) and was packed with parallel arrays of tightly stacked thylakoids (Figures 3.5L, N, and 3.6G, K). The lamella was made up of two to six thylakoids (Figures 3.5L and 3.6G). The prominent pyrenoid found in the basal part of the chloroplast was centrally located (Figures 3.5N and 3.6K). The large amorphous core of the pyrenoid was surrounded by a variable number of large starch grains. The individual starch grains had a grey core surrounded by a halo of electron-lucent material (Figures 3.5N and 3.6K). Starch grains were also found in distal parts of the chloroplast, where they were (not usually) surrounded by the electron-lucent material (Figures 3.5L, N and 3.6G, K).

Single thylakoids also penetrated into the pyrenoid matrix and attached to the pyrenoid core (Figure 3.6K). Small electron-dense plastoglobuli (lipid storage bodies) were also scattered throughout the chloroplast (Figures 3.5N and 3.6K). The eyespot was well developed and lateral (Figure 3.6E).

The outer rim of the chloroplast's cup-shaped plastid extended into the anterior part of the cell, and enclosed the zone where most of the main cytoplasmic organelles were located (Figures 3.4A 3.5N). The nucleus was found in the anterior region of the cell (Figure 3.5N). It was a large nucleus and the nuclear envelope with inner and outer membranes was present. It was spherical in shape with concavity in the site associated with dictyosomes of the Golgi body (Figure 3.5N). In addition, the nuclear pores could be clearly seen (Figure 3.5N, red arrows). Ovoid to capsule-shaped (Figure 3.5N) or branched (Figure 3.6I) mitochondrial profiles were also scattered throughout the anterior region of the cytoplasm, usually lying close to the chloroplast envelope and around the nucleus (Figures 3.5N and 3.6I).

The endoplasmic reticulum (ER) was found directly under the cell membrane. Furthermore, it was parallel to it and the ribosomes found on the outer surface of the ER (Figure 3.6A, red arrow). Two Golgi dictyosome profiles were seen, closely associated with the nuclear envelope oriented towards the basal bodies of the flagellum at the anterior end of the cell (Figures 3.5N, and 3.6A and C). One Golgi dictyosome was perpendicular to the longitudinal axis of the cell, while the other was parallel to it (Figure 3.6A). They were surrounded by several cytoplasmic vesicles lying between the dictyosome and nucleus (Figures 3.5N and 3.6A). Small electron-lucent vacuoles were also present in the cytoplasmic anterior zone of the cell. However, in these actively growing cells, lipid globules were rarely observed (Figure 3.5N).

3.3.1.2 Ultrastructure of 14-day-old stationary phase cells

D. salina cells from a 14-day-old stationary phase culture had a much altered cytoplasm, compared with their actively growing counterparts (Figure 3.5O). The chloroplast remained the largest and most conspicuous organelle, and in stationary cells occupied approximately 64% of cell volume (Figures 3.5O and 3.7), which represented an approximately 15% increase compared with normal actively growing cells. There was no significant difference between the chloroplast volume fraction of the active phase growing cells and that of the stationary phase growing cells (Table 3.3, Figure 3.7). However, the statistical analysis of volume fractions of the chloroplast constituents

(thylakoid membranes, pyrenoid, matrix and starch) showed significant differences between active phase growing cells and stationary phase growing cells. The most conspicuous change within chloroplast constituents was that, in stationary cells, the whole plastid appeared to be packed with starch grains which had their usual grey core and electron-lucent outer region (Figure 3.50). There was a significant increase in starch mean volume fraction between the active phase growing cells (mean = 14.1%, 95% CI: (11.8, 16.9)) and the stationary phase growing cells (mean = 41.9%, 95% CI: (38.4, 45.5))(t- test, Table 3.3, Figure 3.7). In contrast to starch, the thylakoid content of the plastid showed a significant decrease in volume fraction (Figure 3.7). There was a statistically significant reduction in mean volume fraction of thylakoid membranes in active phase growing cells (mean = 27.8%, 95% CI: (26.0, 30.9)) compared to that in the stationary phase growing cells (mean= 19.1%, 95% CI: (16.8, 21.4)) (t-test, Table 3.3, Figure 3.7). The thylakoid membranes were stacked and condensed into each other (Figure 3.6H), in contrast to actively growing cells where they formed a grana-like structure composed of 2-6 thylakoids membranes (Figure 3.6G). Furthermore, there was a significant reduction in mean volume fraction of matrix between active phase growing cells (mean = 9.7%, 95% CI: (8, 11.3)) and stationary phase cells (mean = 2%, 95% CI: (1.4, 2.6)) (t-test, Table 3.3, Figure 3.7). The pyrenoid also was present in the stationary phase cells (Figure 3.6L), although there was no statistically significant difference in median volume fraction between growth phases (Mann-Whitney *U*-test, Table 3.4, Figure 3.8).

In addition to the increase in plastid starch grains, stationary phase cells of D. salina also had large lipid globules located between the nucleus and plastid (Figure 3.3O). There was a statistically significant difference in the median lipid volume fraction between the active phase growing cells (median = 0.00%, 95% CI: (-0.02, 0.05)) and stationary phase growing cells (median = 7.12%, 95% CI: (5.22, 9)) (Mann-Whitney U-test, Table 3.4 Figure 3.8).

The dictyosomes of the Golgi apparatus became attached to each other, were increased in number and were separated by vacuoles (Figure 3.6B). The vacuoles had electrondense content (Figure 3.6B, D). On the other hand, there was no statistically significant difference in median volume fraction of vacuoles between growth phases (Mann-Whitney *U*-test, Table 3.4, Figure 3.8).

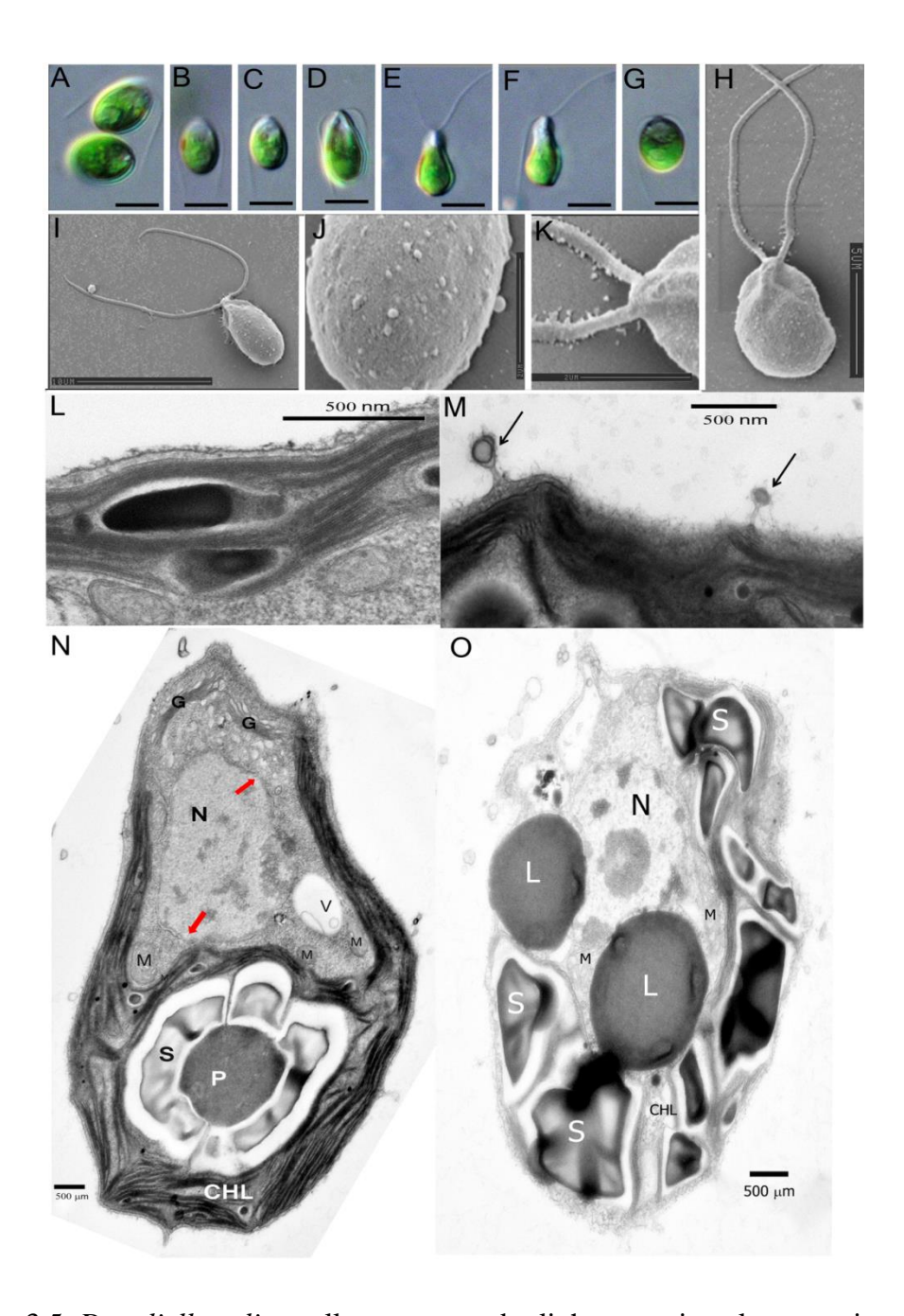
There was a statistically significant reduction in the volume fraction of the mitochondria of the stationary phase growing cells (mean = 2%, 95% CI: (1.2, 6.7)) compared with that of actively growing cells (mean = 3.2%, 95% CI: (1.2, 5.2)) (t-test, Table 3.3, Figure 3.7). The eyespot/stigma in stationary cells had the same characteristics of this organelle in active phase cells (Figure 3.6E, F), although the number of plastoglobuli appeared greater in stationary phase cells (Figure 3.6L) than in active phase cells (Figure 3.6K). There was no statistically significant difference in median volume fractions of plastoglobuli in the active phase and stationary phase growing cells (Mann-Whitney U-test, Table 3.4, Figure 3.8). Finally, no change in cell size was detected, as the mean cell length was 9 μ m for both active and stationary growth phases, and the mean cell width was 5 μ m for both.

Table 3.3: Results of t-tests for volume fractions of cytoplasm, mitochondria, chloroplast, matrix, thylakoid membranes and starch in *Dunaliella salina* active and stationary phase cells

Organelle	t	DF	P
Cytoplasm	4.86	58	< 0.001
Mitochondria	5.92	29	< 0.001
Chloroplast	-3.07	59	0.003
Matrix	9.75	29	< 0.001
Thylakoid membranes	6.24	58	< 0.001
Starch	-12.01	58	< 0.001

Table 3.4: Results of Mann-Whitney tests for volume fractions of nucleus, lipid, vacuoles, plastoglobuli and pyrenoid in *Dunaliella salina* active and stationary phase cells

Organelle		W	n	p
	Active		30	
Nucleus	Stationary	1169	30	0.001
Lipid	Active	548.5	30	< 0.001
	Stationary	348.3	30	<0.001
Vacuoles	Active		30	
vacuoles	Stationary	937.5	30	0.741
	Stationary		30	
Dlastoglobuli	Active	914.0	30	0.993
Plastoglobuli	Stationary	914.0	30	0.553
	Active		30	
Pyrenoid	Stationary	934.5	30	0.774
	Stationary		30	



Figur 3.5: *Dunaliella salina* cell structure under light, scanning electron microscopy and comparison between exponential and stationary growth phases of *Dunaliella salina* under lower magnification transmission electron microscopy

A-G) Light microscopy images of *D. salina* showing the variable cell shapes and the two flagella. Scale har 5 µm. H-D Scanning electron micrographs of *D. salina* showing

two flagella. Scale bar 5 μ m. H-I) Scanning electron micrographs of *D. salina* showing the equal length flagella and the granulated cell coat. Scale bars mentioned on each figure. J) Higher power magnification of the flagellar apparatus base Scale bar 2 μ m. K) Higher magnification of the cell coat showing different-sized granules. Scale bar 2 μ m (L) Higher magnification of the cell coat under transmission electron microscope. Scale bar 0.5 μ m. M) Higher magnification of the cell coat under transmission electron microscope. Scale bar 0.5 μ m. N) Transmission electron micrograph of exponentially growing cells. Scale bar 0.5 μ m. O) Transmission electron micrograph of stationary phase cells. Scale bar 0.5 μ m. Chl: chloroplast; G: Golgi; L: lipid bodies; M: mitochondria; N: nucleus; P: pyrenoid; S: starch; V: vacuoles.

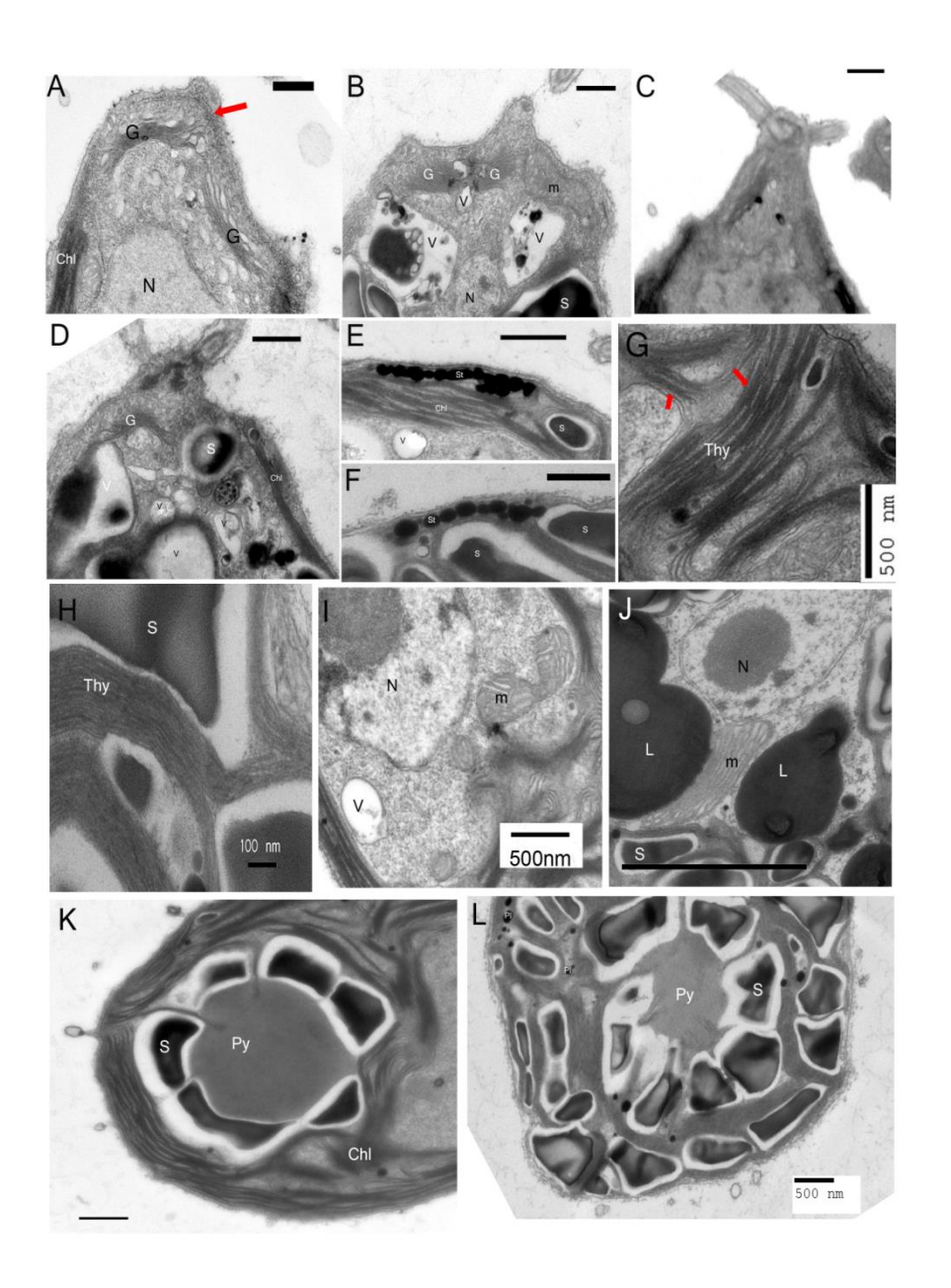


Figure 3.6: Comparison of exponential and stationary growth phases of *Dunaliella salina* at higher magnification of transmission electron microscope
A) Golgi apparatus in exponential growth phase. Scale bar 0.5 μm. B) Golgi apparatus in stationary growth phase. Scale bar 0.5 μm. C) Golgi apparatus in exponential growth phase with flagella origin. Scale bar 0.5 μm. D) Golgi apparatus in stationary growth phase with flagella origin. Scale bar 0.5 μm. E) Stigma in exponential growth phase. Scale bar 0.5 μm. F) Stigma in stationary growth phase. Scale bar 0.5 μm. G) Thylakoid membranes in exponential growth phase. Scale bar 0.5 μm. H) Thylakoid membranes in stationary growth phase. Scale bar 0.1 μm. I) Mitochondria in exponential growth phase. Scale bar 0.5 μm. L) Pyrenoid in stationary growth phase. Scale bar 0.5 μm. Chl: chloroplast; G: Golgi; L: lipid bodies; M: mitochondria; N: nucleus; Pl: plastoglobuli; Py: pyrenoid; S: starch; St: stigmata; Thy: thylakoid; V: vacuoles.

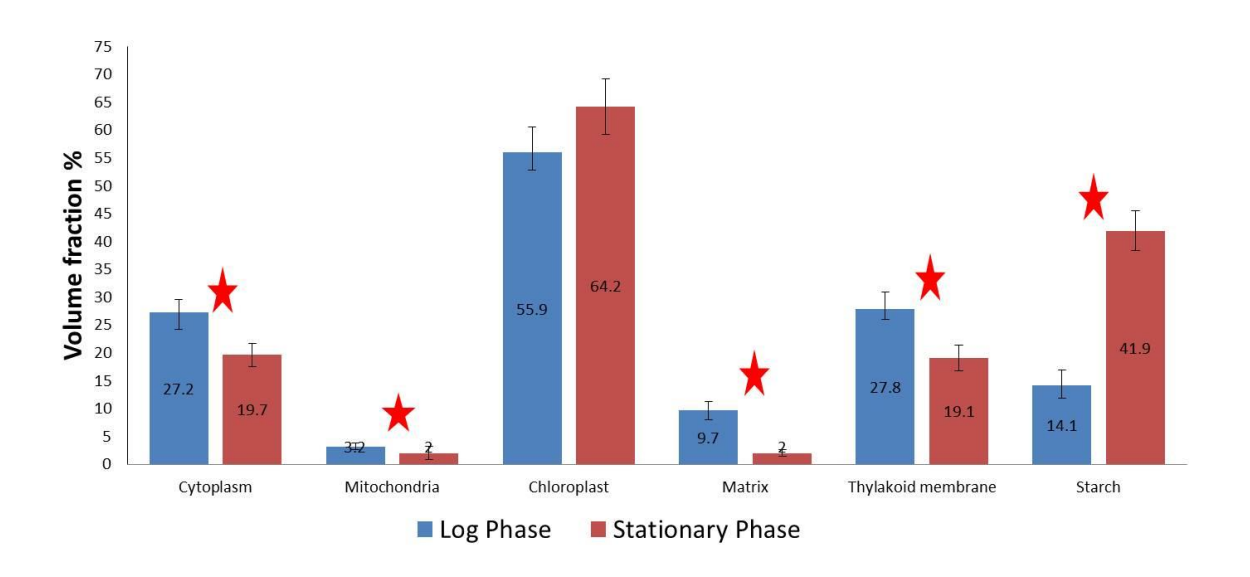


Figure 3.7: Mean and 95% confidence intervals of volume fractions of the cell organelles in *Dunaliella salina* log and stationary phase cells The volume fraction data for each organelle were subjected to a separate t-test. Stars indicate significant differences between log and stationary phase volume fractions of an organelle.

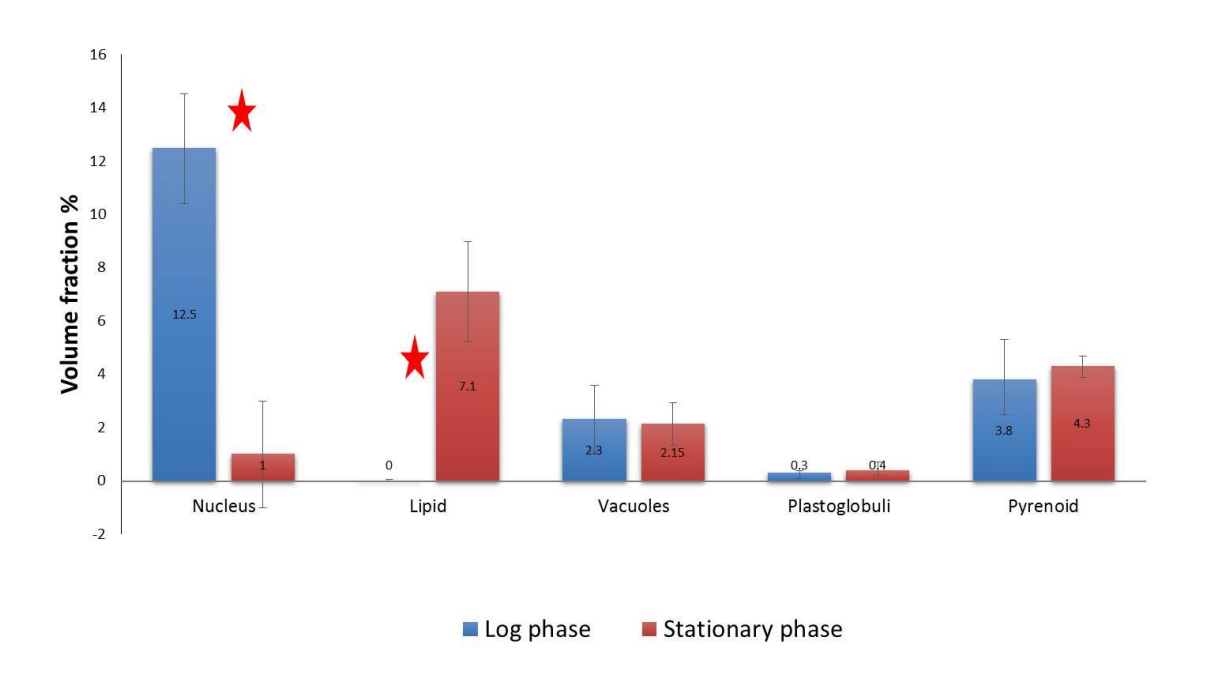


Figure 3.8: Median and 95% confidence intervals of volume fractions of the cell organelles in *Dunaliella salina* log and stationary phase cells Data of each organelle were tested using the Mann-Whitney test. Each pair represents a separate test. Pairs with stars show significant differences.

3.3.1.3 Ultrastructure of decadienal-treated cells

Two control samples were used: one of 0 μ M decadienal, and the other a solvent blank using methanol (Figures 3.9A, G). A comparison of actively growing cells (Figure 3.5N), control cells (Figure 3.9A, G) and those treated with 2.5 μ m decadienal (Figure 3.2N) indicated that ultrastructural differences were rare. There were no clear differences between the methanol control (Figure 3.9G-K) and normal actively growing cells (with 0 μ M decadienal) (Figure 3.9A-F). Only samples treated with 50 μ M decadienal showed ultrastructural alterations. Its effect on the ultrastructure of *D. salina* cells varied. Some cells remained intact and preserved their shape (Figure 3.11B), whilst others became more rounded in shape without leakage of intracellular content (Figure 3.10A). In contrast, other cells were lysed and cytoplasmic consumption was obvious as all cellular organelles disappeared except for starch granules with intact cell membranes (Figure 3.11E, F). Alterations to specific organelles are described below.

The ovoid to pyriform cell shape was maintained in all treatments (Figure 3.9A, G), as was the variability in cell size. The mean cell length was 9 μ m (ranging from 6 μ m to 12 μ m) and mean cell width 5 μ m (ranging from 1 μ m to 8 μ m) for 0 μ M decadienal. For the methanol control, the mean cell length was 8 μ m (ranging from 7 μ m to 11 μ m) and mean cell width 5 μ m (ranging from 4 μ m to 7 μ m). The basal cup-shaped chloroplast with a prominent central pyrenoid (Figure 3.9 A, G) constituted more than 50% of the volume fraction (57.4% for untreated cells, 55.7% for methanol control, 56.6% 2.5 μ M decadienal-treated cells and 55.9% for 50 μ M decadienal-treated cells). There was no significant difference in the median volume fractions of the chloroplast (Kruskal-Wallis test, Table 3.6, Figure 3.13).

The chloroplasts were packed with parallel arrays of tightly stacked thylakoids that constituted 30% of cell volume fraction, with the pyrenoid found in the basal part. The structure of thylakoids and photosynthetic lamellae showed alterations in 50 μ M decadienal treatments. This varied between cells, with some having no changed structures, where the thylakoids formed a grana-like structure (Figure 3.11B, C). Other cells had condensed thylakoid membranes (Figure 3.11A). In other cells, both structures were found (Figure 3.11D). There was a statistically significant difference in mean volume fraction of the thylakoid membranes between different treatments (ANOVA test, Table 3.5, Figure 3.12). Post-hoc Tukey pairwise comparison (P = 0.05) showed that the thylakoid volume fraction was significantly lower in samples treated with 2.5

μM decadienal (mean = 25.1%, 95% CI: (23.3, 26.8)) than in samples treated with 0 μM decadienal (mean = 29.6%%, 95% CI: (27.7, 31.9)) and the methanol control (mean = 30.1%%, 95% CI: (28.2, 32.1)). The starch grains surrounded the pyrenoid and were found to be separated throughout the chloroplast (Figure 3.9A, G). There was no significant difference in the median volume fractions of the pyrenoid (Kruskal-Wallis test, Table 3.6, Figure 3.13). There were also no statistically significant differences in the mean volume fractions of the starch between different treatments (ANOVA test, Table 3.5, Figure 3.12). However, the matrix volume fraction showed significant differences between the different treatments (ANOVA test, Table 3.5, Figure 3.12). Small electron-dense plastoglobuli (lipid storage bodies) were also scattered throughout the chloroplast (Figure 3.9A, G). There was no significant difference in the mean volume fractions of plastoglobuli (Kruskal-Wallis test, Table 3.6, Figure 3.13). The eyespot was well developed and lateral (Figure 3.9F, L).

The plastid again extended into the anterior part of the cell, and enclosed the zone where most of the main cytoplasmic organelles were located (Figure 3.9A, C, G). The cytoplasm density increased in samples treated with 50 µM decadienal, and some membranous organelles were hardly detectable, such as the Golgi dictyosome and endoplasmic reticulum (Figure 3.11A, B). Cytoplam median volume fraction was not significantly different between different treatments (ANOVA test, Tables 3.5, Figure 3.12).

The nucleus was located in the anterior region of the cell (Figure 3.6A, C, G). It was a large nucleus and the nuclear envelope was present with inner and outer membranes. It was spherical in shape with concavity in the site associated with dictyosomes (Figure 3.9A, C, D, and G). Cells treated with 50 μ M decadienal showed an increased gap in the nuclear envelope, whose size in 50 μ M decadienal-treated cells was 125 nm (Figures 3.10B, 3.11B and C) while it was only 30 nm in control cells (Figure 3.9A, G). In addition, some cells showed chromatin condensation and margination (Figure 3.11A, C, and D), and others showed karyolysis (chromatin dissolution) (Figure 3.11B). There was a statistically significant difference in the median volume fractions of the nucleus between different decadienal treatments (Kruskal-Wallis test, Table 3.6, Figure 3.13). The median volume fractions of the nucleus in samples treated with 50 μ M decadienal (median = 8.2%, 95% CI: (6.3, 10)) were significantly lower than in all other treatments (0 μ M decadienal median = 12.66%, 95% CI: (10.06, 15.36); 2.5 μ M decadienal median

= 14.9%, 95% CI: (12.7, 14.86); and methanol control median =13.7%, 95% CI: (11.75, 15.7) (Kruskal-Wallis test, Tables 3.6, 3.7, Figure 3.13).

The profiles of mitochondria were ovoid to capsule-shaped (Figure 3.9A, B, C, G, K) and they were scattered throughout the anterior region of the cytoplasm, usually lying close to the chloroplast envelope and around the nucleus (Figure 3.9 A, C, D, G). The mitochondrial profiles in samples treated with 50 µM decadienal showed evidence of lysis and rupture (Figures 3.10B and 3.11A-D). Cavities appeared in the cytoplasm in the region where mitochondria were usually present in the cell (Figure 3.11A-D). There was a statistically significant difference in median volume fractions of mitochondria between different decadienal treatments (Kruskal-Wallis test, Tables 3.6 and 3.7, Figure 3.13). The mitochondria median volume fraction in sample treated with 50 µM decadienal (median = 0%, 95% CI: (-0.6, 0.6)) were significantly lower than in all other treatments (0 µM decadienal median = 2.9%, 95% CI: (2.1, 3.7); 2.5 µM decadienal median = 2.62%, 95% CI: (2.02, 3.22); and $methanol\ median = 9.5\%$, 95% CI: (9, 10)) (Kruskal-Wallis test, Tables 3.6 and 3.7, Figure 3.13). The mitochondria median volume fractions in samples treated with 2.5 μ M decadienal (median = 2.62%, 95% CI: (2.02, 3.22)) were significantly less than those in 0 μ M decadienal (median = 2.9%, 95% CI: (2.1, 3.7)) and methanol (median = 9.5%, 95% CI: (9, 10)) (Kruskal-Wallis test, Tables 3.6 and 3.7, Figure 3.13). The mitochondria median volume fractions in samples treated with 0 μ M decadienal (median = 2.9%, 95% CI: (2.1, 3.7) and methanol control (median = 9.5%, 95% CI: (9, 10)) were not significantly different from each other (Kruskal-Wallis test, Tables 3.6 and 3.7, Figure 3.13).

Two Golgi dictyosome profiles were seen, closely associated with the nuclear envelope and oriented towards the basal bodies of the flagellum at the anterior end of the cell (Figure 3.9A, D, G, J). They were surrounded by several cytoplasmic vesicles lying between the dictyosome and nucleus (Figure 3.9D, J). Small electron-lucent vacuoles were also present in the cytoplasmic anterior zone of the cell.

When compared to controls and 2.5 μ M decadienal-treated cells, the 50 μ M decadienal-treated cell structure showed lipid production, with volume fractions of lipids increasing from 0 for 0 μ M, methanol and 2.5 μ M decadienal to 0.72% in 50 μ M decadienal. These observations revealed the presence of lipid bodies in 50 μ M decadienal (Figures 3.10B and 3.11A-D, G, H). These lipid bodies resembled lipid bodies found in the

stationary phase samples (Figure 3-5O). There was a statistically significant difference in median volume fractions of lipid between different decadienal treatments (Kruskal-Wallis test, Table 3.6). The lipid median volume fractions in samples treated with 50 μ M decadienal (median = 0.72%, 95% CI: (0.12, 1.22)) were significantly higher than all other treatments 0 μ M decadienal (median = 0%, 95% CI: (0, 0)), 2.5 μ M decadienal (median = 0%, 95% CI: (-0.007, 0.04)) and methanol (median = 0%, 95% CI: (0, 0)) (Kruskal-Wallis test, Tables 3.6, 3.7 and Figure 3.13). There were no significant differences between the remaining three treatments.

The distinctive alteration that presented frequently in 50 µM decadienal-treated cells was extensive cytoplasmic vacuolation. Compared with the control, decadiena-treated D. salina showed vacuoles with a larger volume which contained different types of inclusions varying in shape and electron density (Figure 3.11A-D). The only alteration in the ultrastrucuture of cells treated with 2.5 µM decadienal was that the vacuoles contained electron dense (osmiophilic) inclusions (Figure 3.10C). There was a statistically significant difference in median volume fractions of vacuoles between different decadienal treatments (Kruskal-Wallis test, Table 3.6). The vacuole median volume fractions in samples treated with 50 μ M decadienal (median = 8.1%, 95% CI: (6.3, 10)) were significantly higher than in 2.5 μ M decadienal (median = 1.2%, 95% CI: (0.5, 1.9), 0 µM decadienal (median = 0.96%, 95% CI: (0.46, 1.56)) and methanol (median = 0.15%, 95% CI: (-0.41, 0.85)) (Kruskal-Wallis test, Tables 3.6, Mann-Whitney *U*-test, 3.7, Figure 3.13). The vacuole median volume fractions in samples treated with 0 μ M decadienal (median = 0.96%, 95% CI: (0.46, 1.56)) and 2.5 μ M (median = 1.2%, 95% CI: (0.5, 1.9)) were not significantly different (Kruskal-Wallis test, Tables 3.6 and Mann-Whitney *U*-test, 3.7, Figure 3.13). The vacuole median volume fractions in samples treated with methanol (median = 0.15%, 95% CI: (-0.41, 0.85)) were significantly lower than those in 2.5 μ M decadienal (median = 1.2%, 95%) CI: (0.5, 1.9), 0 μ M decadienal (median = 0.96%, 95% CI: (0.46, 1.56)) and 50 μ M decadienal (median = 8.1%, 95% CI: (6.3, 10)) (Figure 3.13).

Table 3.5: Results of ANOVA tests on the effects of decadienal treatments on the volume fraction of cytoplasm, thylakoid membranes, starch, and matrix in *Dunaliella salina*

Organelle	DF	F-statistic	P
Cytoplasm	3	1.17	0.323
	116		
	119		
Thylakoid	3	5.47	0.001
membranes	116		
	119		
Starch	3	0.19	0.900
	114		
	117		
Matrix	3	2.8	0.038
	116		
	119		

Table 3.6: Results of Kruskal-Wallis tests for volume fraction of nucleus, mitochondria, lipid, vacuoles, chloroplast, pyrenoid and plastoglobuli in *Dunaliella salina* decadienal-treated cells

Organelle	Н	DF	P
Nucleus	18.39	3	< 0.001
Mitochondria	39.58	3	< 0.001
Lipid	69.3	3	< 0.001
Vacuoles	61.11	3	< 0.001
Chloroplast	1.3	3	0.722
Pyrenoid	2.84	3	0.416
Plastolobuli	1.9	3	0.594

Table 3.7: Results of Mann-Whitney tests for significant differences between volume fractions of nucleus, mitochondria, lipid and vacuoles in *Dunaliella salina* decadienal-treated cells

Organelle	Tested concentrations	n	W	P
	0 μM Vs M	30, 30	877.5	0.583
	0 μM Vs 2.5 μM	30, 30	837.0	0.25
	0 μM Vs 50 μM	30, 30	1073.5	0.019
Nucleus	2.5 μM Vs M	30, 30	982.0	0.3255
	2.5 μM Vs 50 μM	30, 30	1188.0	0.0001
	50 μM Vs M	30, 30	677.5	0.0005
	0 μM Vs M	30, 30	930.0	0.8294
	0 μM Vs 2.5 μM	30, 30	1245.0	< 0.001
Mitochondria	0 μM Vs 50 μM	30, 30	1298.0	< 0.001
Mittochondra	2.5 μM Vs M	30, 30	488.0	< 0.001
	2.5 μM Vs 50 μM	30, 30	1255.0	< 0.001
	50 μM Vs M	30, 30	473.0	< 0.001
	0 μM Vs M	30, 30	919.5	0.909
	0 μM Vs 2.5 μM	30, 30	946.5	0.292
Lipid	0 μM Vs 50 μM	30, 30	595.5	< 0.001
Lipid	2.5 μM Vs M	30, 30	886.0	0.3298
	2.5 μM Vs 50 μM	30, 30	536.0	< 0.001
	50 μM Vs M	30, 30	1271.0	< 0.001
Vacuoles	0 μM Vs M	30, 30	1120.0	0.0023
	0 μM Vs 2.5 μM	30, 30	859.0	0.4095
	0 μM Vs 50 μM	30, 30	528.0	< 0.001
	2.5 μM Vs M	30, 30	1170.5	0.0002
	2.5 μM Vs 50 μM	30, 30	543.5	< 0.001
	50 μM Vs M	30, 30	1333.5	< 0.001

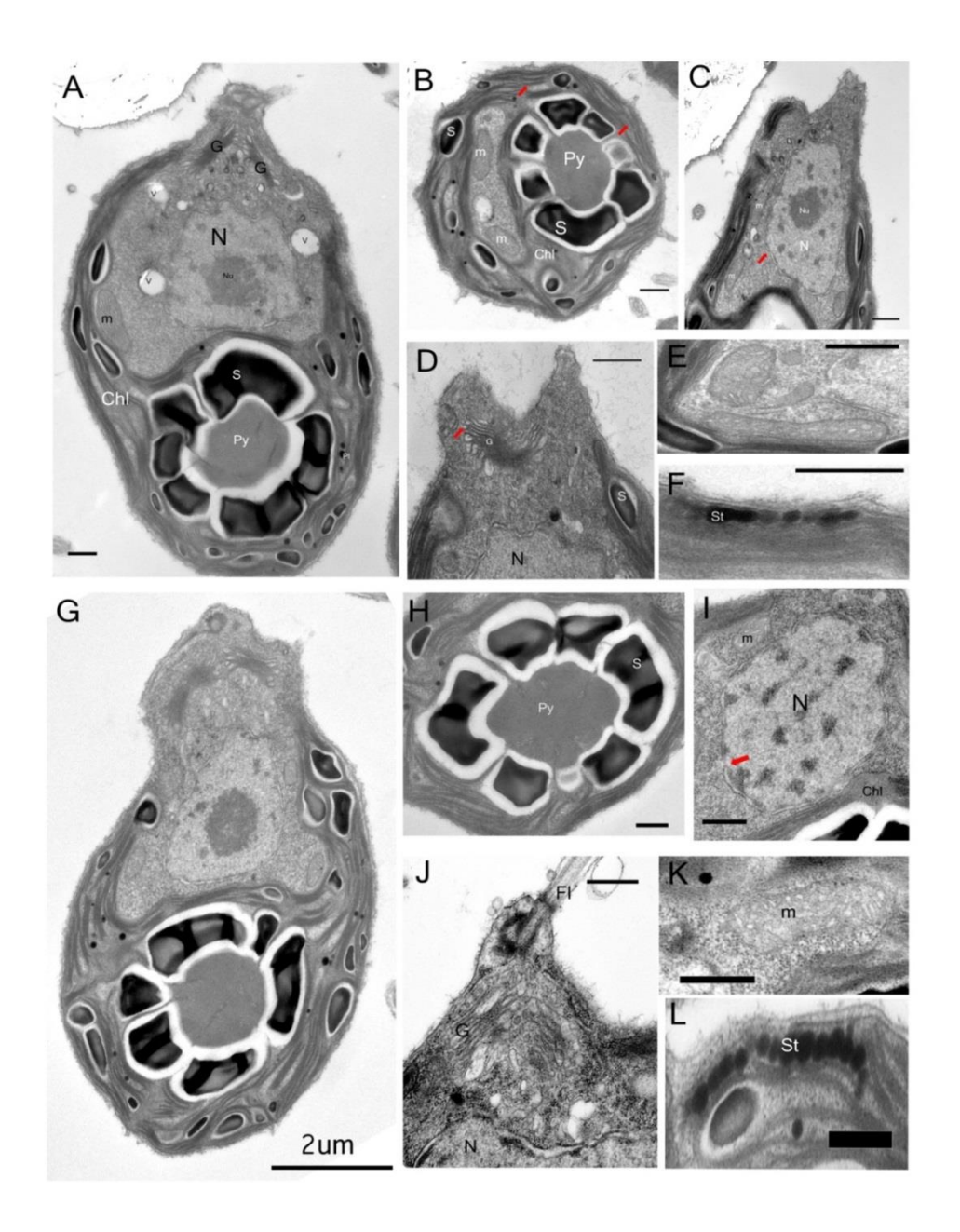


Figure 3.9: Comparisons of cell structures of two *Dunaliella salina* control samples A-F) Negative control (0 μ M decadienal-treated cells). G-K) Methanol control cells. A) Median longitudinal section of whole cell. Scale bar 0.5 μ m. B) Transverse section of lower part of the cell. Scale bar 0.5 μ m. C) Enlarged section of the nucleus. Scale bar 0.5 μ m. D) Higher magnification of Golgi apparatus. Scale bar 0.5 μ m. E) Higher magnification of mitochondrial profiles. Scale bar 0.5 μ m F) Higher magnification of stigmata. Scale bar 0.5 μ m. G) Median longitudinal section of whole cell of methanol control. Scale bar 0.5 μ m. H) Transverse section of lower part of the cell. Scale bar 0.5 μ m. I) Enlarged section of the nucleus. Scale bar 0.5 μ m. J) Higher magnification of Golgi apparatus. Scale bar 0.5 μ m. K) Higher magnification of mitochondrial profiles. Scale bar 0.5 μ m. L) Higher magnification of stigmata. Scale bar 0.5 μ m. Chl: chloroplast; G: Golgi; M: mitochondria; N: nucleus; Nu: nucleolus; Py: pyrenoid; S: starch; St: stigmata; V: vacuoles.

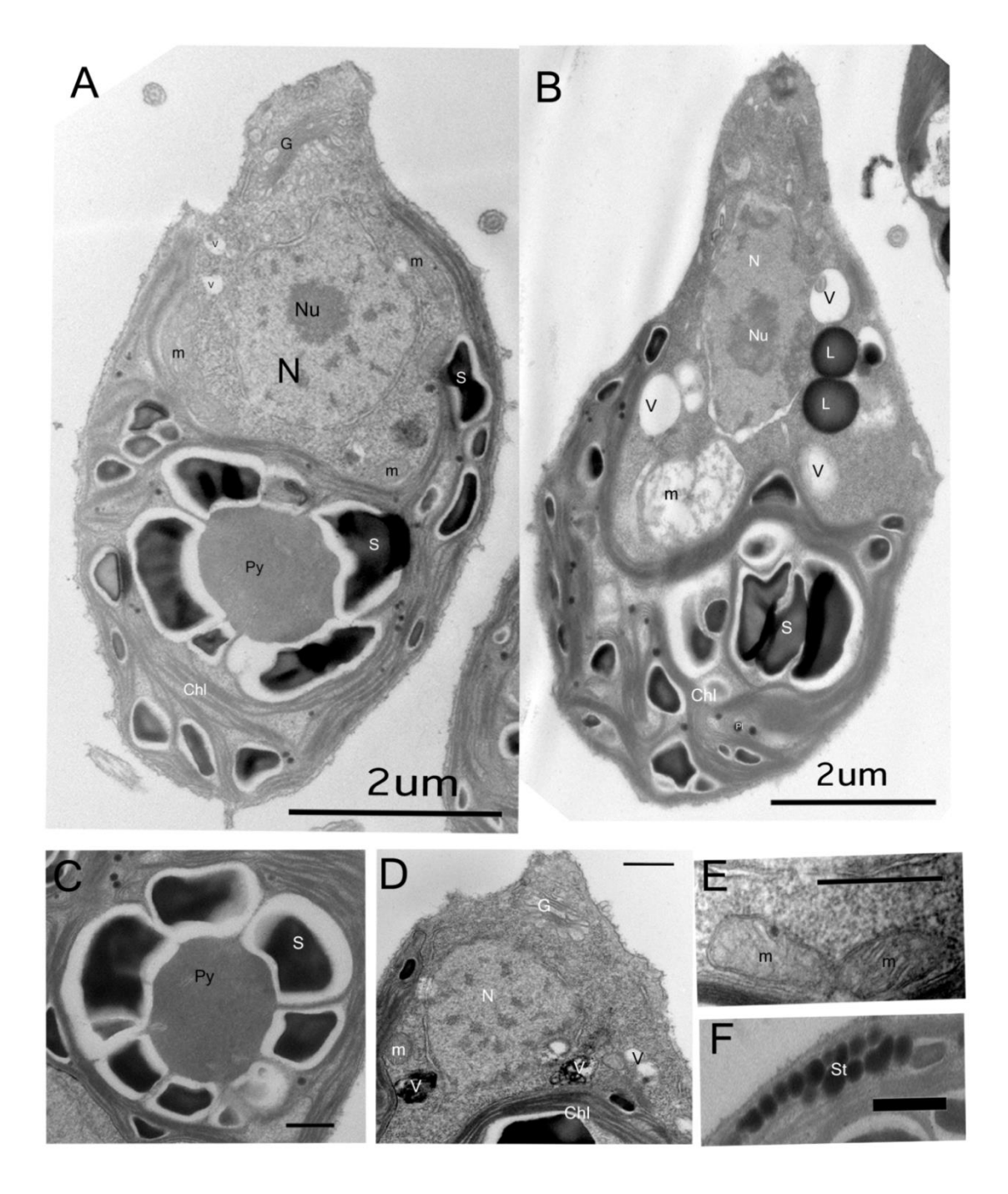


Figure 3.10: *Dunaliella salina* decadienal-treated cells
A) Median longitudinal section of whole cell treated with 2.5 μM decadienal. Scale bar 2 μm. B) Median longitudinal section of whole cell treated with 50 μM decadienal. Scale bar 2 μm. C) Transverse section of lower part of cell treated with 2.5 mM decadienal. Scale bar 0.5 μm. D) Enlarged section of the nucleus and Golgi apparatus cell treated with 2.5 μM decadienal. Scale bar 0.5 μm. E) Higher magnification of mitochondrial profiles of cell treated with 2.5 μM decadienal. Scale bar 0.5 μm F) Higher magnification of stigmata of cell treated with 2.5 μM decadienal. Scale bar 0.5 μm.Chl: chloroplast; G: Golgi; L: lipid bodies; M: mitochondria; N: nucleus; Nu: nucleolus; Pl: plastoglobuli; Py: pyrenoid; S: starch; St: stigmata; V: vacuoles.

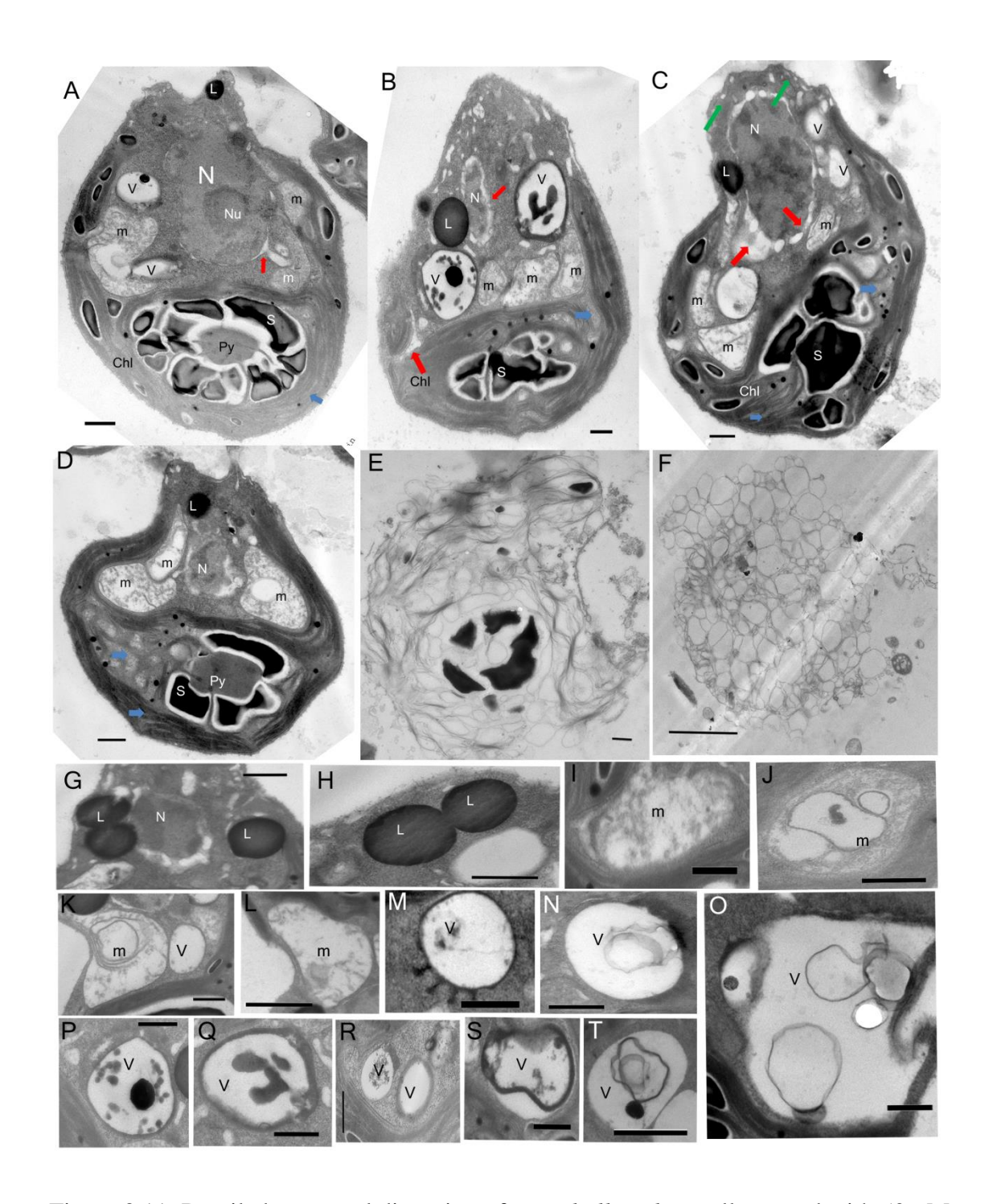


Figure 3.11: Detailed structural distortion of Dunaliella salina cells treated with 50 μM decadienal

A-D) Median longitudinal sections of whole cell treated with 50 μM decadienal. Scale bar 0.5 μm unless mentioned. E-F) Membrane residuals of lysed cells. Scale bar 0.5 μm . G-H) Lipid bodies of different shapes and sizes. Scale bar 0.5 μm . I-L) Different lysed mitochondrial profiles. Scale bar 0.5 μm . M-T) Different values appear in 50 μM treated cells only. Scale bar 0.5 μm .Chl: chloroplast; L: lipid bodies; M: mitochondria; N: nucleus; Nu: nucleolus; Py: pyrenoid; S: starch; V: vacuoles.

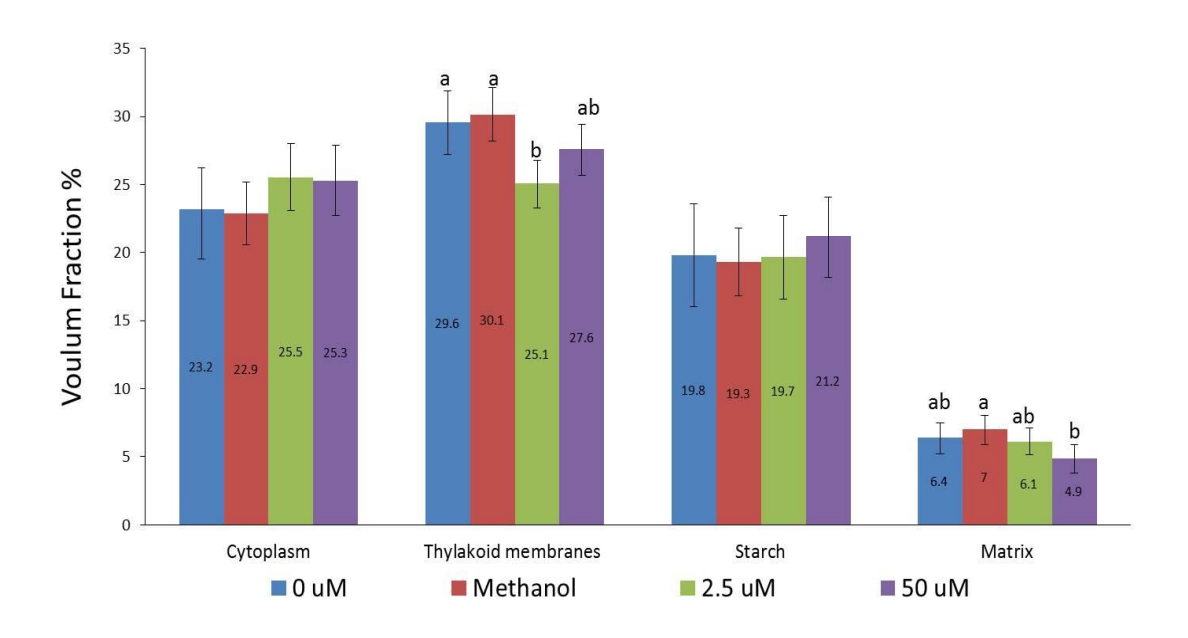


Figure 3.12: Means and 95% confidence intervals of volume fractions of the cytoplasm and chloroplast constituents in *Dunaliella salina* treated with decadienal Data for each organelle were tested with a separate ANOVA test. Treatments with the same letters are not significantly different from each other (Post-hoc Tukey pairwise comparison).

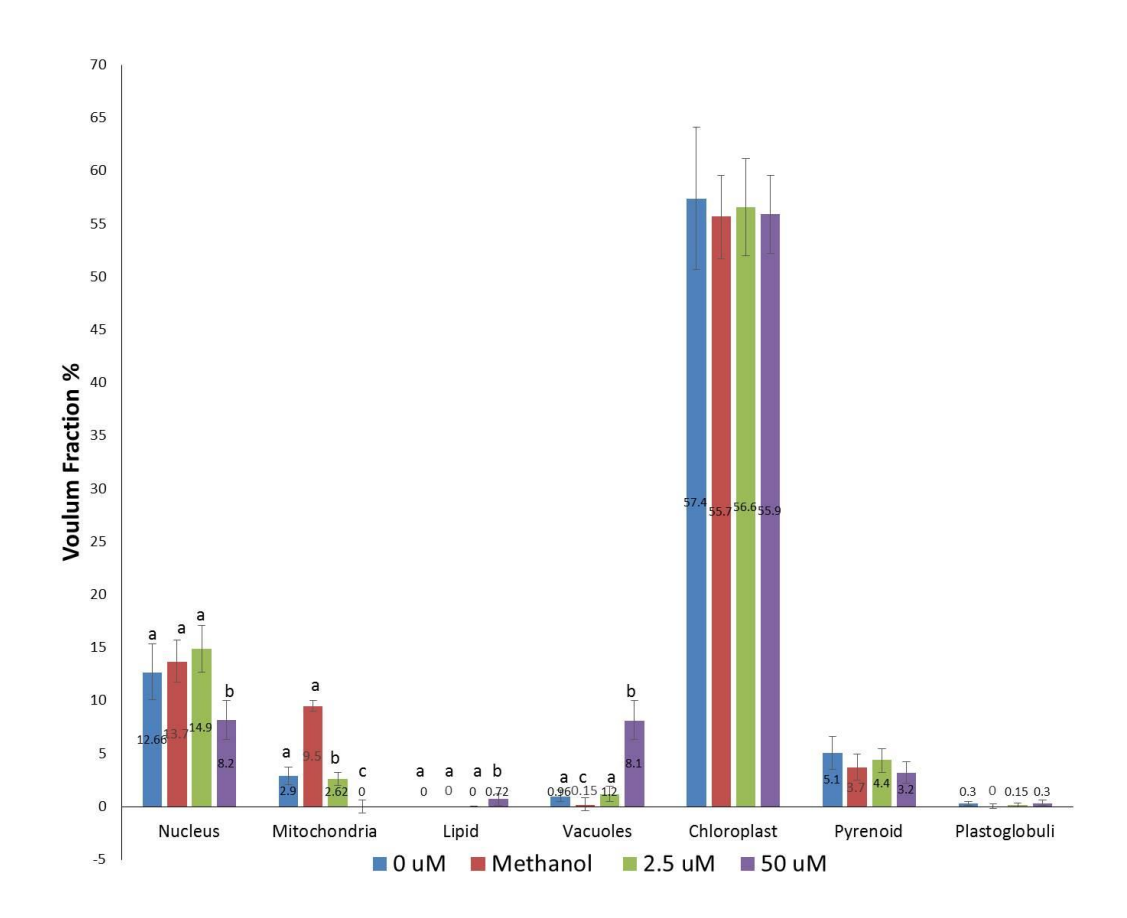


Figure 3.13: Medians and 95% confidence intervals of volume fractions of organelles in *Dunaliella salina* treated with decadienal Data for each organelle were tested with a separate Kruskal-Wallis test (P=0.05). Treatments with the same letters are not significantly different from each other (Mann-Whitney test (P=0.05)).

3.3.2 Nannochloropsis oculata ultrastructure

3.3.2.1 Ultrastructure of actively growing 6-day-old cells

Under the light microscope *Nannochloropsis oculata* (CCAP849/1) cells were small, ovoid, non-motile (Figure 3.14A, B) and somewhat variable in size, with an average cell length of 4 μ m (ranging from 3 μ m to 4.5 μ m), and an average cell width of 2.6 μ m (ranging from 1.5 μ m to 3.1 μ m). Each cell contained a single cup-shaped chloroplast which gives the cells their overall green appearance (Figure 3.14C). Under the SEM cells were ovoid (Figure 3.14D-E) and usually rather crumpled in appearance, even after critical point drying (Figure 3.14D-E). The cells often appeared as if dried down onto the coverslip with a halo of matrix material around them (Figure 3.14E arrowed).

The internal cytoplasmic organisation of 6-day-old active growth phase N. oculata is shown in Figure 3.14G-H. The simple round to ovoid cells were enclosed in a thin uniformly electron dense wall (8.9 µm) (Figure 3.14G-H). The cells of N. oculata had a comparatively simple organisation, containing a single cup-shaped chloroplast, a nucleus, several mitochondria and a number of small lipid droplets and assorted vacuoles (Figures 3.14 and 3.15). The most prominent organelles were the cup-shaped peripheral chloroplasts, which enclosed the other organelles (Figure 3.14G, H) and occupied around half the cell volume (57%, Figure 3.18). The chloroplast was packed with linear bands of 3-ply thylakoids (Figures 3.14G, H and 3.15A) that typify the chromophyte algae. Under the TEM, in most sections two chloroplast profiles were seen (Figure 3.14G, H). Each lamella was made up of three closely adpressed thylakoids, which always ran parallel to the long axis of the chloroplast. In this species there was no girdle lamella running around the outer perimenter of the plastid (Figure 3.14G, Figure 3.15A). The plastid matrix contained granular ribosomes, which were particularly clearly seen in the more electron-lucent regions where the thylakoids were less closely packed (Figure 3.15A, black star). Also scattered throughout the chloroplast stroma were small electron-dense plastoglobuli (lipid storage bodies) (Figure 3.14G). No pyrenoid, grana-like stacks or starch grains were observed. The chloroplast was surrounded by four closely adpressed membranes, which gave the plastid envelope its characteristically electron-dense appearance (Figure 3.15A). The outer membrane was the chloroplast endoplasmic reticulum (cER) and the inner membrane was the chloroplast envelope.

The main cytoplasmic organelles were located in the centre of the cell (Figure 3.14G, H). The central nucleus was spherical to ovoid in shape, although often had an irregular profile in thin sectioned material (Figure 3.14G, H). Two mitochondrial profiles were also present in the cell lying close to the chloroplast envelope and nucleus, near the cell wall (Figure 3.14G, H and Figure 3.15C, E). Ribosomes were found in high density throughout the cytoplasm (Figure 3.14G, H). Several cytoplasmic vacuoles which were electron-lucent surrounded the nucleus (Figure 3.14G, H). Lipid globules were observed in these actively growing cells (Figure 3.15D).

3.3.2.2 Ultrastructure of 14-day-old stationary phase cells

Nannochloropsis oculata from a 14-day-old stationary phase culture had a similar overall appearance to those in actively growing cultures (e.g. Figure 3.14G, H) but had a much altered cytoplasm (Figure 3.16A-D). The cytoplasm mean volume fraction of stationary phase cells (mean = 15.9%, CI: (13.9, 17.9)) was significantly lower than the mean volume fraction of log phase (mean = 18.7%, CI: (14.97, 21.7)). The nucleus appearance showed no difference between the actively growing cultures (e.g. Figure 3.14G, H) and the stationary phase cells (Figure 3.16A-D). This was confirmed through statistical analysis as there was no significant difference in median volume fraction of stationary phase cells (median = 6.9%, CI: (4.09, 9.26)) and log phase cells (median = 4.5%, CI: (2.3, 7.6)) (Mann-Whitney test, Table 3.9, Figure 3.19). One of the most obvious changes was that the homogeneous cell walls were thicker in stationary phase cells (Figures 3.14 and 3.15), with a mean thickness of around 46 µm, compared with 8.9 µm in actively growing cells. The average total volume fraction of the cell wall in stationary phase cells (mean =14.06%, CI: (12.8, 15.26)) was significantly different, at nearly double that of active phase cells (mean = 7.2%, CI: (6.3, 8)) (t-test Table 3.8, Figure 3.18).

In contrast, the mean volume fraction of the chloroplast was significantly reduced (t-test, Table 3.8) in stationary phase cells (mean = 20.59%, CI: (14.99, 26.39)), compared to active phase cells (mean = 57.4%, CI: (52.5, 62.3)) (Figures 3.16A-D and Figure 3.18, Table 3.8).

From the volume fraction analysis for chloroplast constituents, both thylakoid membranes and matrix content of plastid decreased from 36.46% and 20.9% to 15.15% and 5.25% respectively (Figure 3.18). The thylakoid membranes in some stationary

cells often appeared broader, with homogeneous contents, and their lamellae had fused resulting in stacks of <6 thylakoids, as shown in Figure 3.17A. However, their volume fractions decreased significantly in stationary phase cells which were (mean = 15.15%, CI: (11.85, 19.25)) compared to active growth cells (mean = 36.4%, CI: (32.96, 39.96)) (t-test, Table 3.8, Figure 3.18). The mean volume fraction of matrix was significantly decreased from 20.9% (CI: (17.5, 24.2)) in actively growing cells to 5.25% (CI: (3.45, 7.09)). The number of plastoglobuli remained statistically the same in stationary phase cells (Figure 3.17A), compared to active phase ones (Figure 3.14G and Figure 3.19).

Mitochondria tended to be clustered around the nucleus (Figure 3.16C, D) and were often irregular in shape (Figure 3.17B) but still packed with tubular cristae.

Mitochondrial median volume fraction of stationary phase cells (median = 4.49%, CI: (2.49, 6.49)) was significantly lower than that of active phase cells (median = 8.3%, CI: (6.01, 10.71)) (Mann-Whitney, Table 3.9, Figure 3.19). Stationary stage cells were characterised by containing many more conspicuous vacuolar vesicles (Figures 3.16A, B, and 3.17C-E) which contained rectangular inclusion bodies (IB) usually with fine parallel lamellae (Figure 3.17C-E). These vascular vesicles were absent in the log phase cells, which prevented the statistical analysis. In contrast, the cytoplasm of the log phase cells contained more vacuoles than stationary phase cell cytoplasm. This was confirmed statistically as the median volume fraction of active phase cells (median = 0.76%, CI: (-0.6, 0.6)) was significantly higher than for stationary phase cells (median = 0%, CI: (0.09, 0.09)) (Mann-Whitney, Table 3.9, Figure 3.19).

Stationary phase cells of *N. oculata* contained one large lipid globule or more (Figure 3.16 A-D, (L)) located near the nucleus which occupied around 28% of the cell volume (Figure 3.19). The median volume fraction of the lipids significantly increased (Mann-Whitney test, Table 3.9) in stationary phase cells (median = 28.25%, CI: (23.65, 32.85)), compared to active phase cells (median = 0%, CI: (-0.2, 0.2)) (Figures 3.16A-D and 3.19, Table 3.9).

Table 3.8: Results of t-tests of volume fractions of cytoplasm, cell wall, chloroplast, matrix and thylakoid membranes and starch in *Nannochloropsis oculata* active and stationary phase cells

Organelle	t	DF	P
Cytoplasm	11.36	29	< 0.001
Cell wall	-9.59	50	< 0.001
Chloroplast	23.67	29	< 0.001
Matrix	12.42	29	< 0.001
Thylakoid membrane	20.86	29	< 0.001

Table 3.9: Results of Mann-Whitney tests of volume fractions of nucleus, lipid, vacuoles, plastoglobuli and mitochondria in *Nannochloropsis oculata* active and stationary phase cells

Organelle		W	N	P
	Active		30	
Nucleus	Stationary	861.0	30	0.429
Lipid	Active	490	30	<0.001
	Stationary	490	30	
Vacuoles	Active	1169.0	30	0.0002
vacuoles	Stationary		30	
	Stationary		30	
Plastoglobuli	Active	835.0	30	0.2398
	Stationary		30	
	Active		30	
Mitochondria	Stationary	1075	30	0.0184
	Stationary		30	

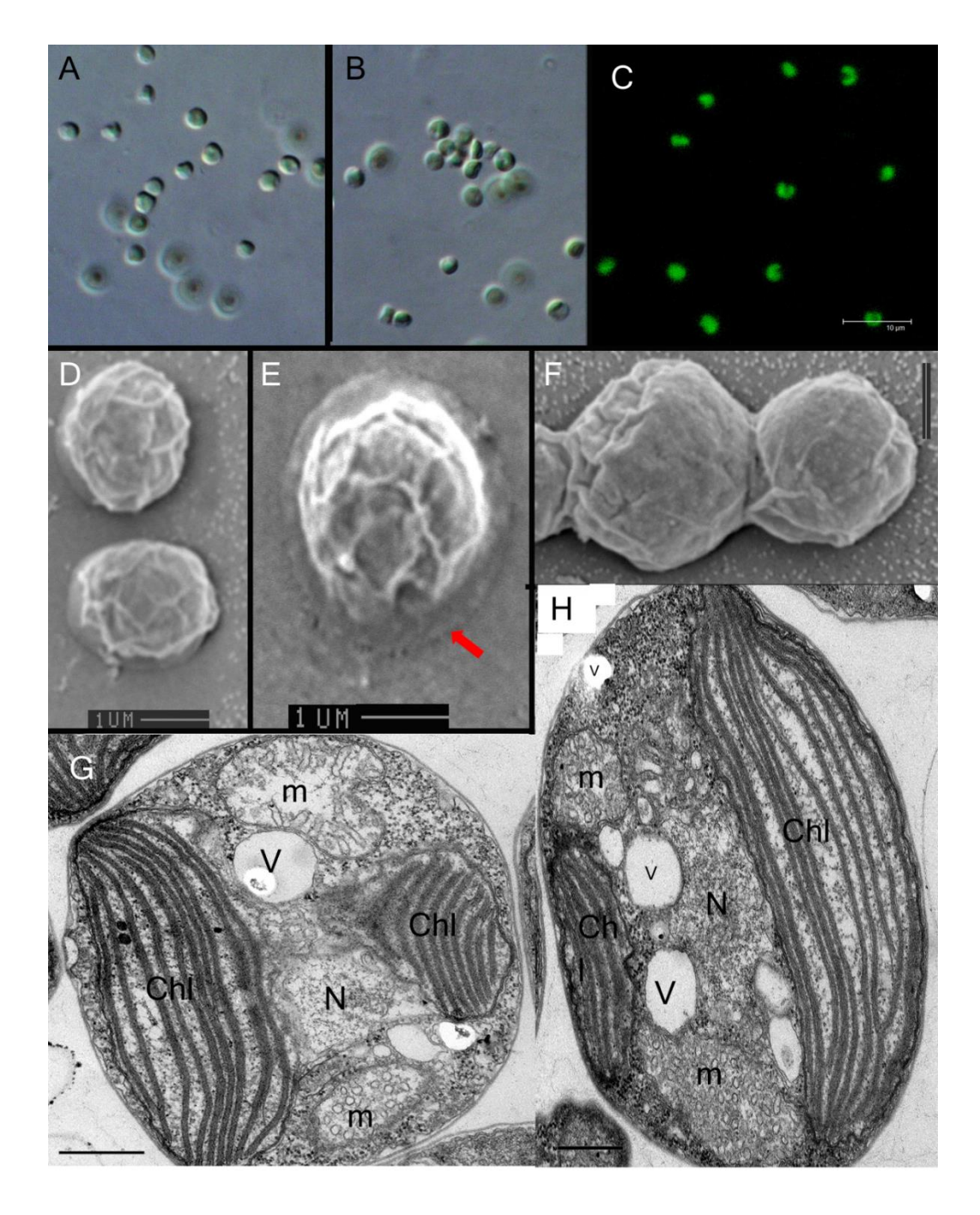


Figure 3.14: *Nannochloropsis oculata* cell structure under light and scanning electron microscopy and exponential growing cells under electron microscopy A-B) Light microscopy images of *N. oculata* showing coccoid cell shape. C) Fluorecsent microscopy showing the choloroplast cup shape. Scale bar 10 μm. D-F) Scanning electron microscopy images showing the surrounding matrix (red arrow). Scale bar 1 μm. G-H) Transmission electron microscopy showing internal cell organelles. Scale bar 0.5 μm. Chl: chloroplast; M: mitochondria; N: nucleus; V: vacuoles.

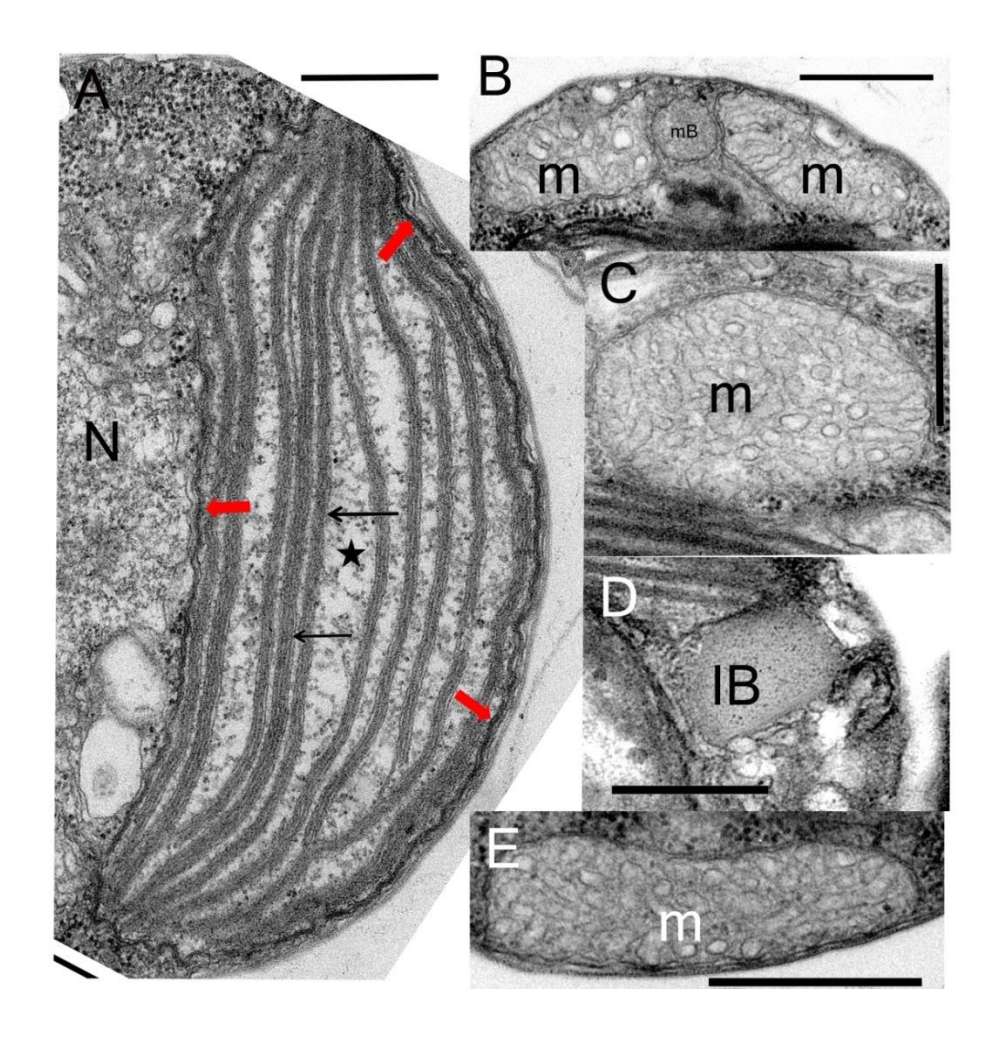


Figure 3.15: Higher magnification of the fine structure of exponentially growing cells of *Nannochloropsis oculata*

A) Cross section showing the chloroplast structure. The chloroplast envelope surrounded by two extra membranes of endoplasmic reticulum (red arrows) appears as a thick membrane with high osmiophility. Thylakoids are in clusters of three membranes (black arrows) and the matrix is indicated by a black star. B) Microbody surrounded by two mictochondrial profiles which indicate a metabolically active cell, as the cell is in the linear exponential growth phase. C) Higher magnification of a cross-section of mitochondrial profile. D) Higher magnification of lipid body. E) Higher magnification of a vertical section of a mitochondrial profile. Scale bars 0.5 µm. IB: inclusion bodies; M: mitochondria; mB: microbody; N: nucleus; V: vacuoles.

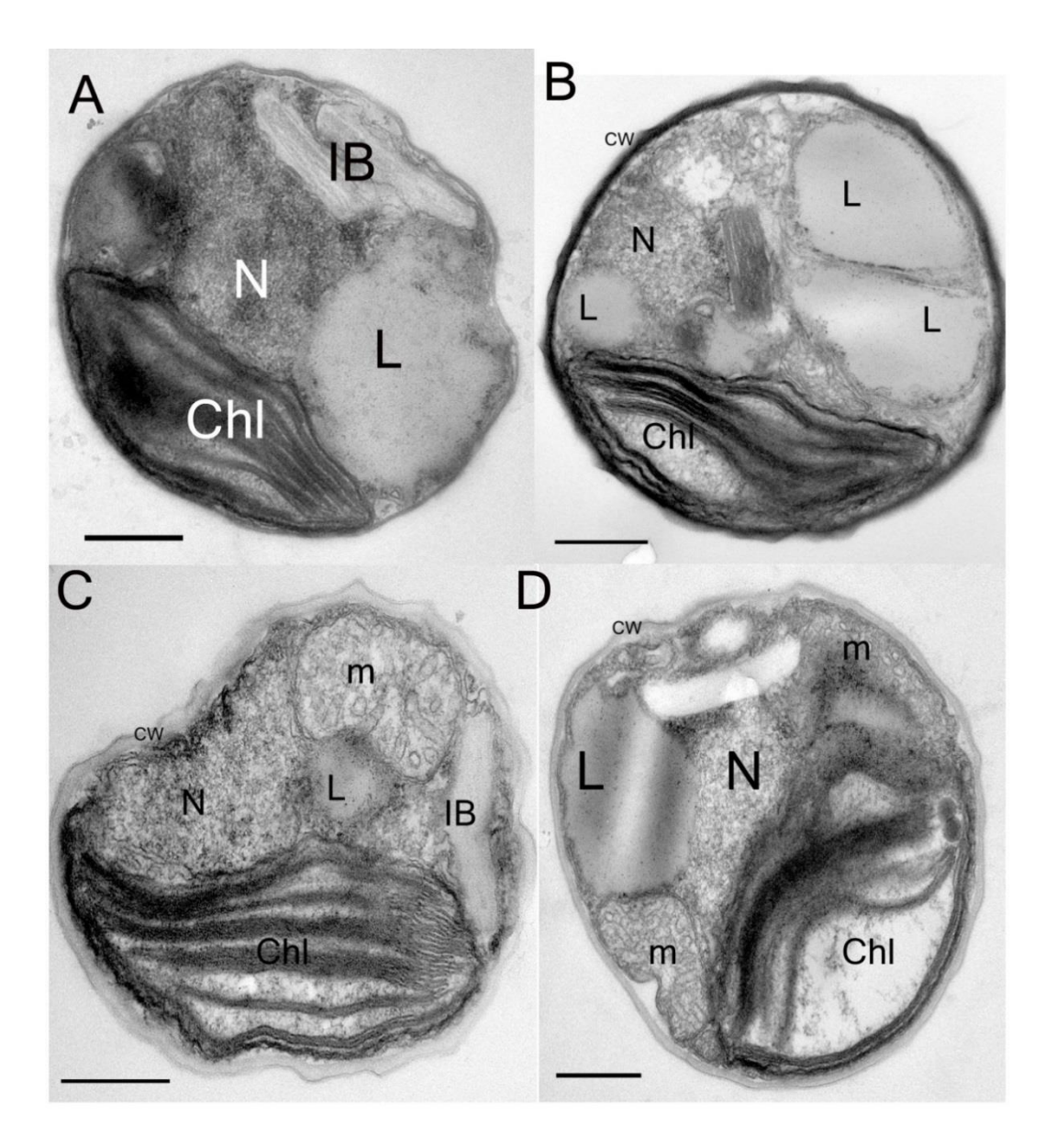


Figure 3.16: *Nannochloropsis oculata* stationary phase growing cells A-D) The cell structure changes significantly as the lipid droplets occupy the vast majority of cell volume and with the presence of inclusion bodies. The cell wall becomes thicker. Scale bars 0.5 μ m Chl: chloroplast; CW: cell wall; IB: inclusion bodies; L: lipid bodies; M: mitochondria; N: nucleus; V: vacuoles.

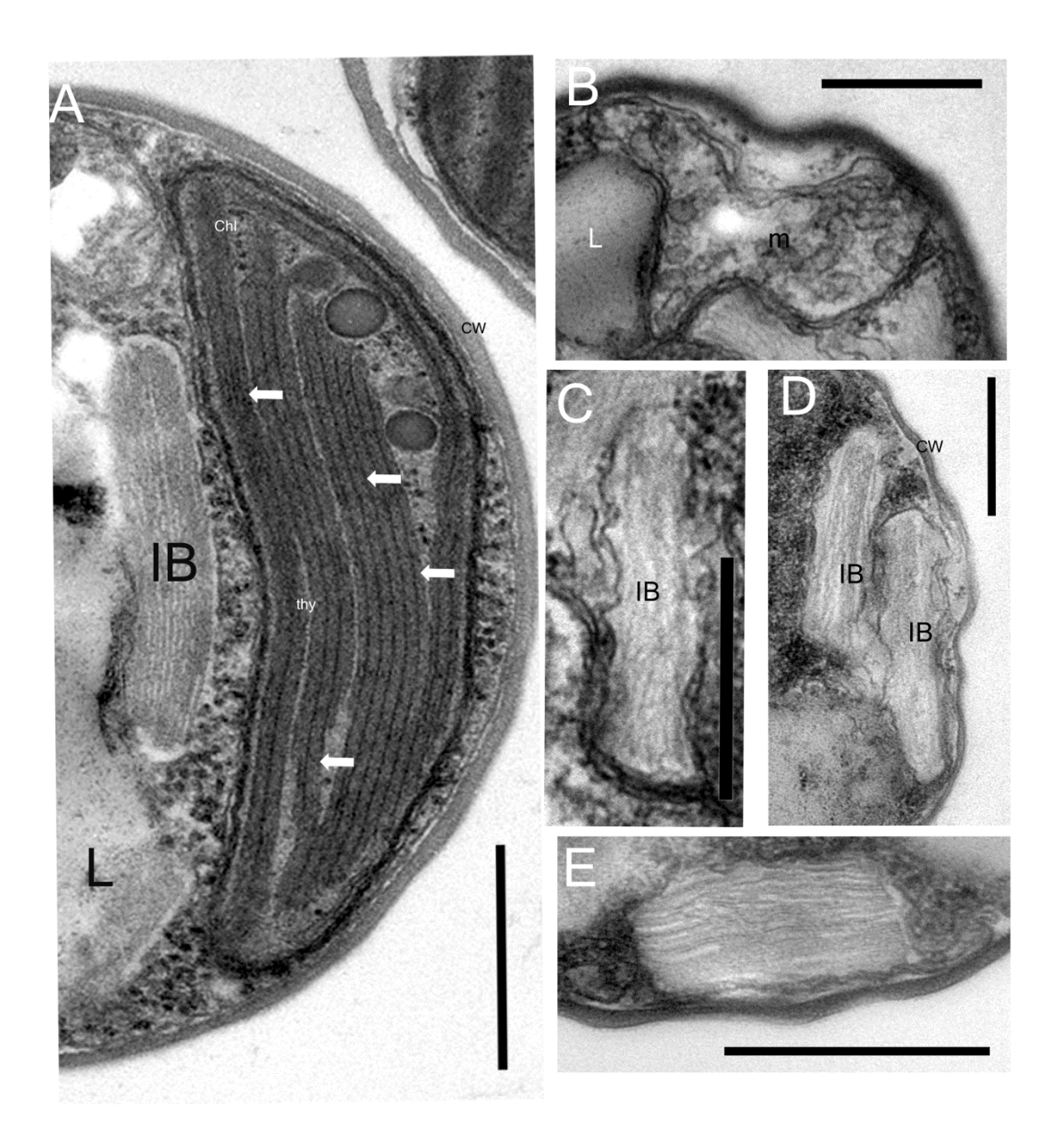


Figure 3.17: Higher magnification of fine structure of stationary phase growing cells of *Nannochloropsis oculata*

A) Cross section showing the chloroplast structure, the chloroplast envelope surrounded by two extra membranes of the endoplasmic reticulum and appears as a thick membrane with high osmiophility. Thylakoids are condensed and backed onto each other in clusters of 3-6 membranes (white arrows). B) Irregular shaped mictochondrial profile. C-E) Higher magnification inclusion bodies that contain membranous structures. Scale bars 500 μ m. Chl: chloroplast; CW: cell wall; IB: inclusion bodies; L: lipid bodies; M: mitochondria; N: nucleus; Thy: thylakoid; V: vacuoles.

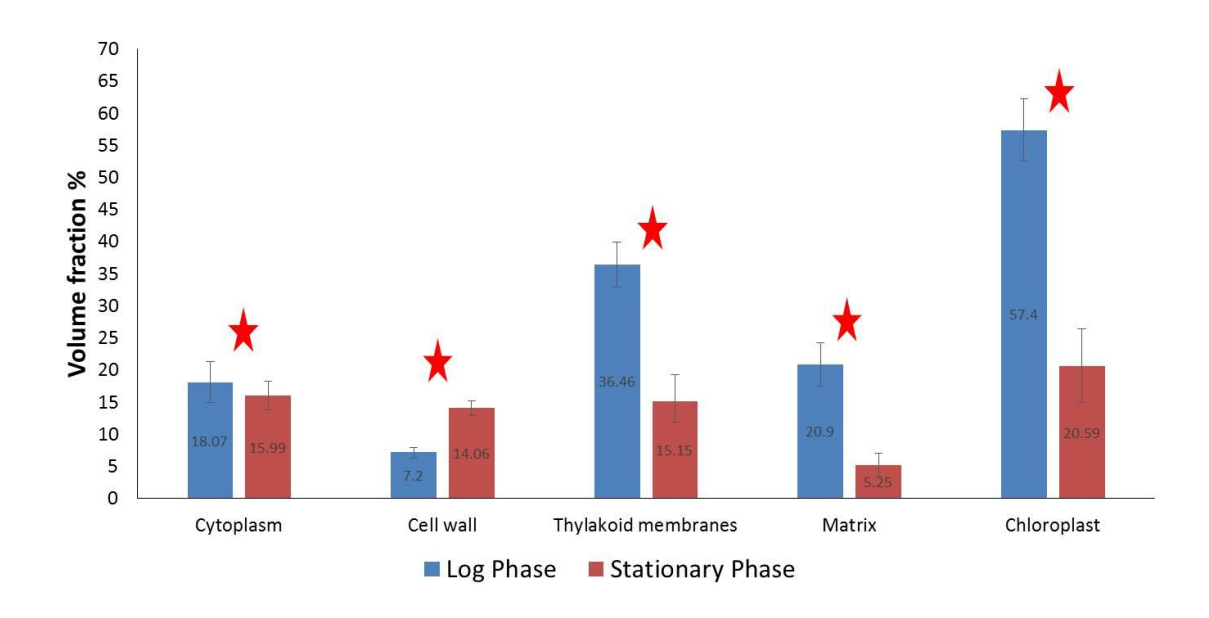


Figure 3.18: Mean and 95% confidence interval of volume fractions of the cell organelles and chloroplast constituents in *Nannochloropsis oculata* log and stationary phase samples

The volume fraction data for each organelle were subjected to a separate t-test. Stars indicate significant differences between log and stationary phase volume fractions of an organelle.

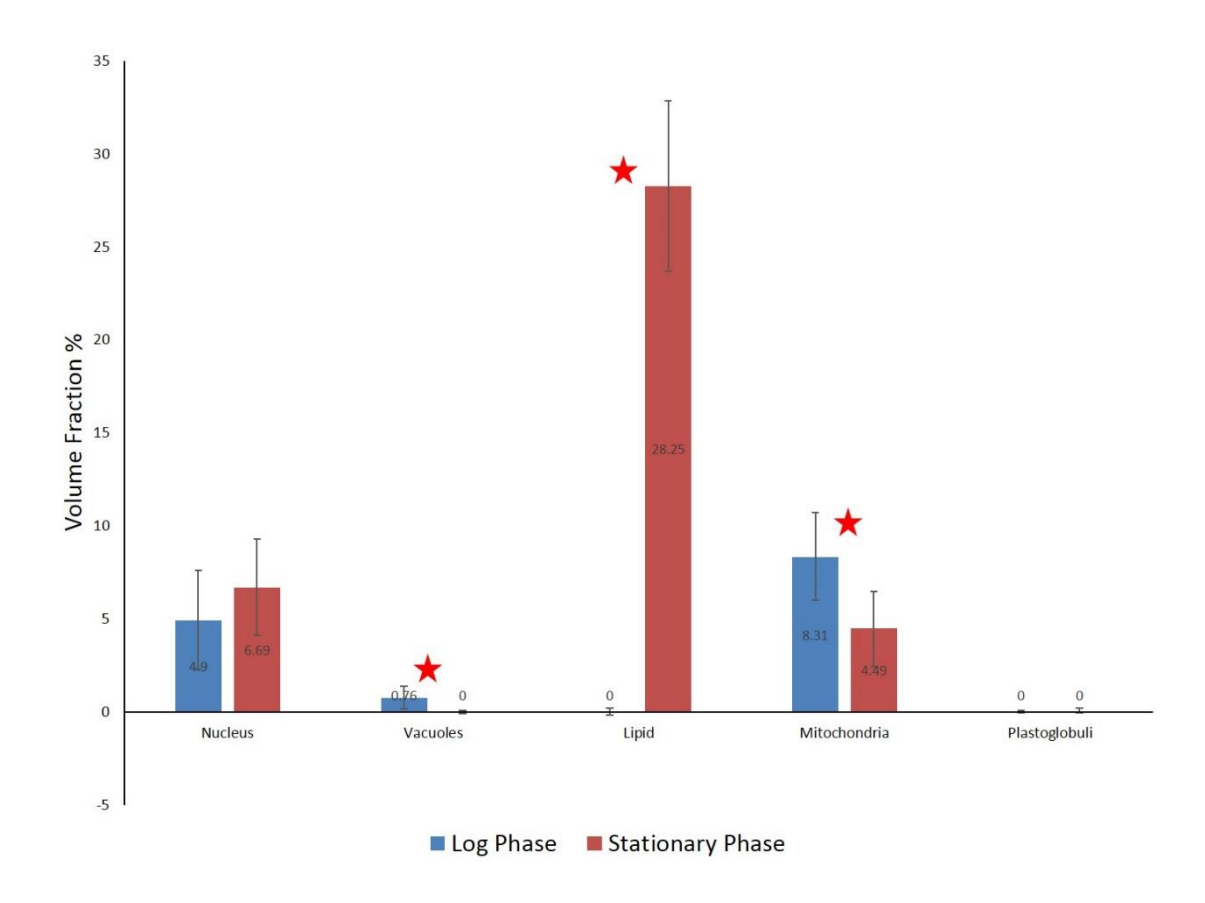


Figure 3.19: Median and 95% confidence interval fractions of cell organelles and chloroplast constituents in *Nannochloropsis oculata* log and stationary phase samples The significance of differences was tested using the Mann-Whitney test, P= 0.05. Each pair represents a separate test. Pairs with stars show significant differences.

3.3.2.3 Ultrastructure of decadienal-treated cells

Two control samples were used; one treatment had no additions (indicated by 0 in tables and Figures 3.28 and 3.29) (Figure 3.20A), while the second control had ethanol added (Figure 3.20B-D).

The spherical cell shape was maintained (Figure 3.20A-D). The mean cell size was 3.5 μ m (ranging from 2.8 μ m to 4.3 μ m) by 2.2 μ m (ranging from 1.5 μ m to 3 μ m) for the untreated control and 3.5 μm (ranging from 2.3 μm to 5 μm) by 2.6 μm (ranging from 1.8 µm to 7.2 µm) for the ethanol-treated control. Some cells in the ethanol-treated suspension appeared to be surrounded by an additional outer wall layer (Figure 3.20B, arrowed), which often occurs during internal autospore formation. The chloroplast (Figure 3.20A-D) constituted approximately 50% of the volume fraction; 48% for the 6day-old control cultures and 45% in the ethanol-added control (Figure 3.29). The overall volume occupied by the chloroplast showed no significant difference between the two controls and all the decadienal-treated samples (Kruskal-Wallis test, Table 3.11, Figure 3.29). In both control samples, the chloroplasts were packed with parallel arrays of tightly stacked thylakoid lamellae, which constituted more than 30% of cell volume fraction and with no significant differences in volume fraction in comparison to decadienal-treated cells (Kruskal-Wallis test, Figure 3.16A-D, Figure 3.29, Table 3.11). In control cells, the individual thylakoids were closely associated, and in sections the three lamellae often appeared to be helically twisted around each other (Figure 3.21A, C). In the ethanol-treated control (Figure 3.21E), the matrix appeared denser and the thylakoid membranes often appeared to reveal a negative contrast. Small numbers of electron-dense plastoglobuli were also scattered throughout the chloroplast (Figure 3.20A, B, D and Figure 3.21A-C). The matrix volume fraction of control samples was statistically insignificant in comparison to that of decadienal-treated cells (ANOVA test, Table 3.10, Figure 3.29).

The single nucleus was often located toward the margin of the cell (Figure 3.20A, D) and was generally ovoid (Figure 3.20 A-D), but often with an irregular outline. An electron-dense nucleolus was also found (Figure 3.20A). Mitochondria were ovoid or capsule shaped (Figure 3.21B, D) and occasional looped profiles were seen (Figure 3.20A). They were packed with tubular cristae, although these were often difficult to resolve against the granular matrix (Figure 3.21B, D). There was no statistically significant difference between the median volume fraction of both nucleus and

mitochondria in control and decadienal-treated samples (Kruskal-Wallis test, Table 3.11, Figure 3.29).

Small electron-lucent vacuoles were also present in the cytoplasm of the cell (Figures 3.20C and Figure 3.21A). The only significant difference between the normal cells and the culture to which 8.5 µl of 99% ethanol had been added was the presence of lipid bodies (Figure 3.16B- D), which occupied just under 10% of the cell volume (Figure 3.29).

Cells treated with decadienal all showed altered cell structure, although generally with few significant differences in the overall volume fractions of the major cell components (Figure 3.29). The only significant difference compared with the untreated controls was an increase in lipid (Figure 3.29), but this was comparable to that observed when ethanol was added on its own to the cultures (Figure 3.29). The Kruskal-Wallis test for the volume fractions of lipids showed a significant difference (Table 3.11). The volume fraction of lipid in decadienal-untreated samples (median = 0.0%, CI: (-2, 2)) was significantly lower compared to all other treatments (ethanol, median = 8.3%, CI: (5.2, 11.7); 1 μ M, median = 6.6%, CI: (4.5, 9.3); 10 μ M, median = 6.5%, CI: (3.8, 9.2); and 50 μ M, median = 3.4%, CI: (0.2, 6.5) (Mann-Whitney test, Table 3.12).

The appearance of individual organelles was altered by the addition of increasing concentrations of decadienal. The cells appeared to have an overall increased cytoplasmic density, which often made discerning individual organelles more difficult (Figures 3.22 and 3.27). Cell appearance was much more variable, and whilst some cells looked healthy (Figure 3.22D), others appeared to be in advanced stages of degeneration and autolysis with no clear cytoplasmic organelles (Figure 3.26E). Although some micrographs showed evidence of cytoplasmic shrinkage (Figures 3.22C and 3.26D) the statistical analysis showed that the volume fraction of cytoplasm in decadienal-untreated samples (mean = 15.35%, CI: (12.8, 17.85) was significantly lower compared to samples treated with 10 μ M decadienal (mean = 21.2%, CI: (18.5, 24.1)) and 50 μ M decadienal (mean = 25.15%, CI: (21.6, 28.65)) (ANOVA test, Table 3.10, Figure 3.28).

Even cells treated with the lowest concentration (1 μ M) of decadienal contained many membranous structures in their cytoplasm (Figure 3.23C, F), which were not observed in either set of control cells. These structures appeared to be composed of concentric whorls of membrane, and are thought to be elaborations of the vacuole system (Figures

3.23C, F; 3.25C and 3.27G). Cells contained vacuoles with osmiophilic inclusion (Figure 3.23B, D; 3.25C and 3.27E, G). Some cells had detached cell walls (Figures 3.22A, C arrow and 3.26D, arrow) and the Kruskal-Wallis test for the volume fractions of cell wall showed a significant difference (Table 3.11). The volume fraction of cell wall in decadienal-untreated samples (median = 7.2%, CI: (6.4, 8)) was significantly lower compared to treatments with ethanol (median = 8.7%, CI: (7.7, 9.8)), 1 μ M decadienal (median = 8.9%, CI: (8, 9.9)) and 50 μ M decadienal (median = 7.9%, CI: (6.5, 9.3)) (Mann-Whitney test, Table 3.12).

One of the major changes that took place in higher levels ($10~\mu M$ and $50~\mu M$) of decadienal was the increasing (but variable) disruption of the thylakoid membrane system. The individual thylakoids seemed to have separated and simply formed a continuous whorled array with the plastid matrix (Figures 3.21F, 23A-C, 3.24A-D and 2.25F). In general, it was much more difficult to discern the usual electron-dense lamellar bands in decadienal-treated plastids. However, there was no significant difference in thylakoid volume fractions between different treatments (Kruskal-Wallis test, Table 3.11). Cells with $10~\mu M$ decadienal showed numerous of membranous structures in their cytoplasm (Figure 3.24A-D and 2.25C). Cells contained vacuoles with membranous inclusion (Figures 3.22A, C and 3.23).

Table 3.10: Results of ANOVA tests on the effects of decadienal treatments on the volume fractions of cytoplasm and matrix in *Nannochloropsis oculata*

Organelle	DF	F-statistic	P
Cytoplasm	4	5.72	< 0.000
	145		
	149		
Matrix	4	1.57	0.184
	145		
	149		

Table 3.11: Results of Kruskal-Wallis test of volume fractions of nucleus, mitochondria, lipid, vacuoles, chloroplast, cell wall, plastoglobuli and thylakoid membranes in *Nannochloropsis oculata* decadienal-treated cells

Organelle	Н	DF	P
Nucleus	5.23	4	0.264
Mitochondria	6.57	4	0.161
Lipid	31.9	4	< 0.001
Vacuoles	3.7	4	0.448
Chloroplast	4.72	4	0.317
Cell wall	15.42	4	0.004
Plastoglobuli	5.93	4	0.431
Thylakoid membrane	3.21	4	0.524

Table 3.12: Results of Mann-Whitney tests for significant differences between volume fractions of lipid and cell wall in *Nannochloropsis oculata* decadienal-treated cells

Organelle	Tested concentrations	n	W	P
	0 μM Vs E	30, 30	657	< 0.001
	0 μM Vs 1 μM	30, 30	591	< 0.001
	0 μM Vs 10 μM	30, 30	567	< 0.001
	0 μΜ Vs 50 μΜ	30, 30	675.0	< 0.001
Lipid	1 μM Vs E	30, 30	891	0.725
	1 μM Vs 10 μM	30, 30	913	0.982
	1 μM Vs 50	30, 30	986	0.292
	10 μM Vs E	30, 30	910	0.946
	10 μM Vs 50 μM	30, 30	992.5	0.255
	50 μM Vs E	30, 30	853	0.354
	0 μM Vs E	30, 30	744	0.011
	0 μΜ Vs 1 μΜ	30, 30	726	0.005
	0 μM Vs 10 μM	30, 30	906	0.900
Cell wall	0 μM Vs 50 μM	30, 30	793	.0730
	1 μM Vs E	30, 30	949	0.620
	1 μM Vs 10 μM	30, 30	1111	0.003
	1 μM Vs 50	30, 30	1004	0.190
	10 μM Vs E	30, 30	743	0.011
	10 μM Vs 50 μM	30, 30	797	0.083
	50 μM Vs E	30, 30	849	0.332

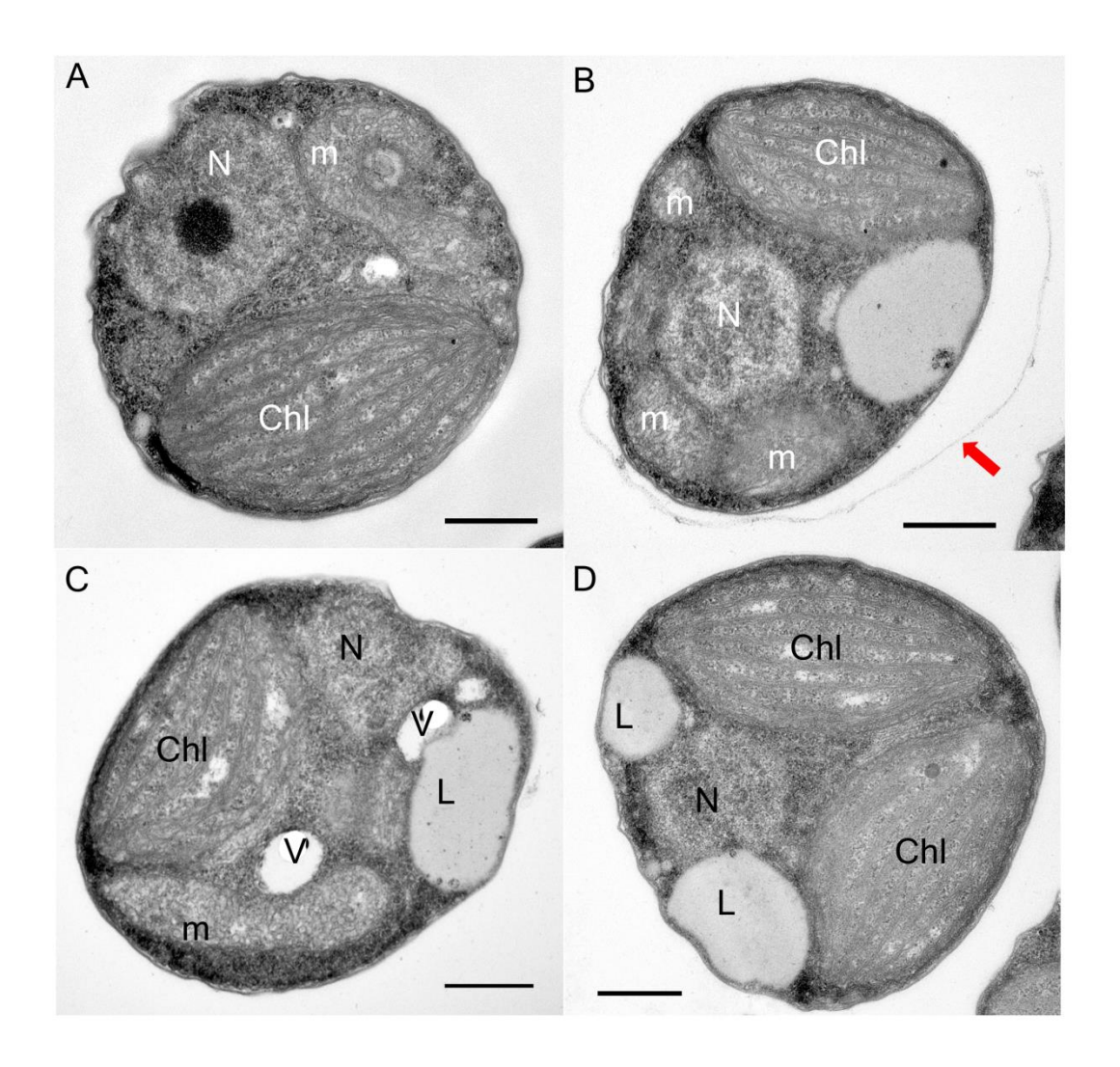


Figure 3.20: Nannochloropsis oculata controls A) Untreated control (0 μ M decadienal) cells looks normal. B-D) Ethanol control cell structures are similar to some decadienal-treated cells as the cell wall detached (red arrow); lipid bodies and vacuoles present in large volumes. Scale bar 0.5 μ m. Chl: chloroplast; G: Golgi; L: lipid bodies; M: mitochondria; N: nucleus; V: vacuoles.

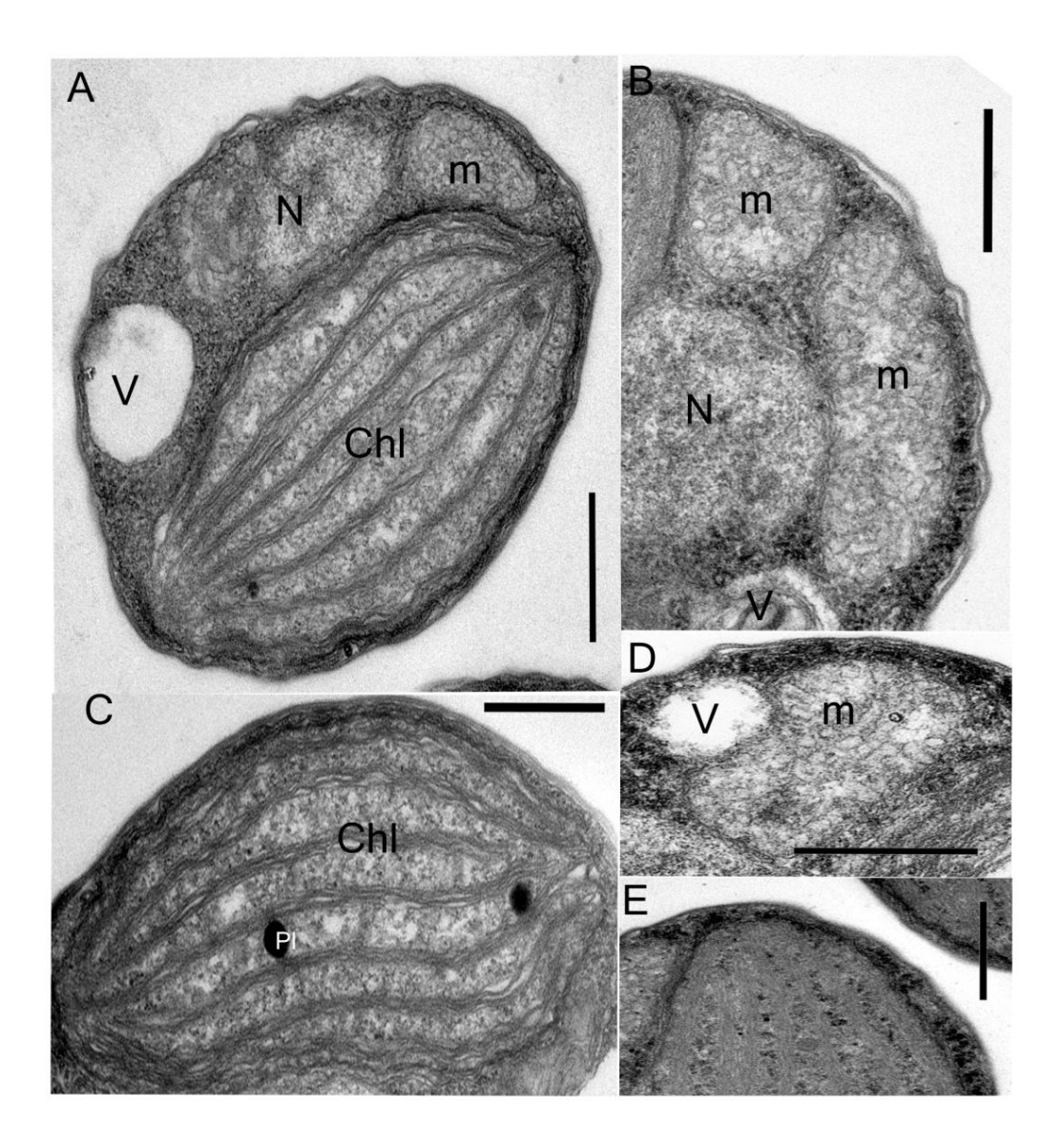


Figure 3.21: Higher magnification of *Nannochloropsis oculata* cell organelles of both 0 μ M decadienal and ethanol control cells
A) Whole cells of 0 μ M decadienal. B) Mitochondrial profiles of 0 μ M decadienal. C) chlroplast of 0 μ M decadienal. D) Vacuoles mitochondrial profiles of 0 μ M decadienal. E) Chloroplasts of ethanol control cells. Scale bars 0.5 μ m. Chl: chloroplast; L: lipid bodies; M: mitochondria; N: nucleus; Pl: plastoglobuli; V: vacuoles.

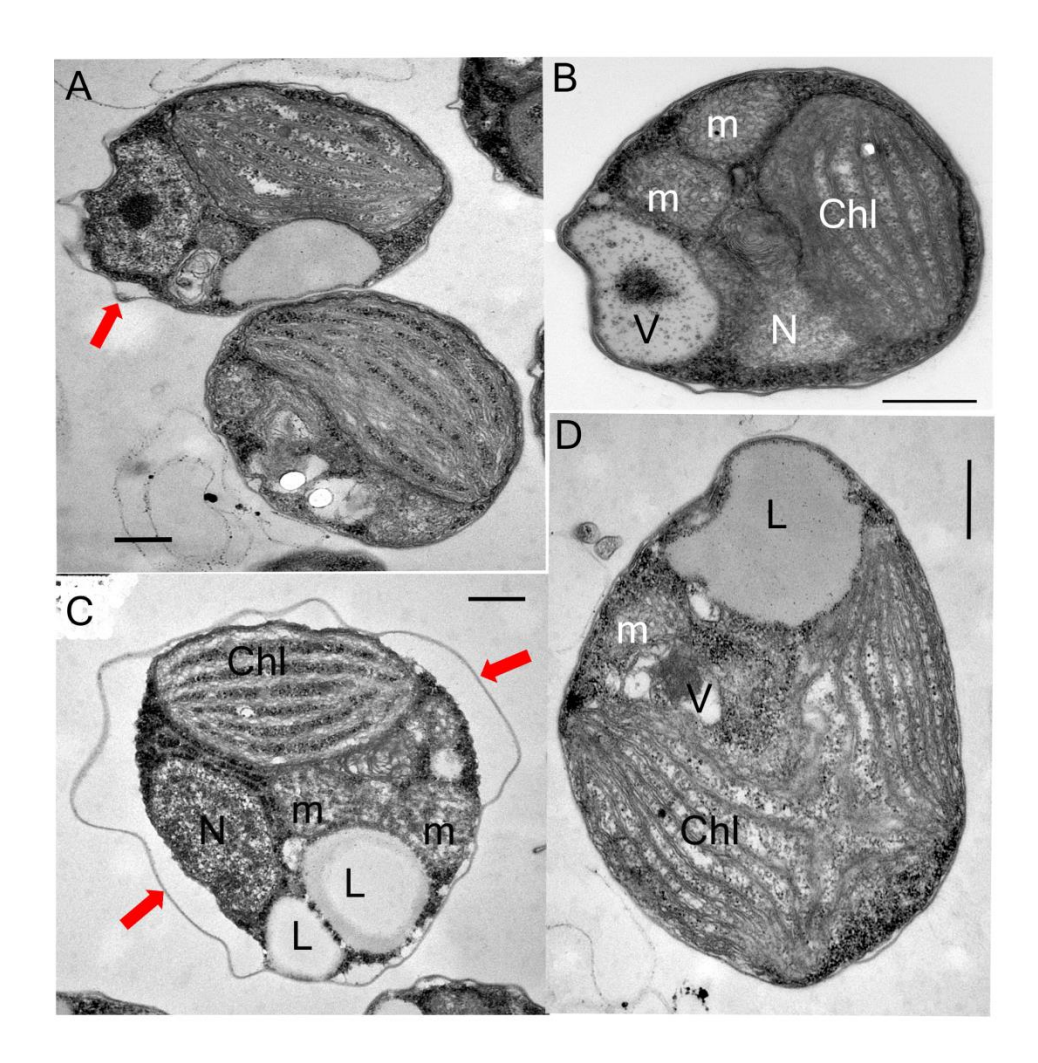


Figure 3.22: Nannochloropsis oculata cells treated with 1 μ M decadienal Red arrow shows detached cell walls. Visible membrane inclusion, vacuoles and lipid bodies. Scale bars 0.5 μ m. Chl: chloroplast; L: lipid bodies; M: mitochondria; N: nucleus; V: vacuoles.

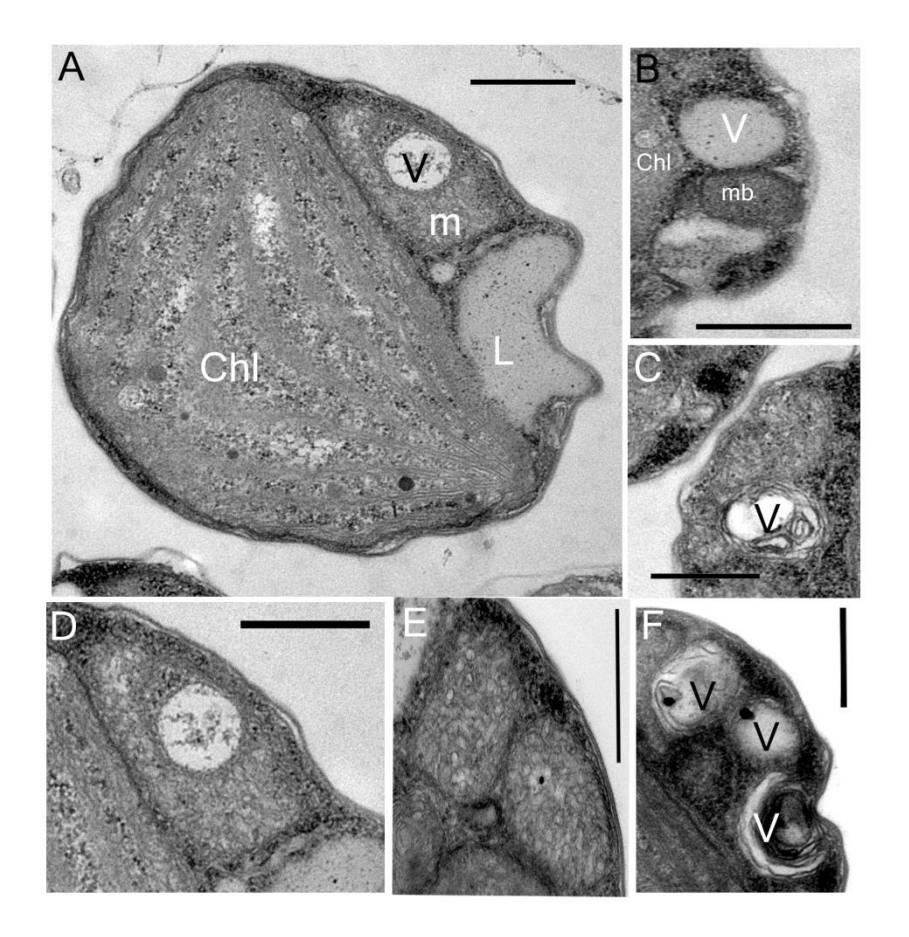


Figure 3.23: Higher magnification of Nannochloropsis oculata cells treated with 1 μM decadienal

A) Section in a whole cell through the chloroplast amd showing mictochondria surrounded by vacule and irregular-shaped lipid body. B) Vacuoles surrounded by microbody which might be involved in lipid metabolism or cell detoxification. C) Vacuoles with membranous inclusions. D-E) Mitochondrial profiles with altered and condensed cristae. F) Vacuoles with membranous inclusions. Scale bars 0.5 μ M. Chl: chloroplast; L: lipid bodies; M: mitochondria; mb: microbody; V: vacuoles.

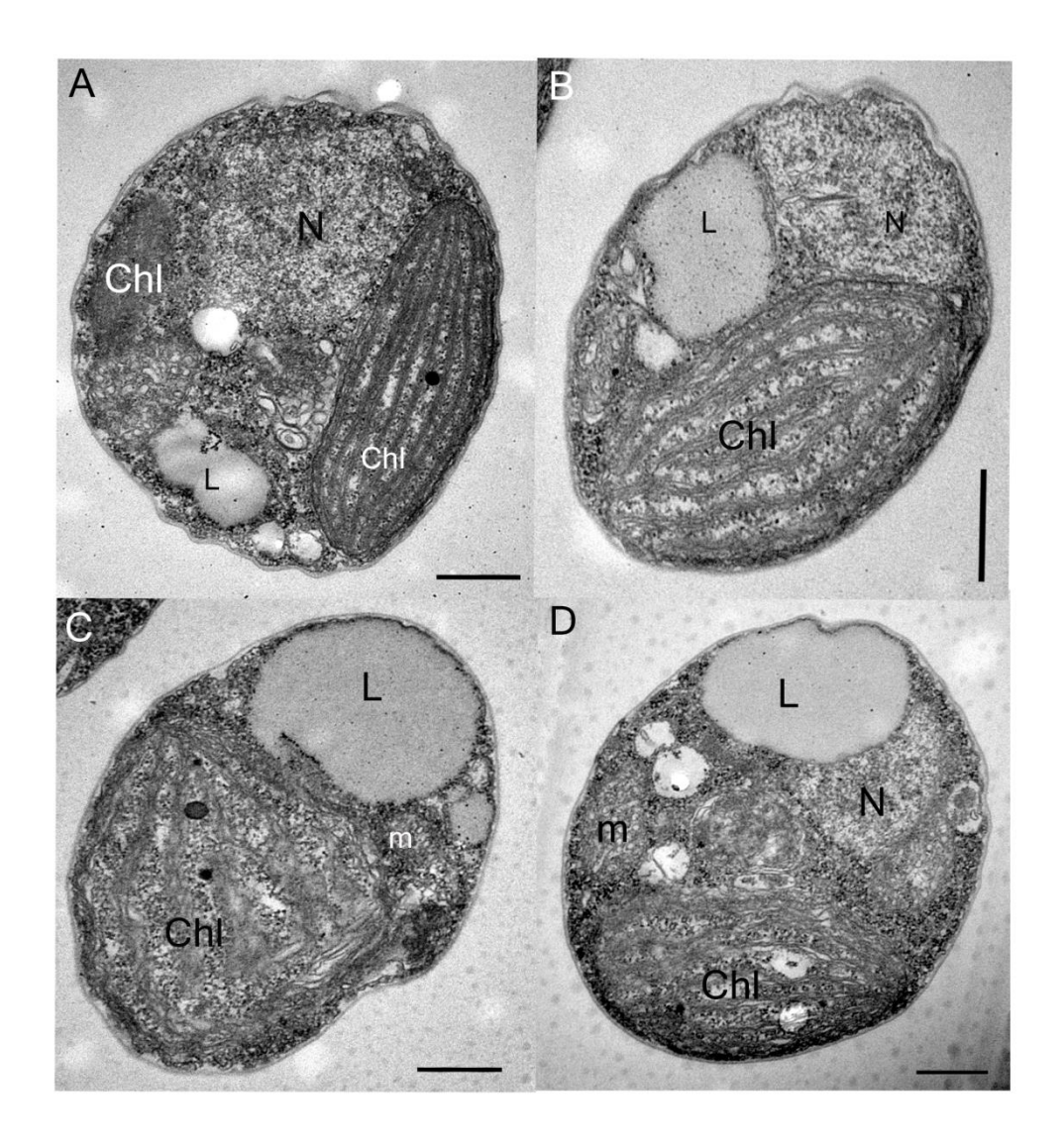


Figure 3.24 : Nannochloropsis oculata cells treated with 10 μM decadienal A-D) Thin sections of different cells showing the various signs af cell structutre modification: the presence of lipid bodies, membranous inclusion with vacuoles, increased vacuoles within the cytoplasm. Scale bars 0.5 μm . Chl: chloroplast; L: lipid bodies; M: mitochondria; N: nucleus.

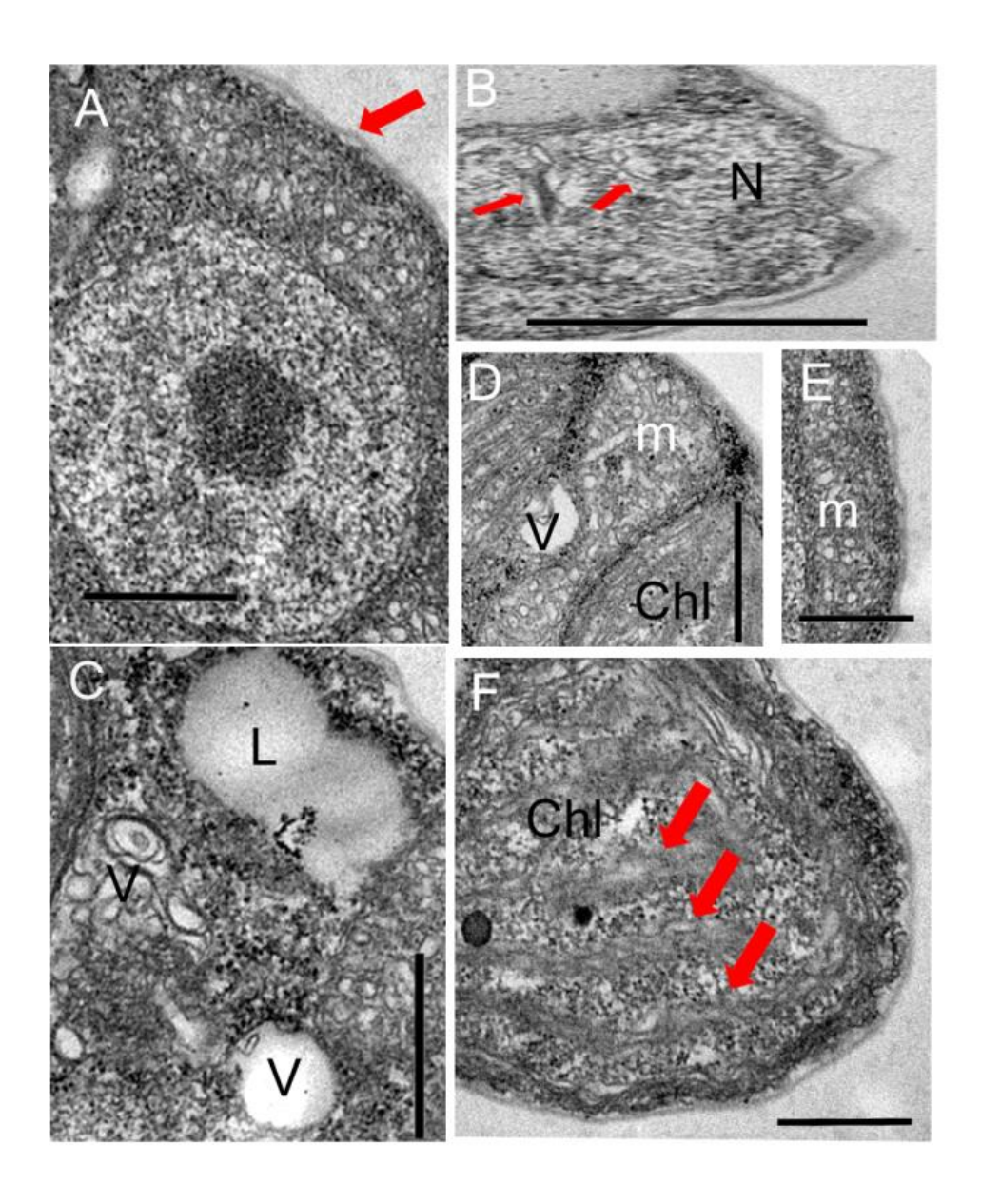


Figure 3.25: Higher magnification of Nannochloropsis oculata cells treated with 10 μM decadienal

A) Detached cell wall (red arrow). B) Membranous invagination in nucleus. C) Lipid bodies with various vacuoles in the cytoplasm. D-E) Mitochondrial profiles. F) The individual thylakoids seem to have separated and simply formed a continuous whorled array with the plastid matrix. Scale bars 0.5 μ m. Chl: chloroplast; L: lipid bodies; M: mitochondria; N: nucleus; V: vacuoles.

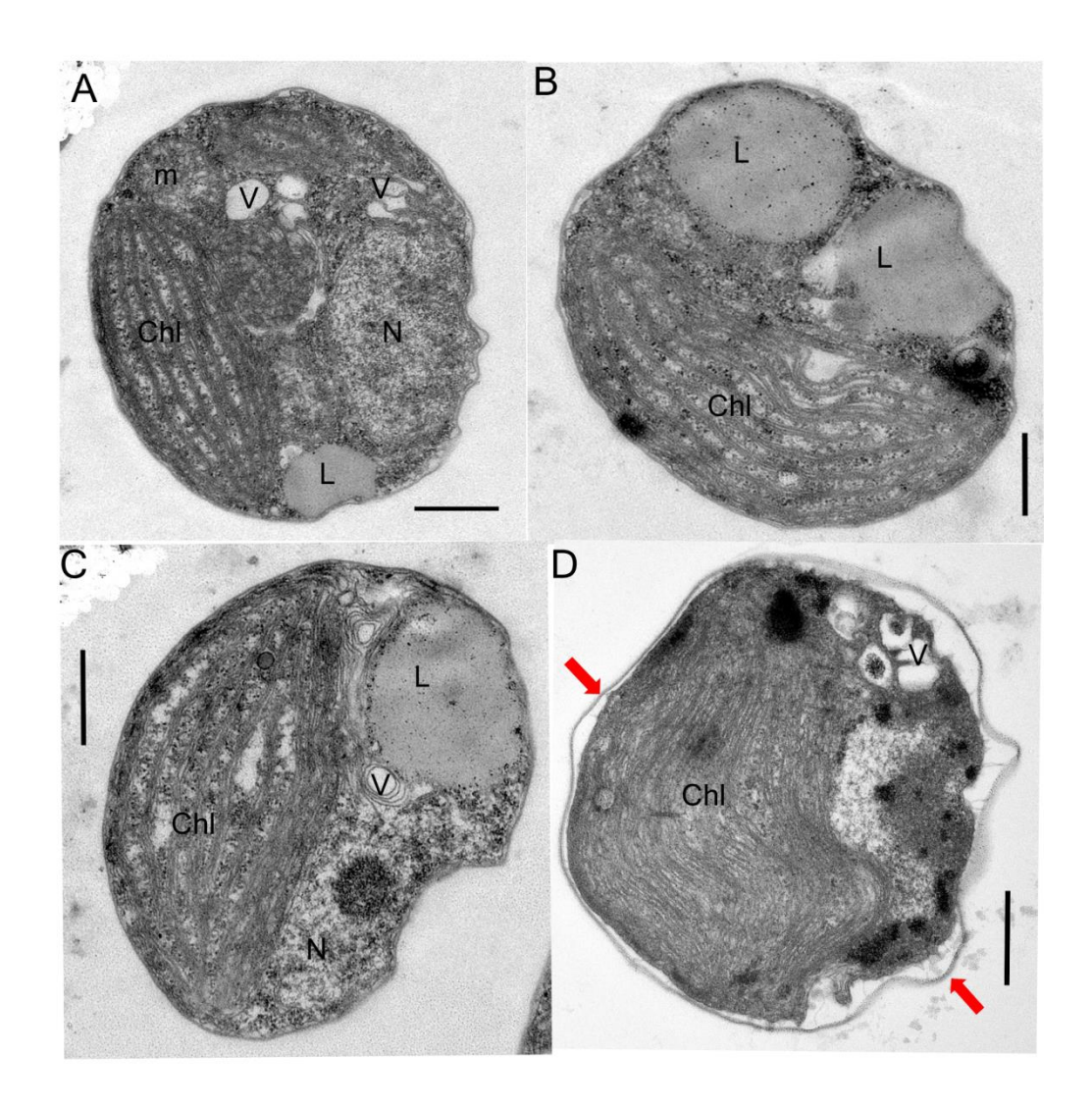


Figure 3.26: Nannochloropsis oculata cells treated with 50 μ M decadienal A-D) Thin sections of different cells showing the various signs of cell structure modification: the presence of lipid bodies, membranous inclusion with vacuoles, increased vacuoles within the cytoplasm, cytoplasmic shrinkage. Scale bars 0.5 μ m. Chl: chloroplast; G: Golgi; L: lipid bodies; M: mitochondria; N: nucleus; V: vacuoles.

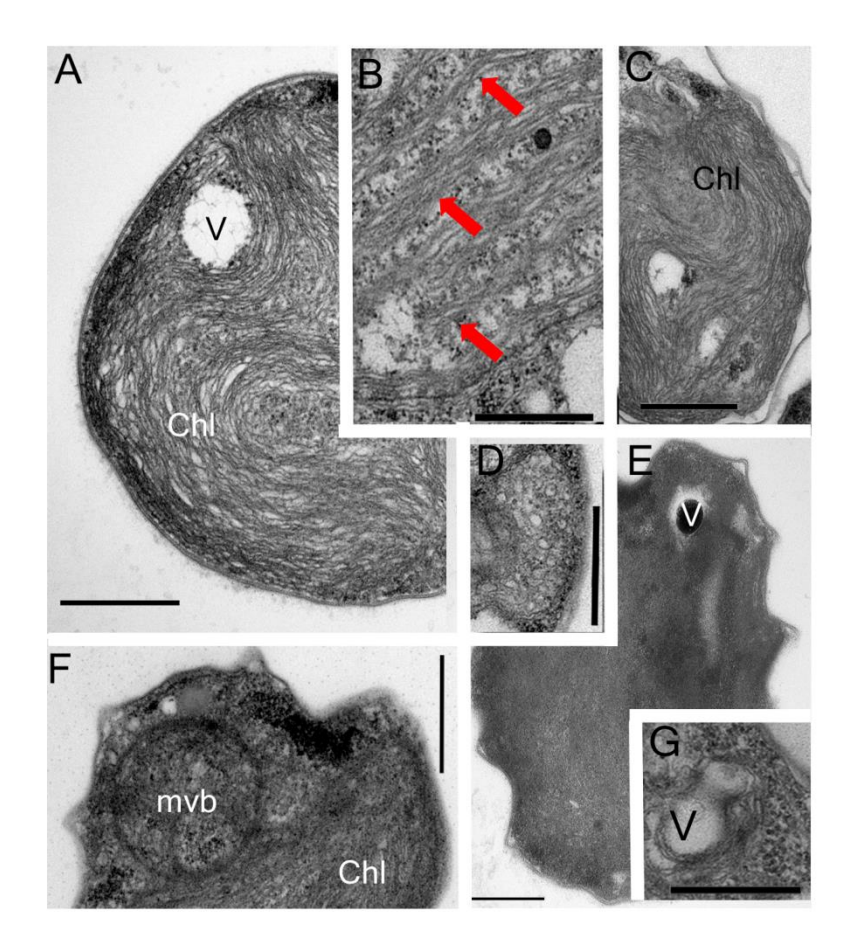


Figure 3.27: Higher magnification of Nannochloropsis oculata cells treated with 50 μM decadienal

A-C) Altered thylakoid structure, separated and simply forming a continuous whorled array with the plastid matrix. C) Detached cell wall. D) Mitochondrial profile. E) Cell with dark cytoplasm and vacule. F) Multivascular body in the proximity of the chloroplast. G) Vacuoles with membranous inclusions. Scale bars 0.5 μ m. Chl: chloroplast; mvb: multivascular body; V: vacuoles.

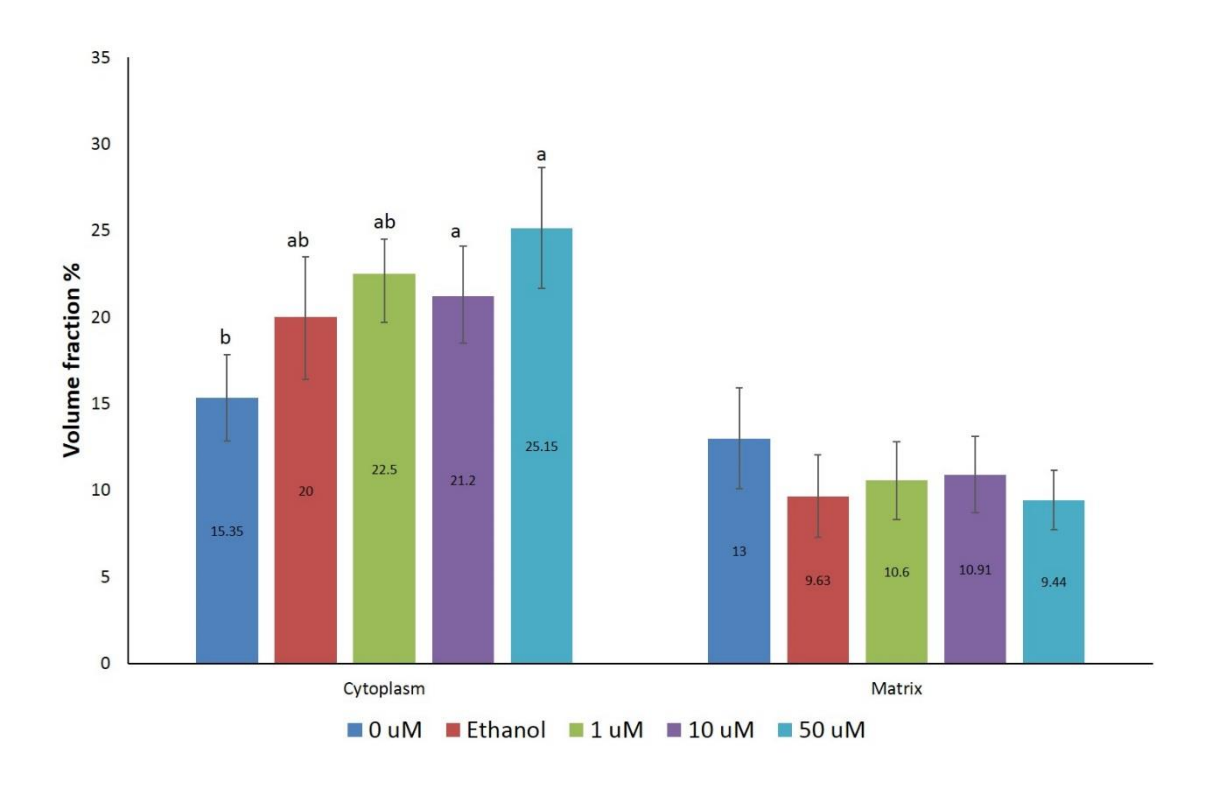


Figure 3.28: Mean and 95% confidence intervals of volume fraction of the cytoplasm and matrix in *Nannochloropsis oculata* cells treated with deacadienal Data for each organelle were tested with a separate ANOVA test (P=0.05).

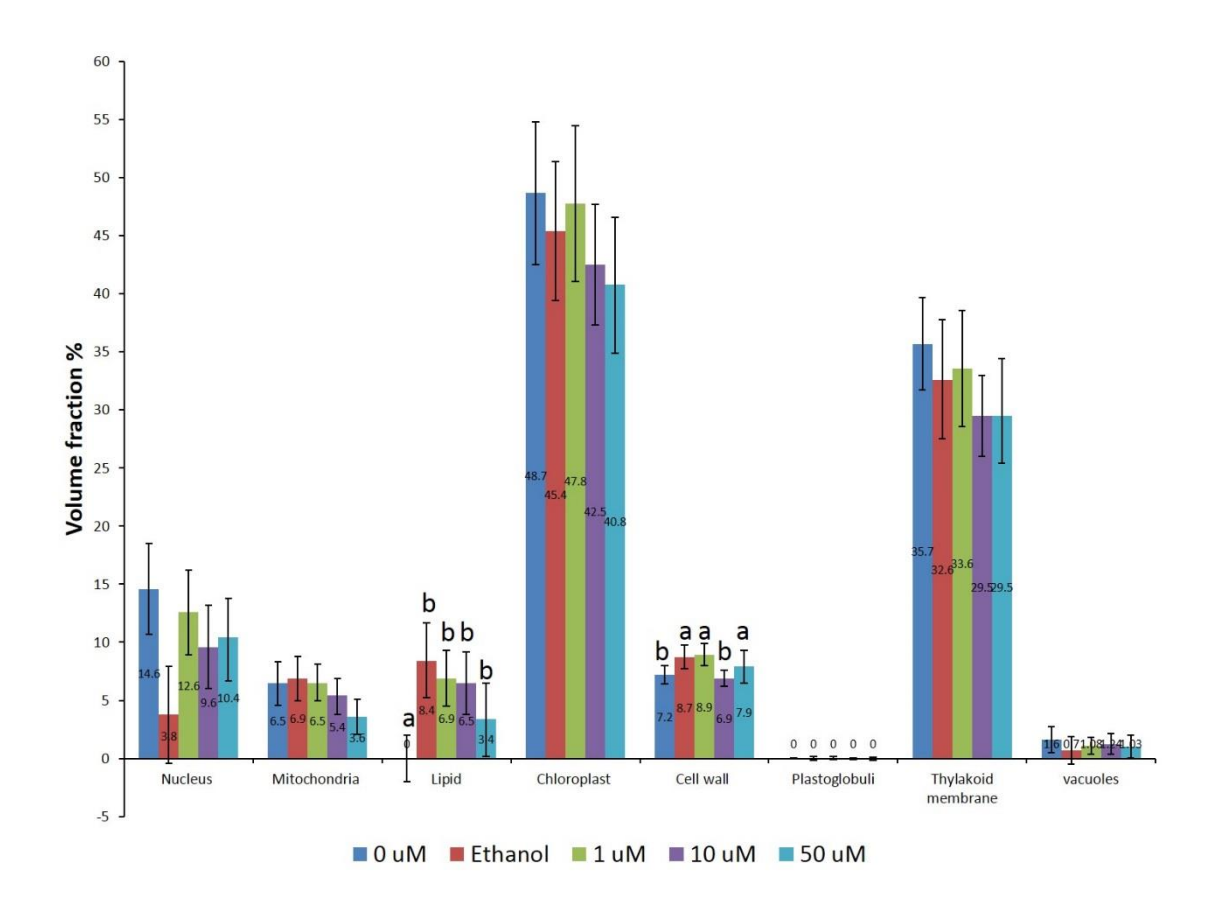


Figure 3.29: Median and 95% confidence intervals of volume fraction of the cell organelles in *Nannochloropsis oculata* cells treated with deacadienal Data for each organelle were tested with a separate Kruskal-Wallis test (P=0.05). Treatments with the same letters are not significantly different from each other (Mann-Whitney test, P=0.05).

3.4 Discussion

It is well established that lipid accumulation in microalgae increases as the cells age and enter the stationary phase, generally as a result of stressful environmental conditions (Hu et al. 2008; Sharma et al. 2008). Eyden (1975) concluded that lipid accumulation in ageing or stationary cultures could be explained on the basis that exponentially growing cells use all lipids synthesised in the formation of new membranes, whilst in cells in stationary phase, the synthesised lipids are accumulate in lipid bodies.

Exposure to certain infochemicals such as decadienal are also known to lead to faster lipid accumulation (Taylor et al. 2012) and to changes in the life cycle of some organisms (Caldwell et al. 2002, 2004; Adolph et al. 2004; Ribalet et al. 2007; Taylor et al. 2007). Therefore, a main objective of this study was to investigate the effect of decadienal on lipid production and cell ultrastructure in two microalgal species, *Dunaliella salina* and *Nannochloropsis oculata*; both of which are cited as potential candidates for biofuel production (Sharma et al. 2012). A comparison was also made between naturally senescent stationary cells and cells treated with decadienal, to determine if the main effect of this compound was simply to induce premature senescence. The results of this study are discussed with reference to three main themes: comparing the ultrastructural differences between active and stationary phase growing cells in relation to the existing literature for the species studied; discussing the effects of decadienal on lipid production; and, finally, discussing the effects of decadienal on ultrastructure.

3.4.1 Ultrastructural differences between actively growing and stationary cells

3.4.1.1 Dunaliella salina

3.4.1.1.1 General morphology

Although describing features of taxonomic interest is not the primary aim of this chapter, some of the differences in ultrastructure observed in this study of *D. salina* and previously published studies will be highlighted. *Dunaliella* classification is based on physiological and ultrastructural differences between different species. Previous ultrastructural studies of *Dunaliella* are comparatively few and they are secondary resources. They depend on the earliest intensive revision of *Dunaliella* taxonomy by Massyuk in 1973 (in Borowitzka and Siva 2007). This was originally written in Russian and summarized by Ginzburg (1987) and Preisig (1992). Borowitzka and Siva (2007)

revised the traits used to classify *Dunaliella* by studying all the isolates available to them.

According to Ginzburg (1987), the genus *Dunaliella* has two groups with different cell forms, which he gave species level assignation. The first is represented by *Dunaliella salina*, which has rounded cells and is reddish or orange in colour (due to carotenoid accumulation); the cell axes are 10-20 μm long. These cells move slowly and the two flagella are short relative to cell length (Ginzburg 1987). When grown at low light intensities, the cells lose their carotenoid colouration, making the green chloroplast visible. *D. salian* chloroplast volume occupies no more than half of the cell volume (Ginzburg 1987). The second type of cells is represented by *Dunaliella viridis*, which are cylindrical to ovoid in shape and coloured green (Ginzburg 1987). The two flagella are attached to the front of the cell and point backwards and they are usually longer than the cell length (Ginzburg 1987). Cells measure 3-5 μm by 6-8 μm and are similar to the green cells referred to as chlamydomonads, or of the Volvocalean type. These cells move comparatively quickly. The chloroplast appears to occupy most of the cell body (Ginzburg 1987).

The strain D. salina CCAP 19/30 used in this present study showed morphological features shared by both D. salina and D. viridis as defined by Ginzburg (1987) and D. bioculata reported by Borowitzka and Siva (2007). Firstly, the cell shape varied from rounded to cylindrical to ovoid. Secondly, the cell length was closer to D. salina, as it measured from 10-20 µm. Thirdly, the chloroplast occupied most of the cell body, which is a feature of D. viridis. Finally, the flagellar length was larger than cell length, which is different from the finding of Borowitzka and Siva (2007). They found that D. salina CCAP 19/30 had a flagellar length shorter than the cell length. Further, they found D. bioculata cells to have flagella 1.5-2 times the cell length (Borowitzka and Siva 2007). In addition, they described *D. salina* species that had green to dark red cells, which accumulated β -carotene as a droplet in the chloroplast stroma, and their flagella length was approximately equal to cell length. This study showed that the D. salina CCAP 19/30 flagella were 1.6 times the cell length (similar to *D. bioculat*a) and were always green, wide from the posterior end and gradually narrowing towards the anterior end. These are all characteristics of *D. bioculata* as reported by Borowitzka and Siva (2007).

These differences in morphological features may be due to a number of reasons. One factor could be the validity of the feature chosen to identify or classify the species. As mentioned previously, the flagellar length was varied in this present study from that in the literature. This could indicate it was not a stable feature to consider or there was misidentification in the culture collections. The flagellar length could be unreliable because observations were based on limited samples and isolates and there was not much detail in the literature about their materials and methods. Therefore, it is possible that the flagellar length could be either intraspecific (different within the species itself) or interspecific (different between different species). However, because of the scarcity of data this could not be unequivocally confirmed. Another reason for this variation could be cultural misidentification. In support of the claim of misidentification, the molecular studies by Gomez and Gonzalez (2004) indicated that there was genetic diversity which supported the observed physiological diversity within the studied strains of D. salina, indicating that more than one species could be found among them. This diversity could reflect on ultrastructure. This might explain the difference described in this study and the literature. However, the present writter does not have genetic information regarding the strains used in ultrastructural studies.

3.4.1.1.2 Chloroplast structure and lipid reserves

The differences between the present findings and previous work might be due to different culture conditions and age. This could be demonstrated by the effect of age and stress factors affecting the plastid organization and cellular lipids location in the cell. The internal cytoplasmic organisation of 10-day-old active phase D. salina cells revealed a structure similar to that previously described for this species (Preisig 1992). Chloroplast structure of 14-day-old stationary cells had noticeable ultrastructural changes in the stationary phase cells. However, Leonardi and Caceres (1994) showed that the lamellae (of their stationary phase cells) were made up of 2 to 9 thylakoids. These findings match this study of actively growing cells. Leonardi and Caceres (1994) used a 7-day-old culture as stationary phase cells and 4-day-old culture as actively growing cells (leaner). In addition, Leonardi and Caceres (1994) showed that the chloroplast in stationary phase cells was filled with lipid globules and only the pyrenoid was surrounded by 1 to 2 layers of starch plates. In this study, stationary phase (14-dayold) chloroplasts were mostly occupied by starch granules, resulting in the thylakoid membranes becoming densely compacted. The lipid globules were largely in the cytoplasm, rather than in the plastid stroma. Further, the strain of Leonardi and Caceres

(1994) was a brackish water strain, while in this study F/2 media with a salinity of sea water was used. Borowitzka and Siva (2007) reported that the *Dunaliella* chloroplast was smooth and changed to a granular appearance due to starch accumulation, as a result of being stressed by higher salinities and/or the ageing of the culture, as found in this study. However, they did not mention if their findings were based on laboratory grown cultures. However, in the same paper, they presented micrographs resembling field samples that show lipid globules in the chloroplast, which contradicts their statement. This variation could be due to the culturing system, as the laboratory culturing conditions result in the presence of starch in the chloroplast with ageing, while in natural environment lipids are synthesised instead of starch due to limited carbon availability and the differences of light intensity (Stoynova-Bakalova and Toncheva-Panova 2003; Su et al. 2011). Furthermore, lipid accumulation in the eyespot increased with age, the number of eyespot lipid droplets doubling between log and stationary phases (Ginzburg 1987; Preisig 1992). In this present study there was no doubling in droplet number between exponentially growing and stationary phase cells, but their size did double (250 nm cf 125 nm) (Figure 3.6E and F).

Another lipid containg structure, which appears to be of taxonomic significance, is the prominent red eyespot or stigma (Hoshaw and Maluf 1981). The stigmata of D. tertiolecta and D. primolecta seemed to lie free in the chloroplast matrix, whereas in D. bioculata and D. salina they were more closely associated with the chloroplast lamellae. This present study showed that the stigma lipids of D. salina CCAP 19/30 occurred between closely adpressed chloroplast thylakoids, which is similar to the observations of Preisig (1992), being located within the anterior and peripheral part of the chloroplast in both exponential and stationary phase cells. This is consistent with the findings of Leonardi and Caceres (1994) but contradicts those of Melkonian and Preisig (1984), who only found the eyespot sporadically and, when found, it was only one layer of lipid globules. Eyden (1975) reported that the eyespot of *D. primolecta* was plate-like and occured in the matrix, being composed of 1 or 2 layers of closely packed lipid globules 100-200 nm in diameter. The eyespot of *D. tertiolecta* also lay in the matrix, but in *D*. salina it was connected with the thylakoids (Preisig 1992). Ginzburg (1987) reported that the eyespot was made up of one or two rows of lipid globules and its presence differed between strains.

Hoshaw and Maluf (1981) also described some differences in characteristics between log and stationary phase cells. Lipid droplets accumulated in the cytoplasm. The

osmiophilicity of cytoplasmic lipid droplets was different from that of the chloroplast. This variation in osmiophilicity could be as a result of the variable effects of growth phase on lipid composition and yield (Dunstan et al. 1993; Brown et al. 1996; Lv et al. 2010). In stationary phase cells, the plastid thylakoids were stacked in 8 to 10 layers and were tightly compacted, compared to those in exponentional phase cells. In the latter, the thylakoid stacks were typically composed of only 2 to 4 layers. Finally, amounts of both starch and lipid increased in stationary compared with exponential phase cells. Whilst Hoshaw and Maluf (1981) found that starch deposits only increased slightly, the number of lipid droplets increased twofold. However, they did not quantify these changes as done in this present study.

Another explanation is that the presence of oil or starch in the *Dunaliella* chloroplast or cytoplasm could be a species-specific (intraspecific) characteristic. Ginzburg (1987) reported that in *D. tertiolecta* starch increased in the stationary phase and chloroplasts contained oil droplets which were not as conspicuous as in D. salina. Eyden (1975) reported that the chloroplast of stationary phase cells in *D. primolecta* also had very large and numerous starch granules. Preisig (1992) reported that the starch grains, which were plentiful in older cultures, encased the pyrenoid and were also found at other sites in the chloroplast. In exponentially growing D. primolecta cultures, lipid inclusions were sparsely scattered (Eyden 1975) throughout the chloroplast which had interconnected groups of thylakoids in a fine granular matrix. Furthermore, the refractive granules (probably representing intracellular lipid) were considered to be amongst the most stable *Dunaliella* species characteristics (Butcher 1959; in Hoshaw and Maluf 1981). For example, in D. tertiolecta the granules were present in the cytoplasm and considered one of its main distinguishing features (Hoshaw and Maluf 1981). It is well known that both D. salina and D. parva accumulate large quantities of β -carotene in oily globules within the inter-thylakoid spaces of the chloroplast, which changes the cell colour to orange-red (Preisig 1992). This was not seen in the current D. salina strain (CCAP19/30).

3.4.1.1.3 Other cell organelles

There are certain cytoplasmic organelles which develop ultrastructural features changed by age and cannot be related to specific species. Rather, they with concerned to a physiological function such as enabling survival in poor conditions in the exponential growth phase or in stressful conditions. Examples of these organelles are mitochondria, Golgi and vacuoles. Melkonian and Preisig (1984) and Leonardi and Caceres (1994) noted that both exponential and stationary phase cells contained a single branched mitochondrion. In the present study, the mitochondria profiles were always located between the chloroplast and nucleus, although without serial sectioning it could not be ascertained whether or not these represented a single branched organelle. Ginzburg (1987) and Preisig (1992) reported the presence of mitochondrial profiles in other parts of the cell, such as in proximity to the basal bodies and in more peripheral positions between the chloroplast and the plasmalemma. Vladimirova's study in 1978 (in Ginzburg 1987) reported that the mitochondrial profiles were surrounded by extensions of the chloroplast membrane, which was never observed in this study. The 1989 study by Klut et al. (in Preisig 1992) showed that the number and size of mitochondria may vary among cells at different stages of growth (Preisig 1992). In this present study, 2 Golgi dictyosomes were found in both active and stationary phase cells, as described by Melkonian and Preisig (1984). In contrast, Leonardi and Caceres (1994) reported that the Golgi apparatus was always made up of 3 dictyosomes in young cells and 6 to 8 dictyosomes in older cells. However, stress conditions may affect the Golgi apparatus in different ways. In this present study it was noted that the number of cisternae in a single Golgi dictoysome in stationary cells exceeded that of actively growing cells. Stoynova-Bakalova and Toncheva-Panova (2003) considered that the Golgi usually appeared to be rather non-functional in D. salina stressed cells and there were fewer in number compared with D. bioculata. Under UV-B radiation, the cisternae in Golgi dictyosomes became loosely associated (Tian and Yu 2009).

In this present study it was observed that vacuoles were present in both active and stationary phase cells of *D. salina*, and although there was no significant difference in volume fraction their ultrastructure differed markedly. Active phase vacuoles were electron-lucent while stationary phase vacuoles contained electron-dense granules, as has been illustrated in stationary phase vacuoles in many green flagellates (Dodge 1973). This was also reported by Eyden (1975), who noted that the vacuoles contained either mitochondria or cytoplasm and ER; however, these may have been fixation artefacts. Electron-transparent vacuoles have been described in exponentially growing cells in *D. primolecta* (Eyden 1975), *D. viridis* (Anghel et al. 1980; in Parra et al. 1990) and *D. salina* (Leonardi and Caceres 1994). Hoshaw and Maluf (1981) showed an increase in vacuole number in stationary phase cells. Many studies have reported that the vacuolar content of exponential phase cells was quite variable, ranging from

granular and thread-like material to concentric arrays of membrane (Trezzi et al. 1964; in Hoshaw and Maluf 1981; Marano-LeBaron and Izard 1972; in Visviki and Rachlin 1994a); but, again, these may be fixation artefacts. Despite the nature of vacuolar inclusions in most organisms being poorly understood, it has been reported that stationary phase cell vacuoles often contained a compact, dark-staining material surrounded by numerous small vesicles and they might contain small lipid-like granules (Preisig 1992). However, this present study showed that the stationary phase cell vacuoles had only a compact, dark staining material with no vesicles.

3.4.1.2 Nannochloropsis oculata

3.4.1.2.1 General morphology

There have been very few previous ultrastructural studies on *Nannochloropsis oculata*, and most published studies describe other species in the genus. The cells of Nannochloropsis are only 2-4 µm in size and were originally considered to be related to Chlorella in the Chlorophyceae (Droop 1955; in Maruyama et al. 1986). However, Hibberd (1981) placed *Nannochloropsis* in the Eustigmatophyceae, within what are now defined as the Ochrophyta clade of algae. Even with the advent of electron microscopy the cells proved difficult to fix and had relatively few non-ultrastructural anatomical characteristics (Hibberd 1981). Karlson et al. (1996) described the ultrastructure of N. granulata using a much improved fixation protocol. This species had globose cells which contained one to two chloroplasts, a mitochondrion with tubular cristae, and a nucleus. The cell wall was thin and appeared to consist of a single electron-dense layer. However, Mohammady et al. (2005) reported that N. salina cells had a multi-layered cell wall, which appeared to be covered by an irregular network of rib-like structures. This present study showed that *N. oculata* CCAP849/1 had a rounded to globose cell shape and its cell wall consisted of a single electron-dense layer similar to N. granulate (Karlson et al. 1996) and not N. salina (Mohammady et al. 2005).

3.4.1.2.2 Chloroplast morphology and structure and lipid reserves

Nannochloropsis has a single chloroplast with three thylakoid lamellae, which is a typical feature of chromophyte algae (Antia et al. 1975). The occurrence of pyrenoids is problematic as they were not detected in *N. oculata* (CCAP849/1) by Maruyama et al. (1986) but were described in an earlier study by Antia et al. (1975). Further, no girdle lamella or pyrenoids were observed (Antia et al. 1975). However, another feature of *N*.

oculata that differs from those of typical chromophytes is the absence of a chloroplast-associated endoplasmic reticulum (Hibberd and Leedale 1972). Neither pyrenoid nor girdle lamella were observed in *N. oculata* CCAP849/1 in the present study.

Solomon et al. (1986) reported few inclusions in the stationary phase chloroplast and lipid droplets present in both exponentially and stationary growing populations. Lipid droplets were adjacent to mitochondria. Vesicles with finely lamellate contents as reported by Solomon (1985) were also seen in the results of the present study. The presence of membrane-bound lamellate vesicles in the cytoplasm of stationary phase *N. oculata* (CCAP849/1) cells is a characteristic shared with other eustigmatophytes (Hibberd 1981). The present writer did not observe any lamellate vesicles in the chloroplasts of *N. oculata*, contrary to reports of lamellate inclusions within the plastids in *N. oculata* and *N. salina* (Antia et al. 1975), but in this study lamellate structures did occur in the cytoplasm. However, it is not clear whether these represent homologous structures.

Cells are typically surrounded by multiple layers of an electron-lucent substance (Solomon et al. 1986). Mohammady et al. (2005) also reported that in *N. salina* the plastid thylakoids consisted of groups of three and the stroma contained plastoglobuli (lipid bodies). There were no girdle lamellae. However, in this species they reported that the chloroplast was associated with a stalked pyrenoid penetrated by thylakoids. Under light microscopy, the eyespots in *N. oculata* were observed in this present study and this appears similar to what Droop (1955; in Maruyama et al. 1986) described as a circular pale orange-red stigma. When viewed at certain angles it appeared to be present in the chloroplast, but generally appeared as a free body in the cytoplasm. Antia et al. (1975) reported "copious cytoplasmic lipid accumulation" in ageing cells of *N. oculata*.

3.4.2 Effects of decadienal and culture age on lipid accumulation in *Dunaliella* salina and *Nannochloropsis oculata*

A major aim of this chapter is to investigate the effects of decadienal on cell ultrastructure and lipid production following on from the study of Taylor et al. (2012). The effects of decadienal on cell structure of *D. salina* and *N. oculata* has been described after subjecting these two organisms to different decadienal concentrations as described in section 3.2.2. The assumption is that decadienal can trigger cells to shift from normal growth phase to stationary phase quickly. This was investigated through comparison of the ultrastructure of stationary phase cells and the decadienal-treated

cells. In this present study, both ultrastructural changes and the volume fractions of the stationary phase cells were different from decadienal-treated cells. The stationary phase cells of D. salina had an increased volume fraction of both lipid bodies (7.1%) and starch (41.1%) and decreased thylakoid membranes volume fraction (19.1%). The low decadienal concentration (2.5 µM) did not trigger lipid production and did not differ from the actively growing cell ultrastructure. There was no significant difference in cell organelle volume fractions between 2.5 µM decadienal-treated and untreated control (0 μM decadienal-treated) cells, except for a significantly higher thylakoid membrane volume fraction in control cells. In contrast, the higher concentration (50 μM) resulted in more lipid globules in the cytoplasm, but did not affect starch volume fraction in D. salina and vesicular bodies volume fraction in N. oculata. In addition 50 μM decadienal decreased the volume fraction of nucleus, mitochondria and matrix in D. salina. The N. oculata cell treated with ethanol and decadienal had a significant increase in lipid bodies and cell wall fraction volumes (which might be attributed to either decadienal or ethanol or their synergistic effects). Although, there was a significant increase in cell wall volume fraction within 50 μM decadienal-treated cells of *N. oculata* compared with untreated cells, this was still much lower than that in normal stationary phase cells (the mean cell wall volume fraction of stationary cells was 14%, whereas for the highest decadienal treatment it was 9%). Increasing cell wall volume is a general mechanism to adapt to harsh conditions (Fogg 2001). It should also be remembered that the cell wall is an important cytological factor to consider in biofuel production as it can make cells difficult to break and lipid extraction difficult. These observations suggested that decadienal does not trigger the cells of D. salina and N. oculata to shift from the normal growth phase to stationary.

On the other hand, the ultrastructural changes induced by decadienal indicated here cytoplasmic changes similar to those induced by other types of stressors. The stressors are divided into physical and mechanical factors such as visible radiation, UV-radiation, temperature osmotic pressure and desiccation. The other types of factors are nutritional and biochemical such as nutrient (N, P, C) deficiency, pH and toxic substances. Lipid production is a general response mechanism that is caused by several factors. The response mechanism is different and depends on the type of stressor, exposure period and concentration. Lipid production has been reported in *D. tetriolecta* cells grown in allantoic acid to develop frequently, in contrast with cells grown in nitrate, urea or hypoxanthine (Oliveira and Huynh 1989) and in nitrogen depleted

conditions (Mendoza et al.1999). Similarly, subjecting *D. salina* to UV light also triggered lipid globule formation (Tian and Yu 2009). These stress factors produced lipid granules similar to those revealed by this study. However, previous studies did not include any volume fraction measurements.

Cells treated with low concentrations (2.5 µM) showed only minor effects on the major cell organelles. In contrast, cells treated with the high concentration (50 µM) showed more significant but variable changes to cell structure. Exposing D. salina to 50 μM decadienal resulted in some cells remaining intact and maintaining their ovoid shape, whilst others became more rounded and other cells lysed. This variation in response was reported in the response of *Dunaliella* to salinity (Stoynova-Bakalova and Toncheva-Panova 2003). Further, Stoynova-Bakalova and Toncheva-Panova (2003) reported the formation of lipid globules in D. salina when stressed by 220 µmol m⁻² s⁻¹ irradiance. However, in their study the droplets were of different sizes and electron-densities (osmiophility) compared with cells growing normally. Although these lipid droplets were found in the cytoplasm, they were mainly located under the plasma lemma (Stoynova-Bakalova and Toncheva-Panova 2003). The authors attributed the production of lipid globules under the plasma membrane to the cell defence mechanism, which forms a layer that prevents high irradiation from damaging the cells. In comparison, the results of the present study showed that lipid globules formed following exposure to 50 μM decadienal were uniformly electron-dense and had variable sizes. These results suggest that lipid induction from irradiation differs from lipid induction from decadienal.

Furthermore, lipid globules in *D. salina* have been reported to be formed under carotenogenic conditions such as high light intensity and salinity nutrient starvation (Ben-Amotz et al. 1982; Rabbani et al. 1998). More recently, β -carotene accumulation in *D. salina* caused by different stress factors was studied by Lamers et al. (2010). They studied eight stress combinations in batch experiments, of which five combinations resulted in increased β -carotene levels. β -carotene production was induced by high light intensities, even if accompanied by other factors such as high salinity, low temperature and nitrogen depletion. However, only the low light intensity when combined with nitrogen depletion induced β -carotene production. Also, Alhassan (1987) reported that elevated salinity induced numerous, small lipid globules in the cell periphery. The carotenoid lipid globules differed in size, location and number from

those triggered by decadienal, as they were found in the cytoplasm, were larger in size and fewer in number. This supports the earlier premise that ultrastructure variations could be due to age and cultural conditions (section 3.4.1.1.2).

An example that supports the premise that the cellular response mechanism varies under different conditions, even to the same stressor, is the study by Visviki and Rachlin (1994a). In their study, lipid production in *D. salina* in response to copper and cadmium was dependent on time and concentration. Acute exposure of *Dunaliella* to 4.55 µM Cd⁺⁺ resulted in increased relative lipid volume by 91.7%, significantly increased cell volume, and decreased relative nuclear volume. In contrast, combining copper and cadmium decreased the relative lipid volume by 68.3%, with no changes in the mean total cell volume or relative nuclear volumes. In addition, constantly exposing Dunaliella to 4.9 x 10⁻⁴ mM copper and 4.5 x 10⁻⁶ mM Cd resulted in significantly increased relative lipid volume (211.7% and 143% respectively). Although lipid production increased, the overall culture growth decreased (Visviki and Rachlin 1994b). These results resemble the decadienal results, which showed increased lipid production at 50 µM but not in 2.55 µM treatment (The increase is 72% from control). Decadienal also reduced culture growth (Taylor et al. 2012). In the case of N. oculata, the increase in the lipid volume fraction was 840% for the ethanol control, 690% for 1 µM decadienal, 650% for 10 µM decadienal, and 340% for 50 µM decadienal, suggesting that ethanol could also be used as a stress factor and that decadienal may potentially interfere with its effect. Ethanol has been reported to increase phospholipid production in *Chlamydomonas eugametos* gametes (Musgrave et al. 1992).

Another example that support the premise the cellular response mechanism varies under different conditions is the study by Solomon et al. (1986), which reported increased cytoplasmic and chloroplast lipid droplets as a result of nutrient starvation in *N. salina*. The chloroplast lipid droplets were more electron dense than those in the cytoplasm. In addition, the presence of vesicles within the chloroplast disrupted the thylakoid arrangement, and lipid droplets were surrounded by crystalline structures in some cells. These structures were not found in this present study, which showed decadienal induced lipid bodies in the cytoplasm only in the case of *N. oculata*. In addition, they reported that the mitochondria were in close association with the lipid droplets and chloroplasts, suggesting close metabolic relationships between these organelles (Solomon et al. 1986).

Although decadienal resulted in the accumulation of lipid globules in active growth cells, the amount of lipid did not approach that observed in the stationary phase cells. The lipid volume fraction of 50 µM decadienal-treated cells was 10% of the lipid volume fraction of the stationary phase D. salina cells. For N. oculata, the lipid volume fraction in the stationary phase was 28% and decadienal-treated cells had a lipid volume fraction of 3.4%. However, these values are the volume fraction of lipid bodies only, in contrast to chemical extraction methods that quantify the total lipids in the cell, including membrane lipids. Therefore, the volume fraction of thylakoid membranes in the decadienal-treated cells was similar to untreated cells, approximately constituting 30% of cell volume of both D. salina and N. oculata. These findings suggest that decadienal did induce the production of pure lipid bodies (TAGs) in the cytoplasm of an actively growing cells, which supports the findings of Taylor et al. (2012). This is consistent with the results reported regarding other environmental factors that can affect lipid production (Boussiba et al. 1987; Roessler 1990; Thompson 1996; Khozin-Goldberg et al. 2002; Zhekisheva et al. 2002; Guschina and Harwood 2006; Solovchenko et al. 2008). However, the volume fraction of lipid bodies induced by decadienal suggests that it did increase the lipid bodies volume (which contains a pure lipid, that will facilitate lipid extraction), but not in quantities that exceed the normal lipid production rate of normal elderly cells. Therefore, decadienal would not be a suitable lipid inducer for a cost-effective lipid extraction plant.

It was hoped that volume fractions of lipid in cells determined by electron-microscopy could be related to actual levels of lipids in cells (by dry mass). However, in the absence of quantitative analysis of lipids in the cultures that were fixed for electron microscopy, it was found that it was not practical to undertaken this.

3.4.3 Effect of decadienal on other cell organelles of *Dunaliella salina* and *Nannocloropsis oculata*

The present detailed ultrastructural study showed that when *D. salina* cells were exposed to an increasing dose of decadienal, increased cell damage and lysis were found. This is the first study to document the effects of decadienal on cell ultrastructure in *D. salina* and *N. oculata*. The knowledge of how decadienal affects algal cells is incomplete, decadienal has variable effects depending on the eukaryotic cell being tested. For example, it is toxic to liver and kidney cells (Hageman et al. 1991) but apparently increases the number of gastrointestinal epithelial cells (National Toxicology

Program 1993). Decadienal has been reported to trigger programmed cell death (PCD) or survival pathways in human cells (Sansone et al. 2014) and is reported to have irreversible effects due to covalent modifications of proteins or DNA (van Iersel et al. 1997; Ishii et al. 2003). Decadienal can break DNA strands by oxidative damage and adduct formation (Nappez et al. 1996; Young et al. 2010). Membrane blebbing is reported only in high concentrations in copopod embryos (Hansen et al. 2004). Furthermore, it disrupts tubulin organisation and cell spindle formation during cell division (Buttino et al. 1999). In addition, it is also reported as genotoxic (Hansen et al. 2004; Romano et al. 2010), and high doses induce oxidative stress and ROS production in immortalized BEAS-2B (a human lung cancer cell line) (Chang et al. 2005) and oxidative DNA damage in A549 cells (another human lung cancer cell line) (Wu and Yen 2004). Since *D. salina* and *N. oculata* are eukaryotic cells any of the previously mentioned effects could occur. In the following, the possible effects based on the ultrastructural features reported in this present study will be discussed, supported by the evidence available in the literature.

This study suggests that decadienal is toxic to *D. salina* and *N. oculata* as it generates cell morphological changes that resemble PCD. However, the mechanism of PCD can only be confirmed by both the ultrastructural changes and the specific biochemical inhibitors and activators that induce them and this study was limited to ultrastructural analysis. Therefore, drawing firm conclusions about the precise PCD mechanism invoked by decadienal is difficult. However, comparing the results here with information present on the effects of decadienal on other eukaryotic cells may prove helpful through determining the ultrastructural characteristics of different PCD mechanisms (since different PCD mechanisms have unique ultrastructural features) (Table 3.13). PCD is a universal biological phenomenon that has been identified in both multicellular and single cell organisms with the same characteristics (Ameisen 2002). It is a highly controlled process through which cells control their death in response to injury, although it is often difficult to distinguish the different types of PCD and, despite having specific and clearly defined characteristics, even apoptosis can be difficult to recognise in cell model systems (Vaux 1999). Table 3.13 lists the types of PCD and their signs and characteristics. In spite of this difficulty, a normal apoptotic-like PCD pathway has been widely reported in vascular plants (Greenberg 1996; Pennell and Lamb 1997; Lam et al. 2001) as well as in some unicellular eukaryotic organisms such as chlorophytes (Berges and Falkowski 1998; Segovia et al. 2003; Segovia and Berges

2005), dinoflagellates (Vardi et al. 1999; Dunn et al. 2004; Franklin and Berges 2004), diatoms (Casotti et al. 2005), yeasts (Frohlich and Madeo 2000), and kinetoplastids and slime moulds (Cornillon et al. 1994). It has even been described in prokaryote groups such as bacteria (Lewis 2000) and cyanobacteria (Berman-Frank et al. 2004). This almost universal occurrence of PCD suggests that the origin of programmed cell death is very ancient (Berman-Frank et al. 2004). Therefore, any one of *D. salina* and *N. oculata* could have this mechanism. However, how PCD has evolved in unicellular organisms is controversial (Deponte 2008).

Table 3.13: Programmed cell death mechanisms, their signs and mediator with the key reference

PCD	Signs	Mediator
Necrosis	Cell swells, incomplete	Passive process, not being
Identified by Rudofi Virchow	degradation of plasma membrane	controlled by genes (Bredesen
(Linkermann and Green 2014)		2007)
Apoptosis	Cytoplasmic shrinkage occurs but	Gene-directed mechanism
	the cell remains surrounded by an	controlled by an energy-
	intact plasma membrane	dependent process (Strasser et
		al. 1994; Martin et al. 1995;
		Gottlieb et al. 1996; Zhai et al. 1996)
Paraptosis	Characterized by cytoplasmic	Mitogen-activated protein
	vacuolization and mitochondrial	kinases (MAPKs) (Sperandio
	swelling in the absence of caspase	et al. 2000, 2004)
	activation or nuclear changes such	
	as pyknosis (chromatin	
	condensation followed by nuclear	
	fragmentation) and DNA	
	fragmentation	
Autophagy/vacuolar-like cell	Characterized by the degradation	Lysosomal degradation
death	of target organelles (damaged	pathway because of the
	mitochondria; aggregates of	evidence from similar
	misfolded proteins) within the	lysosome-like organelles in
	lysosomal vacuolar system	plants (Swanson et al. 1998)
	without loss of cell integrity as	
	the plasma membrane remains	
	intact. Nuclear degradation and	
	pyknosis perhaps be also occurs	
	during this process (Jones 2000)	

Various PCD mechanisms could be induced by decadienal, one could be apoptosis. In this present study of *D. salina*, the integrity of the plasma membrane was maintained, and there appeared to be no significant cell shrinkage due to leaking cell contents. Both of these features are considered as hallmarks of apoptosis (Lennon et al. 1991). In addition, the cells of *D. salina* exposed to decadienal showed the condensation and margination of heterochromatin in their nuclei. However, some of the other ultrastructural hallmarks of apoptosis seen in animal cells, such as membrane blebbing, and the formation of apoptotic bodies, were not seen (Bredesen 2007).

D. salina appeared to show mitochondrial lysis despite other organelles remaining intact. This may indicate that decadienal could have induced intrinsic (mitochondrialinitiated) apoptosis-like PCD. If this was the case, then had the cultures been given sufficient time the nucleus would have lysed, followed by the full cell. There are various studies that support this premise. Decadienal induces the release of calcium transients and the generation of free radicals (Vardi et al. 2006). Vardi et al. (2006) reported that, in diatoms, decadienal stimulated a dramatic increase in intracellular calcium that persisted for several minutes. These authors suggested that this was a signalling pathway by which decadienal induced cell death in diatoms. First, the diatom perceives the decadienal and this is followed by changes in intracellular calcium that may activate a plant-type NOS to subsequently generate NO. The reactive oxygen species are known to participate in various biological processes, such as apoptosis and DNA damage (Wiseman and Halliwell 1996; Ren et al. 2001). In addition, it has been reported that in animal cells (Jones 2000) and in plants (Levine et al. 1994) high levels of calcium will lead to the release of cytochrome c, and, in turn, this will cause ROS generation, causing the mitochondria to start PCD. From this present study, it also appeared that lysis first started in the mitochondria. Decadienal is known to induce reactive oxygen stress (Chang et al. 2005), which, in turn, triggers mitochondria to become PCDinducing organelles in unicellular microalgae (Jones 2000).

The presence of extracellular signal-regulated kinase (ERK) in *Dunaliella* (Jimenez et al. 2004) may provide another mechanism for PCD induction. Since both *D. viridis* (Jimenez et al. 2004) and mammalian cell (Jimenez et al. 2007) division is regulated by extracellular signal-regulated kinase (ERK). Furthermore, ERK has been proven to cause different death mechanisms in different cell types (Wong et al. 2003; Arany et al. 2004; Schweyer et al. 2004; Subramaniam et al. 2004, Kim et al. 2005; Subramaniam and Unsicker 2006). In ascidians, the caspase-3 is activated by NO (Comes et al. 2007),

which finally activates ERK (Castellano et al. 2014). ERK is a direct target for decadienal in ascidians (Castellano et al. 2015). Subramaniam and Unsicker (2006) reported that the inhibition of ERK in neurons prevented plasma membrane damage. The intact plasma membrane was the hallmark sign reported in the results of the present study of *Dunaliella*. Therefore, the decadienal could have used the ERK as a target and the inhibition of ERK induced the PCD without damaging the plasma membrane. Nevertheless, cell death with non-apoptotic morphology and which is independent of caspase activation depends on the activation of ERK (Castro-Obregon et al. 2004), and this could support the possibility of the other non-apoptotic pathways.

Another possibility is the autophagy type of PCD. The signs of autophagy in *Dunaliella* cells treated with 50 μM decadienal were clear, in the present study, including the lysis of cytoplasm and other cell organelles. Other stress factors such as nitrogen starvation caused the autophagy of the ribosomes and chloroplast membranes in *Chlamydomonas reinhardtii* (Wang et al. 2009). In another study, nitrogen starvation was shown to cause the degradation of the cytochrome *b*6-cytochrome *f* complex of the photosynthetic apparatus (Bulte and Wollman 1992). A close inverse relationship between lipid body formation and autophagy in mammalian systems has recently been reported (Singh et al. 2009). Signs of autophagy PCD were reported in prokaryotic and eukaryotic phytoplankton (Segovia et al 2003; Berman-Frank et al. 2004), such as the increased vacuolization and degradation of the internal cellular content while the plasma membranes remained intact; this was present in *D. salina* cells subjected to 50 μM decadienal.

Segovia et al. (2003) described the effect of darkness on *D. tertiolecta* as autocatalysed cell death that resembled apoptotic cell death with increasing caspase-like activity and expression. The ultrastructural changes were chromatin condensation, loss of the nucleus, and lysis of the starch layer that surrounded the pyrenoid; but the pyrenoid and mitochondria did not change. Hyposalinity also caused heterochromatin condensation (Hoshaw and Maluf 1981). In contrast, the present results showed that all cell organelles lysed except for the starch granules, which indicates that a different cell death mechanism had occurred. This is not a new finding since different cell-death phenotypes were reported in *D. viridis* (Jimenez et al. 2009) in response to different lethal stressors. For example, heat shock resulted in a necrosis-like cell death process, and UV radiation triggered a cell death morphotype transitional between apoptotic and necrotic features which resembled the aponecrotic type. Further, hyperosmotic shock

triggered cell death represented by a paraptotic-like phenomenon. Finally, incubating *D. viridis* under nitrogen starvation resulted in a PCD resembling the autophagic/vacuolar-like cell death. The present results showed a lysis of all cell constituents in the case of *D. salina*, while the membranes remained intact. Therefore, the degradation process of *D. salina* cell constituents could be similar to those found in plant cells: a process of vacuolar autophagy, plastolysony (Krishnamurthy et al. 2000), or secondary necrosis (Bianchi and Manfredi 2004). Table 3.14 summarizes the similarities and differences between the results of the present study and those of Jimenez et al. (2009).

The case of *Nannochloropsis* is quite different. Although lipid production was similar in all samples the ultrastructural changes were comparable to those seen following fixation with glutaraldehyde alone (Chapter 2, protocols one, two, three). Decadienal, of course, is also an aldehyde. The noticeable ultrastructual changes within N. oculata cells treated with decadienal was an increase in overall cytoplasmic density that made it difficult to discern cell organelles such as the nucleus and mitochondria. These observations resemble those made of the effect of decadienal on cells of the diatom *Thalassiosira* weissflogii as reported by Casotti et al. (2005). Both Nannochloropsis and T. weissflogii belong to the same phylogenetic group. Firstly, the recognised morphological effect of decadienal on T. weissflogii was the granularity of the cytoplasm due to the formation of vesicles and refractive bodies in the cytoplasm (the higher the decadienal concentration, the higher the granularity) (Casotti et al. 2005). This present study indicates that at 50 µM decadienal, some cells were observed to be dense with no clear cytoplasmic organelles. DNA degradation in T. weissflogii was also reported by Casotti et al. (2005), where in cells treated with concentrations equal to or higher than 0.5 mg l⁻¹ the chromatins were scattered within the cell. Finally, DNA fragmentation followed by loss of membrane integrity were reported with T. weissflogii cells subjected to decadienal concentrations equal to or less than 1 mg l⁻¹. Casotti et al. (2005) suggest that these cells were undergoing apoptosis. N. oculata cells subjected to decadienal showed a great alteration in their membranous system, starting from altered or loosened thylakoid membranes in comparison to control cells, to the total loss of organelle membranes in 50 μM decadienal. Furthermore, T. weissflogii had a variable response to decadienal (Casotti et al. 2005), and at 0.18 mg l⁻¹ the cells were able to recover from decadienal stress. Vardi et al. (2006) reported that some marine diatom cells were less sensitive to decadienal and produced a delayed response compared with others in the same culture. They claimed that early response cells could induce an intercellular communication

system that could be transmitted within the diatom population. These observations could explain the variable ultrastructural changes in decadienal-treated *N. oculata* cells in the present study.

Apoptosis is reported to occur in aged cells of vascular plants (Fukuda 1994; Buchanan-Wollaston et al. 2003) and as a mechanism to control phytoplankton blooms (Berges and Falkowski 1998; Vardi et al. 1999). The ultrastructure of dead phytoplankton cells found in the natural environment closely resembles senescent cultured cells (Veldhuis et al. 2001). Jimenez et al. (2009) reported that late stationary phase cells of *D. viridis* die in apoptotic-like pathways that resemble those described in *D. tertiolecta* under light deprivation (Segovia et al. 2003). The ultrastructure of the decadienal-treated cells of both *D. salina* and *N. oculata* never resembled the ultrastructure of the stationary phase cells. This could confirm that different programmed cell death pathways are in operation and confirm the results of section 3.4.2. These showed that decadienal did not shift the cell growth from active phase to stationary phase.

This present study has shown that the vacuolar volume fraction in *Dunaliella* increased from 2% in control cells to 8% in 50 µM decadienal-treated cells. Not only were the vacuoles larger, but they also had a different structure compared to, for example, Dunaliella cells subjected to chronic selenium toxicity. Reunova et al. (2007) described frequent lytic vacuoles associated with cytoplasmic autolysis. In their study, the small "lysosomal" vacuoles fused to form larger ones, and generally these vacuoles surrounded the nucleus or were in intimate contact with it. The vacuoles in 50 µM decadienal-treated D. salina and all decadienal-treated N. oculata cells contained concentric masses of membranes and other particulate fractions. Stoynova-Bakalova and Toncheva-Panova (2003) reported that vacuoles with osmiophilic inclusions occupied the larger area of the cell in samples treated with high salinity concentrations and high irradiance. This type of vacuolar inclusion has been widely described in many different algal species, such as D. tertiolecta (Hoshaw and Maluf 1981) and the diatom Diatoma tenue var. Elongatum (Sicko-Goad and Stoermer 1979). On the other hand, the concentric masses of membranes were reported to increase with lead poisoning in the Diatoma tenue (Sicko-Goad and Stoermer 1979) and poisoning by several heavy metals in *Plectonema boryanum* (Rachlin et al. 1982) and *D. salina* and *Chlamydomonas* bullosa (Visviki and Rachlin 1994a). The latter authors proposed that the lipids and proteins of these membranes act as reservoirs to store the excess quantities of intracellular cations as a mechanism to counter metal poisoning. The hypothesis behind

this detoxification mechanism is that the membranes can increase the surface area within the cell in which metals can react with sulphydryl groups and thus prevent the excess cations from reacting with susceptible and important cellular organelles or machinery. This mechanism of detoxification could be applicable to decadienal exposure, since the volume fraction and number of cells with membranous vacuoles increased under 50 μM decadienal exposure in *D. salina* and in all exposed *N. oculata* cells. The vacuoles contained several layers of thick or thin membranes.

In conclusion, microalgae have superiority over conventional land-crop biofuels for biodiesel production (Chisti 2008). One vital advantage of particular interest to this present study is that they have the ability to produce large amounts of lipids, including triacylglycerides (TAGs), which can be converted into biodiesel through transesterification (Chisti 2007). The use of microalgae species for commercial products, including biofuel production, is an important area of research. The species D. salina is already successfully used to produce β -carotene commercially and N. oculata is successfully used commercially to feed fisheries (Boussiba et al. 1987). The focus of this study was on the effect of decadienal on the ultrastruvture of two microalgae species, D. salina and N. oculata as sources of lipids and subsequent biodiesel production. The lipid volume fraction percentages under high and low decadienal as well as stationary phase cells were compared for D. salina and N. oculata in 30 randomly selected micrographs. The highest lipid volume fraction percentage was found in *N. oculata* stationary phase cultures. The highest lipid volume fraction percentage induced by decadienal was found at 50 µM in N. oculata cells. This study demonstrated that although decadienal could increase the species lipid bodies production, the lipid bodies volume fraction constituted a very low fraction of cell volume. Furthermore, signs of PCD, which limit population growth, were induced by decadienal. This was also revealed by Taylor et al. (2012), who showed that decadienal induced significant lipid production and reduced the growth rate of *N. oculata*. Therefore, the main obstacle in this area of research is the compromise between cell health and lipid productivity. With reference to the results obtained, the smaller volume fraction in cells treated with higher decadienal concentration 50 µM suggests that the total lipid content of the cell is important, not only the lipid bodies that contain TAGs, although TAGs are easier to convert to biofuel by transesterification. Finally, with reference to the ultrastructural changes induced by decadienal in the present study, different programmed cell death mechanisms could be induced by decadienal in D. salina. These include, apotosis,

apoptitic-like PCD, paraptosis, autophagy because the main ultrastructural effect on *D*. *salina* was mitochondrial cell lysis with intact plasma membrane. In *N. oculata* the main ultrastructural effect was dense granules in the cytoplasm.

Table 3.14: Similarities and differences between results of this present study for *Dunaliella salina* programmed cell death and the results of Jimenez et al. (2009)

Factor	Hyperosmotic shock	Results of this study	UV radiation	Results of this study	Acute heat-shock	Results of this study	Nutrient starvation and nitrogen limitation	Results of this study	Stationary phase	Results of this study
Cell death process	Paraptotic		Necrosis and apoptosis (aponecrosis)		Necrotic-like		Autophagic/vascular cell death			
	Swollen	X	Cell swelling	X	Swelling	X	Migration of the nucleus	X	Chromatin aggregation	?
Characteristics	Chromatin condensation	√	Disruption of organelle membranes	X	Nuclear oedema	X	Pyknosis (nucleus condensation)	√	Karyorrhexis (nuclear fragmentation)	?
	Extensive cytoplasmic vacuolation	V	Condensation of mitochondria	X	Mitochondrial rupture	√	Intact cell membrane	√	Membrane blebs	X
			Formation of cytoplasmic blebs	X or ??	Disrupted organelle membranes	X	Blebbing	X		
	Absence of nuclear fragmentation	V	Intact cell membrane	1	Altered plasma- membrane typical of necrosis	X	Absence of leakage of intracelluar content	√	Cytoplasmic disassembling	V
	and cellular				Chromatin clusters		Cytoplasmic consumption	$\sqrt{}$	disassembing	
	blebbing		Neat membrane blebbing	X	can be identified as spots within the nucleus	$\sqrt{}$	Disappearance of chloroplast and other organelles	1		

Chapter 4. Gametogenesis of Pseudostaurosira trainorii

4.1 Introduction

4.1.1 Diatom classification: historical perspectives based on morphological characteristics

Diatoms were described for the first time in the eighteenth century, and their classification has been greatly affected by technological developments (Mann and Evans 2007). An historical analysis shows many different attempts to classify diatoms by many scientists (reviewed by Mann and Evans 2007; Williams 2007; Williams and Kociolek 2011). The key systems are briefly described here to clarify the current state of diatom classification. The earliest attempts at diatom classification were by Carl Adolph Agardh in 1832, followed in 1843 by Friedrich Traugott Kutzing. Their classifications were based on the microscopic characteristics of living organisms, arranging diatoms based on the shape of siliceous valves (Williams 2007). In 1871, Ernst Pfitzer suggested a classification system for diatoms based on chloroplast structure. He proposed two divisions of Coccochromaticae (numerous plastids) and Placochromaticae (one or two plastids) (Mann and Evans 2007). In the following year (1872), Smith used the silica valve parts as a criterion for classifying diatoms. The main feature was the presence of the raphe, which is a true cleft generally on the valve (Williams 2007), which meant that the diatoms were divided into three groups: the Raphidieae, with a true raphe (equivalent to raphid diatoms); the Pseudo-raphidieae (equivalent to araphid diatoms); and the Crypto-raphidieae (equivalent to centric diatoms). Following on from the two systems of Pfitzer and Smith, Schutt, in 1896, introduced two major groups, the Centricae and Pennatae, using a complex system composed of four taxonomic levels (Williams and Kociolek 2011). In 1937, Hendey reclassified diatoms as one order, Bacillariales, which he subdivided into ten sub-orders. In 1966 Patrick elevated Hendey's sub-orders to orders, and in 1979 Simonsen resurrected Schutt's classification by considering Centrales and Pennales as the major division in diatom classification. He considered frustule symmetry to be the main criterion for categorizing them, which was also reflected in differences in

sexual reproduction. All Centrales reproduce by oogamous sexual reproduction with motile sperm, whereas all pennates undergo conjugative sex (Williams 2007). In 1990, Round et al. (1990) reused the three group system, dividing diatoms into classes based on cell morphology using scanning electron microscopy. The first class is the Coscinodiscophyceae, including the centric diatoms which have frustules with radial and bipolar symmetry. The second class is the Bacillariophyceae which include pennate diatoms having a raphe (so-called raphid pennates). The final class is the Fragilariophyceae, which contains pennate diatoms that lack a raphe (so-called araphid pennates). However, Williams and Kociolek (2007) suggested that the classification system of Round et al.'s (1990) could be represented in two ways. In the first, all three groups are considered as equal; whereas in the second the araphid and raphid diatoms are included in the same group encompassing the majority of bilaterally symmetrical species. This is because they considered that "the araphid diatoms are more closely related to raphid diatoms" (Williams and Kociolek 2007).

4.1.2 Diatom classification: molecular phylogeny and ultrastructural characteristics

The molecular phylogeny of the diatoms has progressed in several stages. Phylogenetic studies conducted in the 1990s based on the nuclear-encoded small subunit ribosomal RNAs (SSU rRNAs) revealed that diatoms have heterokont algal lineages (Bhattacharya et al. 1992; Leipe et al. 1994). In the late 1990s, Guillou et al. (1999) demonstrated that they were most closely related to a group of free-living phytoplankton in the Bolidophyceae (Guillou et al. 1999). Several molecular phylogenetic studies have suggested that, within the diatoms, the araphid pennate diatoms evolved from a lineage of centric diatoms (Kooistra et al. 2003 a, b). Two molecular phylogenetic analyses were particularly significant. The first by Medlin and Kaczmarska (2004) revealed that diatoms could be divided into two major subdivision-level clades. The first subdivision was defined as the Coscinodiscophytina (Clade 1), which includes centric diatoms that have valves with radial symmetry (representing the class Coscinodiscophyceae). The other major clade represents the subdivision Bacillariophytina (Clade 2) which has two subgroups (class level): Clade 2a includes the bi- or multipolar centrics and the radial Thalassiosirales (resembling traditional Mediophyceae); and Clade 2b that

includes all pennate diatoms (resembling traditional Bacillariophyceae) (Medlin and Kaczmarska 2004). Therefore, there are three major clades. The second major molecular phylogenetic analysis was by Mann (in Adl et al. 2005) which, although using the same phylogenetic tree as Medlin and Kaczmarska (2004), considered that the centric state was paraphyletic, although no further details were given about other groups.

Following these molecular phylogenetic studies, there has been growing concern about how to reconcile their conclusions with the morphological characteristics on which diatom classification has traditionally depended. Both the morphological and cytological evidence has been reviewed in Medlin et al. (2000) and Medlin and Kaczmarska (2004), who concluded that it correlates with their molecular phylogeny clades as summarized in Table 4.1. However, some morphological features that have traditionally defined different diatom classes, such as pattern centres, reproduction and plastid morphology, and the features that define different orders, such as labiate and strutted processes, were found not to map well onto molecular trees (Medlin et al. 2000). Nevertheless, these structures can still be used to describe the more recent branches in the molecular tree at the order level in diatom taxonomy (Medlin et al. 2000).

4.1.2.1 Golgi apparatus

Medlin (2009) and Medlin and Kaczmarska (2004) proposed that Golgi body arrangement could help in classification, based on their analysis of data from the available literature on Golgi bodies in diatom cells because the structure of the Golgi apparatus correlates well with the major clades of diatom. Golgi bodies have been classified into three types. In type 1, the dictyosomes (G) are associated with endoplasmic reticulum (ER) cisterna and mitochondria (M) and with the so-called G-ER-M unit found in species such as *Coscinodiscus* (Schmid 1988), *Stephanopyxis* (Medlin et al. 2000) and *Ellerbeckia* (Schmid and Crawford 2001). The type 2 Golgi apparatus consists of dictyosomes that surround the nucleus and form a perinuclear shell or ring (Medlin and Kaczmarska 2004) and it is associated with the Thalassiosirales, Aulacoseirales, and the majority of pennates and bipolar centric diatoms. An example of genera that have these arrangements is *Stephanodiscus niagare* (Drum et al. 1966; in Medlin and Kaczmarska 2004).

There are two varieties of the type 2 Golgi. Variation 2.1 occurs in *Synedra ulna*, where the nuclear envelope, nuclear matrix and RNA form two long tentacles which extend until they reach the cell poles (Schmid 1989). The tentacles have two different sides, one with nuclear pores and the other with Golgi dictysomes lining up along the outside (Figure 4.1). Golgi variation 2.2 is found in *Pinnularia*, where the tentacles spread out in multipolar directions with Golgi dictysomes arranged on both sides (Medlin et al. 2000). In type 3, the Golgi bodies are paired with filose tentacles formed by the periplasmic nuclear membrane, and an example of genera that have this arrangement is *Biddulphiopsis titiana* (Coscinodiscophycidae) (Clade 1) (Medlin and Kaczmarska 2004). Golgi variations correlate with the molecular phylogeny tree, where type 1 Golgi are found in Clade 1 (Subdivision Coscinodiscophytina) with the exception of *Odontella sinensis* (G-ER-M unit). Type 2 Golgi, 2.1, 2.3, and type 3 Golgi variations are found in Clade 2 (Subdivision Bacillariophytina), and therefore they could all be considered as a variant of one type called the perinuclear shell (Medlin 2009).

148

Table 4.1: Comparison of morphological features across the three molecular clades (Source: Medlin and Kaczmarska 2004)

Feature	Clade 1	Clade 2a	Clade 2b
Morphological symmetry	Radial centrics	Bipolar centrics plus the radial	Pennates
		Thalassiosirales	
Golgi	G-ER-M, one exception	Perinuclear, one exception	Perinuclear and its variations, no
			exceptions
Pyrenoid	enoid One pore plastid, lamellae cross		One per plastid, very complicated
pyrenoids not connected to		plastid usually not crossed by	structures, lamellae crossing
	thylakoids		pyrenoids are connected to
		periphery of pyrenoids,	thylakoids
		occasionally like clade 1; not	
		connected to thylakoids	
Sexual reproduction	Oogamy, mostly merogenous	Oogamy, mostly hologenous,	Isogamy
	sperm with elongated nuclei	sperm with rounded nuclei	
Auxospore	Isometric	Nonisometric properizonia	Perizonium
Processes raphae	Marginal	Central, also marginal in	Central
		Thalassiosirales	

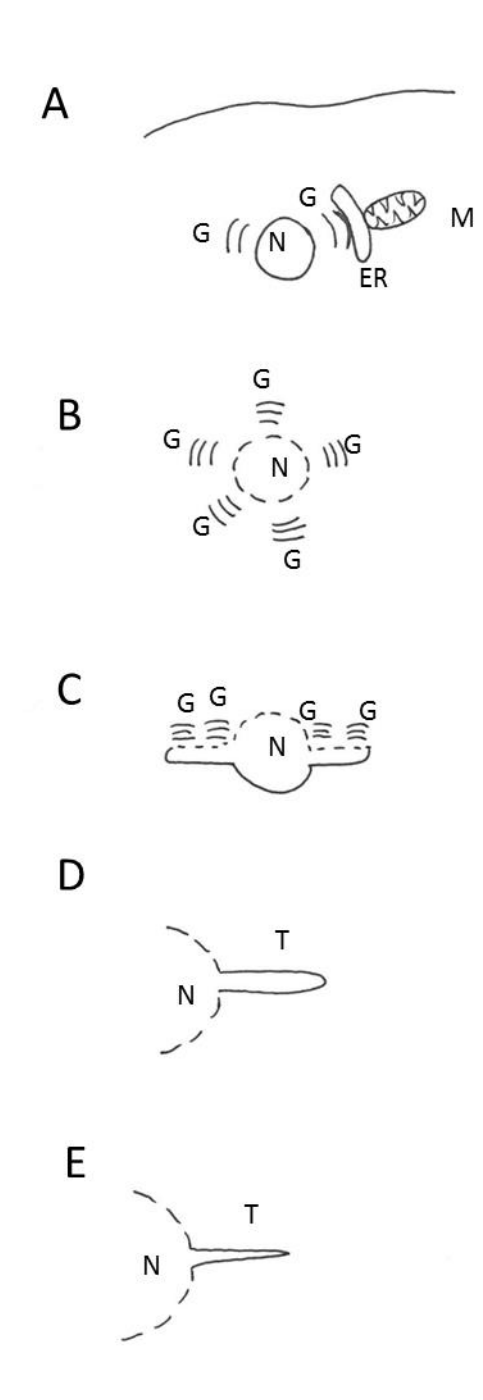


Figure 4.1: Golgi arrangements A) Type one Golgi arrangement, the G-ER-M unit. B) Type two perinuclear shell Golgi arrangement. C) Type 2 variation 2.1. D) Type 2 variation 2.3. E) Type 3 Golgi. (Source: Medlin et al. 2000)

4.1.2.2 Pyrenoid structure

Pyrenoid structure could help in the classification and phylogeny of diatoms, according to the primary results of Mann (1996) and Schmid (2001). Their findings have been summarized by Medlin and Kaczmarska (2004). Table 4.2 shows a detailed summary and brief sketches of the major types of byrenoid structures. The first characteristic is the presence or absence of a membrane that surround the pyrenoid. The second characteristic is the presence or absence of lamellae inside the pyrenoid. The lamellae, if present, have different arrangement and could be associated with chloroplast or not (Schmid 2001). Clade 1 contains centric species which have a single membrane-bound embedded pyrenoid that is traversed by one set or more of lamella. Clade 2a diatoms also have single membrane-bound embedded pyrenoids but with two variations. The first is in the radial centrics of the Thalassiosirales, where the pyrenoid is free of traversing membranes and some species have lamellae invading the pyrenoid periphery (Medlin and Kaczmarska 2004). The second variation occurs in the bi- or tripolar species of clade 2a, whose their pyrenoids resemble those of Clade 1 (crossed by a single thylakoid); however, they differ from Clade 1 in that they form plastids with many pyrenoids. The pyrenoid structure in Clade 2b (the pennate diatoms) is either embedded or protruding, and these include a wide variety of pyrenoid morphologies even in the same species (Schmid 2001). Therefore, the pyrenoids of phylogenetic Clade 2 are more diverse than those of Clade 1 (Table 4.2).

4.1.2.3 Sexual reproduction

Regarding diatom sexual reproduction in relation to ultrastructure and molecular phylogeny this has involved two scientific debates. The first concerns the evolution of the diatom within the algal groups. For example, ultrastructural studies (listed in Medlin and Kaczamarska 2004, non-English literature) have shown that male gametes in both clades of centric diatoms have two transitional plates in the helix, a feature that they share with the sister group of diatoms, the Bolidophyceae (Medlin and Kaczmarska 2004). The second debate is over the evolution of isogamy from anisogamy from oogamy, which contradicts that of other algae as the evolutionary direction is reversed (Edlund and Stoermer 1997).

Sexual reproduction in diatoms is linked to the maximum cell size recovery, as the diatom cell progressively decreases in size through asexual division. Early research focused on vegetative cells only and it was not untill 1950, with von Stosch's study of Melosira mrians, that oogamous sexual reproduction was first described in centric diatoms (Rao 1970). In contrast, conjugative sex in pennate diatoms shows great variability, although the proportion of species in which sexual reproduction has been described is small (Round et al. 1990). The patterns of sexual reproduction (including gametogenesis, gamete behaviour and auxosporulation) include changes that occur independently in different periods, and therefore could not reflect the evolutionary relationships among higher rank taxa (Mann 1993). However, based on phonetic diatom classification, the three diatom groups have developed two different sexual reproduction patterns (Edlund and Stoermer 1997). It is thought that centric diatoms (Coscinodiscophyceae) were the earliest to evolve and are ancestral to the pennates (Chepurnov et al. 2004). The centric diatoms reproduce by oogamy, which is characterized by the presence of morphologically non-similar gametes. The egg (female gamete) is large and non-motile while the sperm (male gamete) is small, motile and anteriorly flagellated (reviewed by Drebes 1977) (Figure 4.2 1a, 2a and b). Meanwhile the two other groups, Fragilariophyceae (araphids) and Bacillariophyceae (raphids), reproduce by isogamy or behavioural anisogamy in which the gametes are morphologically similar but exhibit behavioural differences. The isogamy or behavioural anisogamy starts through contact and/or the production of mucilage envelopes or copulation tubes (Edlund and Stoermer 1997), and pheromones have recently been reported (Sato et al. 2011). These different types of sexual reproduction are discussed next (sections 4.1.2.3.1 and 4.1.2.3.2).

Table 4.2: Summary of pyrenoid characteristics as described by Schmid (2001) together with diagrammatic interpretations of the present writer

Clade	Pyrenoid characteristics	Sketch
Clade 1	Single Membrane bound Embedded pyrenoid per plastid Traversed by one set more of membranes, discontinuous with thylakoids	Cytoplasm Consister Crass
Clade 2a, variation 1	Single. Membrane bound. Embedded pyrenoid. Lack membranes traversing the pyrenoid.	Cytoplasm Chloroplast Pyrenoid
Clade 2a, variation 1, exception 1	The genus <i>Stephanodiscus</i> has a large undulating band with two membranes traversing the pyrenoid	Cytoplasm Chloroplast Chyrenoid
Clade 2a, variation 1, exception 2	Some species have only a fold of pyrenoid membrane slightly projecting along the pyrenoid periphery into the matrix: Cyclotella, Planktoniell, Skeletonema, Stephanodiscus	Cytoplasm Chloroplast Chloroplast
Clade 2a, variation 2:	Single Membrane bound Embedded pyrenoids Tendency to form mega- plastids with several pyrenoids Pyrenoids are traversed by membranes not continuous with the thylakoids	Cytoplasm Chloroplast Chloroplast Chyroplast

Table 4.2: Summary of pyrenoid characteristics as described by Schmid (2001) together with diagrammatic interpretations of the present writer (continued)

together with diagrammatic interpretations of the present writer (continued)					
Clade 2b,	Membrane bound				
embeded	with intra-pyrenoidal membranes				
	that are not continuous with the	Nucleus			
	thylakoids, which completely surround them				
	Number of pyrenoids varies in	Cytoplasm			
	different plastids; some contain	Chloroptes			
	many small pyrenoids while others	Fyrenoid**			
	contain single large pyrenoid.				
Cl. 1 21	Doctor dia comment de comment de c				
Clade 2b,	Protruding pyrenoids occupy the space between the thylakoids and				
Peripheral	the chloroplast envelope facing the	Nucleus			
	cell interior	Nucleus			
	Not separated by membrane	Cytoplasm			
	Not traversed thylakoids	Pyrenoid			
	Not traversed by membranes	Thylakoid			
		Chloroplast			
Clade 2b,	Not separated by membrane				
· ·	Not traversed by membranes				
Peripheral, non-		Nucleus			
protruding					
		Cytoplasm			
		Thylakoid			
		Pyrenoid			
		Chloroplast			
Clade 2h	Membrane bound with transverse				
Clade 2b,	membranes continuous with				
Achnanthes	thylakoids	(Nucleus)			
brevipes					
		Cytoplasm			
		Thylakoid			
		Pyrenoid			
		Chloroplast			
Eexo-	Single, large, peripheral,				
thylakoidal	panduriform pyrenoid				
, ,	projects conspicuously towards the	(Nucleus)			
	vacuole and consists of amorphous dense matrix				
	Transgressed by irregular tubular	Vacuole			
	cytoplasm channels	Pyrenoid			
		100000			
		Chloroplast Thylakoid			
	j	1			

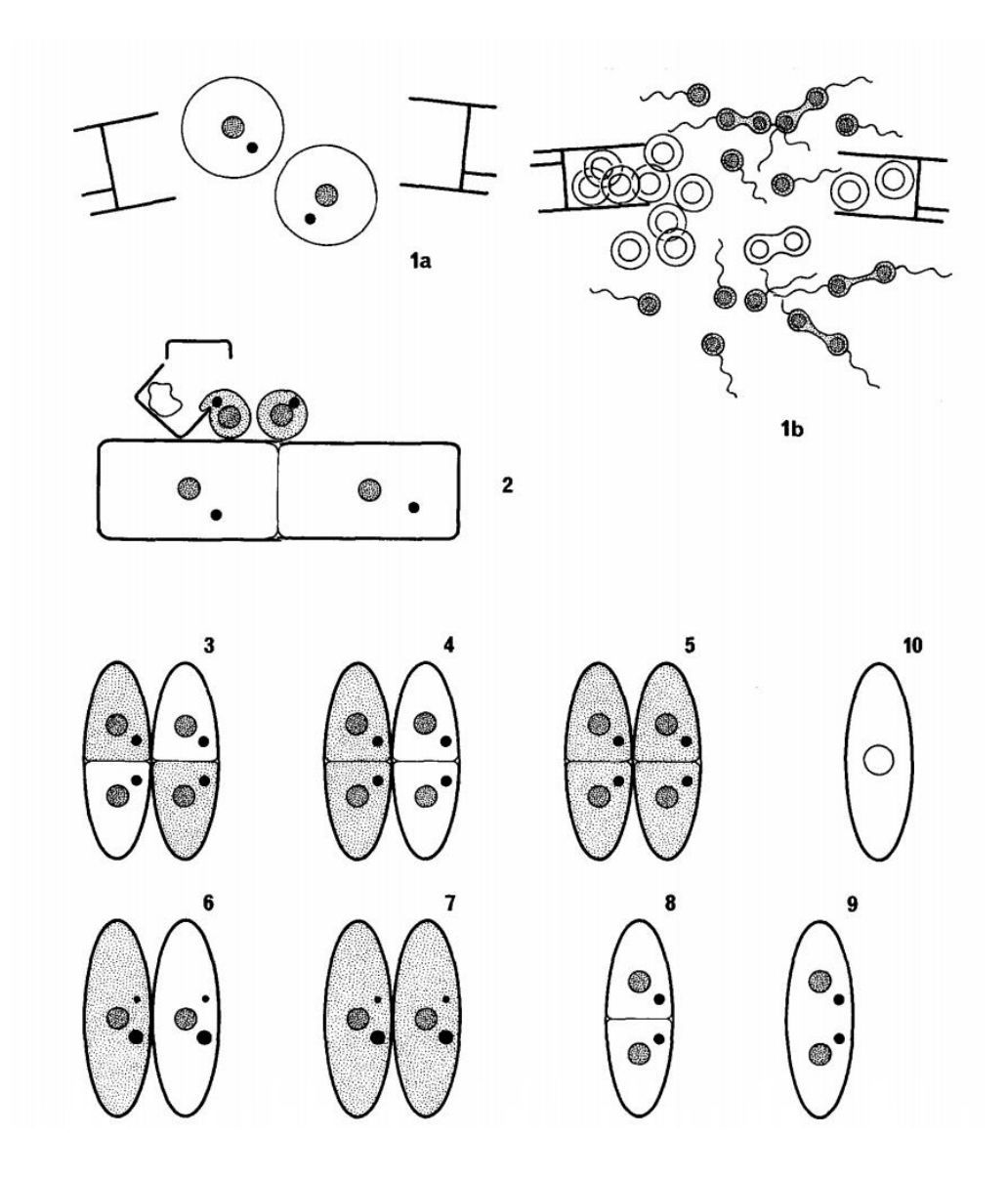


Figure 4.2: Different types of sexual reproduction in different diatom groups as summarised by Mann (1993)

1) Oogamy in centric diatoms: 1a) The oogonium produce two eggs. 1b) The male gametes are flagellated and motile. 2) Morphological anisogamy in *Rhabdonema arcuatum*. The female gametes are larger in size and non-motile while the male gametes are flagellated and motile and smaller in size and during gametogenesis leave a residual body. 3)-7) Allogamous reproduction in pennate diatoms. 3) Two identical male and female gametangia produce one active gamete per each. 4) The two active gametes produced by the same gametangium. 5) Isogamy where both gametes are identical. 6, 7) One gamete produced per gametangium. 8) Paedogamy. 9) Autogamy. Stipple: Motile gametes. Heavy stipple: Functional haploid gametic nuclei. Black: Degenerating, non-functional nuclei. Open circle: Unreduced diploid nucleus or meiotic nucleus.

4.1.2.3.1 Sexual reproduction in centric diatoms

Since diatoms have a deplonitic life cycle, meiosis is a key step in the formation of gametes in sexual reproduction, and the process by which eggs and sperm are produced is known as gametogenesis (Round et al. 1990). Some centric diatoms have a cell wall surrounding the gametangium and undergo what is known as merogenous spermatogenesis, in which nuclei in the spermatogonia undergo the first meiotic division without cytokinesis, resulting in the production of a binucleate plasmodium which undergoes a second meiotic division and forms four flagellated gametes and a residual body (Figure 4.3A). However, other centric diatoms have non-shelled (frustule-less) spermatogonia which undergo a hologenous process in which cytokinesis occurs in two meiotic nuclear divisions, and, therefore, four sperm are produced with no residual body (Figure 4.3B).

In centric diatoms, the female gametes are large and sessile, and only one or two are produced per gametangium (Chepurnov et al. 2004). The female gametangium is produced directly from the vegetative cell and serves as the mother cell of the resulting zygote or auxospore. However, auxospore formation is not limited to sexual reproduction and can arise through automixis and asexually (Chepurnov et al. 2004). The process of oogenesis normally starts with cell elongation in the girdle region, associated with an enlarged nucleus (in the prophase of meiosis I) and an increase in pigmentation due to the increased number and size of chloroplasts (Chepurnov et al. 2004). Meiosis consists of two divisions resulting in the segregation of chromatids into haploid nuclei, prior to the formation of eggs (oogenesis). Again, three distinct patterns of behaviour have been described, with oogonia containing two eggs, oogonia with one egg and a polar body, and oogonia with just a single egg (Drebes 1977). After the egg is fertilized, the oogonium cell (zygote) is transformed into an auxospore, which not only is considerably enlarged but has its own unique structure.

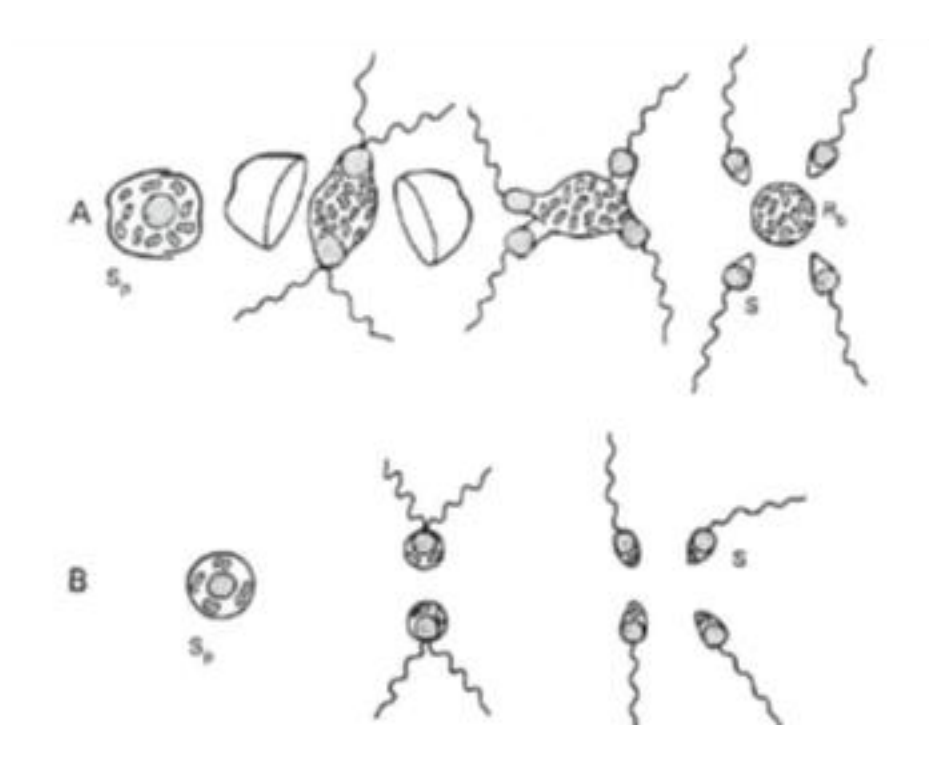


Figure 4.3: Sperm formation in centric diatoms A) In the merogenous type, a spermatocyte (S_p) undergoes two meiotic nuclear divisions to form four sperms (S) with a residual body (Rb). B) In the hologenous type, two meiotic nuclear divisions are accompanied by cytokinesis in each, resulting in four sperms (Source: Drebes 1977).

4.1.2.3.2 Sexual reproduction in pennate diatoms

Sexual reproduction in pennate diatoms takes different forms. One of the earliest studied genera of pennate diatoms is *Rhabdonema*, whose patterns of sexual reproduction appear to be somewhat intermediate between those of centric and pennate diatoms (Figure 4.2 (2)). This genus is classified in the pennate diatoms; however, it shares the characteristics of centric diatom mitosis in male gametogenesis. This supports the hypothesis that isogamy evolved from oogamy in diatoms. The pennate diatom *Rhabdonema* reproduces by oogamy, but this is different from centric oogamy because the male gametes in Rhabdonema are nonmotile and naked (Round et al. 1990), but it matches centric oogamy in that the male gametes are significantly smaller than the female gametes due to an imbalance in the mitotic division plane. In addition, two pycnotic nuclei are also produced during male Rhabdonema gametogenesis, whereas all meiotic nuclei survive in centric male gametogenesis. Gametogenesis in the male produces two amoeboid gametes per male gametangia, which is a characteristic of pennate gametogenesis (Edlund and Stoermer 1997). The female gametangia represent centric diatom oogenesis by producing one or two eggs per gametangium (Edlund and Stoermer 1997). This has led to the hypothesis that the *Rhabdonema* lineage is likely to be an early diverging member of the pennates, and is the most closely related to the centric diatoms (Chepurnov et al. 2004). However, subsequent molecular studies have not confirmed this hypothesis, since *Rhabdonema* does not have a stable position in the phylogenetic tree (Medlin et al. 2000; Kooistra et al. 2003a). Although Rhabdonema had for a long time been considered to be orgamous, von Stosch (1982) considered it to be morphologically and physiologically anisogamous. Other ultrastructural features that match well with molecular phylogeny are the merogenous forms found in Clade 1 and the hologenous forms found in Clade 2a, though with some exceptions (Jensen et al. 2003).

Other pennates do not form motile (non-flagellated) male gametes. They have variable reproduction patterns, as summarized by Mann (1993) in Figure 4.2 (3-7). Their reproduction is by allogamy (cross-fertilization as in plants) where the gametes are anisogamous (Chepurnov et al. 2004). Furthermore, in anisogamous sexual reproduction, the male gametes differ morphologically and behaviourally from female gametes; however, they usually have the same overall morphology

(Chepurnov and Mann 2003). In addition, because the male gametes in pennate diatoms do not have flagella, the gametangia conjugate first, followed by the gametes. It has been reported that the male gametes of *Rhabdonema adriaticum* show amoeboid movement (von Stosch 1958b; in Drebes 1977), whilst the female gametes remained attached to their parental frustule. Two female gametes are produced per gametangium and one haploid nucleus degenerates after the second meiosis.

Only a few studies (mentioned in Chepurnov et al. 2004) have been carried out on sexual reproduction in the araphid pennate diatoms. They are heterothallic and the induction of gametogenesis requires interactions between sexual partners of opposite mating types (Chepurnov et al. 2004). Recently, it has been shown experimentally that they produce pheromones to induce gametogenesis (Sato et al. 2011). The gametes differ in behaviour as the female gametes remain attached within the gametangial valves/frustule/theca and are, therefore, described as passive (stationary) gametes. On the other hand, the male gametes are discharged from the parental frustule and move towards the female gametes, and are therefore described as the active (migratory) gametes. These differ from other pennate diatoms in having flagella-like structures called threads because their morphology is quite different from a flagellum (Sato et al. 2011). The ultrastructure of these threads will confirm whether they are flagella or not.

The raphid pennate diatoms are allogamous (isogamous) with most of them having morphologically identical male and female gametes (Drebes 1977; Round et al. 1990). However, some of them reproduce by anisogamy, as reported in araphid pennate diatoms (Chepurnov et al. 2004). The raphid gametes are motile and pairing is active, and one or two gametes are produced per gametangium, in the first step by gamete angiogamy. The combinations of gametogenesis fertilization and auxospore development are extremely diverse (Figure 4.2).

4.1.2.4 Auxospore formation and structure in relation to molecular phylogeny

The auxospore is the cell resulting from sexual reproduction (Chepurnov et al. 2004) as a result of the fusion of male and female gametes. It may contain a diploid nucleus, or two haploid nuclei with a number of pycnotic nuclei, depending on the species (Kaczmarska et al. 2001). However, auxospore types do not correlate well

with classical diatom systematics based on phenotypic characteristics. The centric group has two types of auxospore structure (isodiametric and anisodiametric properizonia auxospore) and pennate diatoms which have anisometric perizonium auxospores (Kaczmarska et al. 2001). Thus, diatoms are divided into the centric group, which have isodiametric auxospore and anisodiametric properizonia auxospores, and araphid and raphid pennates which both have a perizonium (Kaczmarska et al. 2001). According to Kaczmarska et al. (2001) and Medlin and Kaczmarska (2004), the correlation between auxospore types and molecular phylogeny (Table 4.1) is as follows. Clade 1 has isodiametric auxospores that can swell in all directions and have only scales. Clade 2a has non-isometric auxospores with scales and hoops or bands (aproperizonium) to restrict the swelling to the bipolar or multipolar directions. Finally Clade 2b has anisodiametric auxospores that form a complex tubular perizonium, usually consisting of transverse hoops and longitudinal bands. These three main types of auxospore structure described in the literature are illustrated in Figure 4.5, taken from Kaczmarska et al. (2001). These findings accord with the hypothesis of von Stosch (1982), which suggests the evolution of auxospore structure from a scaled auxospore wall with isometric growth, to anisometric auxospore growth controlled by properizonial closed hoops, then to anisometric growth controlled by closed hoops and open bands, and finally to anisometric auxospore growth controlled by open bands. The Rhabdonema auxospore shares the features of centric auxospores which are a scale-invested auxospore (von Stosch 1982); however, it shares the pennate auxospore features of a siliceous perizonium made of open hoops and longitudinal bands in the perizonia (von Stosch 1982).

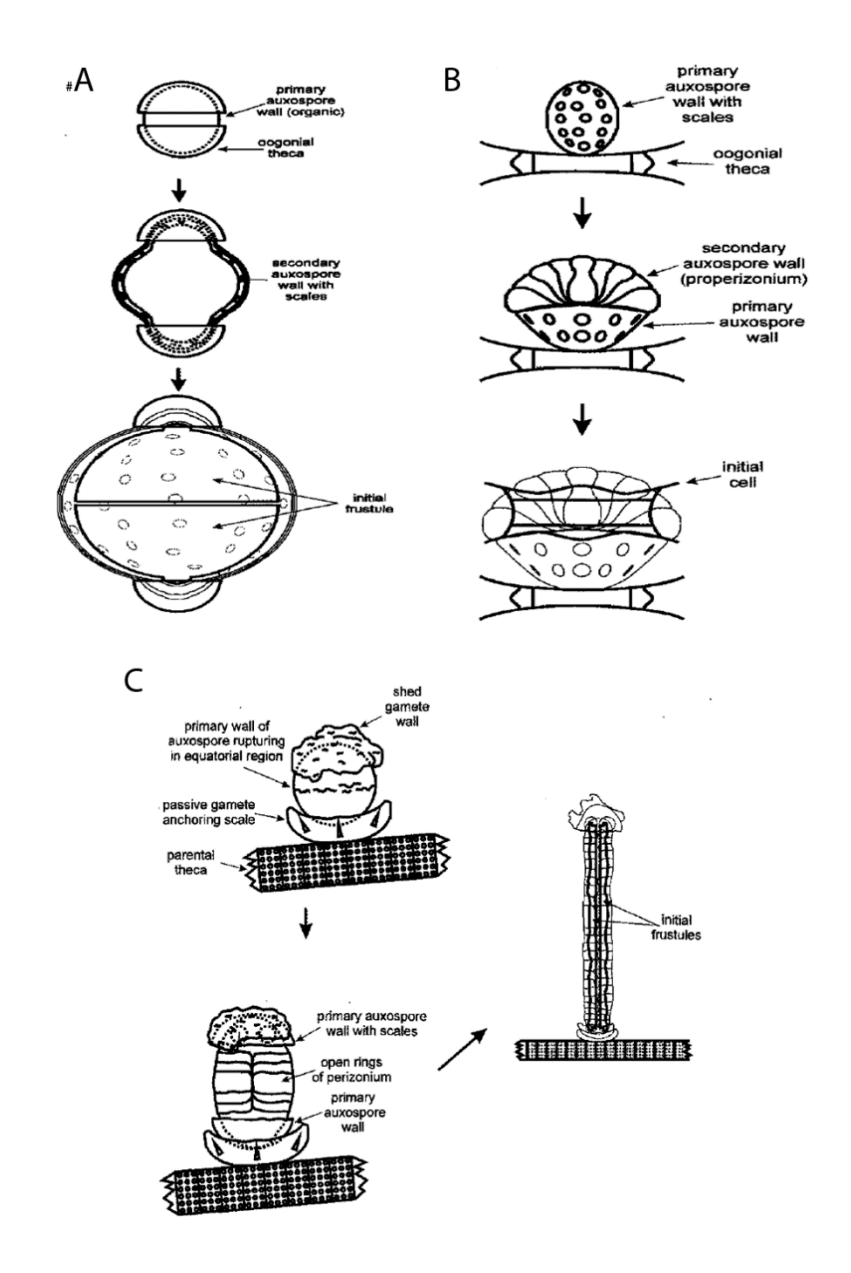


Figure 4.4: The three types of auxospore

A) Isometic auxospore: In the auxospore's intial stage, as the auxospore enlarged the primary wall shed to the poles, followed by the development of a secondary auxospore wall with scales, and finally the auxospore maintains a globular shape with scales on the initial frustule. This is common in Clade 1. B) Properizonial auxospore: the properizonium is a secondary wall built of siliceous rings produced inside and coalescent with the primary scaly wall. The bands, rings, loops, and hoops are laid at various orientations relative to the direction of the initial valve. The primary scaly wall is modified and not replaced by these structures, helping the expansion of the auxospore in different directions. This is common in Clade 2a. C) Perizonial auxospore: the perizonium is a secondary wall of the bilateral auxospore consisting of closed or open rings laid at fixed orientations relative to the direction of initial valve expansion. This is common in Clade 2b. (Source: Kaczmarska et al. (2001))

Pseudostaurosira trainorii belongs to the araphid diatoms, which are paraphyletic (Williams and Kociolek 1988, Medlin et al. 2008). The earliest molecular phylogeny for the araphid diatoms (included Clade 2b of Medlin and Kaczmarska 2004) showed that they are divided into two major clades (Kooistra et al. 2003a). Chepurnov et al. (2004) stated that the sexual reproduction of Clade 1 (Kooistra et al. 2003a), which includes Asterionellopsis, Asterioplanus and Rhaphoneis, had not been studied and there was little information available about the second clade. The second clade contains the genus Striatella and is considered as the sister group of the raphid diatoms (Kooistra et al. 2003a).

4.1.3 Aims of this diatom study

Available studies describing the genus *Pseudostaurosira* were summarized in the general introduction (Chapter 1, section 1.3.2). This chapter aims to add to existing knowledge obtained by light and scanning electron microscopy using the transmission electron microscope, which will enable firstly, description of the cell structure of *P. trainorii* in different life cycle stages (vegetative cells, male and female heterothallism, gametes, auxospore and initial cells), which has never been done before. Secondly, the thread-like ultrastructure of the male gametes that have been reported by Sato et al. (2011) is investigated to confirm whether or not it resembles the flagella. Thirdly, the molecular phylogeny of diatoms described by Medlin and Kaczmarska (2004) is correlated with ultrastructural features.

4. 2 Methods

Methods were described in Chapter 2, section 2.1.1 and section 2.3.3

4.3 Results

4.3.1 Vegetative cells

Pseudostaurosira trainorii is a chain-forming (filamentous) diatom (Figure 4.5A, B, G) that on first appearance looked very like a centric species such as *Melosira* (Figure 4.5 C-F). The adjacent cells were linked to each other with small interlocking spines (Figure 4.5B-F). Valves had parallel striae (11 in 5 μm) and diatom dimensions of 6.5 μm x 5.5 μm in size, and were decorated with uniseriate rows of linear to slightly curved striae, each with between 12 and 20 areoloae

(Figure 4.5C). The valve showed the typical bilateral symmetry of a pennate diatom, with the striae being divided by a central sternum (approx. 0.4 µm in width), which was only differentiated from the rest of the valve by the absence of areolae (Figure 4.5C and D).

Both male and female vegetative cells had the same structure. The vegetative cell was bounded by the typical electron dense valve, and contained a single nucleus, chloroplasts, vacuoles, dictyosomes, and mitochondria (Figure 4.5 G-J). The vegetative cells prior to gamete formation were of rectangular shape in girdle view and were on average 6.5 µm x 5.5 µm in size (Figure 4.5J, H and J) and circular to elliptical in valve view (Figure 4.5I). Each vegetative cell contained a single nucleus which was normally located at one end of the cell adjacent to the chloroplast and Golgi dictyosomes at the site of the epitheica (Figure 4.6A, D). The nucleus was bordered by a nuclear envelope interrupted by nuclear pores (Figure 4.6D-F). The nucleoplasm was usually homogenous, with a fine granular appearance and interspersed with small patches of more electron-dense heterochromatin. Each nucleus also contained a prominent nucleolus, which is an electron-dense granular spherical body situated at one peripheral side of the nucleus close to the nuclear envelope (Figure 4.6A, D). It was intimately associated with a cup-shaped plastid and perinculear Golgi dictyosomes (Figure 4.6A-F) and near the tonoplast of vacuoles (Figure 4.6A, B). The nucleus was closely associated with the endomembrane system of the cell, particularly the Golgi system and endoplasmic reticulum (Figure 4.6C-F). Both girdle (Figure 4.7A, B; Figure 4.9A, B) and valve (Figure 4.7C and 4.9C) sections of the vegetative cells revealed 2-3 Golgi dictyosome profiles associated with the nucleus. Each dictyosome consisted of 4-6 cisternae (Figure 4.6E), which were formed by the fusion of vesicles produced from the nuclear envelope (Figure 4.6D, E).

From the valve plane (Figure 4.5; 4.7A-B) and girdle (Figure 4.5J) sections it could be seen that the chloroplast was restricted to the periphery of the cell, where it formed an open cup around the cell. In thin-sectioned material each cell usually contained one to three plastid profiles, which in the girdle plane could be seen to underlie the valve (Figure 4.5H). Each plastid contained many electron-dense lamellae that ran parallel to the cell surface. Each lamella consisted of three closely stacked thylakoids (Figure 4.6A-C and F). The outermost lamella formed a

continuous loop underlying the plastid envelope, and this is called the girdle lamella (Figure 4.6A-C and F). The thylakoid lamella was separate around the prominent pyrenoid region (Figure 4.6A, C), which was traversed by a single lamella extending across the centre of the pyrenoid from the perimeter (Figure 4.6A, C). The chloroplast also contained scattered electron-dense plastoglobuli (osmiophilic granules), that might occur singly or in groups of up to seven (Figure 4.6A-C).

The nuclear envelope and periplastid membrane formed electron-transparent cisternae where the plastid abutted the nucleus (Figure 4.6A, C and F). There was an additional cisternum of smooth ER which completely enveloped the chloroplast, which is where the nucleus abuts the plastid in common with the nuclear envelope. Where the plastid curved around to the other side of the cell, it enveloped the large lipid droplet (Figure 4.6B).

The mitochondria were variable in shape but mostly rounded and containing tubular cristae. They mainly lay at the periphery of the cell (Figure 4.7A). Storage products in relatively electron-transparent droplets were found in the cytoplasm near vacuoles and chloroplasts (Figure 4.5H). The most obvious storage product was the large droplet of lipid (oil) which formed a large droplet that lay directly in the cytoplasm and was not bounded by a membrane (Figure 4.6B). The lipid droplet in vegetative cells appeared to abut both the nucleus and chloroplast (Figure 4.5H). The side of the cell opposite where the nucleus resided was is mainly occupied by the large electron-lucent vacuole(s) – this is shown clearly in Figure 4.5H; 4.6A.

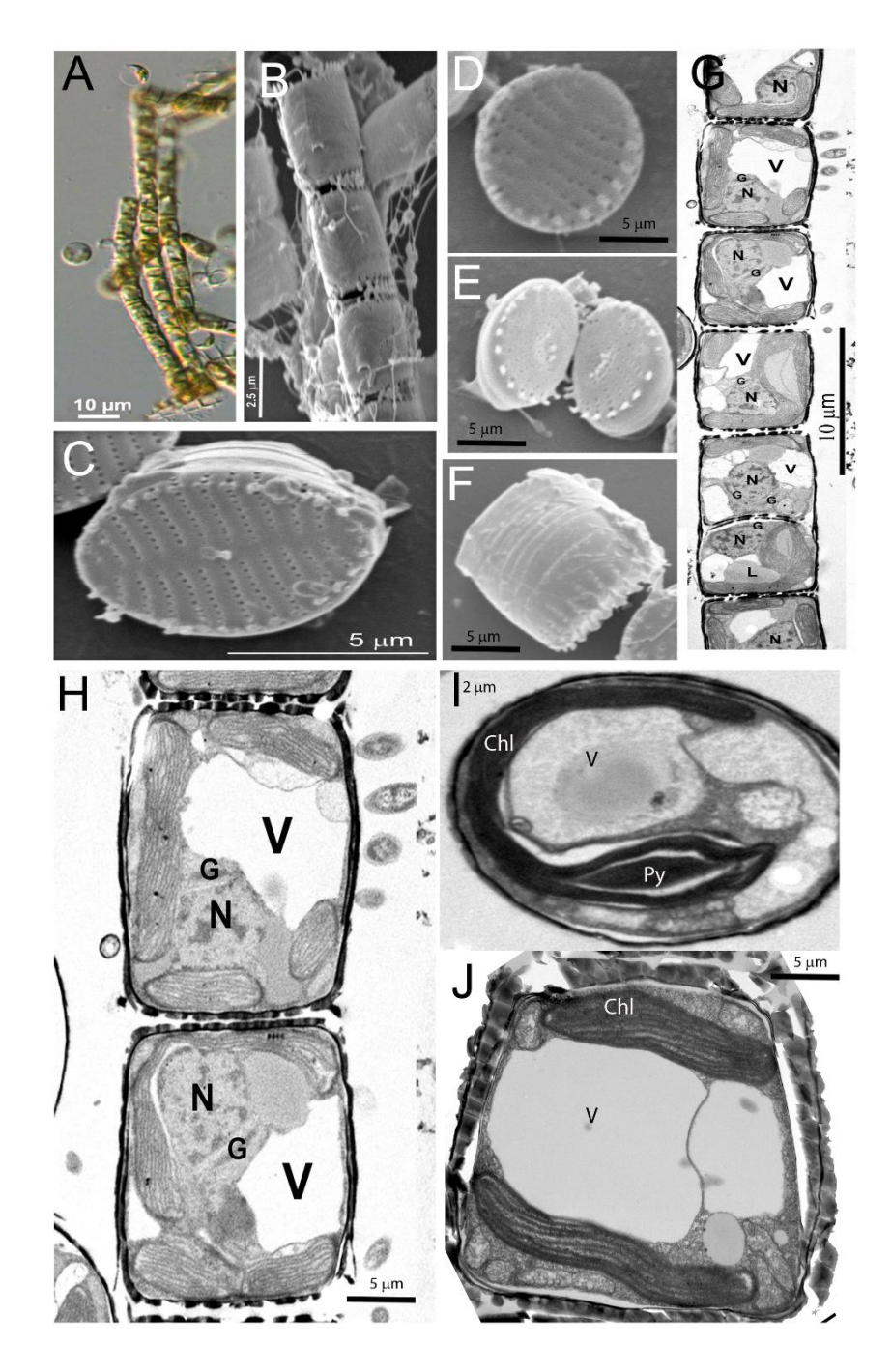


Figure 4.5: Light, scanning and transmission electron micrographs of *Pseudostaurosira trainorii*

A) *P. trainorii* under light microscope forming chain-like colony. Scale bar 10 μm. B) Chain like colony under scanning electron microscopy of *P. trainorii*. Scale bar 5 μm. C-F) Scanning electron microscopy micrographs of *P. trainorii*. G) Girdle view of chain of *P. trainorii* cells. Scale bar 10 μm. H) Higher magnification of two vegetative cells. I) Valve view of the cell. G) Girdle view of the cell. Chl: chloroplast; G: Golgi; L: lipid bodies; N: nucleus; Py: pyrenoid; V: vacuoles.

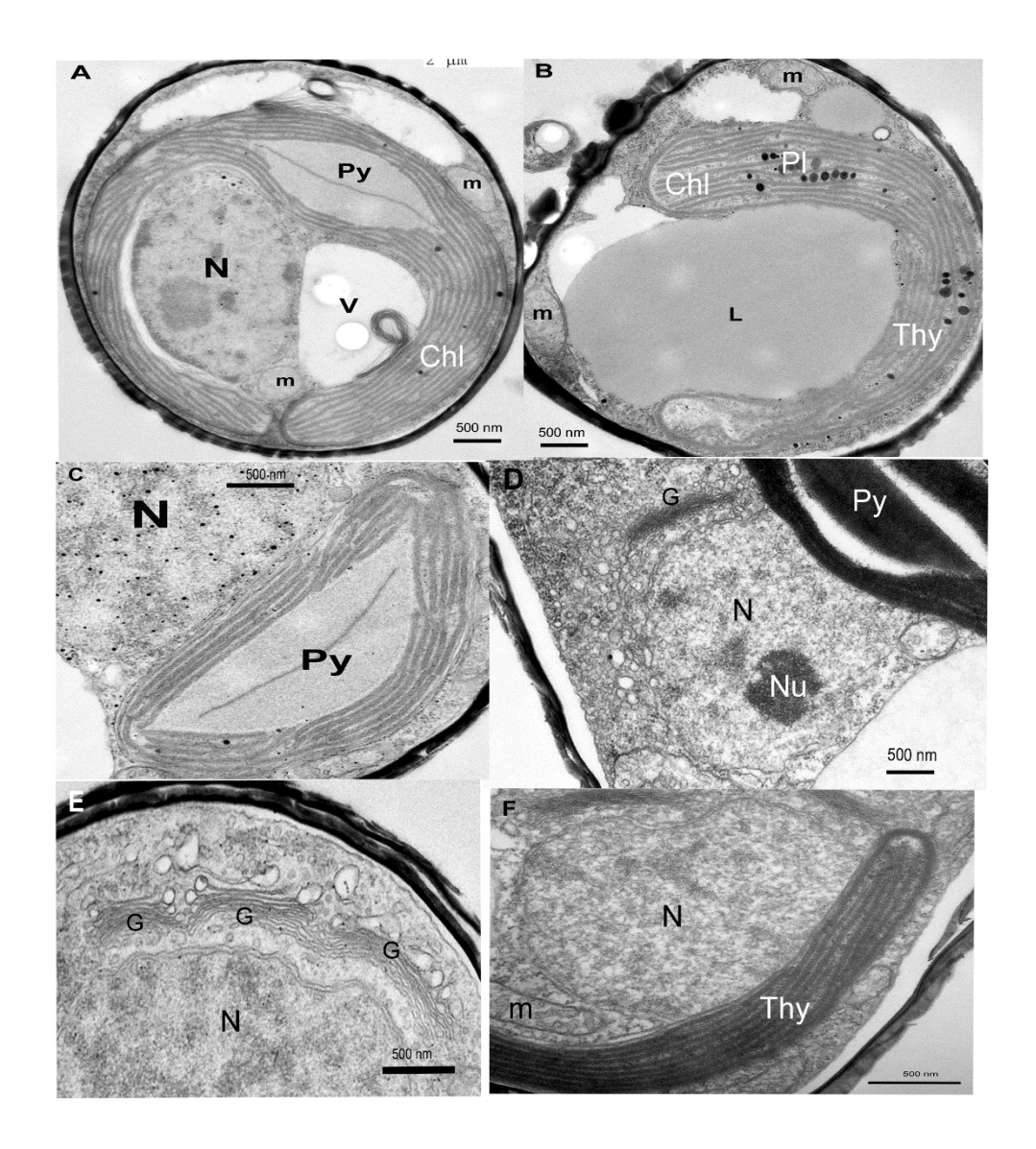


Figure 4.6: Cytological features of *Pseudostaurosira trainorii*A) Cross-section from valve view through the nucleus and pyrenoid. B) Cross-section from valve view through lipid droplet. C) Higher magnification of chloroplast through the pyrenoid. D, E) Higher magnification of nucleus and Golgi body. F) Higher magnification of chloroplast through the girdle lamella. Chl: chloroplast; G: Golgi; L: lipid bodies; M: mitochondria; N: nucleus; Nu: nucleolus; Pl: plastoglobuli; Py: pyrenoid; Thy: thylakoid; V: vacuoles.

4.3.2 Gametogenesis

From the detected stages of both fertilized samples (20 minutes and 24 hours), the first evidence of gametogenesis in both induced male and female clones was the appearance of dividing vegetative cells, in which cells elongated to up to 12 µm (male Figure 4.7A-B, female Figure 4.9A-B). At this stage, the interphase nuclei were spherical and ranged in size from ca 2.5 x 2 µm and had an average volume of around 50 µm³ (male Figure 4.7A-D, female Figure 4.9A-D). Following enlargement, differences could be detected in the fine structure of male and female gametes, although they appeared almost identical under light microscopy (Sato et al. 2011). Subsequent male and female gametogenesis are now be described in separate sections.

4.3.2.1 Male gametogenesis and gametes

Cultures of *P. trainorii* were induced to produce male gametes as described in Chapter 2 (section 2.1.2). As gametogenesis progressed, the developing spermatogonia cells were elongated (in girdle plane) to around 12 µm in length (Figure 4.7B). This contrasted with the <9 μm in length of recently divided vegetative cells (Figure 4.5H). The nucleus in non-dividing cells was located at the cell periphery (Figure 4.5G, H) whereas when a cell was dividing the nucleus migrated to the centre of the cell (Figure 4.7B). The elongated spermatogonia cell had a basally located nucleus that had increased in size to approximately 4-4.5 x 3 μm (Figure 4.7B). These findings are indicative that meiosis was about to take place. The volume of these nuclei had increased to around 250 µm³ (Figure 4.7D). In spite of the increase in overall cell size, there had not been any increase in the size and volume of other organelles, such as vacuoles and lipids (Figure 4.7B). In some of the nuclei, paired electron-dense structures could be seen (Figure 4.57B) which might be indicative of a pre-synaptonemal complex stage. In these spermatogonia cells, the Golgi was more compact and the chloroplasts appeared smaller and had a denser overall appearance than in vegetative cells (Figure 4.7B). A pyrenoid was still present but appeared to be surrounded by a zone of electron-lucent material (Figure 4.7B) which was also present, but less obvious, in vegetative cells (Figure 4.6A, C). Following cell enlargement, the gametangium formed two male gametes per gametangium. They were different in size (Figure 4.7D).

The fully differentiated male gametes were rounded or spherical in shape. When observed under the light microscope with differential interference contrast light microscopy (DIC), living sperm cells appeared remarkably pleomorphic and constantly changed shape. As Sato et al. (2011) have reported, the sperm produced fine protoplasmic threads, along which the cells appeared to glide (Figure 4.8A). In the sequence of still images taken from a captured video sequence, a non-motile sperm cell was approached by a motile cell (masked with an asterisk) which was trailing its fine, almost flagellum-like protoplasmic thread. This was retracted as the asterisked cell became more irregular in shape as it moved around the static cell. Although these threads could be easily observed using DIC microscopy, they had been very difficult to find in thin sectioned samples (Figure 4.8D-G). However, one profile showed evidence of what could be a thread (Figure 4.8E, arrow). The male gamete was motile, and Figure 4.8C shows the pseudopodia movement.

Thin-sectioned differentiated sperm cells had relatively small vacuoles and contained a single functional nucleus (Figure 4.8D-G). However, there was also a second smaller body, which had very electron-dense membranes and was presumed to be a non-functional or partially degenerate nucleus (Figure 4.8B and D). The gamete nucleus was significantly smaller than the spermatogonial nucleus, having a volume of around $40 \ \mu m^3$ which was slightly less than that of a typical diploid vegetative nucleus (Figure 4.7D). The volume of the electron-dense non-functional nucleus was less than that of the functional nucleus (Figure 4.7D).

The male gamete also contained many mitochondrial and vacuole profiles, although these were only was occupying a relatively small volume compared to those in the female gamete. The sperm cell chloroplasts were much denser and narrower than those in vegetative cells and up to four separate profiles could be seen (Figure 4.8B, D-G). In contrast to the vegetative cells, the dense plastids were not closely associated with the nucleus, although they remained in close contact with the single prominent lipid globule. The Golgi bodies were of the perinuclear type (Figure 4.8D, E and G).

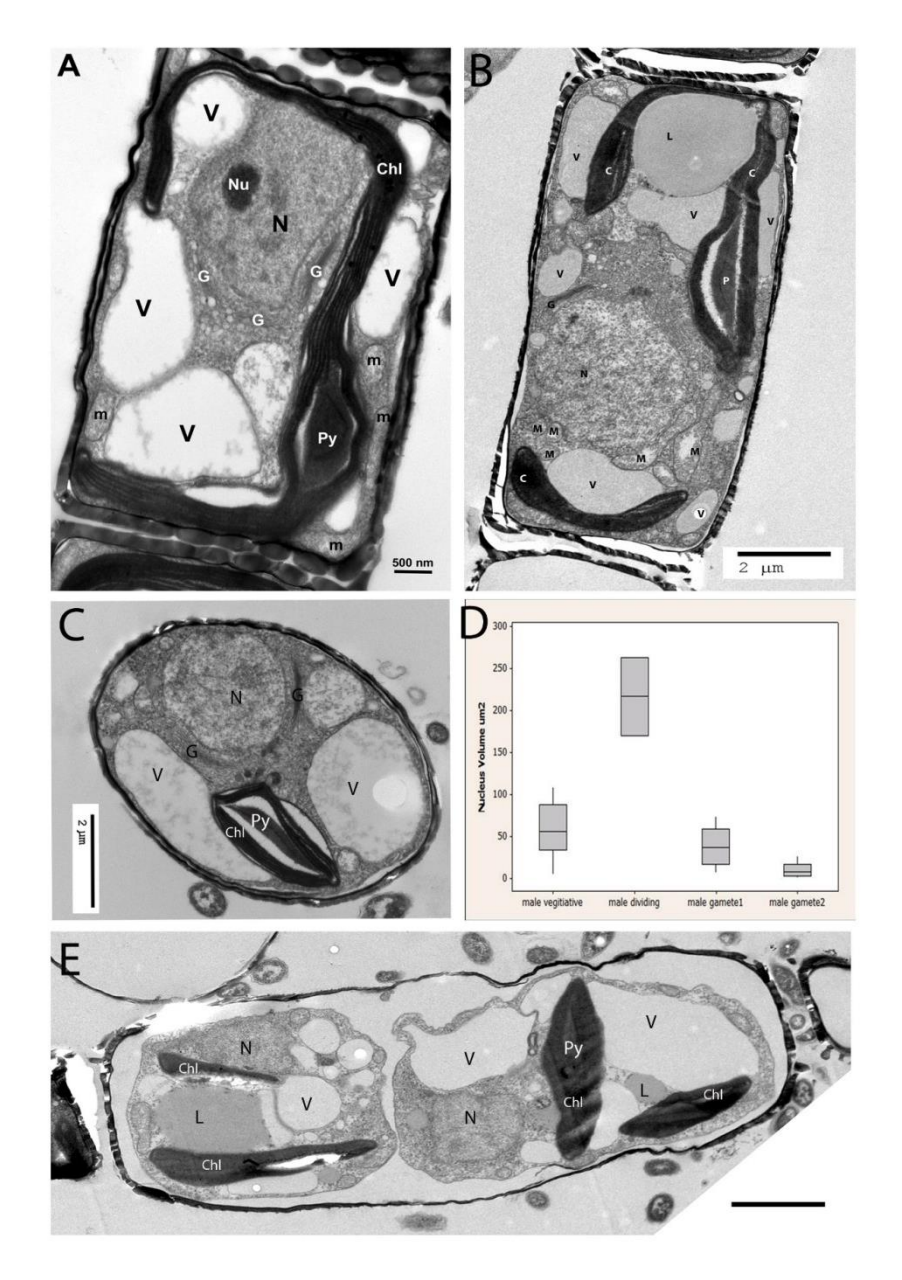


Figure 4.7: Male dividing cells and gametogenesis A) Cell before dividing, girdle view. B) Dividing cell, girdle view. C) Dividing cell, valve view. D) Box plot of nuclei volume for male vegetative, male dividing, and male gamete 1 which resemble the normal nucleus appearance profiles in the male gamete; and male gamete 2 which resembles the degenerated nucleus within the male gamete. E) Gametangium containing two male gametes. Scale bar 2 μ m. Chl: chloroplast; G: Golgi; L: lipid bodies; M: mitochondria; N: nucleus; Nu: nucleolus; Py: pyrenoid; V: vacuoles.

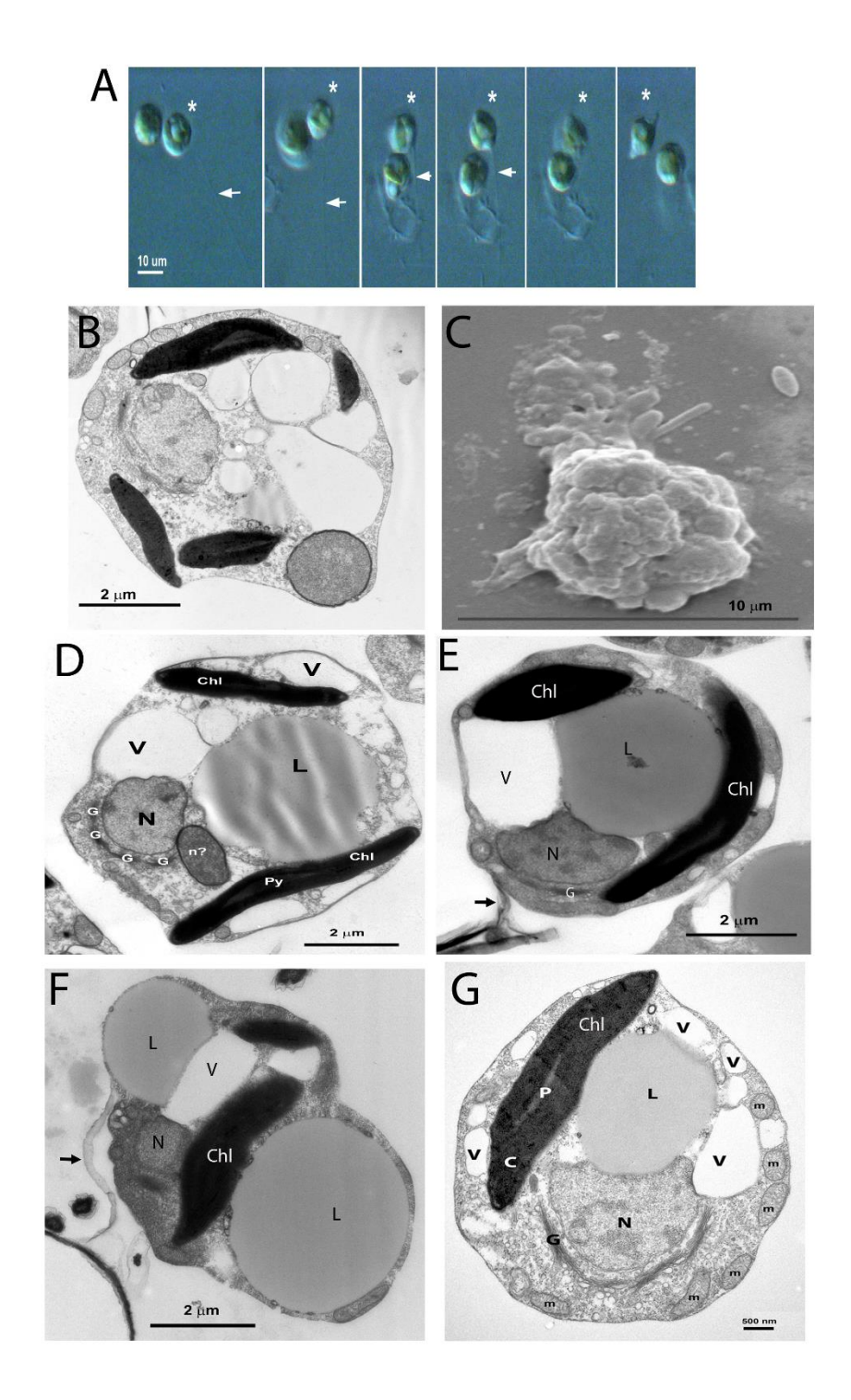


Figure 4.8: Mature male gamete
A) Successive light microscopy graphs for motile male gamete (asterisk). B)
Scanning electron micrograph. C-G) Different cross-sections of male gametes. Chl: chloroplast; G: Golgi; L: lipid bodies; M: mitochondria; N: nucleus; N?: partially degenerate nucleus; Py: pyrenoid; V: vacuoles..

4.3.2.2 Female gametogenesis and gametes

The female gametangium (egg) cell was also recognised by its greatly increased size and large nucleus located at its centre (Figure 4.9A, B, E). Following division, the egg cells were largely occupied by vacuoles which occupied nearly two thirds of the cell volume. The chloroplasts also replicated and migrate to the gametangium poles so that each egg (gamete) contained a single plastid (Figures 4.9E and 4.10A). Since the nucleus always remained at the hypotheca side of the cell, this implies an unequal division plane. Unfortunately, the final stage where a fully differentiated egg is seen within the gametangium was not observed. The most frequently observed stage in female gametogenesis was after the upper hypovalve had already been shed, exposing the naked egg cell to the environment (Figure 4.10B-D). The differentiated egg cell was much more vacuolated than its male equivalent (Figure 4.10B-D). The retaining epivalve was very elongated (<8 µm – Figure 4.10B-C) compared with typical vegetative cells where it rarely exceeded 5 µm (Figure 4.5H). In female gametogenesis, following the shedding of the upper valve, the rather elongated naked female gamete was still held in place by the parent frustule. As the female gametes matured they appeared to slide out of the basal frustule and became more rounded in shape. At this stage, they each had two large polar vacuoles and a narrow crescent of cytoplasm containing the two gametic nuclei, which were completely separated from the plastid (Figure 4.10C). At this stage, each egg cell contained 2 nuclei (Figure 4.10C, enlarged E, and F), and one or two relatively small, centrally located lipid globules (Figure 4.10B, C). The two small centrally located egg nuclei lay equatorially (Figure 4.10C) and were of similar overall appearance but tended to be of unequal size, one having a volume of around 40 μ m³ and the other only 20 μ m³ (Figure 4.9D). Only the larger nucleus tended to be associated with Golgi dictyosomes (Figure 4.10F). The developing egg had two nuclei and it seemed in the later stages the second nucleus degenerated as the thin section showed a highly vesicular membranous area besides the larger nucleus (Figure 4.10G).

The female gamete also contained a large expanding vacuole initially located towards the cell poles (Figure 4.10C) and which appeared to occupy nearly half of the egg volume. There were one or two dense but narrow (0.5-1.0 μ m wide) plastids (Figure 4.10B, C), which were usually basally located. As development progressed, the eggs moved out of the valve and became more rounded in shape and the mature

egg cells were highly vacuolated (Figure 4.10D). The scanning electron microscope showed a mucilaginous region around the female gamete (Figure 4.10H).

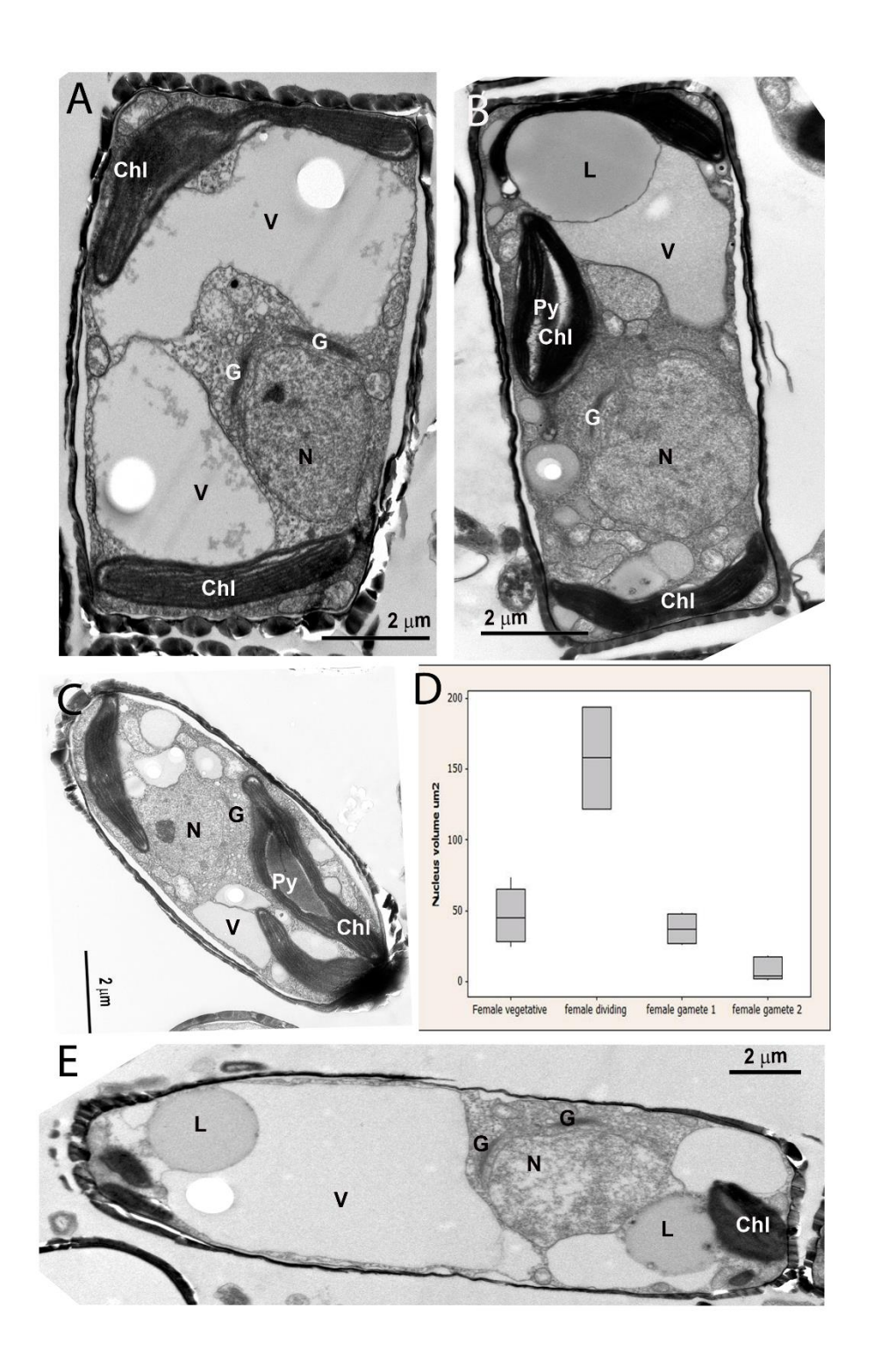


Figure 4.9: Female dividing cells and gametogenesis A) Cell before dividing, girdle view. B) Dividing cell, girdle view. C) Dividing cell, valve view. D) Box plot of nuclei volume for female vegetative, female dividing, and female gamete1 which resembles the first nucleus in the female gamete, and female gamete 2 which resembles the second nucleus within the female gamete. E) Large size of the gametangium. Chl: chloroplast; G: Golgi; L: lipid bodies; M: mitochondria; N: nucleus; Py: pyrenoid; V: vacuoles.

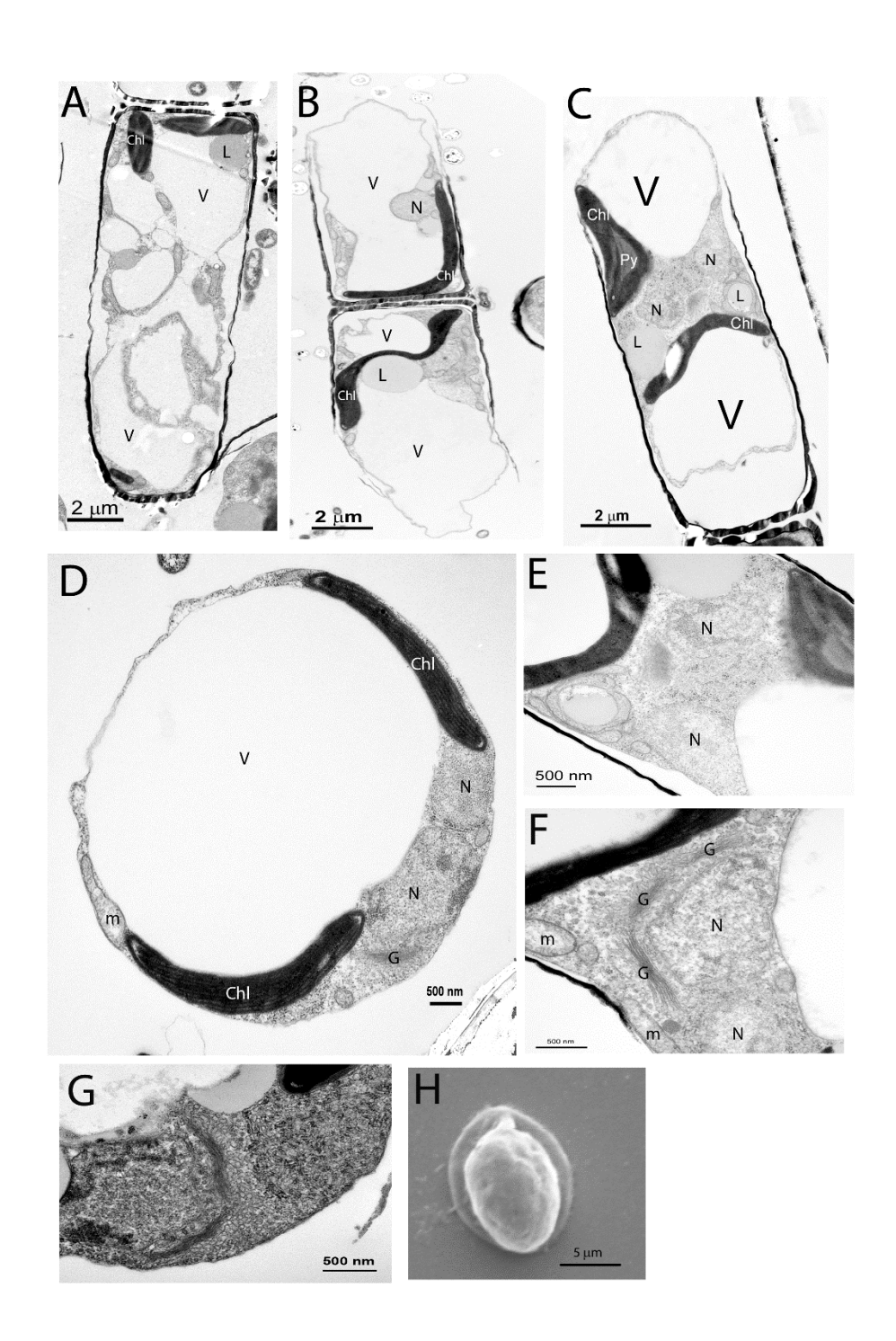


Figure 4.10: Egg differentiation and maturation A-C) Different stages in egg gametogenesis. D) Mature egg. E-G) High magnification of the nucleus. H) Scanning electron micrograph of egg. Chl: chloroplast; G: Golgi; L: lipid bodies; M: mitochondria; N: nucleus; V: vacuoles.

4.3.2.3 Fertilization and auxospore development

A thin section showing a male sperm cell lying close to a female gamete (egg) is shown in Figure 4.11A and a possible post-fertilization cell is shown in Figure 4.11B. As P. trainorii is heterothallic and differentiated into compatible clones, one male and the other female, the presence of a male gamete opposite a female gamete in the same thallus could indicate a fertilized egg at the earlier stages (Figure 4.11B). Figure 4.11C shows an enlarged fertilized egg, where the nucleus size was large (radius is 4 µm, 3.5 µm) and the male's degenerated nucleus had started to lyse as its double membrane had become detached. The SEM micrograph shows the size of what could be interpreted to be a fertilized egg in the 20 minutes sample, which was huge in comparison to the normal gamete, far exceeding the frustule size, and the shape was rounded (Figure 4.11D). Following this stage, the auxospore was reshaped into the typical elongated bilateral cell embedded in a copious mucilaginous matrix (Figure 4.11E). The transmission microscope thin sections showed two cells that might represent auxospore initials, which were surrounded by a thin wall which clearly differentiated them from male gametes (Figure 4.11F, J). The 24 hours zygote sample showed a dramatically increased size of auxospores, which by then were encased in open transverse bands, with the widest bands in the centre (Figure 4.12B).

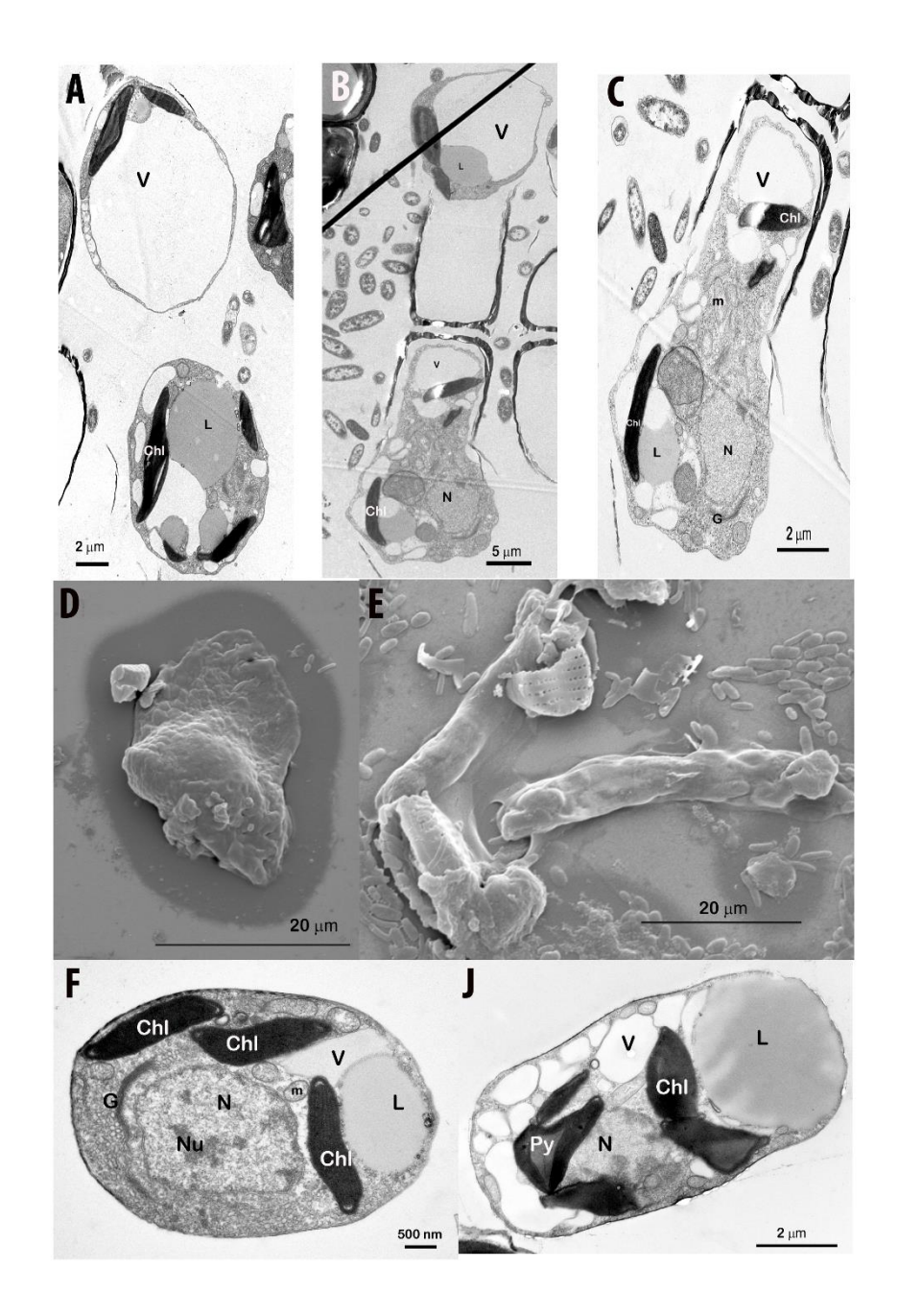


Figure 4.11: Fertilization and auxospore in the 20 minutes fertilized sampleA) Male gamete approaching female gamete. B) *Pseudostaurosira trainorii* thallus containing female gamete (upper one) and fertilized female gamete (lower one). C) High magnification of the fertilized egg in B. D) Scanning electron micrograph of a zygote showing the huge volume in comparision with the frustule size. E) Expanded auxospore within the mucilaginous material. F-J) Cross-sections through the expanded auxospore showing the organic cell wall. Chl: chloroplast; G: Golgi; L: lipid bodies; M: mitochondria; N: nucleus; Nu: nucleolus; Py: pyrenoid; V: vacuoles.

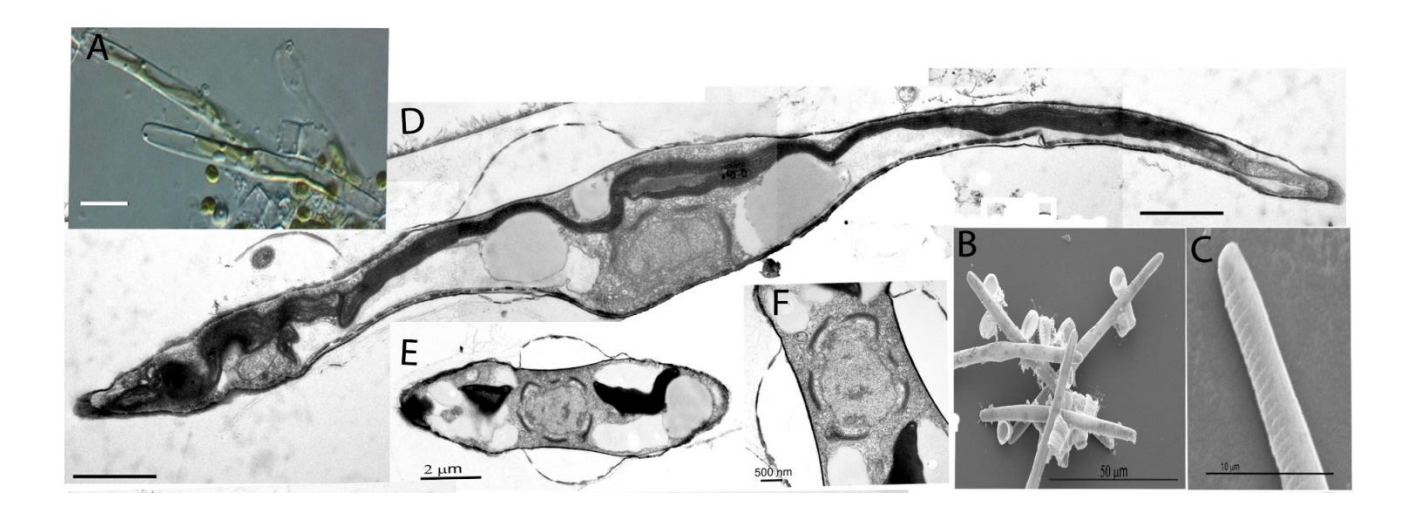


Figure 4.12: Mature auxospore from 24 hours fertilized sample

A) Light microscopy of the auxospore. Scale bar $10 \, \mu m$. B-C) Scanning electron microscopy of the auxospore. D) Thin section montage of the mature auxospore showing the huge volume of the cell and the two cell wall layers. Scale bar $10 \, \mu m$. E-F) Cross-section of the central part of the auxospore with the nucleus surrounded by preinuclear Golgi apparatus.

4.4 Discussion

Advances in molecular approaches have changed views about diatom classification systems and increased interest in reviewing old hypotheses and findings such as those concerning the relationship between cell structure and classification (Kooistra et al. 2003a). The main reason for this is that molecular phylogenetic approaches differ from those of phenetic phylogeny (Kaczmarska et al. 2001). The discovery of difficult-to-place diatom species further complicates the situation. Therefore, elucidating the hitherto undescribed ultrastructure of *Pseudostaurosira trainorii* vegetative cells and gametogenesis, in one such anomalous genus, could help in resolving differing morphological and molecular concepts of diatom relationships. A discussion of the implications of ultrastructural features for molecular phylogeny will follow.

4.4.1 Organelles with significance for molecular phylogeny

This present study showed partial agreement with the morphological and cytological support for the major clades and taxonomic revision proposed by Medlin and Kaczmarska (2004). To start with, this study revealed that the structure of the Golgi apparatus in *P. trainorii* resembled type 2 Golgi associations; that is, an array of perinuclear Golgi that surround the nucleus. This arrangement was found in different life cycle stages (i.e. vegetative cells; gametes and zygotes) and is a characteristic of the Clade 2b diatoms to which *P. trainorii* belongs. Therefore, this present study supports the conclusion of Medlin and Kacmarska (2004) concerning the relation of Golgi structure to the major molecular phylogenetic clades. This is unlike the Bedoshvili and Likhoshway (2012) study, which showed limitations in the application of cell ultrastructure features to phylogenetic reconstruction, where two types of Golgi arrangement are found in *Ditylum brightwellii*; the G-ER-M unit and perinuclear dictyosomes (Bedoshvili and Likhoshway 2012). This species is a member of the Clade 2a diatoms; therefore, this hypothesis may need more study.

This study also showed that the pyrenoid structure of *P. trainorii* resembles the commonly found form of the pyrenoid in the genera studied that belong to the class Bacillariophyceae (Clade 2b of Medlin and Kaczmarska (2004)) as it is non-membrane-bounded and contains lamellae. However, results of this present study showed that the lamella was connected to the thylakoid in some micrographs and not connected in others. This could indicate that the lamella was found as a sheath within the pyrenoid and has different widths at different levels that are not continuous with thylakoids.

Medlin and Kaczmarska (2004) state that Clade 2b have pyrenoids with lamellae that are continuous with thylakoids (Table 4.1, section 4.2.1); however, results of this present study showed that P. trainorii is an exception to this rule. Examples of results resembling the findings of this present study regarding traverse pyrenoid lamellae are in Achnanthes minutissima, which also belong to Clade 2b and where the pyrenoid lamella was not associated with the chloroplast thylakoids (Bedoshvili and Likhoshway 2012), and in the genus Aulacoseira which belongs to Clade 1. In Aulacoseira granulata the pyrenoid is crossed by lamellae not associated with other thylakoids (Drum et al. 1966; in Medlin and Kaczmarska 2004). Meanwhile, in Aulacoseira baicalensis, the transverse lamellae are associated with chloroplast thylakoids. No information is available about how many thin or serial sections were taken in these studies; therefore, their results could be variable due to a lacking of appropriate sectioning. The present study has shown the presence of both states (association and non-association of lamella with the thylakoids) at different levels of the chloroplast. In addition, recent studies revealed more exceptions in other major clades. For example, the absence of a membrane surrounding the pyrenoid in genera belonging to the Clade 2a, Chaetoceros muelleri and Attheya ussurensis, contradicts Medlin and Kaczmarska's (2004) hypothesis (Bedoshvili and Likhoshway 2012). Furthermore, the same study also revealed a new type of pyrenoid structure found in Clade 1. The pyrenoid of Aulacoseira baicalensis has several lamellae associated with other thylakoids. This is an exception for Clade 1 to which this species belongs. Thus, more research is needed to confirm the cytological evidence concerning the molecular phylogeny of clades suggested by Medlin and Kaczmarska (2004), since diatom diversity has not been well studied. As Mann et al. (2013) state "the proportion of the studied species is still extremely small.".

4.4.2 Sexual reproduction, gametogenesis and auxosporulation

Chepurnov et al. (2004) believe that the diatom life cycle and size-dependent control of sexuality have played an important role in the diatom's evolutionary success. They postulated that understanding sexual reproduction in diatoms would help in determining the relationship between lifecycle dynamics, population biology and evolution (Chepurnov et al. 2004). Therefore, these authors developed six rules for the lifecycle of diatoms, as follows. Firstly, the life cycle is diplontic and gametogenesis involves the process of meiotic division; secondly, the vegetative cells are reduced in size as a result of successive mitosis; and, thirdly, therefore, the auxospore developed as a result of

sexual reproduction to restore the normal cell size. Fourthly, vegetative cells continue to divide by mitosis until they die if they are unable to reproduce sexually; fifthly, the small cells can be triggered to switch from meiosis to mitosis; and, finally, the auxospore is not a dormant stage. However, although these rules are meant to apply uniformly to all diatoms, variations in gametogenesis and sexual reproduction are, in fact, common (Chepurnov et al. 2004).

Many studies support the first rule of Chepurnov et al. (2004), that meiosis is found in all diatom sexual life cycles. For example, Mann and Stickle (1995; in Chepurnov et al. 2004) state that diatom meiosis is ordinary with no distinctive characteristics and a review by Kociolek and Stoermer (1989; in Chepurnov et al. 2004) showed that meiosis is a predominant feature of diatom gametogenesis. However, there are different mechanisms of cytokinesis after meiosis I, which result in variations in the numbers of gametes and of functional nuclei. In egg gametogenesis, the results of this present study showed that *P. trainorii* produced two eggs per gametangium. However, Sato et al. (2011) state that the *P. trainorii* female egg has one nucleus. The production of two eggs could be explained by an equal cytokinesis occurring after meiosis I but not after meiosis II; therefore, one haploid nucleus has degenerated (Round et al. 1990). This is clearly shown by the results of the present study as the nucleus volume indicated the smaller size of one nucleus in the gametes (see section 4.3.2, Figures 4.7 and 4.9). The conflict between these results and those of Sato et al. (2011) regarding the number of nuclei in the female gametes could be explained by the dependence of the latter on light microscopy and DAPI staining which might not be absorbed by the degenerating nucleus, whereas the TEM showed the presence of two nuclei in some sections. The results of the present study suggest that the process of gametogenesis in *P. trainorii* resembles that of *Rhabdonema* (which is considered to have gametogenesis intermediate between the centric and pennate groups) (Drebes 1977). In the genus Rhabdonema, the number of eggs per oocyte is different in different species. R. adriaticum produces one egg per gametangium; this is explained by the unequal cytokinesis after meiosis I (Round et al. 1990). Meanwhile, in R. minutum and R. arcuatum two cells are produced per oocyte (Round et al. 1990). P. trainorii has two eggs per oocyte, and so the number of eggs per oocyte could be variable with no constant tendency within the genus.

In addition, in the genus *Rhabdonema*, the male gametangia form two male gametes (consistent with results of this present study) and the male gametes have two nuclei, one

of which is degenerated (Drebes 1977). Chepurnov and Mann (2003) reviewed the types of gametogenesis in pennate diatoms and concluded that anisogamy, in which one gamete is active (movable) and the other is passive (sessile), represents the most primitive type of reproduction within this group. *P. trainorii* gametogenesis differs from that in *Rhabdonema*, which has "passive" male gametes (Derbes 1977), while in *P. trainorii* the male gametes actively move along threads to reach the females (Sato et al. 2011). However, the male gametes of *Rhabdonema* were not reported to have either flagella or thread-like structures. The male gametes in *P. trainorii* were non-flagellated and had thread-like structures, which might indicate that these structures could have developed as an adaptation to environmental conditions after the loss of flagella. In addition, the fine structures of male and female gametes were dissimilar.

The flagella structure of male gametes has been shown to be an important feature that reflects diatom evolution (Round et al. 1990). Earlier research suggested that the ancestor of the diatom could be a flagellated cell (Manton and Stosch 1966; in Chepurnov et al. 2004) and the flagella were retained only in sexual reproduction (Mann and Marchant 1989). Therefore, research has been conducted on the structure of the flagella of the diatom male gametes to investigate its evolutionary history. It has been revealed that the structure of the flagella axoneme is a 9+0 configuration in both genera closer to the diatom roots (Jensen et al. 2003; Theriot et al. 2010, 2011; Idei et al. 2013) as well as genera not closer to diatom roots (Round et al. 1990; Graham and Wilcox 2000). In centric diatoms, the male gametes are flagellated, whereas those in pennates are non-flagellated. The pennate diatoms are considered to be the most recently evolved of the diatom lineages, and this suggests that the loss of flagella in diatoms is a relatively recent development. However, it is not known, for instance, if there are any non-flagellate centric diatoms and whether flagella loss occurred before or after the emergence of pennate diatoms (Sato et al. 2011). Sato et al. (2011) speculated that the threads observed in the centric-like pennate P. trainorii might represent some form of reduced flagellum as an intermediate stage in the flagellar loss process. They showed that the threads produced by the male gametes are rich in tubulin. However, the results of this present study showed that the male gamete cell structure in P. trainoii lacked any indication that they might have possessed a flagellum, since pennate gamete flagella normally form a pair of nucleus-associated kinetosomes shortly after the completion of meiosis I and they are always closely associated with the poles of the spindle (Idei et al. 2013; Round et al. 1990). The results her showed no evidence of any such basal body

associated with the gamete nuclei of *P. trainorii*. Rudimentary structures which might possibly represent thread sections also showed no evidence of an axonemal structure. This indicates that the threads investigated by Sato et al. (2011) almost certainly are not homologues of flagella and are more likely to be filopodia-like structures. The lack of flagella in this species does add support the view that *P. trainorii* is a typical araphid diatom. The presence of slender, non-ramified cytoplasmic projections which expand and retract in accordance with cell movement was reported by Davidovich et al. (2012), who stated that araphid sexual reproduction mechanisms vary and further new gamete movement patterns may be discovered; however, their study was limited to light microscopy (Davidovich et al. 2012).

4.4.3 Auxospore development

Auxospore formation and development is important for the cytology and reproductive behaviour of diatoms and their taxonomy (Mann 1982). Results of the present study regarding for the auxospore structure of the *P. trainorii* revealed that it resembled the Clade 2b auxospore structure, which is a perizonium with bilateral symmetry. It develops out of the parental theca, which is consistent with the descriptions by Mann (1993); Kaczmarska et al. (2001) and Sato and Mann (2012).

The auxospore cell wall is made up of organic matter and siliceous elements (von Stosch 1982; Round et al. 1990; Kaczmarska et al. 2001). It is clear that the results of the present study showed the presence of different cell wall layers, one being thicker than the other. The TEM results for *P. trainorii* confirmed that, as described by Medlin and Kaczmarska (2004), the auxospore starts in a spherical shape with a delicate primary cell wall (which is the organic constituents), as such a phase was detected in the 20 minutes fertilised sample. Medlin and Kaczmarska (2004) state that the valves of the primary wall may be retained by the older auxospore as apical caps and may or may not remain as integral parts of the expanding cells. Results of this present study showed that the auxospore of *P. trainorii* expanded in both directions and the primary wall ruptured and surrounded the auxospore and covered the new walls of the perizonium, which expanded to reach the size of the young auxospore. However, it retained a circular shape at the centre of the auxospore in the TEM results. The scanning electron microscope results of this study (section 4.2.3, Figure 4.16) showed that no scales and caps were detected and the auxospore contained transverse bands with the widest in the centre in the 24 hours mature sample. This is consistent with the results of Sato et al. (2011).

However, they indicated the presence of longitudinal bands beneath the transverse ones. This present study aimed to study this using TEM with scanning electron microscopy as an auxiliary tool, whereas Sato and Mann (2012) used SEM extensively. However, there are no published micrographs for comparison. The TEM micrographs showed a perinuclear Golgi arrangement in the auxospore and the nucleus was huge in size. Bedoshvili and Likhoshway (2012) reported that the number of Golgi dictyosomes was proportional to the cell size where the larger cell volume had the higher number of Golgi dictyosomes. This present study showed that the auxospore stage had the higher number of Golgi dictyosomes, and this could be related to the physiological state of the cell, which is growing and increasing in size at an astonishing rate (Sato and Mann 2012).

In conclusion, diatom classification is a controversial field as the taxonomic features are variable and molecular phylogeny adds another dimension of complexity. Araphids are very abundant and have important environmental and economic implications (Round et al. 1990), but their taxonomy has long been ignored, perhaps because of their morphological simplicity (Round et al. 1990). The distinctive features of the main groups of araphid diatoms are not fully established, and many new species are classified as araphids that have characteristics intermediate between centric and araphid diatoms. P. trainorii is an araphid pennate species that morphologically looks much more like a typical centric species and for which there has been no previous ultrastructural description. It has recently been shown to have a unique pattern of gametogenesis, with motile male gametes that appear to glide along fine cytoplasmic threads which may or may not be related to flagella (Sato et al. 2011). Transmission electron microscopy resolved this issue and confirmed that the thread-like structures in P. trainorii are not flagella, due to the absence of any basal body associated with the gamete nuclei of P. trainorii. Further, gametogenesis in P. trainorii could be induced in the male and female strains separated by agar through the pheromones, this species made an ideal model in which to follow the separate ultrastructural differentiation of male and female gametes and auxospore structure. Therefore, gametes were mixed and the development of their resting zygotes followed. The results of the present study showed that the fine structures of the male and female gametes were different, although they appeared similar under light microscopy. Furthermore, the fine structure of the auxospores had phylogenetic significance at higher taxonomic levels (Medlin and Kaczmarska 2004); however, auxospore evolution is still not fully understood and further investigation is

needed. The ultrastructural features of *P. trainorii*'s auxospore resembled the Clade 2b auxospore structure, in the context of the modern molecular phylogeny of diatoms as defined by Medlin and Kaczmarska (2004). Further, the results of this study supported the conclusion that the Golgi arrangement relative to the nucleus was consistent with the characteristics of phylogenetic clades proposed by Medlin and Kacmarska (2004), and that the pyrenoid structure was more variable than was previously supposed (Schmid 2001).

Chapter 5. Conclusion

Understanding cell ultrastructure has greatly enhanced the knowledge of how cells work. Identifying the internal organization of cellular components and following their changes during biological processes such as cell division (Pickett-Heaps et al. 1975), gametogenesis (Jensen et al. 2003) and their response to environmental stressors (Alhasan et al. 1987) has greatly enhanced the understanding of these processes. The main aim of this thesis was to satisfy the requirements of the Kuwait Government Scholarship so that the present writer can become qualified in microalgae ultrastructure. To this end, two different scientific problems using the transmission electron microscope (TEM) were investigated and described in this thesis. Firstly, the effects of decadienal on cell structure and lipid production were investigated by quantifying lipid production in two important biofuel producing algae, Dunaliella salina and Nannochloropsis oculata. Secondly, for the first time, the ultrastructure of the phylogenetically interesting araphid pennate diatom *Pseudostaurosira trainorii* was documented. The ultrastructure of cellular organelles and gametogenesis was placed in the context of current theories of diatom taxonomy based on molecular phylogeny. Electron microscopy is the only technique that enables the distribution and structure of intracellular organelles to be examined at high resolution.

Chapter 3 of this thesis summarised the first investigation of the effects of the so-called infochemical decadienal on cell ultrastructure in two important biofuel producing microalgal species. The sustainability of biofuel production depends on many factors, one of them being the lipid content of algal cells. The higher the lipid content, the more cost-effective the biofuel production will be. It has recently been shown that decadienal induced lipid production in *Nannochloropsis* (Taylor et al. 2012), which could make the process of biofuel production more economical. However, little is known about how decadienal work. One assumption was that it may be bringing about premature senescence of cells. Therefore, as part of this investigation, the effects of decadienal on cell ultrastructure in *Dunaliella* and *Nannochloropsis* was compared with the ultrastructural changes that occurred in naturally senescing (stationary) cultures. In, addition, how lipid is structurally organised in cells, whether as discrete lipid globules or as part of cellular structures such as membranes, will clearly impact on how easily it can be extracted and, thus, on the cost effectiveness of biofuel production. Neutral lipids are found in the cell as separate lipid bodies, and an increase in their volume may be

directly relevant to biofuel production. The use of electron microscopy can differentiate between these discrete lipid bodies and structural lipids (Wang et al. 2009), which cannot be discriminated by chemical extraction. This study showed an increase in lipid production in *D. salina* at very high decadienal concentrations, which induced cell apoptosis. This is consistent with the results of Taylor et al. (2012) who reported significant increases in lipid production at high decadienal concentrations, which limited cell growth. This present study quantified lipid production based on well-known mathematical concepts using electron microscopy to estimate the lipid volume fraction (Steer 1981), whereas, previous studies have quantified lipids by dry mass (Sharma et al. 2012); or as arbitrary fluorescence units per cell (Tylor et al. 2012). It is difficult to reconcile these different measurements and to compare dry mass values directly with volume fractions. These results, together with the apparent induction of apoptosis, support the conclusion that decadienal acts as a stressor. However, it does not appear to cause the cell to enter the stationary phase prematurely, since it induced less lipid production than in normal stationary phase cells.

The use of electron microscopy as a quantitative method may have some limitations, as the volume fraction percentages based on microscopy might reflect the status within the cell rather than the whole population (Solomon et al. 1985). On one hand, using stereological principles to estimate the fraction volume of lipid droplets overcomes this limitation as some sections contained lipid droplets while others did not due to random sampling of the sections themselves, and the thickness of a section is tiny in comparison to total cell thickness (Russ 1986). On the other hand, it has been reported that lipid accumulation in *Ankistrodesmus* can be assessed on a daily basis using epifluorescence microscopy, and it has been demonstrated that the number of cells accumulating lipid increased over time rather than the quantity of lipid per individual cell increasing (Solomon et al. 1986). In addition, Vardi et al. (2006) suggested that early responding cells can induce intracellular communication that could be transmitted within a diatom population in response to decadienal. Therefore, the volume fraction of the lipid body in this present study was very small; however, the chemical extraction of lipid from the whole population showed significant results (Taylor et al. 2012).

In order to reach a better understanding of lipid production and to increase its potential using decadienal or any other similar chemical inducers, it is clear that two levels of understanding are required: firstly, of lipid production and storage within a single (or model) cell; and, secondly, of lipid production within a population. For example, the

real mechanism of lipid induction by decadienal could not be detected, although one of its effects is the induction of oxidative stress (Vardi et al. 2006) and recent research has shown that oxidative stress could increase lipid production in *D. salina* species (Yilancioglu et al. 2014). Another example is the results found here for N. oculata. The cell responses in this species to ethanol and decadienal seemed to result in similar ultrastructural changes. Analysis of such results could indicate that it is a general biological response of N. oculata to a chemical stressor or it may simply be an induced artefact of fixation. The apparent induction of lipid in ethanol-treated cells as well as in decadienal-treated cells suggests the induction of lipids by both of these chemicals (Musgrave et al. 1992; Taylor et al. 2012). Furthermore, it could indicate a synergistic effect of decadienal and ethanol. Previous reports suggest that decadienal was working synergistically with heavy metals (Caldwell et al. 2005; Taylor et al. 2005). The presence of ultrastructural changes seen in the present study were comparable to those seen following fixation with glutaraldehyde alone (Chapter 2, protocols one, two, three) and their absence in ethanol-treated samples may indicate that ethanol could make decadienal stronger or that the fixation protocol did not work with ethanol and decadienal together because of their synergistic effect. This indicates the importance of understanding the effect of all chemical factors on the cell, as it is very problematic to fix and embed N. oculata successfully (Hibberd 1981; Lubian 1982 in Solomon et al. 1986). As the electron microscope is expensive, the repetition of experiments using methanol as solvent was difficult.

One important point that results from this study is that more detailed signs of apoptosis were observed, as the internal apoptosis lesions that are invisible with light microscopy are clearly visible with TEM. There is an active debate about the evolution of programmed cell death and its origins in phytoplanktonic photosynthetic organisms (Bidle and Falkowski 2004). The signs of apoptosis were different in *D. salina* and *N. oculata*, and these two organisms evolved from two different algal groups from the green and red lineages. Given the premise that metacaspases were found in *Chlamydomonas reinhardtii*, which belongs to the green lineage, and the marine diatom *Thalassiosira pseudonana*, which belong to the red lineage, the present results indicate that both *D. salina* and *N. oculata* could have different programmed cell death mechanisms in response to decadienal. This might indicate that the evolving mechanisms of PCD in the two different lineages of microscopic algae are different.

Chapter 4 documented the cell ultrastructure of *Pseudostaurosira trainorii* for the first time and permitted a detailed comparison with other diatom species in the context of modern diatom classification based on molecular phylogeny. Regarding P. trainorii the findings here support the classification of diatoms based on the type of Golgi, yet it has an undescribed pyrenoid structure. Available information is very sparse, as diatom research has shifted from description to a focus on silica biomineralization (Lopez et al. 2005) and nanotechnology (Gordon et al. 2008). On the other hand, molecular phylogeny itself is a subject of extensive research. Molecular phylogeny techniques vary in their accuracy and results. For example, the current status of the class Mediophyceae is under debate, having been accepted by Medlin and Kaczmarska (2004) and questioned by Alverson and Theriot (2005) and Williams and Kociolek (2007). In addition, some features may be acquired separately as a result of other factors, for example environmental pressure or natural selection, and may not indicate the same ancestor. For example, *Toxarium* is a centric diatom with an elongated shape. Studies have shown that it acquired its elongated shape separately (Kooistra et al. 2003b). Therefore, the molecular phylogeny and ultrastructural correlation evidence provided by Medlin and Kaczmarska (2004) needs further investigation.

The detection of gametogenesis in *P. trainorii* has many limitations, because it is an expensive and time-consuming procedure. In addition, the random sectioning of samples makes it difficult to obtain micrographs for all of the stages of the gametogenesis process. However, the present study provides significant information concerning ultrastructure. Sato et al. (2011) reported that both male and female gametes under light microscopy were similar; however, various differences between them have been detected in this study. It has been confirmed that *P. trainorii* male gametes are non-flagellated.

In conclusion, on the one hand, the transmission electron microscope, confirmed that the lipid bodies volume fraction induced by decadienal constituted a very low fraction of cell volume. Thefore, the induction of lipid bodies' by high concentration decadienal as here would not be suitable for commercial use and total lipid content of the cell is an important factor in improving the cost effectiveness of biofuel extraction plants. The use of the electron microscope is valuable to study structures that cannot be seen using a light electron microscope. It was used in this study to detect the effects of decadienal on the cell structure of *D. salina* and *N. oculata*. The effect of decadienal on the cell structure of *D. salina* suggests it is a stress factor (or a toxin); at high concentration (50)

 μM) it induced signs of programmed cell death. The cell could provide a suitable detoxification mechanism for decadienal at very low concentrations (2 μM) as the cell structure was similar to controls.

On the other hand, the transmission electron microscope was useful in confirmaing that the thread-like structures in the *P. trainorii* male gamete were not flagella. The results of this present study showed partial agreement with the hypothesis of Medlin and Kaczmarska (2004) as it confirmed that the Golgi structure in *P. trainorii* matched their hypothesis, while the pyrenoid structure did not. Therefore, more studies are needed in the future to investigate the relation between the ultrastructure and molecular phylogeny.

6. Appendices

Appendix 1

Specimen processing for transmission electron microscopy

- Fix in 2% Glutraldehyde in Cacodylate buffer.
- Rinse in Cacodylate Buffer 2 X 15 minutes then leave in the buffer at 4 °C for 3 changes over several hours.
- Secondary fix in 1% Osmium Tetraoxide in buffer for 1 hr, dispose of waste in container provided in fume hood
- Rinse in buffer for a minimum of 2 X15 minutes (can be left in buffer overnight at 4 °C so rest of schedule can be completed in 2 days.
- Dehydration

25% acetone	30 min
50% acetone	30 min
75% acetone	30 min

From this point on, use acetone stored in dessicator (not from wash bottles)

100% acetone 1 hr 100% acetone 1 hr

- Using TAAB epoxy resin kit, mixed to manufacturer's specifications:
- Impregnate with

25% resin in acetone	1 hr
50% resin in acetone	1 hr
75% resin in acetone	1 hr
100% resin in acetone	1 hr

(can be left overnight on rotator at this stage, store the liquid resin in the dessicator)

100% resin	1hr
100% resin	1hr
100% resin	at least 3 hrs

- Embed in fresh 100% resin at 60 °C oven overnight
- Polymerise all items contaminated with resin in 60 °C oven overnight before appropriate disposal

Appendix 2

Statistical analysis

Dunaliella salina: testing the differences between volume fractions of log and stationary phase

Testing normality for linear and stationary growing cells

Table A1: Results of Anderson-Darling tests of original data of organelles' volume fractions in *Dunaliella salina* log phase cells

Organelle	A^2	n	p
Nucleus	0.511	30	0.181
Mitochondria	0.425	30	0.296
Lipid	9.356	30	< 0.005
Vacuoles	2.191	30	< 0.005
Chloroplast	0.227	30	0.798
Cytoplasm	0.340	30	0.474
Thylakoid membrane	0.286	30	0.601
Starch grains	0.370	30	0.403
Plastoglobuli	1.803	30	< 0.005
Pyrenoid	1.621	30	< 0.005
Matrix	0.345	30	0.461

Table A2: Results of Anderson-Darling tests of original data of organelles' volume fractions in *Dunaliella salina* stationary phase cells

Organelle	A^2	n	p
Nucleus	2.561	30	< 0.005
Mitochondria	3.764	30	< 0.005
Lipid	0.295	30	0.574
Vacuoles	0.898	30	0.019
Cytoplasm	0.453	30	0.254
Chloroplast	0.348	30	0.454
Thylakoid membrane	0299	30	0.562
Starch grains	0.518	30	0.173
Plastoglobuli	1.443	30	< 0.005
Pyrenoid	6.328	30	< 0.005
Matrix	0.885	30	0.021

Table A3: Results of Anderson-Darling tests of transformed data of organelles' volume fractions in *Dunaliella salina* log phase cells. Transformation formula: =ASIN (SQRT(A3/100))

Organelle	A^2	n	p
Lipid	9.578	30	< 0.005
Vacuoles	2.055	30	< 0.005
Plastoglobuli	2.035	30	< 0.005
Pyrenoid	2.885	30	< 0.005

Table A4: Results of Anderson-Darling tests of transformed data of organelles' volume fractions in *Dunaliella salina* stationary phase cells. Transformation formula: =ASIN (SQRT(A3/100))

Organelle	A^2	n	p
Nucleus	2.063	30	< 0.005
Mitochondria	0.808	30	0.032
Matrix	0.707	30	0.059

Test of variance

Table A5: Results of F-tests to test the variances for *Dunaliella salina* log phase and stationary phase volume fractions of different organelles

Organelle	DF	F	P value
Cytoplasm	29	0.58	0.374
Mitochondria	29	0.61	< 0.005
Chloroplast	29	2595.58	0.07
Matrix	29	0.5	< 0.005
Thylakoid membrane	29	356.57	0.183
Starch grains	29	1.40	0.15

${\it Dunaliella\ salina:}$ testing the differences between volume fractions of decadienal-treated cells

Table A6: Results of Anderson-Darling tests for original data of organelles' volume fractions in *Dunaliella salina* cells treated with 0 μ M decadienal

Organelle	A^2	n	p
Nucleus	1.478	30	< 0.005
Mitochondria	0.953	30	< 0.005
Lipid	error		
Vacuoles	1.941	30	< 0.005
Chloroplast	0.369	30	0.405
Cytoplasm	0.294	30	0.578
Thylakoid membrane	0.475	30	0.223
Starch grains	0.537	30	0.155
Plastoglobuli	1.760	30	<0.005
Pyrenoid	0.813	30	0.031
Matrix	0.292	30	0.582

Table A7: Results Anderson-Darling tests of transformed data of organelles' volume fractions in *Dunaliella salina* cells treated with $0~\mu M$ decadienal

Organelle	A^2	n	p
Nucleus	1.557	30	< 0.005
Mitochondria	1.138	30	< 0.005
Lipid	Error		
Vacuoles	0.840	30	0.027
Plastoglobuli	1.557	30	<0.005

Table A8: Results of Anderson-Darling tests of original data of organelles' volume fractions in *Dunaliella salina* sample treated with methanol

Organelle	A^2	n	p
Nucleus	0.625	30	0.094
Mitochondria	0.244	30	0.741
Lipid	error		
Vacuoles	1.332	30	<0.005
Chloroplast	0.412	30	0.319
Cytoplasm	0.480	30	0.217
Thylakoid membrane	0.541	30	0.152
Starch grains	0.657	30	0.078
Plastoglobuli	2.960	30	<0.005
Pyrenoid	1.044	30	0.008
Matrix	0.425	30	0.296

Table A9: Results of Anderson-Darling tests of original data of organelles' volume fractions in *Dunaliella salina* sample treated with $2.5~\mu M$ decadienal

Organelle	A^2	n	p
Nucleus	0.681	30	0.068
Mitochondria	0.889	30	0.020
Lipid	11.090	30	< 0.005
Vacuoles	1.671	30	< 0.005
Chloroplast	0.666	30	0.074
Cytoplasm	0.358	30	0.431
Thylakoid membrane	0.216	30	0.831
Starch grains	0.182	30	0.905
Plastoglobuli	2.358	30	<0.005
Pyrenoid	1.536	30	<0.005
Matrix	0.499	30	0.194

Table A10: Results of Anderson-Darling tests for original data of organelles' volume fractions in *Dunaliella salina* sample treated with 50 μ M decadienal

Organelle	A^2	n	p
Nucleus	0.668	30	0.073
Mitochondria	5.914	30	<0.005
Lipid	1.103	30	0.006
Vacuoles	0.223	30	0.809
Chloroplast	0.349	30	0.451
Cytoplasm	0.323	30	0.512
Thylakoid membrane	0.551	30	0.142
Starch grains	0.242	30	0.7848
Plastoglobuli	2.331	30	<0.005
Pyrenoid	1.012	30	0.010
Matrix	0.387	30	0.367

Table A11: Results of Levene's tests of normally distributed data of organelles' volume fractions in *Dunaliella salina* samples treated with methanol, 0 μ M, 2.5 μ M, and 50 μ M decadienal

Organelle	L	p
Chloroplast	3.82	0.012
Cytoplasm	2.19	0.092
Thylakoid membranes	0.68	0.568
Starch grains	1.02	0.385
Matrix	0.17	0.917

$Nannochloropsis\ oculata$: testing the differences between volume fraction of log and stationary phase

Table A12: Results of Anderson-Darling tests of original data of organelles' volume fractions in *Nannochloropsis oculata* log phase sample

Organelle	A^2	n	p
Nucleus	1.34	30	0.005
Mitochondria	0.37	30	0.407
Lipid	11.09	30	0.005
Vacuoles	2.10	30	0.005
Chloroplast	0.53	30	0.165
Cytoplasm	0.51	30	0.177
Thylakoid membrane	0.44	30	0.276
Cell wall	0.34	30	0.481
Plastoglobuli	7.55	30	0.005
Matrix	0.40	30	0.339

Table A13: Results of Anderson-Darling tests of original data of organelles' volume fractions in *Nannochloropsis oculata* stationary phase sample

Organelle	A^2	n	p
Nucleus	1.02	30	0.010
Mitochondria	1.28	30	0.005
Lipid	0.43	30	0.286
Vacuoles	9.35	30	0.005
Cytoplasm	0.77	30	0.039
Chloroplast	1.11	30	0.005
Thylakoid membrane	1.20	30	0.005
Cell wall	0.39	30	0.360
Plastoglobuli	4.50	30	0.005
Matrix	1.11	30	0.006
Storage bodies	1.11	30	0.006

Table A14: Results of Anderson-Darling tests of transformed data of organelles' volume fractions in *Nannochloropsis oculata* log phase sample. Transformatioin formula: =ASIN (SQRT(A3/100))

Organelle	A^2	n	p
Lipid	11.09	30	0.005
Vacuoles	1.31	30	0.005
Plastoglobuli	7.87	30	0.005
Nucleus	1.26	30	0.005

Table A15: Results of Anderson-Darling tests of transformed data of organelles' volume fractions in *Nannochloropsis oculata* stationary phase cells. Transformation formula: =ASIN (SQRT(A3/100))

Organelle	A^2	n	p
Cytoplasm	0.30	30	0.553
Mitochondria	0.91	30	0.017
Chloroplast	0.50	30	0.190
Matrix	0.47	30	0.227
Thylakoid membrane	0.48	30	0.216

Table A16: Results of F-tests to test the variances for *Nannochloropsis oculata* log phase and stationary phase volume fractions of different organelles

Organelle	DF	F	p value
Cytoplasm	29	5726.21	<0.001
Chloroplast	29	9180.67	<0.001
Matrix	29	5876.72	< 0.001
Thylakoid membrane	29	8785.65	< 0.001
Cell wall	29	0.43	0.027

${\it Nannochloropsis\ oculata:}$ testing the differences between volume fractions of decadienal-treated cells

Table A17: Results of Anderson-Darling tests of original data of organelles' volume fractions in *Nannochloropsis oculata* sample treated with 0 µM decadienal

Organelle	A^2	n	p
Nucleus	0.48	30	0.218
Mitochondria	0.37	30	0.407
Lipid	2.26	30	0.005
Vacuoles	1.57	30	0.005
Chloroplast	0.38	30	0.383
Cytoplasm	0.49	30	0.205
Thylakoid membrane	0.44	30	0.279
Cell wall	0.73	30	0.052
Plastoglobuli	10.19	30	0.005
Matrix	0.25	30	0.712

Table A18: Results of Anderson-Darling tests of original data of organelles' volume fractions in *Nannochloropsis oculata* sample treated with ethanol

Organelle	A^2	n	p
Nucleus	1.40	30	0.005
Mitochondria	0.27	30	0.644
Lipid	0.97	30	0.013
Vacuoles	2.11	30	0.005
Chloroplast	0.53	30	0.159
Cytoplasm	0.49	30	0.210
Thylakoid membrane	0.44	30	0.277
Cell wall	0.43	30	0.282
Plastoglobuli	7.15	30	0.005
Matrix	0.62	30	0.100

Table A19: Results of Anderson-Darling tests of original data of organelles' volume fractions in *Nannochloropsis oculata* sample treated with 1 μ M decadienal

Organelle	A^2	n	p
Nucleus	0.44	30	0.277
Mitochondria	1.72	30	0.005
Lipid	0.79	30	0.035
Vacuoles	1.87	30	0.005
Chloroplast	1.06	30	0.007
Cytoplasm	0.21	30	0.851
Thylakoid membrane	0.78	30	0.039
Cell wall	0.26	30	0.685
Plastoglobuli	4.76	30	0.005
Matrix	0.38	30	0.385

Table A20: Results of Anderson-Darling tests of original data of organelles' volume fractions in *Nannochloropsis oculata* sample treated with 10 μM decadienal

Organelle	A^2	n	p
Nucleus	0.83	30	0.029
Mitochondria	0.33	30	0.493
Lipid	0.67	30	0.071
Vacuoles	2.40	30	0.005
Chloroplast	0.29	30	0.600
Cytoplasm	0.37	30	0.405
Thylakoid membrane	0.33	30	0.490
Cell wall	0.62	30	0.097
Plastoglobuli	4.96	30	0.005
Matrix	0.35	30	0.445

Table A21: Results of Anderson-Darling tests for original data of organelles' volume fractions in *Nannochloropsis oculata* sample treated with 50 μ M decadienal

Organelle	A^2	n	p
Nucleus	0.68	30	0.068
Mitochondria	1.43	30	0.005
Lipid	1.92	30	0.005
Vacuoles	2.30	30	0.005
Chloroplast	0.18	30	0.906
Cytoplasm	0.80	30	0.034
Thylakoid membrane	0.13	30	0.979
Cell wall	1.82	30	0.005
Plastoglobuli	5.12	30	0.005
Matrix	0.30	30	0.566

Table A22: Results of Anderson-Darling tests of transformed data of organelles' volume fractions in *Nannochloropsis oculata* samples treated with different decadienal treatments

Sample	Organelle	A^2	n	p
0 μM decadienal	Plastoglobuli	10.33	30	0.005
	Vacuoles	0.39	30	0.365
	Lipid	1.24	30	0.005
Ethanol	Nucleus	1.31	30	0.005
	Vacuoles	1.36	30	0.005
1 μM decadienal	Mitochondria	1.02	30	0.009
	Thylakoid membranes	1.59	30	0.005
	Chloroplast	1.54	30	0.005
	Vacuoles	1.26	30	0.005
10 μM decadienal	Vacuoles	1.04	30	0.008
50 μM decadienal	Mitochondria	1.96	30	0.005
	Cytoplasm	0.54	30	0.154
	Cell wall	1.28	30	0.005
	Vacuoles	1.81	30	0.005

Table A23: Results of Levene's tests of normally distributed data of organelles' volume fractions of *Nannochloropsis oculata* samples treated with ethanol, 0 μ M, 1 μ M, 10 μ M and 50 μ M decadienal

L	p
0.35	0.844
2.37	0.055

7. References

- Aaronson S (1973) Effect of incubation temperature on the macromolecular and lipid content of the phytoflagellate *Ochromonas danica*. Journal of Phycology 9: 111-113.
- Adl SM, Simpson AGB, Farmer MA, Andersen R A, Anderson OR, Barta JR, Bowser SS, Brugerolle G, Fensome RA, Fredericq S, James TY, Karpov S, Kugrens P, Krug J, Lane CE, Lewis LA, Lodge J, Lynn DH, Mann DG, Mccourt RM, Mendoza L, Moestrup O, Mozley-Stanridge SE, Nerad TA, Shearer CA, Smirnov AV, Spiegel FW, Taylor MFJR (2005) The new higher level classification of eukaryotes with emphasis on the taxonomy of protists. Journal of Eukaryotic Microbiology 52: 399-451.
- Adl SM, Simpson AGB, Lane CE, Lukes J, Bass D, bowser SS, Brown MW, Burki, F, Dunthorn M, Hampl V, Heiss A, Hoppenrath M, Lara E, Gall L, Lynn DH, Mcmanus H, Mitchell EAD, Mozley-Stanridge SE, Parfrey LW, Pawlowski J, Rueckert S, Shadwick L, Schoch CL, Smirnov A, Spiegeln FW (2012) The revised classification of eukaryotes. Journal of Eukaryotic Microbiology 59: 429-493.
- Adolph S, Bach S, Blondel M, Cueff A, Moreau M, Pohnert G, Poulet SA, Wichard T, Zuccaro A (2004) Cytotoxicity of diatom-derived oxylipins in organisms belonging to different phyla. Journal of Experimental Biology 207: 2935-2946.
- Alhasan RH, Ghannoum MA, Sallal A-K, Abu-Elteen KH, Radwan SS (1987)

 Correlative changes of growth, pigmentation and lipid composition of

 Dunaliella salina in reponse to halostress. Journal of General Microbiology
 133: 2607-2616.
- Alonso DL, Belarbi EH, Fernández-Sevilla JM, Rodríguez-Ruiz J, Grima EM (2000)

 Acyl lipid composition variation related to culture age and nitrogen concentration in continuous culture of the microalga *Phaeodactylum tricornutum*. Phytochemistry 54: 461-471.

- Alverson AJ, Theriot EC (2005) Comments on recent progress toward reconstructing diatom phylogeny. Journal of Nanoscience and Nanotechnology 5: 57-62.
- Ameisen JC (2002) On the origin, evolution, and nature of programmed cell death: a timeline of four billion years. Cell Death and Differentiation 9: 367-393.
- Antia NJ, Bisalputra T, Cheng JY, Kallery JP (1975) Pigment and cytological evidence for reclassification of *Nanochloris oculata* and *Monallantus salina* in the Eustigmatophyceae. Journal of Phycology 11: 339-343.
- Arany I, Megyesi JK, Kaneto H, Price PM, Safirstein RL (2004) Cisplatin-induced cell death is EGFR/src/ERK signaling dependent in mouse proximal tubule cells. American Journal of Physiology and Renal Physiology 28: F543-F549.
- Archibald JM (2005) Jumping genes and shrinking genomes: probing the evolution of eukaryotic photosynthesis with genomics. IUBMB Life 57: 539-547.
- Archibald JM (2008) Plastid evolution: Remnant algal genes in ciliates. Current Biology 18: R663-R665.
- Ban S, Burns C, Castel J, Chaudron Y, Christou E, Escribano R, Umani SF, Gasparini S, Ruiz FG, Hoffmeyer M, Ianora A, Kang HK, Laabir M, Lacoste A, Miralto A, Ning X, Poulet S, Rodriguez V, Runge J, Shi J, Starr M, Uye S, Wang Y (1997). The paradox of diatom-copepod interactions. Marine Ecology Progress Series 157: 287-293.
- Barnwal BK, Sharma MP (2005) Prospects of biodiesel production from vegetables oils in India. Renewable and Sustainable Energy Reviews 9: 363-78.
- Bedoshvili YD, Likhoshway YV (2012) The cell ultrastructure of diatoms: implications for phylogeny? In: The Transmission Electron Microscope, Maaz K (ed.), ISBN: 978-953-51-0450-6, InTech, available from http://cdn.intechopen.com/pdfs-wm/34882.pdf. Accessed 13 October 2015
- Bedoshvili YD, Popkova TP, Likhoshway (2009) Chloroplast structure of diatoms of different classes. Cell and Tissue Biology 3: 297-310.
- Belarbi EH, Molina E, Chisti Y (2000) A process for high yield and scaleable recovery of high purity eicosapentaenoic acid esters from microalgae and fish oil.

 Enzyme and Microbial Technology 26: 516-29.

- Beller M, Thiel K, Thul PJ, Jakle H (2010) Lipid droplets: a dynamic organelle moves into focus. FEBS Letters 584: 2176-2182.
- Ben-Amotz A, Avron M (1983) Accumulation of metabolites by halotolerant algae and its industrial potential. Annual Reviews in Microbiology 37: 95-119.
- Ben-Amotz A, Katz A, Avron M (1982) Accumulation of β-carotene in halotolerant algae: Purification and characterization of β-carotene-rich globules from *Dunaliella bardawil* (Chlorophyceae). Journal of Phycology 18: 529-537.
- Berges JA, Falkowski PG (1998) Physiological stress and cell death in marine phytoplankton: induction of proteases in response to nitrogen or light limitation. Limnology Oceanography 43: 129-135.
- Berman-Frank I, Bidle K, Haramaty L, Falkowski P (2004) The demise of the marine cyanobacterium, *Trichodesmium* spp., via an autocatalyzed cell death pathway. Limnology Oceanography 49: 997-1005.
- Berner T (1993) Ultrastructure of Microalgae. CRC Press, London.
- Berube K, Dodge J, Ford T (1999) Effects of chronic salt stress on the ultrastructure of *Dunaliella bioculata* (Chlorophyta, Volvocales): mechanisms of response and recovery. European Journal of Phycology 34: 117-123.
- Bhattachary D, Medlin L, Wainwright PO, Ariztia EY, Bibeau C, Stickel SK, Sogin ML (1992) Algae containing chlorophylls a + c are paraphyletic: molecular evolutionary analysis of the Chromophyta. Evolution 46: 1808-1817.
- Bianchi ME, Manfredi A (2004) Chromatin and cell death. Biochimica et Biophysica Acta 1677: 181-6.
- Bidle KD, Falkowski PG (2004) Cell death in planktonic, photosynthetic microorganisms. Nature Reviews Microbiology 2: 643-655.
- Borowitzka LJ, Borowitzka MA (1990) Commercial production of β -carotene by Dunaliella salina in open ponds. Bulletin of Marine Science 47: 244-252.
- Borowitzka MA, Siva CJ (2007) The taxonomy of the genus *Dunaliella* (Chlorophyta, Dunaliellales) with emphasis on the marine and halophilic species. Journal of Applied Phycology 19: 567-590.

- Borowitzka U, Brorowitzka MA, Moulton TP (1984) The mass culture of *Dunaliella* salina for fine chemicals: From laboratory to pilot plant. Hydrobiologia 116/117: 115-134.
- Boussiba S, Vonshak A, Cohen Z, Avissar Y, Richmond A (1987) Lipid and biomass production by the halotolerant microalga *Nannochloropsis salina*. Biomass 12: 37-47.
- Brand N, Arnold C (1986) Improved structural preservation of the mature zygote of *Chlamydomonas reinhardii* by freeze-substitution fixation compared with chemical fixation with special attention to the mitochondria. Endocytobiosis and Cell Research 3: 79-95.
- Bredesen DE (2007) Key note lecture: toward a mechanistic taxonomy for cell death programs. Stroke 38: 652-660.
- Brennan L, Owende P (2010) Biofuels from microalgae review of technologies for production, processing, and extractions of biofuels and co-products.

 Renewable and Sustainable Energy Reviews 14: 557-77.
- Brown MR, Dunstan GA, Norwood SJ, Miller KA (1996). Effects of harvest stage and light on the biochemical composition of the diatom *Thalassiosira pseudonana*. Journal of Phycology 32: 64-73.
- Brown MR, Garland CD, Jeffrey SW, Jameson ID, Leroi JM (1993) The gross and amino acid compositions of batch and semi-continuous cultures of *Isochrysis* sp. (clone T.ISO), *Pavlova lutheri* and *Nannochloropsis oculata*. Journal of Applied Phycology 5: 285-296.
- Buchanan-Wollaston V, Earl S, Harrison E, Mathas E, Navabpour S, Page T, Pink D (2003) The molecular analysis of leaf senescence: a genomics approach. Plant Biotechnology Journal 1: 3-22.
- Bulte L, Wollman FA (1992) Evidence for a selective destabilization of an integral membrane protein, the cytochrome b6/f complex, during gametogenesis in *Chlamydomonas reinhardtii*. European Journal of Biochemistry 204: 327-336.

- Buttino I, Miralto A, Ianora A, Romano G, Poulet SA (1999) Water soluble extracts of the diatom *Thalassiosira rotula* induce aberrations in embryonic tubulin organisation of the sea urchin *Paracentrotus lividus*. Marine Biology 134 147-154.
- Caldwell GS, Bentley MG, Olive PJW (2004) First evidence of sperm motility inhibition by diatom aldehyde 2E, 4E-decadienal. Marine Ecology Progress Series 273: 97-108.
- Caldwell GS, Lewis C, Olive PJW, Bentley MG (2005). Exposure to 2, 4-decadienal negatively impacts upon marine invertebrate larval fitness. Marine Environmental Research 59: 405-417.
- Caldwell GS, Olive PJW, Bentley MG (2002) Inhibition of embryonic development and fertilisation in broadcast spawning marine invertebrates by water soluble diatom extracts and the diatom toxin 2-trans, 4-trans decadienal. Aquatic Toxicology 60: 123-137.
- Cantrell KB, Ducey T, Ro KS, Hunt PG (2008) Livestock waste-to-bioenergy generation opportunities. Bioresource Technology 99: 7941-53.
- Casotti R, Mazza S, Brunet C, Vantrepotte V, Ianora A, Miralto A (2005) Growth inhibition and toxicity of the diatom aldehyde 2-trans, 4-trans-decadienal on *Thalassiosira weissflogii* (Bacillariophyceae). Journal of Phycology 41: 7-20.
- Castellano I, Ercolesi E, Palumbo A (2014) Nitric oxide affects ERK signalling through down regulation of MAP kinase phosphatase levels during larval development of the ascidian *Ciona intestinalis*. PLOS One 9: e102907. doi: 10.1371/journal.pone.0102907.
- Castellano I, Ercolesi E, Romano G, Ianora A, Paluumbo A (2015) The diatom-derived aldehyde decadienal affects life cycle transition in the ascidian *Ciona intestinalis* through nitric oxide/ERK signalling. Open Biology 5: 140182.
- Castro-Obregon S, Rao RV, del Rio G, Chen SF, Poksay KS, Rabizadeh S, Vesce S, Zhang XK, Swanson RA, Bredesen DE (2004) Alternative, nonapoptotic programmed cell death: mediation by arrestin 2, ERK2, and Nur77. Journal of Biological Chemistry 279: 17543-17553.

- Cavalier-Smith T (1999) Principles of protein and lipid targeting in secondary symbiogenesis: euglenoid, dinoflagellate, and sporozoan plastid origins and the eukaryote family tree. Journal of Eukaryotic Microbiology 46: 347-66.
- Chang L, Lo W, Lin P (2005) Trans, Trans-2, 4-Decadienal, a product found in cooking oil fumes, induces cell proliferation and cytokine production due to reactive oxygen species in humans bronchial epithelial cells. Toxicological Sciences 87: 337-343.
- Cheng-Wu Z, Zmora O, Kopel R, Richmond A (2001) An industrialised flat plate glass reactor for mass production of *Nannochloropsis* sp. (Eustigmatophyceae). Aquaculture 195: 35-49.
- Chepurnov V, Mann D (2003) Auxosporulation of *Licmophora communis*(Bacillarophyta) and a review of mating systems and sexual reproduction in araphid pennate diatoms. Phycological Research 51: 1-12.
- Chepurnov V, Mann D, Sabbe K, Vyverman W (2004) Experimental studies on sexual reproduction in diatoms. International Reviews of Cytology 237: 91-154.
- Chisti Y (2006) Microalgae as sustainable cell factories. Environmental Engineering and Management Journal 5: 261-274.
- Chisti Y (2007) Biodiesel from microalgae. Biotechnology Advances 25: 294-306.
- Chisti Y (2008) Biodiesel from microalgae beats bioethanol. Trends in Biotechnology 26: 126-131.
- Christenson L, Sims R (2011) Production and harvesting of microalgae for wastewater treatment, biofuels, and bioproducts. Biotechnology Advances 29: 686-702.
- Comes S, Locascio A, Silvestre F, d'Ischia M, Russo GL, Tosti E, Branno M, Palumbo A (2007) Regulatory roles of nitric oxide during larval development and metamorphosis in *Ciona intestinalis*. Developmental Biology 306: 772-784.
- Converti A, Casazza AA, Ortiz EY, Perego P, Borghi MD (2009) Effect of temperature and nitrogen concentration on the growth and lipid content of *Nannochloropsis oculata* and *Chlorella vulgaris* for biodiesel production.

 Chemical Engineering and Processing: Process Intensification 48: 1146-1151.

- Cornillon S, Foa C, Davoust J, Buonavista N, Gross JD, Golstein P (1994) Programmed cell-death in *Dictyostelium*. Journal of Cell Sciences 107: 2691- 2704.
- Cowan AK, Rose PD, Horne LG (1992) *Dunaliella salina*: a model system for studying the response of plant-cells to stress. Journal of Experimental Botany 43: 1535-1547.
- Cox E (2011) Morphology: cell wall, cytology, ultrastructureal and morphogenetic studies, in the diatom world, cellular origin, life in extreme habitats and astrobiology 19: 21-45.
- Cribb B, Armstrong W, Whittington I (2004) Simultaneous fixation using glutaraldehyde and osmium tetroxide or potassium ferricyanide-reduced osmium for the preservation of monogenean flatworms: an assessment for merizocotyle icopae. Microscopy Research and Technique 63: 102-110.
- Davidovich N, Kaczmarska, Karpov S, Davidovich O (2012) Mechanism of male gamete motility in araphid pennate diatoms from the genus *Tabularia* (Bacillariophyta). Protist 163: 480-494.
- Deponte M (2008) Programmed cell death in protists. Biochemica et Biophysica Acta 1783: 1396-1405.
- Devi S, Santhanam AP, Rekha V, Ananth S, Prasath BB, Nandakumar R, Jeyanthi S, Kumar D (2012) Culture and biofuel producing efficacy of marine microalgae *Dunaliella salina* and *Nannochloropsis* sp.. Journal of Algal Biomass Utilization 3: 38-44.
- Dicke M, Sabelis M (1988) Infochemical terminology: based on cost–benefit analysis rather than origin of compounds? Functional Ecology 2: 131-139.
- Dodge JD (1973) The Structure of Algal Cells. Academic Press, London.
- Drebes G (1977) Sexuality. In: The Biology of Diatoms: Botanical Monographs, Warner D (ed) Vol. 13. Blackwell Scientific Publications, Oxford, pp. 250-283.
- Dunahay TG, Jarvis EE, Dais SS, Roessler PG (1996) Manipulation of microalgal lipid production using genetic engineering. Applied Biochemistry and Biotechnology 5758: 223-31.

- Dunn SR, Thomason JC, Thissler ML, Bythell JC (2004) Heat stress induces different forms of cell death in sea anemones and their endosymbiotic algae depending on temperature and duration. Cell Death and Differentiation 1: 1213-1222.
- Dunstan GA, Volkman JK, Barrett SM, Garland CD (1993) Changes in the lipid composition and maximization of the polyunsaturated fatty acid content of three microalgae grown in mass culture. Journal of Applied Phycology 5: 71-83.
- Edlund MB, Stoermer EF (1997) Ecology, evolution and systematic significance of diatom life histories. Journal of Phycology 33: 897-918.
- Einspahr KJ, Maeda M, Thompson GA (1988) Concurrent changes in *Dunaliella salina* ultrastructure and membrane phospholipid metabolism after hyperosmoic shock. Journal of Cell Biology 107: 529-538.
- El-Sheek MM, Rady AA (1995) Effect of phosphorus starvation on growth, photosynthesis and some metabolic processes in the unicellular green alga *Chlorella kessleri*. Phyton 35: 139-151.
- Eyden BP (1975) Light and electron microscope study of *Dunaliella primolecta* Bucher (Volocida). Journal of Protozoology 22: 336-344.
- Falciatore A, D'Alcala MR, Croot P, Bowler C (2000) Perception of environmental signals by a marine diatom. Science 288: 2363-2366.
- Falkowski PG, Katz M, Knoll AH, Quigg A, Raven JA, Schofield O, Taylor FJR (2004)

 The evolution of modern eukaryotic phytoplankton. Science 305: 354-360.
- Fedorov AS, Kosourov S, Ghirardi ML, Seibert M (2005) Continuous H₂ photoproduction by *Chlamydomonas reinhardtii* using a novel two-stage, sulfate-limited chemostat system. Applied Biochemistry and Biotechnology 121-124: 403-12.
- Fogg GE (2001) Algal adaptation to stress: some general remarks. In: Algal Adaptation to Environmental Stresses: Physiological, biochemical and molecular mechanisms. Rai LC, Gaur JP (eds), Springer-Verlag Berlin, Germany, pp. 1-19.

- Fontana A, d'Ippolito G, Cutignano A, Romano G, Lamari N, Galluci AM, Cimino G, Miralto A, Ianora A (2007) LOX-induced lipid peroxidation mechanism responsible for the detrimental effect of marine diatoms on zooplankton grazers. ChemBioChem 8: 1810-1818.
- Franklin DJ, Berges JA (2004) Mortality in cultures of the dinoflagellate *Amphidinium* carterae during culture senescence and darkness. Proceedings of the Royal Society of London, Biology 271: 2099-2107.
- Frohlich KU, Madeo F (2000) Apoptosis in yeast: a monocellular organism exhibits altruistic behaviour. FEBS Letters 473: 6-9.
- Fukuda H (1994) Programmed cell death of tracheary elements as a paradigm in plants. Plant Molecular Biology 44: 245-253.
- Fukuda H, Kond A, Noda H (2001) Biodiesel fuel production by transesterification of oils. Journal of Bioscience and Bioengineering 92: 405-416.
- Gavrilescu M, Chisti Y (2005) Biotechnology: a sustainable alternative for chemical industry. Biotechnology Advances 23:471-99.
- Gerpen J (2005) Biodiesel processing and production. Fuel Processing Technology 86: 1097-107.
- Ghirardi ML, Zhang JP, Lee JW, Flynn T, Seibert M, Greenbaum E (2000) Microalgae: a green source of renewable H₂. Trends in Biotechnology 18: 506-11.
- Ginzburg M (1987) *Dunaliella*: a green alga adapted to salt. Advances in Botanical Research 14: 93-183.
- Glauert AM, Lewis PR (1998) Biological Specimen Preparation for Transmission Electron Microscopy. Princeton University Press, Princeton, New Jersey, USA.
- Gomez PI, Gonzalez MA (2004) Genetic variation among seven strains of *Dunaliella salina* (Chlorophyta) with industrial potential, based on RAPD banding patterns and on nuclear ITS rDNA sequences. Aquaculture 233:149-162.

- Gordon R, Losic D, Tiffany M, Nagy S, Sterrenburg F (2008) The glass menagerie: diatoms for novel applications in nanotechnology. Trends in Biotechnology 27: 116-127.
- Gottlieb RA, Nordberg J, Skowronski E, Babior BM (1996) Apoptosis induced in Jurkat cells by several agents is preceded by intracellular acidification. Proceedings of the National Academy of Sciences of the United States of America 93: 654-58.
- Gouveia L, Oliveira A (2009) Microalgae as a raw material for biofuels production.

 Journal of Industrial Microbiology and Biotechnology 36: 269-274.
- Graham LE, Graham JM, Wilcox LW (2009) Algae (2nd ed). Pearson Education, San Francisco, California, USA.
- Graham LE, Wilcox LW (2000) Algae. Prentice-Hall, Inc., Upper Saddle River, New Jersey, USA.
- Greenberg JT (1996) Programmed cell death: a way of life for plants. Proceedings of the Natural Academy of Sciences, USA 93: 12094-12097.
- Greenwell HC, Laurens LML, Shields RJ, Lovitt RW, Flynn KJ (2010) Placing microalgae on the biofuels priority list: a review of the technological challenges. Journal of the Royal Society Interface 7: 703-726.
- Griffiths MJ, Harrison SL (2009) Lipid productivity as a key characteristic for choosing algal species for biodiesel production. Journal of Applied Phycology 21: 493-507.
- Guillard RRL, Ryther JH (1962) Studies of marine planktonic diatoms. I. *Cyclotella nana* Hustedt and *Detonula confervaceae* (Cleve) Canadian Journal of Microbiology 8: 229-239.
- Guillou L, Chretiennot-Dinot MJ, Medlin LK, Claustre H, Loiseaux-Degoer S, Vaulot D (1999) *Bolidomonas*, a new genus with two species belonging to a new algal class: the Bolidophyceae. Journal of Phycology 35: 368-381.
- Guschina I, Harwood J (2006) Lipids and lipid metabolism in eukaryotic algae.

 Progress in Lipid Research 45: 160-186.

- Hageman G, Verhagen H, Schutte B, Kleinjans J (1991) Biological effects of short-term feeding to rats of repeatedly used deep-frying fats in relation to fat mutagen content. Food and Chemical Toxicology 29: 689-698.
- Hallmann A, Godl K, Wenzl S, Sumper M (1998) The highly efficient sex-inducing pheromone system of *Volvox*. Trends in Microbiology 6: 185-189.
- Hansen E, Even Y, Geneviere A-M (2004) The $\alpha, \beta, \gamma, \delta$ -unsaturated aldehyde 4-trans4-trans-decadienal disturbs DNA replication and mitotic events in early sea urchin embryos. Toxicological Sciences 81: 190-197.
- Hayat MA (1989) Principles and Techniques of Electron Microscopy: Biological Applications. Third edition, Macmillan Press Scientific and Medical, Toronto, Ontario, Canada.
- Hibberd DJ (1981) Notes on the taxonomy and nomenclature of the algal classes

 Eustigmatophyceae and Tribophyceae (synonym Xanthophyceae). Botanical

 Journal of the Linnean Society 82: 93-119.
- Hibberd DJ, Leedale GF (1972) Observations on the cytology and ultrastructure of the new algal class, Eustigmatophyceae. Annals of Botany 36: 49-71.
- Hill J, Nelson E, Tilman D, Polasky S, Tiffany D (2006) Environmental economic and energetic costs and benefits of biodiesel and ethanol biofuels. Proceedings of the National Academy of Sciences of the United States of America 103: 11206-11210.
- Hoshaw RW, Malouf LY (1981) Ultrastructure of the green flagellate *Dunaliella tertiolecta* (Chlorophyceae, Volvocales) with comparative notes on three other species. Phycologia 20: 199-206.
- Hsieh CH, Wu WT (2009) Cultivation of microalgae for oil production with a cultivation strategy of urea limitation. Bioresource Technology 100: 3921-3926.
- Hu Q, Sommerfeld M, Jarvis E, Ghirardi M, Posewitz M, Seibert M, Darzins A (2008) Microalgal triacylglycerols as feedstocks for biofuel production: perspectives and advances. Plant Journal 54: 621-639.

- Ianora A, Poulet SA, Miralto A (2003) The effects of diatoms on copepod reproduction: a review. Phycologia 42: 351-363.
- Idei M, Osada K, Sato S, Nakayama T, Nagumo T, Mann DG (2013). Sperm ultrastructure in the diatoms *Melosira* and *Thalassiosira* and the significance of the 9+0 configuration. Protoplasma 250: 833-50.
- Illman AM, Scragg AH, Shales SW (2000) Increase in *Chlorella* strains calorific values when grown in low nitrogen medium. Enzyme and Microbial Technology 27: 631-635.
- Ishii T, Tatsuda E, Kumazawa S, Nakayama T, Uchida K (2003) Molecular basis of enzyme inactivation by an endogenous electrophile 4-hydroxy-2-nonenal: identification of modification sites in glyceraldehyde- 3-phosphate dehydrogenase. Biochemistry 42: 3474-3480.
- Jensen KG, Mostrup O, Schmtd AM (2003) Ultrastructure of the male gametes from two centric diatoms, *Chaetoceros laciniosus* and *Coscinodiscus wailesii* (Bacillariophyceae). Phycologia 42: 98-105.
- Jimenez C, Berl T, Rivard CJ, Edelstein C, Capasso JM (2004) Phosphorylation of MAP kinase-like proteins mediates the response of the halotolerant alga *Dunaliella viridis* to hypertonic shock. Biochimica et Biophysica (BBA)-Molecular Cell Research 1644: 61-9.
- Jimenez C, Capasso JM, Edelstein CL, Rivard CJ, Lucia S, Breusegem S, Berl T, Segovia M (2009) Different ways to die: cell death modes of the unicellular chlorophyte *Dunaliella viridis* exposed to various environmental stresses are mediated by the caspase-like activity DEVDase. Journal of Experimental Botany 60: 815-828.
- Jimenez C, Cossio BR, Rivard CJ, Berl T, Capasso JM (2007) Cell division in the unicellular microalga *Dunaliella viridis* depends on phosphorylation of extracellular signal-regulated kinases (ERKs). Journal of Experimental Botany 58: 1001-1011.
- Jones A (2000) Does the plant mitochondrion integrate cellular stress and regulate programmed cell death? Trends in Plant Science 5: 225-230.

- Kaczmarska I, Ehrman JM, Bates SS (2001). A review of auxospore structure, ontogeny and diatom phylogeny. In: 16th Proceeding of International Diatom Symposium, 25 Aug.- 1 Sept. 2000, Athens & Aegean Islands, University of Athens, Greece.
- Kalin M, Wheeler WN, Meinrath G (2005) The removal of uranium from mining waste water using algal/microbial biomass. Journal of Environmental Radioactivity 78: 151-77.
- Karlson B, Potter D, Kuylenstierna M, Andersen RA (1996) Ultrastructure, pigment composition, and 18S rRNA gene sequence for *Nannochloropsis granulata* sp. nov. (Monodopsidaceae, Eustigmatophyceae), a marine ultraplankter isolated from the Skagerrak, northeast Atlantic Ocean. Phycologia 35: 253-260.
- Kelly MG, Bennion H, Cox EJ, Goldsmith B, Jamieson J, Juggins S, Mann DG, Telford RJ (2005) Common freshwater diatoms of Britain and Ireland: an interactive key. Environment Agency, Bristol.
 http://craticula.ncl.ac.uk/EADiatomKey/html/introduction.html. Accessed 1
 September 2015.
- Khairy HM (2009) Toxicity and accumulation of copper in *Nannochloropsis oculata* (Eustigmatophyceae, Heterokonta). World Applied Sciences Journal 6: 378-384.
- Khozin-Goldberg I, Bigogno C, Shrestha P, Cohen Z (2002) Nitrogen starvation induces the accumulation of arachidonic acid in the freshwater green alga *Parietochloris incisa* (Trebouxiophyceae). Journal of Phycology 38: 991-994
- Kilian O, Benemann CS, Niyogi KK, Vick B (2011) High-efficiency homologous recombination in the oil-producing alga *Nannochloropsis* sp. Proceedings of the National Academy of Sciences of the United States of America 108: 21265-21269.
- Kim YK, Kim HJ, Kwon CH, Kim JH, Woo JS, Jung JS, Kim JM (2005) Role of ERK activation in cisplatin-induced apoptosis in OK renal epithelial cells. Journal of Applied Toxicology 25: 374-382.

- King MW (2014) Fatty acid synthesis.

 http://themedicalbiochemistrypage.org/lipids.php. Accessed 1 September 2015.
- Kleinegris DMM, van Es MA, Janssen M, Brandenburg WA, Wijffels RH (2011) Phase toxicity of dedecane on the microalgae *Dunaliella salina*. Journal of Applied Phycology 23: 949-958.
- Klyachko-Gurvich GL (1974) Changes in the content and composition of triacylglyceride fatty acids during restoration of *Chlorella pyrenoidosa* cells after nitrogen starvation. Soviet Plant Physiology 2: 611-618.
- Knights BA, Brown AC, Conway E, Middleditch BS (1970) Hydrocarbons from the green form of the freshwater alga *Botryococcus braunii*. Phytochemistry 9: 1317-24.
- Kooistra WHCF, De Stefano M, Mann DG, Medlin LK (2003a). The phylogeny of the diatoms. Progress in Molecular and Subcellular Biology 33: 59-97.
- Kooistra WHCF, De Stefano M, Mann DG, Salma N, Medlin LK (2003b) The phylogenetic position of *Toxarium*, a pennate-like lineage within centric diatoms (Bacillariophyceae). Journal of Phycology 39: 185-197.
- Krishnamurthy KV, Krishnaraj R, Chozhavendan R, Christopher SF (2000) The programme of cell death in plants and animals: a comparison. Current Science 79: 1169-81.
- Lam E, Kato N, Lawton M (2001) Programmed cell death, mitochondria and the plant hypersensitive response. Nature 411: 848-853.
- Lamers PP, van de Laak CCW, Kaasenbrood PS, Lorier J, Janssen M, De Vos RCH, Bino RJ, Wijffels RH (2010) Carotenoid and fatty acid metabolism in light-stressed *Dunaliella salina*. Biotechnology and Bioengineering 106: 638-648.
- Lee RE (1989) Phycology, (2nd ed.), Cambridge University Press, Cambridge.
- Lee RE (1999) Phycology, (3rd ed.), Cambridge University Press, Cambridge.
- Leipe DD, Wainright PO, Gunderson JH, Porter D, Patterson DJ, Valois F, Himmerich S, Sogin ML (1994) The stramenopiles from a molecular perspective: 16S-

- like rRNA sequences from *Labyrinthuloides minuta* and *Cafeteria roenbergensis*. Phycologia 33: 369-377.
- Lennon, SV, Martin SJ, Cotter TG (1991) Dose-dependent induction of apoptosis in human tumour cell lines by widely divergent stimuli. Cell Proliferation 24: 203-14.
- Leonardi PI, Caceres EJ (1994) Comparative analysis of the fine structure of young and adult individuals of *Dunaliella salina* (polyblepharidaceae, chlorophyceae) with emphasis on the flagellar apparatus. Journal of Phycology 30: 642-653.
- Levine A, Tenhaken R, Dixon R, Lamb C (1994) H₂O₂ from the oxidative burst orchestrates the plant hypersensitive disease resistance response. Cell 79: 583-593.
- Lewis K (2000) Programmed cell death in bacteria. Microbiology and Molecular Biology Reviews 64: 503-514.
- Linkermann A, Green DR (2014) Necroptosis. New England Journal of Medicine 370: 455-465.
- Liu ZY, Wang GC, Zhou BC (2008) Effect of iron on growth and lipid accumulation in *Chlorella vulgaris*. Bioresource Technology 99: 4717- 4722.
- Lopez P, Descles J, Allen A, Bowler C (2005) Prospects in diatom research. Current Opinion in Biotechnology 16: 180-186.
- Lorenz RT, Cysewski GR (2000) Commercial potential for *Haematococcus* microalgae as a natural source of astaxanthin. Trends in Biotechnology 18:160-7.
- Lv X, Zou L, Sun B, Wang J, Sun M-Y (2010) Variations in lipid yields and compositions of marine microalgae during cell growth and respiration, and within intracellular structures. Journal of Experimental Marine Biology and Ecology 391: 73-83.
- Maeda M, Thompson GA (1986) On the mechanism of rapid plasma membrane and chloroplast envelope expansion in *Dunaliella salina* exposed to hypoosmsotic shock. Journal of Cell Biology 102: 289-297.

- Mallick N (2002) Biotechnological potential of immobilized algae for wastewater N, P and metal removal: a review. Biometals 15: 377-90.
- Mann D (1982) Auxospore formation in *Licmophora* (Bacillariophyta). Plant Systematics and Evolution 139: 289-294.
- Mann D (1993) Patterns of sexual reproduction in diatoms. Hydrobiologia 269/270: 11-20.
- Mann DG (1996) Chloroplast morphology, movements and inheritance in diatoms, In: Cytology, Genetics an Molecular Biology of Alagae, Chaudharyb BR and Agrawal SB (eds) SPB Academic, Amsterdam, Netherlands, pp. 249-274.
- Mann DG, Evans KM (2007) Molecular genetics and the neglected art of diatomics. In:
 Unravelling the Algae: The Past, Present, and Future of Algal Systematics,
 Brodie J, and Lewis J (eds) Taylor and Francis, London, pp. 232-256.
- Mann DG, Marchant HJ (1989) The origin of the diatom and its life cycle. In: The Chromophyte Algae: Problems and Perspectives, Green J.C, Leadbeater BSC and Diver WL (eds), Clarendon Press, Oxford, pp. 307-323.
- Mann DG, Sato S, Rovira L, Trobajo R (2013) Paedogamy and auxosporulation in *Nitzschia* sect. *Lanceolatae* (Bacillariophyta). Phycologia 52: 204-220.
- Martin JS, Newmeyer DD, Mathias S, Farschan DM, Wang HG, Reed JC, Kolesnick RN, Green DR (1995) Cell free reconstitution of Fas-UV radiation- and ceramidae induced apoptosis. European Molecular Biology Organization Journal 14: 5191-200.
- Maruyama I, Nakamura T, Matsubayashi, T, Ando Y, Maeda T (1986) Identification of the alga known as "marine *Chlorella*" as a member of the Eustigmatophyceae. Japanese Journal of Phycology 34: 319-325.
- McDonald K and Morphew M (1993) Improved preservation of ultrastructure in difficult-to-fix organisms by high pressure freezing and freeze substitution: I. *Drosophila melanogaster* and *Strongylocentrotus purpuratus* embryos. Microscopy Research and Technique 24: 465-473.
- Medlin LK (2009) Diatoms (Bacillariophyta). In: The Time Tree of Life, Hedges SB and Kumar S (eds), Oxford University Press, Oxford, pp. 127-130.

- Medlin LK, Jung I, Bahulikar R, Mendgen K, Kroth P, Kooistra WHCF (2008)

 Evolution of the diatoms, VI: assessment of the new genera in the araphids using molecular data. Nova Hedwigia, Beiheft 133: 81-100.
- Medlin L, Kaczmarska I (2004) Evolution of the diatoms, V: morphological and cytological support of the major clades and taxonomic revision. Phycologia 43: 245-273.
- Medlin LK, Kooistra WCHF, Schmid AMM (2000) A review of the evolution of the diatoms: a total approach using molecules, morphology and geology. In Witkowski A and Sieminska J (eds). The Origin and Early Evolution of the Diatoms: Fossil, Molecular and Biogeographical Approaches. W. Szafer Institute of Botany, Polish Academy of Sciences, Cracow, Poland.
- Melkonian M, Preisig HR (1984) An ultrastructural comparison between Spermatozopms and Dunaliella (Chlorophyceae). Plant Systematics and Evolution 146: 31-46.
- Mendoza H, Martel A, del Rio MJ, Reina GG (1999) Oleic acid is the main fatty acid related with carotenogenesis in *Dunaliella salina*. Journal of Applied Phycology 11:15-19.
- Metting FB (1996) Biodiversity and application of microalgae. Journal of Industrial Microbiology and Biotechnology 17: 477-89.
- Metzger P, Largeau C (2005) *Botryococcus braunii*: a rich source for hydrocarbons and related ether lipids. Applied Microbiology and Biotechnology 66: 486-96.
- Miao X, Wu Q (2006) Biodiesel production from heterotrophic microalgal oil. Bioresource Technology 97: 841-846.
- Miralto A, Barone G, Romano G, Poulet SA, Ianora A, Russo GL, Buttino I, Mazzarella G, Laabir M, Cabrini M, Giacobbe MG (1999) The insidious effect of diatoms on copepod reproduction. Nature 402: 173-176.
- Mohammady NG, Chen Y-C, El-Mahdy AA, Mohammad RF (2005) Physiological responses of the eustigmatophycean *Nannochloropsis salina* to aqueous diesel fuel pollution. Oceanologia 47: 75-92.

- Molina E, Fernandez FGA, Camacho G, Chisti Y (1999) Photobioreactors: light regime, mass transfer, and scale up. Journal of Biotechnology 70: 231-247.
- Morales EA (2001) Morphological studies in selected fragilarioid diatoms

 (Bacillariophyceae) from Connecticut waters (USA). Proceedings of the

 Academy of Natural Sciences of Philadelphia 151: 105-120.
- Morales EA (2005) Observations of the morphology of some known and new fragilaioid diatoms (Bacillariophyceae) from rivers in the USA. Phycological Research 53: 113-133.
- Morales EA, Edlund MB and Spaulding SA (2010) Description and ultrastructure of araphid diatoms species (Bacillariophyceae) morphologically similar to *Pseudostaurosira elliptica* (Schumann) Edlund *et al.* Phycological Research 58: 97- 107.
- Munoz R, Guieysse B (2006) Algal-bacterial processes for the treatment of hazardous contaminants: a review. Water Research 40: 2799-815.
- Murakami R, Hashimoto H (2009) Unusual nuclear division in *Nannochloropsis* oculata (Eustigmatophyceae, Heterokonta) which may ensure faithful transmission of secondary plastids. Protist 160: 41-49.
- Musgrave A, Kuin H, Jongen M, Wildt PD, Schuring F, Klerk H, van den Ende H (1992) Ethanol stimulates phospholipid turnover and inositol 1, 4, 5-trisphosphate production in *Chlamydomonas eugametos* gametes. Planta 186: 442-449.
- Nappez C, Battu S, Beneytout JL (1996) Trans, trans-2, 4-decadienal: cytotoxicity and effect on glutathione level in human erythroleukemia (HEL) cells. Cancer Letters 99:115-119.
- National Toxicology Program (1993), National Institutes of Health, U.S. Department of Health and Human Services. 2, 4-decadienal CAS No. 25152–84–5. Testing Status of Agents at NTP.

 https://ntp.niehs.nih.gov/ntp/htdocs/st_rpts/tox076.pdf. Accessed 13 October 2015.

- Oliveira L, Huynh H (1989) Ultrastructure and cytochemistry of *Dunaliella tertiolecta*Butcher and *Pavlova luth*eri (Droop) Green, grown on three different sources of organic nitrogen. New Phytologist 113: 481-490.
- Oren A (2005) A hundred years of *Dunaliella* research: 1905-2005. Saline Systems 1: 2, doi:10.1186/1746-1448-1-2.
- Paffenhöfer GA (2002) An assessment of the effects of diatoms on planktonic copepods. Marine Ecology Progress Series 227: 305-310.
- Pal D, Khozin-Goldberg I, Cohen Z (2011) The effect of light, salinity and nitrogen availability on lipid production by *Nannochloropsis* Sp. Applied Microbiology and Biotechnology 90: 1429-1441.
- Parra O, Floyd G, wilcoxl L (1990) Taxonomic identification and ultrastructural characterization of a Chilean strain of *Dunaliella*. Revista Chilean de Historia Natural 63: 239-245.
- Pennell RI, Lamb C (1997) Programmed plant cell in plants. Plant Cell 9: 1157-1168.
- Pfeifhofer AO, Belton JC (1975) Ultrastructure changes in chloroplast resulting from fluctuations in NaCl concentration: freeze-fracture of thylakoid membranes in *Dualiella salina*. Journal of Cell Science 18: 287-299.
- Pickett-Heaps J, McDonald K, Tippit D (1975) Cell division in the pennate diatom *Diatoma vulgare*. Protoplasma 86: 205-242.
- Pohnert G, Steinke M, Tollrian R (2007) Chemical cues, defence metabolites and the shaping of pelagic interspecific interactions. Trends in Ecology and Evolution 22: 198-203.
- Poulet SA, Richer de Forges M, Cueff A, Lennon JF (2003) Double labelling methods used to diagnose apoptotic and necrotic cell degradations in copepod nauplii. Marine Biology 143: 889-895.
- Praveenkumar R, Shameera K, Mahalakshmi G, Akbarsha MA, Thajuddin N (2012) Influence of nutrient deprivations on lipid accumulation in a dominant indigenous microalga *Chlorella* sp., BUM1008: evaluation for biodiesel production. Biomass and Bioenergy 37: 60-66.

- Preisig H (1992) Morphology and taxonomy. In: *Dunaliella*: Physiology, Biochemistry and biotechnology. Avron M and Ben-Amotz A (eds), CRC Press, London.
- Rabbani S, Beyer P, Lintig J, Hugueney P, Kleinig H (1998) Induced β-carotene synthesis driven by triacylglycerol deposition in the unicellular alga *Dunaliella bardawil*. Plant Physiology 116: 1239-1248.
- Rachlin JW, Jensen TE, Baxter M, Jani V (1982) Utilization of morphometric analysis in evaluating the response of Plectonnema boryanum (Cyanophyceae) to exposure to eight heavy metals. Archives of Environmental Contamination and Toxicology 11: 323-333.
- Rao VNR (1970) Studies on *Cyclotella meneghinina* KOTZ. I. sexual reproduction and auxospore formation. Proceedings of the Indian Academy of Sciences 72: 285-287.
- Rebolloso-Fuentes MM, Navarro-Perez A, Garcia-Camacho F, Ramos-Miras JJ, Guil-Guerrero JL (2001) Biomass nutrient profiles of the microalga *Nannochloropsis*. Journal of Agricultural and Food Chemistry 49: 2966-72.
- Reitan KI, Rainuzzo JR, Olsen Y (1994) Effect of nutrient limitation on fatty acid and lipid content of marine microalgae. Journal of Phycology 30: 972-979.
- Ren JG, Xia HL, Just T, Dai YR (2001) Hydroxyl radical-induced apoptosis in human tumor cells is associated with telomere shortening but not telomerase inhibition and caspase activation. Federation of European Microbiological Societies Letters 488: 123-13.
- Renaud SM, Parry DL (1994) Microalgae for use in tropical aquaculture II: effect of salinity on growth, gross chemical composition and fatty acid composition of three species of marine microalgae. Journal of Applied Phycology 6: 347-56.
- Renaud S, Parry D, Thinh L, Kuo C, Padovan A, Sammy N (1991) Effect of light intensity on the proximate biochemical and fatty acid composition of *Isochrysis* sp., and *Nannochloropsis oculata* for use in tropical aquaculture. Journal of Applied Phycology 3: 43-53.
- Reunova YA, Aizdaichera NA, Khristoforovab NK, Reunova AA (2007) Growth and ultrastructure of the marine unicellular alga *Dunaliella salina* (Chlorophyta)

- after chronic selenium intoxication. Russian Journal of Marine Biology 33: 166-172.
- Reyes-Prieto A, Weber APM, Bhattacharya D (2007) The origin and establishment of the plastid in algae and plants. Annual Review of Genetics 41: 147-168.
- Ribalet F, Berges JA, Ianora A, Casotti R (2007) Growth inhibition of cultured marine phytoplankton by toxic algal-derived polyunsaturated aldehdyes. Aquatic Toxicology 85: 219-227.
- Richmond A, Cheng-Wu Z (2001) Optimization of a flat plate glass reactor for mass production of *Nannochloropsis* sp. outdoors. Journal of Biotechnology 85: 259-69.
- Rittschof D, Cohen JH (2004) Crustacean peptide and peptide like pheromones and kairomones. Peptides 25: 1503-1516.
- Rodolfi L, Chini Zittelli G, Bassi N, Padovani G, Biondi N, Bonini G, Tredici MR (2009) Microalgae for oil: strain selection, induction of lipid synthesis and outdoor mass cultivation in a low-cost photobioreactor. Biotechnology and Bioengineering 102: 100-12.
- Rodolfi L, Zittelli CG, Barsanti L, Rosati G, Tredici MR (2003) Growth medium recycling in *Nannochloropsis* sp. mass cultivation. Biomolecular Engineering 20: 243-8.
- Roessler PG (1990) Environmental control of glycerolipid metabolism in microalgae: commercial implications and future research directions. Journal of Phycology 26: 393-399.
- Romano G, Miralto A, Ianora A (2010) Teratogenic effects of diatom metabolites on sea urchin *Paracentrotus lividus* embryos. Marine Drugs 8: 950-967.
- Romano G, Russo GL, Buttino I, Ianora A, Miralto A (2003) A marine diatom derived aldehyde induces apoptosis in copepod and sea urchin embryos. Journal of Experimental Biology 206: 3487-3494.
- Round EF, Crawford RM, Mann DG (1990) The Diatoms: Biology and Morphology of the Genera. Cambridge University Press, Cambridge.

- Russ JC (1986) Practical Stereology. Plenum Press, New York, pp 35-56.
- Sansone C, Braca A, Ercolesi E, Romano G, Palumbo A, Casotii R, Francone M, Ianora A (2014) Diatom-derived polyunsaturated aldehydes activate cell death in human cacer cell lines but not normal cells. PLOS One 9: e101220. doi: 10.1371/journal.pone.0101220.
- Sato S, Beakes G, Idei M, Nagumo T, Mann DG (2011) Novel sex cells and evidence for sex pheromones in diatoms. PLOS One 6: e26923.

 doi:10.1371/journal.pone.0026923.
- Sato S, Mann DG (2012) An astonishing expansion during auxosporulation in the araphid pennate diatom *Psudostaurosira trainorii*. Paper presented at the 22nd International Diatom Symposium, Ghent, Belgium, 26-31 August 2012.
- Sawayama S, Inoue S, Dote Y, Yokoyama S-Y (1995) CO₂ fixation and oil production through microalga. Energy Conversion and Management 36: 729-731.
- Schenk P, Thomas-Hall S, Stephens E, Marx U, Mussgnug J, Posten C (2008) Second generation biofuels: high-efficiency microalgae for biodiesel production. BioEnergy Research 1: 20-43.
- Schmid A-MM (1988) The special Golgi-ER-mitochondrium unit in the diatom genus *Coscinodiscus*. Plant Systematics and Evolution 158: 211-233.
- Schmid A-MM (1989) Geitler's "Plattenband" in the diatom *Synedra cf. ulna* in the light of TEM. Plant Systematics and Evolution 164: 239-252.
- Schmid A-M M (2001) Value of pyrenoids in the systematics of the diatoms: their morphology and ultrastructure. In: Proceedings of 16th International Diatom Symposium, 25 Aug.- 1 Sept. 2000, Athens & Aegean Islands, University of Athens, Greece.
- Schmid A-MM, Crawford RM (2001) *Ellerbeckia renaria* (Bacillariophyta): formation of the auxospores and initial cells. European Journal of Phycology 36: 307-320.
- Schweyer S, Soruri A, Meschter O, Heintze A, Zschunke F, Miosge N, Thelen P, Schlott T, Radzun HJ, Fayyazi A (2004) Cisplatin-induced apoptosis in

- human malignant testicular germ cell lines depends on MEK/ERK activation. British Journal of Cancer 91: 589-598.
- Scott SA, Davey MP, Dennis JS, Horst I, Howe CJ, Lea-Smith DJ, and Smith AG (2010) Biodiesel from algae: challenges and prospects. Current Opinions in Biotechnology 21: 277-286.
- Segovia M, Berges JA (2005) Effect of inhibitors of protein synthesis and DNA replication on the induction of proteolytic activities, caspase-like activities and cell death in the unicellular chlorophyte *Dunaliella tertiolecta*. European Journal of Phycology 40: 21-30.
- Segovia M, Haramaty L, Berges JA, Falkowski PG (2003) Cell death in the unicellular chlorophyte *Dunaliella tertiolecta*: an hypothesis on the evolution of apoptosis in higher plants and metazoans. Plant Physiology 132: 99-105.
- Sharma KK, Schuhmann H, Schenk P (2012) High lipid induction in microalgae for biodiesel production. Energies 5: 1532-1553.
- Sheehan J, Dunahay T, Benemann J, Roessler P (1998) A look back at the US

 Department of Energy's Aquatic Species Program: Biodiesel from Algae. In:

 Closeout Report NREL/TP-580-24190, U.S. Department of Energy's Office

 of Fuels Development, National Renewable Energy Laboratory, Golden,

 Colorado, USA.
- Sicko-Goad L, Stoermer EF (1979) A morphometric study of lead and copper effects on *Diatoma tenue* var. elongatum (Bacillariophyta). Journal of Phycology 15: 316-321.
- Sigma-Aldrich (2015) Trans, trans-2, 4-Decadienal ≥89 %.

 http://www.sigmaaldrich.com/catalog/product/aldrich/w313505?lang=en®

 ion=GB. Accessed 1 September 2015.
- Simionato D, Block M, Rocca NL, Jouhet J, Marechal E, Finazzi G, Morosinotto T (2013) The response of nitrogen starvation includes De Novo biosynthesis of triacylglycerols, a decrease of chloroplast galactolipids, and reorganization of the photosynthetic apparatus. Eukaryotic Cell 12: 665-676.

- Simon CA, Bentley MG, Caldwell GS (2010) 2, 4-Decadienal: exploring a novel approach for the control of polychaete pests on cultured abalone. Aquaculture 310: 52-60.
- Singh J, Gu S (2010) Commercialization potential of microalgae for biofuels production. Renewable and Sustainable Energy Reviews 14: 2596-2610.
- Singh RS, Kaushik Y, Wang Y, Xiang I, Novak M, Komatsu K, Tanaka AM, Cuervo AM, Czaja MJ (2009) Autophagy regulates lipid metabolism. Nature 458: 1131-1135.
- Singh S, Kate BN, Banerjee UC (2005) Bioactive compounds from cyanobacteria and microalgae: an overview. Critical Reviews in Biotechnology 25: 73-95.
- Solomon JA (1985) Ultrastructure evaluation of lipid accumulation in microalgae. In: Aquatic Species Program Review: Proceedings of the March 1985 Principal Investigators' Meeting. Solar Energy Research Institute, US Department of Energy, SERI/CR-23-2700, pp. 71-82.
- Solomon JA, Hand REJr, Mann RC (1986) Ultrastructural and flow cytometric analyses of lipid accumulation in microalgae. Solar Energy Research Institute, US Department of Energy, doi: 10.2172/6757339.
- Solovchenko A, Khozin-Goldberg I, Didi-Cohen S, Cohen Z, Merzlyak M (2008)

 Effects of light intensity and nitrogen starvation on growth, total fatty acids and arachidonic acid in the green microalga *Parietochloris incisa*. Journal of Applied Phycology 20: 245-251.
- Sorrell S, Speirs J, Bentley R, Brandt A, Miller R (2009) Global oil depletion: an assessment of the evidence for a near-term peak in global oil production. A report produced by the Technology and Policy Assessment function of the UK Energy Research Centre.

 https://www.gov.uk/government/uploads/system/uploads/attachment_data/file/43201/1791-uk-erc-report-global-oil-depletion.pdf. Accessed 1 September 2015.
- Sperandio S, de Belle I, Bredesen DE (2000) An alternative, nonapoptotic form of programmed cell death. Proceedings of the National Academy of Sciences, USA 97: 14376-14381.

- Sperandio S, Poksay K, de Belle I, Lafuente MJ, Liu B, Nasir J, Bredesen D (2004)

 Paraptosis: mediation by MAP kinases and inhibition by AIP-1/Alix. Cell

 Death and Differentiation 11: 1066-1075.
- Spolaore P, Joannis-Cassan C, Duran E, Isambert A (2006) Commercial applications of microalgae. Journal of Bioscience and Bioengineering 101: 87-96.
- Steer MW (1981) Understanding Cell Structure. Cambridge University Press, Cambridge.
- Steinke M, Malin G, Liss PS (2002) Trophic interactions in the sea: an ecological role for climate relevant volatiles? Journal of Phycology 38: 630-638.
- Stephenson AL, Dennis JS, Scott SA (2008) Improving the sustainability of the production of biodiesel from oilseed rape in the UK. Chemical Engineering Research and Design 86: 427-440.
- Stoynova-Bakalova E, Toncheva-Panova T (2003) Subcellular adaptation to salinity and irradiance in *Dunaliella salina*. Biologia Plantarum 47: 233-236.
- Strasser A, Harris AW, Jacks T (1994) DNA damage can induce apoptosis in proliferating lymphoid cells via p53-independent mechanisms inhibitable by Bcl-2. Cell 79: 329-39.
- Su C-H, Chein L-J, Gomes J, Lin Y-S, Yu Y-K, Liou J-S, Syu R-J (2011) Factors affecting lipid accumulation by *Nannochloropsis oculata* in a two-stage cultivaton process. Journal of Applies Phycology, 23: 903-908.
- Subramaniam S, Unsicker K (2006) Extracellular signal-regulated kinase as an inducer of non-apoptotic neuronal neuronal death. Neuroscience 138: 1055-1065.
- Subramaniam S, Zirrgiebel U, Bohlen Und HO, Strelau J, Laliberte C, Kaplan DR, Unsicker K (2004) ERK activation promotes neuronal degeneration predominantly through plasma membrane damage and independently of caspase-3. Journal of Cell Biology 165: 357-369.
- Suen Y, Hubbard JS, Holzer G, Tornabene TG (1987) Total lipid production of the green alga *Nannochloropsis sp.* QII under different nitrogen regimes. Journal of Phycology 23: 289-297.

- Sukenik A, Carmeli Y, Berner T (1989) Regulation of fatty acid composition by irradiance level in the eustigmatophytes. Journal of Phycology 25: 686-692.
- Sukenik A, Yamaguchi Y, Livne A (1993a) Alterations in lipid molecular species of the marine eustigmatophyte *Nannochloropsis* sp. Journal of Phycology 29: 620-626.
- Sukenik A, Zamora O, Carmeli Y (1993b) Biochemical quality of marine unicellular algae with emphasis on lipid composition. II. *Nannochloropsis* sp. Aquaculture 117: 313-326.
- Swanson SJ, Bethke PC, Jones RL (1998) Barley aleurone cells contain two types of vacuoles: characterization of lytic organelles by use of fluorescent probes. Plant Cell 10: 685-698.
- Tafresh AH, Shariati M (2009) *Dunaliella* biotechnology: methods and applications. Journal of Applied Microbiology 107: 14-35.
- Tang H, Abunasser N, Garcia MED, Chen M, Ng KYS, Salley SO (2011) Potential of microalgae oil from *Dunaliella tertiolecta* as a feedstock for biodiesel.Applied Energy 88: 3324-3330.
- Taylor R, Caldwell GC, Bentley MG (2005) Toxicity of algal-derived aldehydes to two invertebrate species: do heavy metal pollutants have a synergistic effect?

 Aquatic Toxicology 74: 20-31.
- Taylor R, Caldwell GS, Dunstan HJ, Bentley MG (2007) Short-term impacts of polyunsaturated aldehyde-producing diatoms on the harpacticoid copepod, *Tisbe holothuriae*. Journal of Experimental Marine Biology and Ecology 341: 60-69.
- Taylor R, Rand J, Caldwell G (2012) Treatment with algae extracts promotes flocculation, and enhances growth and neutral lipid content in *Nannochloropsis oculata*: a candidate for biofuel production. Marine Biotechnology 14: 774-781.
- Theriot EC, Ashworth M, Ruck E, Nakov T, Jansen RK (2010) A preliminary multigene phylogeny of the diatoms (Bacillariophyta): challenges for future research. Plant Ecology and Evolution 143: 278-296.

- Theriot EC, Ruck E, Ashworth M, Nakov T, Jansen RK (2011) Status of the pursuit of the diatom phylogeny: are traditional views and new molecular paradigms really that different? In: The Diatom World: Cellular Origin, Life in Extreme Habitats and Astrobiology, Vol. 19, Seckbach J, Kociolek JP (eds), Springer, Dordrecht, pp. 123-142.
- Thompson GA (1996) Lipids and membrane function in green alga. Biochimica et Biophysica Acta 1302: 17-45.
- Tian J, Yu J (2009) Changes in ultrastructure and responses of antioxidant systems of algae (*Dunaliella salina*) during acclimation to enhanced ultraviolet-B radiation. Journal of Photochemistry and Photobiology: B, Biology 97: 152-160.
- Tomaselli L (2004) The microalgal cell. In: Handbook of Microalgal Culture,
 Biotechnology and Applied Phycology. Richmond A (ed) Blackwell Science,
 Hoboken, New Jersey, USA.
- Tonon T, Larson TR, Graham IA (2002) Long chain polyunsaturated fatty acid production and partitioning to triacylglycerols in four microalgae. Phytochemistry 61: 15-24.
- Tsuzuki M, Gantar M, Aizawa K and Miyachi S (1986) Ultrastructure of *Dunaliella tertiolecta* cells grown under low and high CO₂ concentrations. Plant Cell Physiology 27: 737-739.
- Uchida K (1999) Current status of acrolein as a lipid peroxidation product. Trends in Cardiovascular Medicine 9: 109-113.
- Vaishampayan A, Sinha RP, Hader DP, Dey T, Gupta AK, Bhan U, Rao L (2001)

 Cyanobacterial biofertilizers in rice agriculture. Botanical Reviews 67: 453-516.
- van den Hoek C, Mann DG, Jahns HM (1995) Algae: An Introduction to Phycology.

 Cambridge University Press, Cambridge.
- van Iersel M, Ploemen J, Lo Bello M, Federici G, van Bladeren PJ (1997) Interactions of alpha, beta-unsaturated aldehydes and ketones with human glutathione S-transferase P1-1. Chemo-Biological Interactions. 108: 67-78.

- Vardi A, Berman-Frank I, Rozenberg T, Hadas O, Kaplan A, Levine A (1999)

 Programmed cell death of the dinoflagellate *Peridinium gatunense* is mediated by CO2 limitation and oxidative stress. Current Biology 9: 1061-1064.
- Vardi A, Formiggini F, Casotti R, Martino AD, Ribalet F, Miralto A, Bowler C (2006)

 A stress surveillance system based on calcium and nitric oxide in marine diatoms. PLOS Biology 4: e60.
- Vaux DL (1999) Caspases and apoptosis: biology and terminology. Cell Death and Diffentiation 6: 493-4.
- Veldhuis MJW, Kraay GW, Timmermans KR (2001) Cell death in phytoplankton: correlation between changes in membrane permeability, photosynthetic activity, pigmentation and growth. European Journal of Phycology 36: 167-177.
- Vieler A, Brubaker SB, Vick B, Benning C (2012) A lipid droplet protein of *Nannochloropsis* with functions partially analogous to plant oleosins. Plant Physiology 158: 1562-1569.
- Visviki I, Rachlin JW (1994a) Acute and chronic exposure of *Dunaliella salina* and *Chlamydomonas bullosa* to copper and cadmium: effects on ultrastructure.

 Archive of Environmental Contamination and Toxicology 26: 154-162.
- Visviki I, Rachlin JW (1994b) Acute and chronic exposure of *Dunaliella salina* and *Chlamydomonas bullosa* to copper and cadmium: effects on growth. Archive of Environmental Contamination and Toxicology 26: 149-153.
- Vladimirova MG (1978) Ultrastructural organization of the cell of *Dunaliella salina* and functional changes of it in relation to light intensity and temperature. Fiziologiya Rastenii 25: 443-449.
- von Stosch HA (1982) On auxospore envelopes in diatoms. Bacillaria 5: 127-156.
- Walter TL, Purton S, Becker DK, Collet C (2005) Microalgae as bioreactor. Plant Cell Reports 24: 629-41.
- Wang ZT, Ullrich N, Joo S, Waffenschmidt S, Goodenough U (2009) Algal lipid bodies: stress induction, purification, and biochemical characterization in

- wild-type and starchless *Chlamydomonas reinhardtii*. Eukaryote Cell 8: 1856-68.
- Wawra E, Zollner H, Schaur RJ, Tillian HM, and Schauenstein E (1986) The inhibitory effect of 4-hydroxy-nonenal on DNA-polymerases alpha and beta from rat liver and rapidly dividing Yoshida ascites hepatoma. Cell Biochemistry and Function 4: 31-36.
- Weibel E (1969) Stereological principles for morphometry in electron microscopic cytology. International Review of Cytology Supplement 26: 235-302.
- Widjaja A, Chien CC, Ju YH (2009) Study of increasing lipid production from fresh water microalgae *Chlorella vulgaris*. Journal of the Taiwan Institute of Chemical Engineers 40: 13-20.
- Williams DM (2007) Classification and diatom systematics: the past, the present, and the future. In: Unravelling the Algae: The Past, Present, and Future of Algal Systematics. Brodie J, Lewis J (eds). The Systematics Association Special Volume Series 75, CRC Press, Taylor and Francis, London, pp. 57-91.
- Williams DM, Kociolek JP (1988) The araphid diatoms: monophyletic, polyphyletic or paraphyletic? In: The Chromophyte Algae: Problems and Perspectives, Abstracts. Plymouth Polytechnic, England, UK, 1988.
- Williams DM, Kociolek JP (2007) Pursuit of a natural classification of diatoms: History, monophyly and the rejection of paraphyletic taxa. European Journal of Phycology 42: 313-319.
- Williams DM, Kociolek JP (2011) An overview of diatom classification with some aspects for the future. In: The Diatom World, Cellular Origin, Life in Extreme Habitats and Astrobiology 19, Seckbach J, Kociolek JP (eds), Springer, Berlin, Heidelberg, Germany, pp. 47-91.
- Williams DM, Round FE (1978) Revision of the genus *Fragillaria*. Diatom Research 2: 267-288.
- Wiseman H, Halliwell B (1996) Damage to DNA by reactive oxygen and nitrogen species: role in inflammatory disease and progression to cancer. Biochemical Journal 313: 17-29.

- Witz G (1989) Biological interactions of alpha, beta-unsaturated aldehydes. Free Radical Biology and Medicine 7: 333-349.
- Wolf FR, Nonomura AM, Bassham JA (1985) Growth and branched hydrocarbon production in strain of *Botryococcus braunii* (Chlorophyta). Journal of Phycology 21: 388-96.
- Wong JK, Le HH, Zsarnovszky A, Belcher SM (2003) Estrogens and ICI182, 780 (Faslodex) modulate mitosis and cell death in immature cerebellar neurons via rapid activation of p44/p42 mitogen-activated protein kinase. Journal of Neurosciences 23: 4984-4995.
- Wu SC, Yen GC (2004) Effects of cooking oil fumes on the genotoxicity and oxidative stress in human lung carcinoma (A-549) cells. Toxicology In Vitro 18: 571-580.
- Xin L, Hong-ying H, Ke G, Ying-xue S (2010) Effects of different nitrogen and phosphorus concentrations on the growth, nutrient uptake, and lipid accumulation of a freshwater microalga *Scenedesmus* sp. Bioresource Technology 101: 5494-5500.
- Yasumoto K, Nishigami A, Yasumoto M, Kasai F, Okada Y, Kusumi T and Ooi T (2005) Aliphatic sulfates released from *Daphnia* induce morphological defense of phytoplankton: isolation and synthesis of kairomones. Tetrahedron Letters 46: 4765-4767.
- Yilancioglu K, Cokol M, Pastirmaci I, Erman B, Cetiner S (2014) Oxidative stress is a mediator for increased lipid accumulation in newly isolated *Dunaliella salina* strain. PLOS One 9:e91957.
- Young SC, Chang LW, Lee HL, Tsai LH, Liu YC, Lin PP (2010) DNA damage induced by trans, trans-2, 4-decadienal (tt-DDE), a component of cooking oil fume, in human bronchial epithelial cells. Environmental and Molecular Mutagenesis 51: 315-321.
- Yun YS, Lee SB, Park JM, Lee CL, Yang JW (1997) Carbon dioxide fixation by algal cultivation using wastewater nutrients. Journal of Chemical Technology and Biotechnology 6: 451-455.

- Zhai S, Yaar M, Doyle SM, Gilchrest BA (1996) Nerve growth factor rescues pigment cells from ultraviolet-induced apoptosis by up regulation of Bcl-2 levels. Cell Research 224: 335-39.
- Zhekisheva M, Boussiba S, Khozin-Goldberg I, Zarka A, Cohen Z (2002)

 Accumulation of oleic acid in *Haematococcus pluvialis* (Chlorophyceae)

 under nitrogen starvation or high light is correlated with that of astaxanthin esters. Journal of Phycology 38: 325-331.
- Zittelli CG, Lavista F, Bastianini A, Rodolfi L, Vincenzini M, Tredici MR (1999)

 Production of eicosapentaenoic acid by *Nannochloropsis* sp. cultures in outdoor tubular photobioreactors. Journal of Biotechnology 70: 299-312.